

**A Study of the Effectiveness of Ground Penetrating Radar
For Assessing Asphalt Covered Reinforced Concrete
Bridge Deck Deterioration**

by

Christopher L. Barnes

A Thesis Submitted to the
Faculty of Engineering
in Partial Fulfillment of the Requirements
for the Degree of

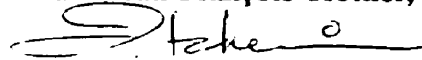
MASTER OF APPLIED SCIENCE

Major Subject: Civil Engineering

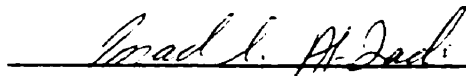
APPROVED:



Dr. Jean-François Trottier, Ph.D., P.Eng., Supervisor



Dr. Farid Taheri, Ph.D., P.Eng.



Dr. Imad Al-Qadi, Ph.D., External Examiner

DALHOUSIE UNIVERSITY – DALTECH

Halifax, Nova Scotia

1999



National Library
of Canada

Acquisitions and
Bibliographic Services

395 Wellington Street
Ottawa ON K1A 0N4
Canada

Bibliothèque nationale
du Canada

Acquisitions et
services bibliographiques

395, rue Wellington
Ottawa ON K1A 0N4
Canada

Your file *Votre référence*

Our file *Notre référence*

The author has granted a non-exclusive licence allowing the National Library of Canada to reproduce, loan, distribute or sell copies of this thesis in microform, paper or electronic formats.

The author retains ownership of the copyright in this thesis. Neither the thesis nor substantial extracts from it may be printed or otherwise reproduced without the author's permission.

L'auteur a accordé une licence non exclusive permettant à la Bibliothèque nationale du Canada de reproduire, prêter, distribuer ou vendre des copies de cette thèse sous la forme de microfiche/film, de reproduction sur papier ou sur format électronique.

L'auteur conserve la propriété du droit d'auteur qui protège cette thèse. Ni la thèse ni des extraits substantiels de celle-ci ne doivent être imprimés ou autrement reproduits sans son autorisation.

0-612-48256-1

Canada

DALTECH LIBRARY

“AUTHORITY TO DISTRIBUTE MANUSCRIPT THESIS”

TITLE:

**A Study of the Effectiveness of Ground Penetrating Radar
For Assessing Asphalt Covered Reinforced Concrete
Bridge Deck Deterioration**

The above library may make available or authorize another library to make available individual photo/microfilm copies of this thesis without restrictions.

Full Name of Author:

Christopher L. Barnes

Signature of Author:

A handwritten signature in black ink, appearing to read 'Chris Barnes', written over a horizontal line.

Date:

6/11/99

TABLE OF CONTENTS

	Page
LIST OF TABLES	vii
LIST OF FIGURES	viii
LIST OF SYMBOLS AND ABBREVIATIONS	ix
ACKNOWLEDGEMENTS	xi
ABSTRACT.....	xii
1. INTRODUCTION	1
1.1 SCOPE OF THE PROBLEM	1
1.2 DELAMINATIONS AND DETERIORATION PROCESSES.....	5
1.3 THE PROBLEM WITH DELAMINATIONS	10
2. DETERMINATION OF APPROPRIATE TECHNOLOGY	12
2.1 TEST METHOD CRITERIA	12
2.2 IDENTIFICATION AND COMPARISON OF CONDITION ASSESSMENT METHODS.....	14
2.2.1 Standard Practice Methods	15
2.2.1.1 Visual Inspection	15
2.2.1.2 Half Cell Potential Survey	17
2.2.1.3 Chain Drag Survey.....	19
2.2.2 Ultrasonic Test Methods	22
2.2.3 Impact Echo	24
2.2.4 Infrared Thermography	27
2.2.5 Ground Penetrating Radar.....	29
2.3 SELECTED TEST METHOD	30

3. GROUND PENETRATING RADAR FOR BRIDGE DECK ASSESSMENT	33
3.1 HARDWARE AND EQUIPMENT SETUP	33
3.2 GPR BACKGROUND THEORY.....	36
3.2.1 Fundamental Concepts.....	36
1.1.2 Interpretation of Layer Characteristics	40
1.1.3 Measurement of Layer Thicknesses.....	44
1.3 EVALUATION OF PAVEMENTS USING GPR.....	50
1.4 DETECTING DETERIORATION IN BRIDGE DECKS	55
1.4.1 Air Gap Detection.....	56
1.1.2 Signal Distortion.....	60
1.1.3 Signal Attenuation	62
1.1.4 High Asphalt/Concrete Interface Reflectivity	64
4. RESEARCH PROGRAM.....	69
4.1 OBJECTIVES	69
4.2 FIELD COLLECTION OF GPR DATA	71
4.2.1 Deck Measurement, Visual Inspection and Marking.....	71
4.2.2 Equipment Setup.....	72
4.2.3 Recording Data and Calibration Files.....	73
4.3 CHAIN DRAG SURVEY DATA COLLECTION	75
4.4 HALF-CELL POTENTIAL SURVEY DATA COLLECTION.....	76
5. PRESENTATION AND DISCUSSION OF DATA ANALYSIS AND RESULTS	79
5.1 AUTOMATIC PROCESSING OF GPR DATA.....	79
5.2 MANUAL PROCESSING OF GPR DATA	82
5.3 CHAIN DRAG DATA PROCESSING.....	85
5.4 HALF-CELL POTENTIAL SURVEY DATA PROCESSING	85
5.5 ISSUES REGARDING DATA INTERPRETATION.....	86

5.5.1	GPR Data	87
5.5.2	Chain Drag Data	94
5.5.3	Half-Cell Potential Data.....	96
5.6	COMPARISON OF BRIDGE DECK SURVEY RESULTS	97
5.6.1	Preliminary GPR Automatic Processing Results.....	99
5.6.2	Glendale Bridge	101
5.6.3	Rough Brook Bridge	105
5.6.4	Victoria Bridge.....	108
5.6.5	Deep Hollow Overpass	112
5.6.6	Grand Pre Overpass	116
5.6.7	Shubenacadie CNR Overpass	120
5.6.8	Baddeck River Bridge.....	124
5.6.9	Skye River Bridge.....	129
5.6.10	Stewiacke River Bridge	133
5.7	NETWORK LEVEL COMPARISON OF RESULTS.....	138
5.8	EFFECTIVENESS OF MANUAL GPR PROCESSING DETERIORATION PREDICTION	144
6.	CONCLUSIONS AND RECOMMENDATIONS	148
7.	REFERENCES	154
8.	APPENDICES	160
APPENDIX A1 GLENDALE BRIDGE		
Appendix A1.1	Manual GPR vs Chain Drag Results	161
Appendix A1.2	Manual GPR vs Half-cell Potential Results	162
Appendix A1.3	Automatic GPR vs Chain Drag Results	163
Appendix A1.4	Automatic GPR vs Half-cell Potential Results	164
Appendix A1.5	Automatic GPR vs Manual GPR Results.....	165

APPENDIX A2 ROUGH BROOK BRIDGE

Appendix A2.1 Manual GPR vs Chain Drag Results.....166
Appendix A2.2 Automatic GPR vs Chain Drag Results167
Appendix A2.3 Automatic GPR vs Manual GPR Results168

APPENDIX A3 VICTORIA BRIDGE

Appendix A3.1 Manual GPR vs Chain Drag Results169
Appendix A3.2 Manual GPR vs Half-cell Potential Results170
Appendix A3.3 Automatic GPR vs Chain Drag Results171
Appendix A3.4 Automatic GPR vs Half-cell Potential Results172
Appendix A3.5 Automatic GPR vs Manual GPR Results173

APPENDIX A4 DEEP HOLLOW OVERPASS

Appendix A4.1 Manual GPR vs Chain Drag Results174
Appendix A4.2 Manual GPR vs Half-cell Potential Results175
Appendix A4.3 Automatic GPR vs Chain Drag Results176
Appendix A4.4 Automatic GPR vs Half-cell Potential Results177
Appendix A4.5 Automatic GPR vs Manual GPR Results178

APPENDIX A5 GRAND PRE OVERPASS

Appendix A5.1 Manual GPR vs Chain Drag Results179
Appendix A5.2 Manual GPR vs Half-cell Potential Results180
Appendix A5.3 Automatic GPR vs Chain Drag Results181
Appendix A5.4 Automatic GPR vs Half-cell Potential Results182
Appendix A5.5 Automatic GPR vs Manual GPR Results183

APPENDIX A6 SHUBENACADIE CANAL CNR OVERPASS

Appendix A6.1 Manual GPR vs Chain Drag Results184
Appendix A6.2 Manual GPR vs Half-cell Potential Results185
Appendix A6.3 Automatic GPR vs Chain Drag Results186
Appendix A6.4 Automatic GPR vs Half-cell Potential Results187
Appendix A6.5 Automatic GPR vs Manual GPR Results188

APPENDIX A7 BADDECK RIVER BRIDGE

Appendix A7.1 Manual GPR vs Chain Drag Results189
Appendix A7.2 Manual GPR vs Half-cell Potential Results190
Appendix A7.3 Automatic GPR vs Chain Drag Results191
Appendix A7.4 Automatic GPR vs Half-cell Potential Results192
Appendix A7.5 Automatic GPR vs Manual GPR Results.....193

APPENDIX A8 SKYE RIVER BRIDGE

Appendix A8.1 Manual GPR vs Chain Drag Results194
Appendix A8.2 Manual GPR vs Half-cell Potential Results195
Appendix A8.3 Automatic GPR vs Chain Drag Results196
Appendix A8.4 Automatic GPR vs Half-cell Potential Results197
Appendix A8.5 Automatic GPR vs Manual GPR Results.....198

APPENDIX A9 STEWIACKE RIVER BRIDGE

Appendix A9.1 Manual GPR vs Chain Drag Results199
Appendix A9.2 Manual GPR vs Half-cell Potential Results200
Appendix A9.3 Automatic GPR vs Chain Drag Results201
Appendix A9.4 Automatic GPR vs Half-cell Potential Results202
APPENDIX A9.5 AUTOMATIC GPR VS MANUAL GPR RESULTS.....203

LIST OF TABLES

	Page
Table 1 - Comparison of test methods to selection criteria.....	31
Table 2 - Predicted peak magnitude of gap of different thicknesses containing different materials.....	59
Table 3 - GPR predictions and actual deterioration quantities on initial structures.....	100
Table 4 – Quantitative and spatial estimate statistics – Glendale Bridge	104
Table 5 – Quantitative and spatial estimate statistics – Rough Brook Bridge	107
Table 6 – Quantitative and spatial estimate statistics – Victoria Bridge.....	110
Table 7 – Quantitative and spatial estimate statistics – Deep Hollow Overpass	115
Table 8 – Quantitative and spatial estimate statistics – Grand Pre Overpass.....	119
Table 9 – Quantitative and spatial estimate statistics – Shubenacadie CNR Overpass	123
Table 10 – Quantitative and spatial estimate statistics – Baddeck River Bridge	128
Table 11 – Quantitative and spatial estimate statistics – Skye River Bridge	132
Table 12 – Quantitative and spatial estimate statistics – Stewiacke River Bridge.....	135
Table 13 – Predicted, ground-truth and actual bridge deck deterioration quantities	139
Table 14 - Statistical comparisons of actual ground-truth and repair quantities to GPR predicted quantities as a percent of the ground-truth or actual quantity	140
Table 15 – Predicted, ground-truth and actual bridge deck deterioration quantities as percentages of the bridge deck surface area.....	141
Table 16 - Statistical comparisons of ground-truth and repair quantities to GPR predicted quantities as a percent of the bridge deck surface area.....	142
Table 17 – Network level statistics of GPR spatial correlation with actual and ground-truth deterioration	143
Table 18 - Actual and estimated deterioration - visual estimation.....	145

LIST OF FIGURES

	Page
Figure 1 - Severely corroded reinforcing bar in a bridge deck	7
Figure 2 - Concrete cover delaminated as a "plate" from underlying reinforcement.....	8
Figure 3 - Concrete cover disintegrated into fragments overlying corroded reinforcement.....	9
Figure 4 - Delamination showing no visible signs of distress on the deck surface.....	9
Figure 5 - Severe staining of deck underside	16
Figure 6 - Van equipped with Penetradar PS-24 Integrated Radar Inspection System	32
Figure 7 - GPR control hardware contained inside research vehicle.....	34
Figure 8 - Exterior antenna assembly on front of van.....	35
Figure 9 - Typical transmitted radar impulse signal.....	40
Figure 10 - Ray diagram of energy reflection and transmission from a bridge deck.....	42
Figure 11 - GPR waveform recorded from typical asphalt paved bridge deck.....	44
Figure 12 - Sample of a flat metal plate calibration file.....	46
Figure 13 - Antenna positioned over the flat metal plate	47
Figure 14 - Sample of a free space calibration file.....	47
Figure 15 - Antenna assembly directed into free space.....	48
Figure 16 - GPR deck data indicating areas of deterioration	67
Figure 17 - Conducting the chain drag survey	76
Figure 18 - Conducting the half-cell potential survey.....	78
Figure 19 - Diagram showing convergence and divergence of test methods.....	86

LIST OF SYMBOLS AND ABBREVIATIONS

a	Angle of incidence of transmitted energy.
A	Peak amplitude of the air/asphalt interface.
ASTM	American Society for Testing and Materials.
c	Speed of light in free space (meters/second).
C	Peak amplitude of the asphalt/concrete interface.
d	Longitudinal reinforcement spacing (meters).
D_l	Diameter of the longitudinal deck reinforcement.
E_i	Incident voltage.
E_r	Energy reflected from the deck surface.
E_{Rn}	Energy reflected from nth interface.
f	Antenna frequency.
F	Intermediate variable for calculations.
F_c	Correction factor, related to conductor spacing, assumed = 0.
FWD	Falling Weight Deflectometer.
GPR	Ground Penetrating Radar.
IE	Impact Echo.
IR	Infrared Thermography.
l	Wavelength of the GPR transmitted pulse.
m₀	Magnetic permeability of free space (Henry/meter).
m_r	Relative magnetic permeability of a given material.
NRP	Net Reflected Pulse.
P_i	Incident power.
R	Voltage reflection coefficient.
R₂	Ratio of peak amplitude of asphalt/concrete interface, C, to air/asphalt interface, A.
R_{n-1,n}	Energy reflected at the interface of the n-1th and nth layers.

RF	Radio Frequency.
SHRP	Strategic Highways Research Program.
T	Voltage transmission coefficient.
$T_{n-1,n}$	Energy transmitted through the interface of the $n-1^{\text{th}}$ and n^{th} layers.
UT	Ultrasonic Testing.
X_n	Thickness of n^{th} layer.
Z_{ri}	Impedance of the i^{th} layer.
α_n	Signal attenuation coefficient of the n^{th} layer.
δ	Loss tangent or dissipation factor.
ϵ	Relative dielectric constant of a given material.
ϵ_0	Permittivity of free space (Farads/meter).
$\epsilon_{\text{asphalt}}$	Relative dielectric constant of asphalt.
$\epsilon_{\text{concrete}}$	Relative dielectric constant of concrete.
ϵ_r	Relative dielectric constant of a given material.
ϵ_m	Relative dielectric constant of the n^{th} material.
v	RF energy propagation velocity through a given material (meters/second).
σ_{dc}	Direct current conductivity or ohmic conductivity (Siemens/meter).
τ	Time required for energy to travel from $n-1^{\text{th}}$ interface to n^{th} interface and back.
φ	Period of transmitted pulse.

ACKNOWLEDGEMENTS

I would like to thank my wife Stacy for her patience and understanding, my supervisor, Dr. J.-F. Trottier, for his encouragement and leadership, Dr Farid Taheri and Dr. Imad Al-Qadi for their valuable assistance and advice in preparing this thesis, Mike Mahoney for the many long hours and advice, and also Blair Nickerson and Dean Forgeron for their assistance and moral support.

I would also like to extend my thanks to the Nova Scotia Department of Transportation and Public Works for the funding and cooperation to make this research project possible. I would specifically like to thank Peter Adams, Tom Guthro, and Gary Pyke of the Nova Scotia Department of Transportation and Public Works for their advice and support and especially for helping me to understand the problem from a management perspective. I would like also to thank the Natural Sciences and Engineering Research Council of Canada for additional funding for this project.

ABSTRACT

The Penetradar Integrated Radar Inspection System (IRIS) Ground Penetrating Radar (GPR) was selected by Dalhousie University DalTech as the most appropriate technology for assessing the condition of reinforced concrete bridge decks because of the ability of the system to penetrate through asphalt concrete overlays and perform data collection at traffic speeds up to 75-80 km/hr. This technology was selected from a list of other nondestructive testing methods such as infrared thermography, ultrasonic methods, and impact echo testing.

A collaborative research program was designed by Dalhousie University DalTech and the Nova Scotia Department of Transportation and Public Works to examine the accuracy and confidence with which GPR can be used to predict the quantity and location of delaminations and concrete scaling on asphalt covered bridge decks. Seventy-two bridge decks were surveyed at traffic speeds using GPR for deterioration estimation. The GPR data was processed manually to determine areas of excess signal attenuation and areas of high concrete relative dielectric constant. Deterioration predictions made using GPR were also compared quantitatively and spatially to ground-truthing data obtained from nine bridge decks using the well-established chain drag and half-cell potential surveys after the asphalt was removed from each bridge deck just prior to repair.

On each of the nine bridge decks, good to excellent correlation between the GPR predicted deterioration quantity and locations was observed on each of the nine bridge decks with the quantity and locations of deterioration found on the decks using the conventional ground-truthing methods. On a network level, the GPR results were observed to underestimate the actual repair quantity by 1.5% of the bridge deck surface area. The 95% upper and lower confidence limits of the GPR prediction of the deterioration quantities as a percent of the deck surface area were observed to be 8.3% underestimation and 4.6% overestimation with respect to the actual repair quantities. These results show improvements in accuracy and variability over traditional visual estimation methods.

From the initial results of this research and comparison to historical records of the visual inspection methods accuracy, GPR provides a valuable pre-tender quantity estimation tool to bridge managers for deck repairs that is more accurate and reliable than traditional visual inspection methods.

1. Introduction

Over the past half-century, the durability and life span of existing reinforced concrete structures have been issues that have received increased priority with government transportation agencies. Focus has shifted from the creation of an infrastructure that permits the rapid movement of people and goods for a strong national economy to the maintenance and longevity of this infrastructure. Significant and increasing portions of annual government expenditures are required to repair and maintain these structures as they age and decay. Gannon and Cady (1993), in their report for the Strategic Highways Research Program, estimated that in the United States alone, the cost of repairing these structures is increasing at \$500 million per annum, or 2.5% of their \$20 billion total replacement value in 1995. These high costs are due, in part, to judgmental errors in formulating estimates of the extent of repairs that are required. Aktan et al. (1995) reported that while state-of-the-art practice had provided a satisfactory level of public safety, inaccurate condition assessment had been identified as the most critical technical barrier to effective management of highway bridges.

This thesis presents a detailed discussion of the problems and costs associated with detecting deck deterioration, presents and critiques several possible test methods as potential resolutions to the problems at hand, and describes the development and implementation of a research program designed to assess the effectiveness of the most appropriate method (ground penetrating radar) for evaluating asphalt-covered reinforced concrete bridge decks..

1.1 Scope of the Problem

Historically, the Nova Scotia Department of Transportation and Public Works, like most transportation agencies, have allocated funds from their annual budgets for

repairs of reinforced concrete bridge decks based upon the subjective and intuitive judgment of project engineers instead of objective measurements of the actual bridge deck conditions. Bridge deck deterioration is normally hidden from view to the inspector by an asphalt pavement layer covering the concrete deck, making an accurate assessment of their extent and location very difficult. Bridges in each district are prioritized for repair by district supervisors based on their perception of the overall condition of the structures. Those bridges that appear to be in the worst condition in each district are compiled into a provincial list that is further prioritized to determine the following season's proposed structures for rehabilitation. Prioritization criteria of the structures on this list have not historically considered actual measurements of deck deterioration, but have been based on subjective condition assessments, usually from visual observations alone. It is not until after deterioration quantities have been estimated based on visual observations, tenders prepared and awarded, and rehabilitation of the structure begun that testing is done to determine the actual extent and location of deterioration in the deck slab. This has been due to costs related to traffic control, physical constraints of test procedures, and time. Conventional deterioration test methods require direct contact with the deck surface and therefore lane closures, traffic control, and removal of the asphalt pavement are needed. Problems in meeting expected rehabilitation costs both on a project level and on a network level have occurred due to variability in the accuracy of individual inspectors to effectively estimate deck deterioration levels prior to tender preparation. On a project level, repair budgets have sometimes been prone to gross overestimates or underestimates of the actual repair costs. Overestimates result in inefficient spending and tend to cause long term price increases while underestimates result in immediate increases to Provincial debt burden. Gross differences between predicted and actual deterioration quantities can result in costs related to improper repair or replacement management decisions.

Variability and excesses in deck repair costs have occurred due to the lack of an objective and accurate means of measuring deterioration in bridge decks prior to their

selection for repair. The major forms of deterioration in reinforced concrete bridge decks are delamination of the concrete cover over the top and bottom mats of steel reinforcement (rebar) and scaling or damage induced by repeated freezing and thawing cycles to the concrete surface. Visual examination of the bridge deck has been the only indicator of the presence of delaminations to the project engineer, but offers no measurement of the true extent or location of delaminations in the deck from the top surface due to the asphalt pavement effectively hiding the deterioration. Instead, methods which involve physical contact with the deck such as the half-cell potential and chain drag surveys have been used for measuring the location and extent of delaminations, but only after the decision had been made to repair the deck and the asphalt has been removed. This has been due primarily to the high cost of removing the asphalt pavement and waterproofing membrane from the deck surface and also traffic control measures and labor. Only the information gathered using visual methods was used in prioritization of structures for repairs or in forecasting repair budgets since half cell potential and chain drag survey methods were typically employed after the decision to repair that structure had been made. The high cost of obtaining accurate information using the half-cell potential or chain drag surveys, along with the cost and difficulty of interrupting traffic and removing the asphalt pavement and waterproofing membrane, has precluded the use of delamination surveys in prioritization and planning of repair budgets. While this system of “judicious guessing” for deterioration estimation appears inefficient, it has been the most cost-effective means of managing the repairs of the provincial bridge population.

Improved prioritization and cost forecasting for repairs of the Provincial bridges would be made possible if an accurate and precise method of quantifying deck deterioration on bridges were available to the project engineers. Savings would be realized on a network level through more efficient spending of the annual repair budget, and also through potential reductions in the unit price of the work. Foreknowledge of deck removal quantities would reduce repair costs on a project level and therefore

decrease time and labor requirements for both traffic control and construction. Improved knowledge of deck conditions prior to removal of the asphalt pavement would eliminate costs associated with unnecessary removal of asphalt pavement on decks that are sound, but were incorrectly perceived to be in need of repair. Furthermore, decks that are excessively deteriorated can be rehabilitated at less cost by replacement rather than by repair of the deteriorations.

There are obvious costs associated with the lack of accurate repair quantities prior to tender preparation. What are not obvious are the effects that these consequences may have on management of the repair budget. Underestimation of the repair quantity will result in an immediate over-run of the repair budget on a project level. This takes funds away from other deserving projects, leading to increased debt and reduced service quality to the public. Overestimation of the repair quantity will cause the contractor to incur losses due to lack of expected work. If chronic overestimation is observed over time, contractors will adjust their unit prices upward to account for the shortfall of work. In the long run, the owners of the bridges lose money due to overestimation by driving the variable unit prices upward. Furthermore, overestimation introduces a budget surplus that may be realized near the end of a fiscal year. To ensure similar annual funding in the future, these excesses may need to be spent quickly and uneconomically.

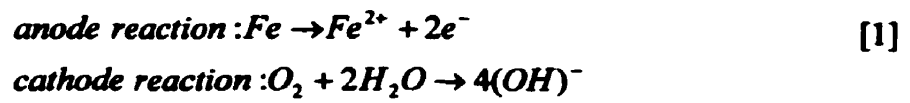
Most importantly, accurate repair quantity estimation will enable economical timing of repairs to ensure that the funding is most appropriately spent. Repairing bridges too early may result in needless early spending on traffic control and asphalt removal for the sake of some minimal deck repairs. Waiting too long to start repairs on a deck may result in spending excessive funding on deck repairs when it may be more economical to replace the deck slab altogether. The proper timing of deck repairs is crucial to effective management of the repair budget.

1.2 Delaminations and Deterioration Processes

Shaw and Xu (1998) refer to what they call the “humidity paradox” in describing the role of water in the life of concrete after it has been placed. Moisture is necessary to develop strength, to establish a proper hardened air-void system in the concrete, to prevent plastic and drying shrinkage cracking in its early stages, and is essential for basically ensuring the highest quality of the concrete when it is placed. On the other hand, water is known to be the prime factor in most of the physical and chemical processes that cause deterioration of concrete after its initial curing.

Bridge deck delaminations are debonded areas of the protective cover layer of concrete that overlies the steel reinforcement embedded in the deck slab. While the term “delamination” may technically be a misnomer since there is not actually a laminar separation of two distinct materials; it has become the accepted term to describe this phenomenon. Delaminations occur in bridge decks due to a combination of physical and chemical processes. The cause of delaminations in reinforced concrete is corrosion of the steel reinforcement in the deck slab. According to Neville (1987), corrosion is an electrochemical process in which iron, Fe^{++} , ions are oxidized in the presence of moisture and chloride, Cl^{-} , ions. Normally, concrete is resistant to corrosion due to the strong alkalinity of the cement hydration product calcium hydroxide, $Ca(OH)_2$, and the passivity of an iron oxide film that forms over the steel in its presence. Carbonation and chloride ion penetration into the concrete deck are two processes which occur that deteriorate the alkaline environment that allows for this passivity to exist. These two processes are accelerated by the presence of cracks in the concrete due to increased surface area for chemical reactions and also increased proximity and passage for water, chloride ions, and other chemical agents to the reinforcing steel. Carbonation is the reaction of carbon dioxide with moisture to produce carbonic acid, which reacts with the calcium hydroxide product of the hydrated cement to produce calcium carbonate. Carbonation neutralizes the alkaline environment in the affected area, beginning at the exposed concrete surface

and proceeding downward into the depth of the slab. If carbonation reaches the reinforcing steel, the passive iron oxide layer is removed along with its corrosion resistant properties. Chloride ions in solution that migrate into the concrete cover react with water to form hydrochloric acid. The acid reacts with the iron oxide film, destroying the protective passivity. Furthermore, concentrations of chloride ions cause anodic and cathodic regions to occur in different location on the steel reinforcement. Transfer of electrons from iron at the anode to water and oxygen at the cathode result in formation of hydroxyl cations (OH)⁻ through the following half-cell reactions:



These hydroxyl cations react with the liberated iron anions (Fe⁺⁺) from the anode reaction to produce ferrous hydroxide Fe(OH)₂, which ultimately results in ferric oxide, or rust. Pitting corrosion also occurs as chloride ions react with water and Fe⁺⁺ to produce ferrous hydroxide and hydrochloric acid, thus increasing rust formation, deterioration of the passivity film on the steel, and inducing further pitting corrosion. Hence, chloride ion intrusion into concrete cover over reinforcement can be considered as a pre-cursor to corrosion problems, or as an initial phase in the deterioration process of a bridge deck. As the steel reinforcing bars in the deck slab are oxidized, rust forms at the steel-concrete interface at the anode resulting in a net increase in volume. This increase in volume leads to development of internal expansive forces in the deck slab. Concrete is a brittle material that is weak in tension and therefore responds to internal expansion by cracking to relieve the stresses. When the concrete cracks, water and chloride ions are allowed easier access to penetrate the concrete cover and reach unaffected steel, increasing the rate of corrosion. It is important to note that chloride ions are not consumed in the corrosion activity, but are continually cycling between formation of hydrochloric acid and reactions with the steel. Figure 1 shows a reinforcing bar that has

been severely corroded to the point that it has become detached from its remaining length embedded in the deck.

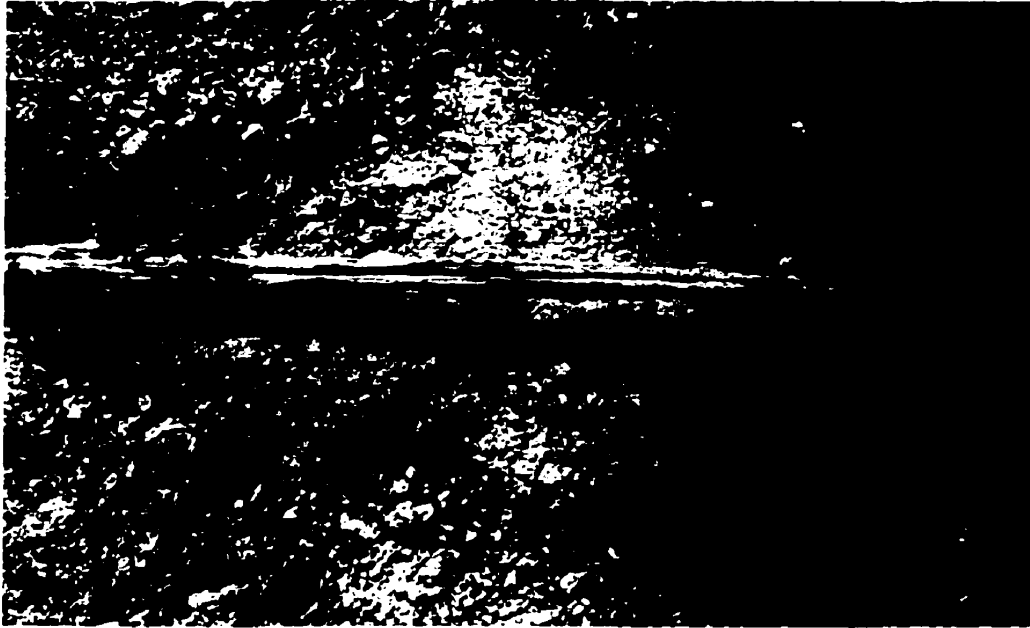


Figure 1 - Severely corroded reinforcing bar in a bridge deck

The problem is further compounded by damage caused to the concrete by repeated freezing and thawing cycles. Properties of concrete such as strength and permeability become worsened through freezing and thawing cycles by increasing the extent of existing micro and macro-cracks. Micro-cracking develops in concrete through buildup of internal expansive pressures during freezing if sufficient resistance is not provided by a well developed hardened entrained air-void system. The surface of the concrete slab at the asphalt/concrete interface may become scaled as freezing and thawing cycles induce cracks which flake and spall away the protective paste layer. The rate of damage to the concrete increases with prolonged exposure to repeated freezing and thawing cycles, worsening the effects on corrosion resistance with increased rates of carbonation and chloride ion ingress. For these reasons, damage due to scaling and

freezing and thawing cycles are often included with delaminations as areas to be repaired on reinforced bridge decks.

Traffic loading is another major contributing factor to the development and growth of delaminations in bridge decks due to flexural fatigue of the concrete. Impact and fatigue loading from truck tires increase stresses, causing an increase in crack growth at delaminations and also aid in spalling the concrete cover from the rebar layer.

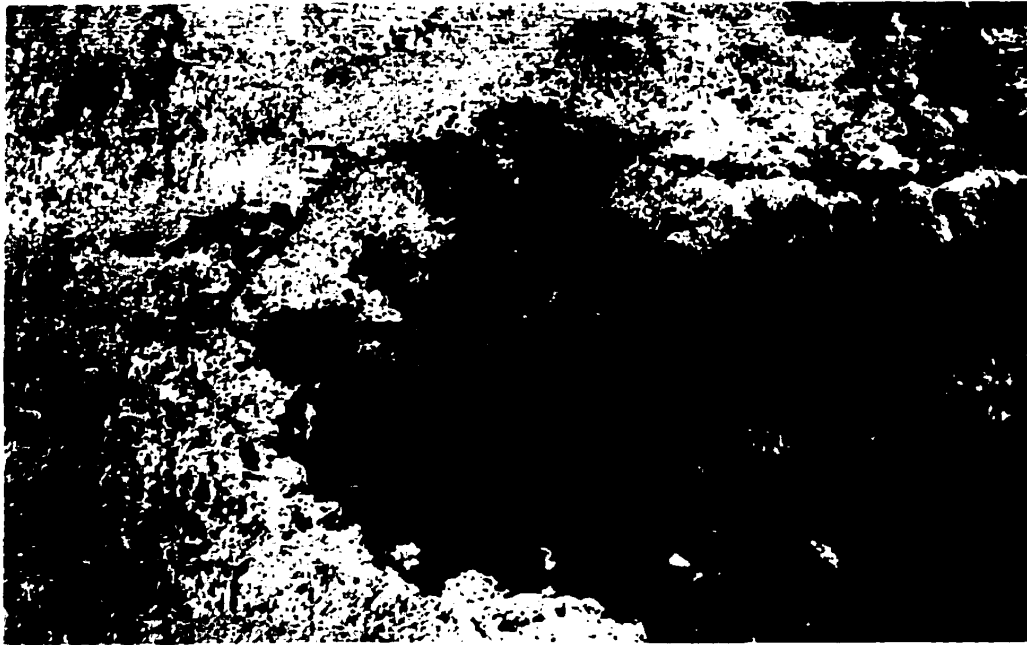


Figure 2 - Concrete cover delaminated as a "plate" from underlying reinforcement

Figure 2 shows a delamination that appears to be a plate of concrete cover that has been separated from a transverse reinforcement bar by internal tensile stresses resulting from corrosion.



Figure 3 - Concrete cover disintegrated into fragments overlying corroded reinforcement

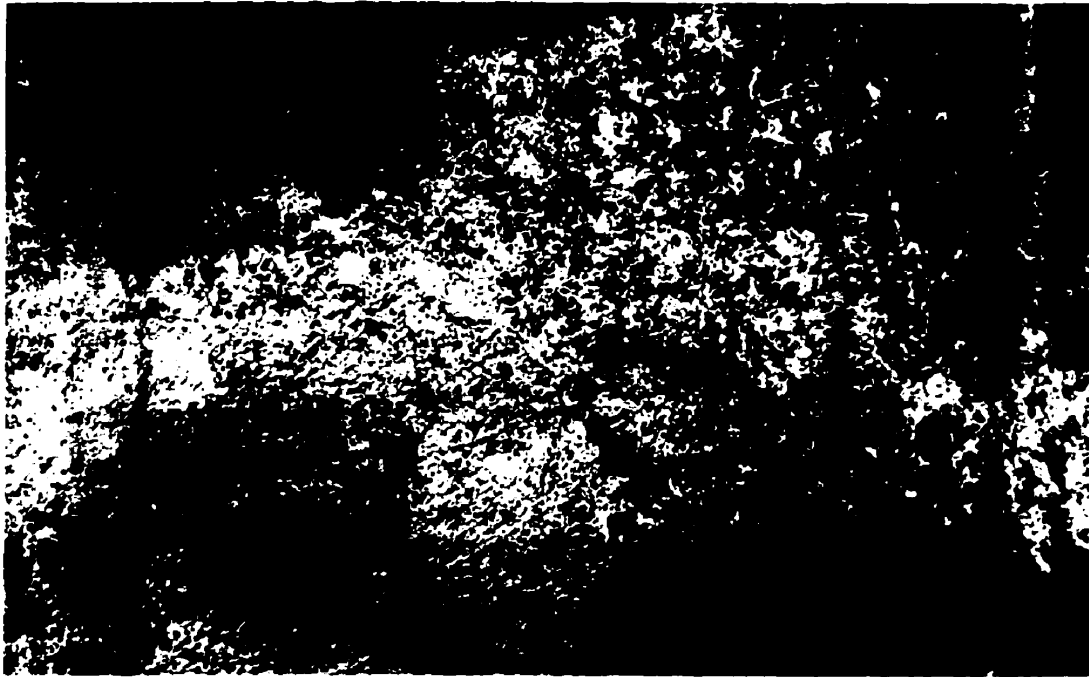


Figure 4 - Delamination showing no visible signs of distress on the deck surface

Figure 3 shows a region of the deck surface that has become pulverized into concrete fragments that overlay corroded reinforcement. Figure 4 shows a delamination that is invisible from the surface. The various levels of effects such as freezing and thawing cycles and traffic loading have on the formation and aging processes of delaminations makes their characteristics difficult to detect using any single test criteria.

1.3 The Problem with Delaminations

Why should delaminations be removed from bridge decks? The answer is based almost entirely upon durability concerns and extending the useful service life of the structure. Deck slabs are designed with respect to shear and flexural strength. These designs incorporate load and resistance factors that serve to increase design loads and reduce design resistances. These factors are developed according to the probabilistic expectations of material performance and service conditions over the design life of the structure. As a result, these designs are highly conservative for usual service conditions, giving the designer some reassurance that the structure will not fail within normal service conditions. The load resistance offered by the in-service materials tends to remain sufficient to carry the in-service loads that are applied to the structure despite reductions in this margin of probability from reinforcement corrosion and concrete deterioration. Increases in material degradation will also serve to increase the rate at which this deterioration and reduction in safety occur. Compounding the problem of dealing with deck deterioration is the question of timing. At what point does it become economical to repair deck deterioration? In discussions with bridge management officials from the Nova Scotia Department of Transportation and Public Works, it was stated that many decks can provide adequate resistance to normal in-service loads, even when they are found to be in excess of fifty to sixty percent deteriorated. From a materials standpoint, if the problem areas are repaired quickly and their causes removed, the lifetime may be increased well beyond the design lifetime of the structure. From the perspective of

management, there must be some compromise between maintenance and replacement costs of a given structure to minimize cost and maximize serviceable life. This compromise ideally describes the point at which it becomes most economical to repair the delaminations to increase the serviceable lifetime of the deck. Repairing decks that are not delaminated enough to warrant the cost of repairs and decks that are so deteriorated that replacement presents a more viable option are both expensive consequences of poor timing of repairs.

This further illustrates the need for an accurate method for predicting deterioration quantities before the decision is made to repair a deck. Not only will this increase in accuracy reduce the margin of error in repair estimates, but also it can allow for effective management decisions regarding the timing of repairs such that the life cycle cost of the structure can be reduced.

2. Determination of Appropriate Technology

There exist many different technologies that may be applicable in solving the problem of accurately predicting delamination quantities in asphalt covered reinforced concrete bridge decks. The following sections describe the establishment of selection criteria for the most appropriate method and how the various methods considered in this research fit those criteria.

2.1 Test Method Criteria

In order to evaluate different methods of assessing asphalt covered reinforced concrete bridge decks, certain criteria were established. These criteria were based on physical conditions and economic factors that have historically precluded delamination surveys from being conducted on many bridges prior to repairs.

There are two primary factors that prevent simple access for personnel to survey the top surface of a reinforced concrete bridge deck. Traffic flow over the bridge surface can not simply be halted during the time required to assess the deck. Usually, a lane closure is required with traffic control measures, consisting of either sign-persons controlling and directing the flow of traffic, or timed signal lights. Furthermore, the surveyed area must be enclosed using safety barriers to prevent injury to personnel inside the area from traffic outside of the area. Therefore, traffic control is expensive and time consuming to establish. Furthermore, there are other expense associated with disruptions in traffic flow such as user delays, and increased risk of accidents. The second factor preventing easy access to the surface of the bridge deck, on the majority of decks in Nova Scotia, is a layer of asphalt pavement overlying the surface of the concrete, sometimes with an asphaltic or rubber waterproofing membrane separating the two materials. The asphalt and membrane provide a driving surface that is similar in

texture to the remainder of the highway, while providing, in principle, a protective layer to retard the ingress of water and chemicals into the concrete deck. Unfortunately, this asphalt layer also prevents bridge inspectors from viewing the surface of the concrete deck and prevents sufficient physical contact to the concrete surface that is necessary for effective traditional delamination survey methods. Providing access to the deck surface has traditionally meant removing the asphalt and waterproofing membrane, usually at a significant cost, plus providing traffic control. In Nova Scotia, there are approximately one thousand reinforced concrete bridge decks, with an estimated ninety-nine percent of them overlaid with asphalt pavement.

Given that some structures would already be in substandard condition, the most appropriate method should be non-destructive so that further damage to the structure would not be incurred and money need not be spent to replace damaged areas or materials.

Experienced bridge inspectors generally make adequately accurate estimates of the condition of a reinforced concrete bridge deck according to the needs of the Department of Transportation and Public Works. Any new method must exhibit accuracy in predicting quantities which meets or exceeds that historically exhibited by bridge inspectors. Equally important as accuracy are subjectivity and reproducibility. The results should be based on a subjective analysis such that any given operator can arrive at the same result with an acceptable level of error. The data recorded using the method must therefore be consistent and reproducible. This will ensure that a reliable end result will be achieved, enabling the deterioration predictions to be readily accepted into a bridge management system.

An important consideration in developing the use of a new technology in an area is simplicity. Ease of data collection and interpretation should be a requirement such that personnel can be trained to use the equipment with little effort.

Given these considerations, the following criteria were established to select or develop the technology to address the problem of predicting the extent of deterioration in asphalt covered reinforced concrete bridge decks in Nova Scotia. The method should be:

- Non-destructive to the pavement and deck slab,
- Non-interfering with normal traffic flow on the structure,
- Accurate in detecting deterioration underneath asphalt overlays on the deck,
- Data must be consistently reproducible,
- Results should be objective,
- Simple to use.

2.2 Identification and Comparison of Condition Assessment Methods

Different bridge deck condition assessment methods were reviewed from available literature and compared against each other using the method criteria established in Section 2.1. From these methods, the one most suited to the constraints of this problem was selected and the necessary equipment was purchased for use in this research project to evaluate its effectiveness for bridge deck condition assessment in Nova Scotia.

From a review of technical literature, conferences and information provided on the internet, the following list of potential methods for the problem of identifying bridge deck deterioration was developed:

- Standard methods – visual assessment, chain drag and half-cell potential surveys
- Ultrasonic test methods

- **Impact Echo test methods**
- **Infrared methods**
- **Ground Penetrating Radar methods**

2.2.1 Standard Practice Methods

The simplest and easiest method of assessing bridge conditions available to a bridge inspector is visual examination. Cracking, rust, efflorescence and moisture staining on the curbs, abutments, and underside of the deck are strong indicators of water permeation through the concrete which may lead to corrosion of the rebars and delaminations in the deck. These indicators may lead one to suspect the existence of delaminations in the deck where they are found, but do not allow one to measure the actual location and extent of delaminations over the whole deck, nor do they give conclusive evidence that delaminations definitely exist at that location. The lack of an actual delamination at a given location may not necessarily mean that corrosion of the reinforcement and other concrete deterioration is not present. There are traditional and also more technical methods which bridge inspectors use to determine the location and extent of delaminations and corrosion rates in the deck to try to gain a better understanding of a particular bridge. Three of these methods are visual inspection, the chain drag and the half-cell potential survey.

2.2.1.1 Visual Inspection

Often an inspector can detect areas in which deterioration may be occurring by observing the surface and underside of the deck. The asphalt surface may exhibit cracks and signs that underlying concrete has deteriorated, providing an unstable base for the asphalt pavement. Cracks in the asphalt pavement and separation from the curb edges

and joints provide easy pathways for water, chloride, and oxygen to penetrate to the concrete deck where ingress into the slab may first be initiated.



Figure 5 - Severe staining of deck underside

The underside of the deck may provide more substantive evidence of deterioration in the slab. Moisture, rust, efflorescence and cracking provide evidence of deterioration processes in the slab above them, but may not necessarily indicate the lateral extent of delaminations in the overlying deck. Furthermore, measurement of the size and location of these indications can be extremely difficult as height and obstacles such as waterways or traffic underneath the structure may limit access to the deck underside surface.

Figure 5 shows extensive staining on the underside of a bridge deck. While the probability of delaminations existing above the stains is high, the lateral or longitudinal extent of the deterioration remains unknown. At best, visual inspection can help the

engineer in assessing probable deterioration in the deck, but still makes formulating a repair quantity estimate difficult.

2.2.1.2 Half Cell Potential Survey

Half-cell potential surveys are used to indicate areas in which there is a high probability of active corrosion present on the reinforcement contained inside the deck. In the corrosion cell within the deck there is a flow of electrical current as electrons migrate from the anode to the cathode. Associated with this current flow are variations in potential along the length of the reinforcement, which may be detected using a half-cell electrode. The results from the half-cell potential survey do not directly indicate the presence of delaminations, but it follows that over time, delaminations will occur in those areas in which there is active corrosion. Active corrosion can be viewed as an intermediate phase in the deck deterioration process, coming after moisture and chloride ingress, but both before and after the formation of a delamination crack.

The test method consists of applying a copper-copper sulfate electrode, connected to the negative terminal of a voltmeter, to the pre-wetted surface of the exposed concrete bridge deck, in which the reinforcing steel is electrically connected to the positive terminal of the voltmeter. The resulting voltage is measured using the voltmeter and recorded along with the location of the test on the deck surface. The voltages are plotted as iso-potential contour maps overlaid on a plan map of the deck surface or on a cumulative frequency distribution for interpretation. According to ASTM C876-91, voltages that are more positive than -0.20 volts CSE (copper-copper sulfate electrode) indicate that there is a greater than 90% probability that no corrosion of the reinforcing steel is occurring at that particular location. Voltages measured between -0.20 volts CSE and -0.35 volts CSE can not be used to predict the existence of corrosion with any certainty. Voltages more negative than -0.35 volts CSE indicate that there is above 90% probability that there is active corrosion at that particular test location. Kemp (1996)

suggests that the standard -0.35 volts CSE limit may indicate a high probability of significant active corrosion, but claims that tests have shown that onset of corrosion may occur at potentials as low as -0.24 volts CSE.

Allred (1996) reports that absolute values of potential alone are not enough for reliable determination of corrosion probability, since the absolute values can vary according to moisture content and, to a lesser extent, the temperature of the concrete. Allred also suggests that inclusion of cover thicknesses with the half-cell survey will allow for correlation between high probability of active corrosion and low cover thicknesses on the deck. There are a number of field conditions that require experience and possibly destructive investigations to aid in interpretation of the half-cell potential test results. Carbonation of the concrete to the depth of the reinforcing steel will increase the negativity of the measurement, resulting in higher prediction rates for corrosion in the deck. Dry concrete will act as an insulating dielectric instead of being more conductive in a wetter state. Concrete that experiences highly variable moisture and oxygen contents at the level of the embedded steel and also rehabilitated structures that have introduced a change in the moisture and oxygen content at the depth of reinforcing steel require analyses that account for these change in rates with respect to corrosion. Volkwein (1995) states that misleading high and low potentials can be observed in concrete that is very dense or wet with poor oxygen supply and in concrete where there is little cover over the reinforcement and that has dried, allowing active corrosion to change into a passive state. Volkwein also notes that potential measurements are the average potential measured over the deck area adjacent to the measuring point and that it is possible to overlook certain small, but active, corrosion locations.

Half-cell potential measurements may or may not be accurate indications of corrosion current. Variable moisture, oxygen, and ion concentrations in the concrete near the reinforcing steel may cause changes in measured voltage that will lead to decreased accuracy in predicting the presence of corrosion activity. ASTM C 876 – 91

recommends that other data be used in conjunction with the half-cell surveys to formulate conclusions concerning the corrosion activity of embedded steel in the deck such as chloride contents, depth of carbonation, delamination survey findings, rate of corrosion results, and environmental exposure conditions. ASTM C 876 – 91 does not specify grid spacing for conducting half-cell potential surveys, but notes that longitudinal and lateral spacing of four feet have been found to be satisfactory for deck slab applications. Measurements that are too close together tend to be redundant and waste time and effort, while spacing that is too large may overlook small areas of active corrosion.

The half-cell potential survey is not a direct measurement of the presence of delaminations, but identifies the potential for delaminations. Given that most bridges are not surveyed using the half-cell electrode until a point in the life span of the deck that delaminations are likely, most areas denoted by the survey are likely to have induced cracking and delaminations in the deck. Some areas will be found in which the probability of active corrosion is high, but the degree of corrosion is insufficient to cause delamination in the deck.

2.2.1.3 Chain Drag Survey

The chain drag may be the simplest and most cost effective means of gathering information on the top rebar delaminations for exposed reinforced concrete decks. Delaminations are detected by the operator listening to the sounds of a length of steel chain being dropped and dragged over the deck surface. Sound concrete will result in a sharp ringing sound from the deck, while delaminated concrete responds with a hollow and dull echo that is lower in pitch as a result of the void or discontinuity between the slab and the delaminated cover. Delaminations are easily located and marked using this technique, but it is much less effective on bridge decks that are overlaid with an asphalt pavement. The pavement tends to have an insulating effect on the transmission of the sound energy to the concrete and back to the surface, reducing the volume and distorting

the reflected sounds. The chain drag method is subject to operator opinion and therefore may not detect all of the delaminated areas. Sometimes, the sound produced by the chain on the deck can make the presence of delaminations questionable. For example, some delaminations produce weak alterations to the sound of the chain that may not be perceived by the operator. Conversely, some slight changes to the sound of the chain on the deck may be perceived by the operator to be a delamination when it is in fact caused by another source. This can be caused by partially debonded pieces of asphalt pavement or membrane that were not removed from the deck surface. With prolonged use over an hour, the operator can tend to become tone-insensitive and may miss audible delamination tones. This problem is aggravated by the traffic noise since traffic flow is not usually discontinued over the entire deck during the survey. Areas that are actively corroding, but have not yet induced sufficient tensile stress in the deck to cause cracking or delamination will not be detected using the chain drag method. Also, areas that have delaminated but in which the crack has been filled with solid corrosion products may not be detectable using the chain drag method. Furthermore, the quantities and locations designated for repair are often determined by visual observation as well as the chain drag method. Surface scaling, embedded objects such as wood and other debris, and severe damage by freezing and thawing action are usually included. Surface macro-texture, reinforcement cover, the size of the chain links used, and operator opinion have an effect on the areas and quantities chosen for repair by using the chain drag method.

In a discussion in the Concrete Repair Digest (1996), three experts were questioned regarding the effectiveness of the chain drag for locating delaminated concrete. It was generally agreed that the chain drag is very effective in locating delaminations, but is limited in depth on an exposed deck from 1 to 3 inches, depending on the size of chain link used. Two of the experts described the accuracy of the chain drag to be within ten and twenty percent of the total delaminated area.

Regardless of the potential for errors, the chain drag method has been the most effective means of quantifying the location and extent of delamination on exposed reinforced concrete bridge decks. The chain drag is the primary method by which the Nova Scotia Department of Transportation and Public Works establishes the removal areas on bridge decks that have been prepared for repair.

Standard test methods for condition assessment of reinforced concrete bridge decks have been the chain drag and half-cell potential survey, precluded usually by a visual survey of the deck. Basically, a visual assessment of the deck underside, which may or may not have included the application of a hammer to the deck underside for detecting delamination in accessible areas, has been the basis of quantity estimates for tendering rehabilitation work. The chain drag and half-cell potential surveys are not practical tools for deterioration estimation prior to the removal of the asphalt pavement from the deck surface. The pavement acts as an insulator to both the half-cell electrode for detecting corrosion currents and to the propagation of sound energy to the underlying concrete and back to the operator's ear. Results obtained by using these methods on decks from which the asphalt pavement has not been removed can be unreliable.

Considering the application of the standard condition assessment methods with respect to the method criteria outlined in Section 1.2, their unsuitability for estimating repair quantities for tender preparation becomes quickly apparent. The success of these methods would require the removal of the asphalt pavement, thus failing to meet the primary criterion of non-destructive testing of bridge decks. Furthermore, removing the asphalt pavement and conducting the surveys requires traffic control and fails to meet the second criterion of non-interference with normal traffic flow. The necessity of asphalt removal for their application to the deck surface fails to meet the third criterion. While the half-cell potential survey is subjective, with minimal operator influence, the chain drag method is not, requiring the operator to decide what is delaminated and what is not. Both methods are simple to use and are cost effective, but the costs associated with

asphalt removal and traffic control are too high to make the use of these standard test methods appropriate for estimating removal quantities for tender preparation. After disqualifying the chain drag and half-cell potential surveys from the list of potential standard test methods for estimating repair quantities, what remains is the current practice of visual examination of the decks.

2.2.2 Ultrasonic Test Methods

Ultrasonic Testing (UT) or ultrasonic pulse velocity measurements have been used world-wide as a non-destructive test for concrete quality. Akroyd and Jones (1963) demonstrated that while there was no unique relationship between pulse velocity and concrete strength, useful empirical relationships could be formulated for predicting concrete strength within $\pm 15\%$ when the composition and curing conditions were carefully controlled. These relationships are based on the assumption that changes in the pulse velocity, or the elastic dynamic modulus, is related to changes in strength properties of the concrete.

Ultrasonic transducers are chosen depending on the path length under scrutiny, or the condition that is sought after, in the concrete specimen. A limiting factor is the degree of signal attenuation and scattering effects due to aggregate size on the concrete. Transducers are usually coupled to the concrete surface using a liquid or grease, then a pulse is transmitted through the specimen. The time required for the pulse to travel from one transducer to the other is recorded along with the peak magnitudes. Pulse velocity is determined based on the travel time between transducers and the measured path distance between transducers, the latter of which may be difficult to accurately measure for slabs and walls where access to the concrete for both transducers may not be available.

Rösch et al. (1995) described how longitudinal, or through-transmission, pulse velocity measurements might be used to locate defects in concrete columns. Low quality

concrete was identified by correlating pulse velocity with the compressive strength of concrete cores drilled from the columns. Pulse velocity measurements were recorded over a grid system established on the columns and three-dimensional modeling was used to produce a simple-to-read diagram of the interior showing areas of low pulse velocity. Areas of poor compaction were associated with slower pulse velocity measurements. These were revealed by increasing the velocity thresholds established for delineating grades of concrete quality. The necessity of a large number of data points and an understanding of the margin of error involved was recommended for reliability and in better locating areas in need of repair.

Wollbold and Neisecke (1995) reported on their continuing development of a single transducer ultrasonic method which incorporated a pulse-echo technique for evaluating concrete structures from one side only, instead of the two-sided transmission technique. Data was presented in B-scan (amplitude intensity changes over time over distance) format in real time to detect defect or backwall reflections, receiving information on the intensity and phase of the signal and their relative changes as the transducer is moved along the concrete surface. Thickness measurements required a separate means of measuring pulse velocity by a transmission method.

Ultrasonic pulse echo has been used to detect and locate air gaps, or cracks and other flaws on concrete structures by identifying shorter pulse time-of-flight from the surface to the defect than is usual for the time-of-flight from the surface to the backwall. Transmission methods detect defects by the attenuation or even the absence of a reflection of the transmitted signal, or by a decrease in pulse velocity.

In terms of the method criteria outlined in Section 1.2, ultrasonic methods can be used to provide non-destructive condition assessment to the slab and other components of reinforced concrete bridge decks, but does not appear viable for detecting deterioration beneath asphalt overlays on the deck. Measurements are objective, but require some

technical expertise in the identification of reflections, understanding internal reflections within concrete members, and in determining the pulse velocity, particularly in the case of deck slabs, where transmission measurements are not possible. The primary reasons for not selecting ultrasonic methods are the time and number of stationary measurements required to survey a complete deck and the necessary interruption of traffic flow and possible removal of the asphalt overlay.

2.2.3 Impact Echo

The Impact Echo (IE) method was developed by Dr. Mary Sansalone and Dr. Nicholas Carino, of Cornell University, from ongoing research that began in 1983. Sansalone and Streett (1995) report using the impact echo method to locate and determine the extent of cracks, voids, delaminations, honeycombing, and debonding in concrete structures. While the point of interest of the impact echo method in the research described within this thesis is dedicated only to reinforced concrete bridge decks, it is also used to evaluate other concrete structures such as pavements, floor slabs, walls, beams, columns, and hollow cylinders like tunnel linings.

The impact echo technique is similar to ultrasonic methods in that the propagation of stress waves is considered in evaluating structures. These waves are generated by a short duration mechanical impact on the specimen produced by striking the surface with a small steel sphere attached to a spring-rod handle. Sphere size is varied, depending on the thickness and material being considered, to produce impacts of different duration to achieve the desired resolution. The impact produces low frequency dilatational (P) and distortional (S) waves that propagate into the specimen and are reflected by internal flaws and external surfaces. Also produced are Rayleigh (R) waves that propagate along the surface of the specimen. Of these three wave types, P-waves are usually considered for analysis purposes since they tend to have the greatest amplitude in the area near the impact. The P-wave reflections from flaws or external surfaces return to the impacted

surface where they are reflected back into the specimen again by the free surface. In this manner, the reflections establish a periodic return to the impacted surface from which layer thicknesses can be measured if the wave speed is known. Displacements caused by the waves arriving at the impacted surface are recorded by a broadband piezoelectric transducer. The signal from the transducer is recorded using a high-speed data acquisition card and a computer. A waveform of amplitude versus time is produced from the data. This waveform is then transformed using a Fast Fourier Transform (FFT) into the frequency domain for analysis. Dominant frequencies arise in the data from multiple reflections between the impact surface and flaws or other external surfaces. Each type of structure exhibits a characteristic frequency response based on its geometry. These resonant frequencies are used to locate flaws according to deviations from the characteristic frequency response. Since the travel time between the surface and an internal flaw must be less than the travel time between the surface and the opposing external surface, flaws appear as dominant resonant frequencies that are higher than the characteristic resonant frequency. In the case of delamination, an additional resonant frequency occurs as the debonded plate vibrates about its longitudinal and transverse axes. This vibration tends to be at much lower frequencies than the characteristic frequency of a sound specimen. Poston and Sansalone (1997) described several cases where the impact echo method was used to detect and establish the extent of cracking in beams and columns based on changes in frequency response and pulse velocity measurements. Sansalone and Carino (1989) reported on the use of the impact-echo method to detect delaminations in a bridge deck through an asphalt overlay. Delaminations were detected in two different asphalt overlaid slabs without prior knowledge of their location. The steel sphere impactor required slight modification by adding a thin steel plate to the sphere so that the impact time would not be increased by the sphere directly contacting the relatively softer asphalt concrete.

Accurate depth measurements are dependent on the speed of the data acquisition, which affects the frequency resolution of the data. Also, the P-wave speed must be

measured accurately. This has historically required direct through-transmission wave speed measurement on a section of the structures that was accessible from both sides. Lin and Sansalone (1997) developed a means of closely estimating the P-wave speed based on the travel time of the Rayleigh wave between two transducers spaced at a known distance. This provides a simple means to determine the P-wave speed on any smooth surface since access is only required from one side.

Impact echo methods have a benefit over conventional ultrasonic methods in that the transducers do not require grease as a couplant to the specimen surface. Instead, a thin sheet of lead is used to provide adequate coupling. Impactors are chosen to provide the contact duration and frequency such that the highest frequencies that are anticipated in the data are contained within the impact pulse, making this test distinct from other ultrasonic methods.

Impact echo testing has been shown to provide accurate and reliable results for detecting delaminations, cracks, and for measuring thicknesses. Structural elements that may cause significant scattering of the waves, such as dense reinforcement or irregular geometry, may reduce the accuracy. The greatest drawbacks to the method are the necessity of contact to the test surface, which may create obstacles in the development of a procedure to test slabs at highway speeds. The reported procedures have involved hand placement of the transducers, sampling on a grid system over a surface, with additional sample points taken when necessary at suspect locations. Software have been developed to process the raw data into a frequency domain format, but still require operator analysis for proper interpretation. A significant amount of time would be required to process the excessive quantity of data that would be generated by a dense survey grid on a typical bridge deck. While the method is simple, purely non-destructive and has been conducted with accurate and reproducible results through asphalt overlays, the amount of time required for testing necessitates lane closure and traffic control. Interference with normal traffic flows and the resulting reduction in cost-effectiveness of this procedure are two

restraints that make network level bridge deck condition assessments using this procedure unattractive, in spite of its excellent reported results as a method of direct delamination measurement.

2.2.4 Infrared Thermography

The technique of Infrared thermography (IR) for detecting delaminations is based on principles of heat transfer. The presence, or lack of, solar heat applied to the deck creates daily cyclical fluctuations in temperature profiles throughout the thickness of the deck. Well-bonded materials transfer heat relatively uniformly, delaminations introduce discontinuities in the heat flow. These discontinuities act to insulate underlying materials, producing localized changes in the heat flow gradient. Infrared cameras are used to scan the bridge deck surface area to detect these anomalous heat gradients, signaling discontinuities that are interpreted as delaminations.

Data is usually collected using an infra-red video camera mounted to a vehicle which is driven over the deck surface. Normal video footage is usually co-recorded with the infrared data to identify cracks, potholes, oil stains, and other surface features which will affect the data interpretation. In the literature encountered during this research, data was collected at slow speeds, not at speeds that would prevent interference with normal traffic flows. Typically, data was collected from deck surfaces that were enclosed within a barrier system so that the deck was open exclusively to the test vehicle.

Manning and Masliwec (1990) report that delaminations can be distinguished from areas of concrete surface scaling by observing a grey-scale intensity plot of the data. Delaminations occur as well defined white spots (hotter areas), compared to the cooler and hence darker areas of surrounding sound deck, while scaling appears as a mottled grey-white tone, with increased mottling occurring as the degree of scaling worsens. Debonding of the asphalt pavement, on the other hand, is less distinguishable, often

appearing as anomalies in the data with the same or greater intensity as delaminations and can sometimes be completely unnoticed.

According to Maser (1989) results from infra-red delamination surveys have been found to be inconclusive, with physical and environmental factors affecting the outcome of the survey. Positive detection results have generally been found to correlate well with existing delaminations, but negative detection results do not necessarily indicate that the deck is in sound condition. Negative detection results may only indicate that conditions at the time of testing were insufficient for detecting some of the deterioration. The presence and thickness of an asphalt pavement overlying the deck affects the magnitude of the thermal anomaly that can be measured, with thicker pavements retarding the rate of heat change at their surface that would indicate a delaminated area. Furthermore, debonded asphalt pavements may introduce thermal discontinuities into the deck system. Surface texture, differential wear, and cracking of the pavement surface also have an effect on the anomalous temperature gradients. The depth of cover and crack opening width of the delamination affects the magnitude of the anomaly as well as the crack contents. Delaminations that are filled with water or corrosion product may not induce thermal anomalies on the deck surface that are measureable. Aside from deck characteristics, infrared thermography is sensitive to availability of sunshine, cloud cover, wind speed, moisture, season, time of day, and stationary shadows. Typically, clear, calm and sunny days are required to adequately detect the presence of delaminations, taking advantage of higher rates of heat absorption of the deck. Water present on the deck surface interferes with the consistency of the data quality.

Manning and Masliwec (1990) state that infrared surveys can generally be conducted successfully except during the hours near sunrise and sunset, where the rate of thermal change approaches zero as the deck goes from a cooling state to a heating state or vice versa. Data collection should be contained to sunny days with ten percent cloud cover or less, since passing clouds can change the grey scale of a portion of the complete

deck data set. Water contained in the delaminations, or in the asphalt pavement, the transfer of heat into the deck becomes affected and deterioration in those areas will not be detected. At pavement thicknesses greater than 75mm, deck deterioration prediction becomes less certain due to the thermal inertia of the thick pavement layer.

Infrared thermography has been shown to be a useful technique in detecting deck deterioration, but inconsistent and inconclusive results that are dependant on the ambient weather conditions make it an undesirable method with respect to the criteria established in Section 1.2 of this thesis. This non-destructive technique meets all method criteria outlined in Section 1.2, except for the reproducibility of the data, accuracy, and the subjectivity of the data interpretation.

2.2.5 Ground Penetrating Radar

Ground Penetrating Radar (GPR) is a nondestructive method of locating and identifying subsurface layers of engineering materials such as soil, rock, and concrete. Information about these layers is gathered by the transmission of high radio frequency (RF) energy into the material and recording the strength of the reflected energy over time. Alongi et al. (1982) reported that GPR developed as a nondestructive method of evaluating bridge decks and pavements from its early applications in detecting buried non-metallic landmines for the United States army in the mid 1960's. Bridge deck assessment followed after the development of GPR technology for determining pavement layer thicknesses and for void detection. Other applications have included reinforcement and metallic duct detection in slabs, detection of excessive moisture in pavements and under slabs on grade, moist rotten areas in timber poles, hydrocarbons in groundwater, and GPR has even been used in forensic science for detecting disturbed soils. Efforts in GPR research have since focussed upon equipment reliability, experience, and automation of the signal processing techniques. Today, GPR technology has advanced to the state of high resolution data collection at maximum

highway speeds of approximately 80 km/hr and partially automated signal analysis for detecting delaminations and measuring layer thicknesses, making it more economically feasible for evaluation of infrastructure on a network level. New efforts are underway to develop the use of multiple antennae for synthetic aperture analysis where data is observed at different locations near a point to produce a three dimensional prediction of the properties of that point.

GPR has been relatively newly established as a bridge investigation tool compared to other conventional and well-accepted techniques, but positive results have been reported by various authors. Its ability to access the deck slab through asphalt pavement layers and in normal traffic flows make this method highly attractive. Commercial systems are available which offer automatic processing software to analyze the data with minimal user input, enabling a more objective result. The use and background theory behind GPR in bridge and highway investigations is discussed more in-depth in the following section.

2.3 Selected Test Method

Ground Penetrating Radar (GPR) best fit the method criteria established in Section 1.2 of this thesis as shown in Table 1. All methods that were examined offer non-destructive testing capability, but not all of them meet the strictest criteria of non-interference with normal traffic flow and effectiveness through asphalt pavement layers. Other test methods meet some of the criteria, but only infra-red thermography and GPR have the capability to collect test data at highway speeds. Of these two methods, only GPR offers software that minimizes user input, simplifying data processing and increasing objectivity in the results. GPR was selected as the most appropriate potential test method for condition assessment of bridge decks in Nova Scotia because of its non-destructive capability to provide accurate results through asphalt pavement layers and non-interference with normal traffic flows. These qualities enable insight to the

condition of the deck before the decision to repair the bridge has actually been made. Furthermore, the automatic processing software permits simple user input in data processing to yield objective results.

Table 1 - Comparison of test methods to selection criteria

	Standard*	UT	IE	IR	GPR
Non-destructive
Does not interfere with normal traffic flow				.	.
Works through asphalt overlays			.	.	.
Reproducible data
Objective with minimal operator influence		.	.		.
Simple to use	.				.

* Half-cell potential and chain drag surveys.

With the identification of the appropriate technology, the Nova Scotia Department of Transportation and Communications was approached by Dalhousie University DalTech with a proposal to lend financial assistance to a five-year term research project in which the use of GPR as a predictive tool for estimating bridge deck deterioration would be undertaken. The GPR system produced by the Penetradar Corporation was selected because of the strong support it had received from the US Federal Highways Administration, Ontario Ministry of Transportation, and many of the above mentioned departments. The five-year research project was approved by the Nova Scotia Department of Transportation and Public Works and the Penetradar Integrated Radar Inspection System (IRIS) shown in Figure 6, was purchased in the summer of 1996.



Figure 6 - Van equipped with Penetradar PS-24 Integrated Radar Inspection System

Further credence was given to the selection of GPR as the most appropriate technology for bridge deck assessment by the SHRP S-325 report describing the application and expected accuracy of the Penetradar PS-24 GPR antenna system. A draft of a standard method for deck assessment was also included in the report that used GPR for detecting delaminated regions of a bridge deck. Furthermore, the use of GPR by many different transportation agencies such as the Ontario Ministry of Transportation and many State departments including New York, Ohio, Texas, Pennsylvania, and West Virginia, lent further credibility to the technology.

3. Ground Penetrating Radar for Bridge Deck Assessment

The following subsections will provide a description of the testing equipment, the theory behind radar energy propagation and reflection from layers, and a discussion of the history and research of the application of GPR to layer thickness measurement and bridge deck condition assessment.

3.1 Hardware and Equipment Setup

The model PS-24 Penetradar system, used in this research program, is a low power solid state ground penetrating radar designed for non-contact inspection and a high data collection rate. The antenna is a monostatic, ultra directive, and ultra broadband air-coupled horn type. The system uses a monocycle transmitter that emits a phase coherent pulse at a very high pulse repetition frequency that allows for a high signal to noise ratio that is required for ground penetrating applications. The IRIS system that incorporates the PS-24 can accommodate and allow for up to three simultaneous radars to be used at one time. A 100 Hz linear range scan provides continuous ground coverage at vehicle speeds up to 80 km/hr. Each transmitted pulse has a period of approximately one nanosecond, equal to the inverse of the center frequency of one GHz, and over one million pulses are generated transmitted every second. The radar hardware, shown in Figure 7, is integrated as a system inside a Ford E250 cargo van and manipulates a signal emitted from the distance measuring instrument of the ABS braking system into the data for spatial alignment of the data to the deck surface.

A workstation is contained within the van for personnel to collect and process GPR data. The workstation includes a rack-mounted computer, monitor, power inverter, radar battery pack, master control unit, and distance measuring device control. The power inverter draws electrical charge from the heavy-duty alternator installed in the

cargo van and is also used to charge 2 large wet-cell batteries located in the rear storage area of the van. These two batteries are used to power the equipment if the van is not running and also for charging the radar battery pack. The radar battery pack provides a short-term supply of relatively constant voltage to the radar control unit, enabling constant transmitted signal power. Since the inception of this research project the battery pack has been replaced with a circuit supplying constant power to the radar control unit. This eliminated the need to recharge the battery pack and tends to produce output of a more uniform amplitude. The master control unit controls the timing and shape of the transmitted signal, signaling the transmitter/receiver unit which is located on the exterior hardware that is installed on the antenna configuration on the front of the van. The distance measuring device control receives electronic pulses from the ABS braking system and has them recorded along with the radar data for distance measurement.



Figure 7 - GPR control hardware contained inside research vehicle.

Exterior hardware includes the transmitter/receiver unit, antenna, and antenna support structure. This assembly is shown in Figure 8 below.

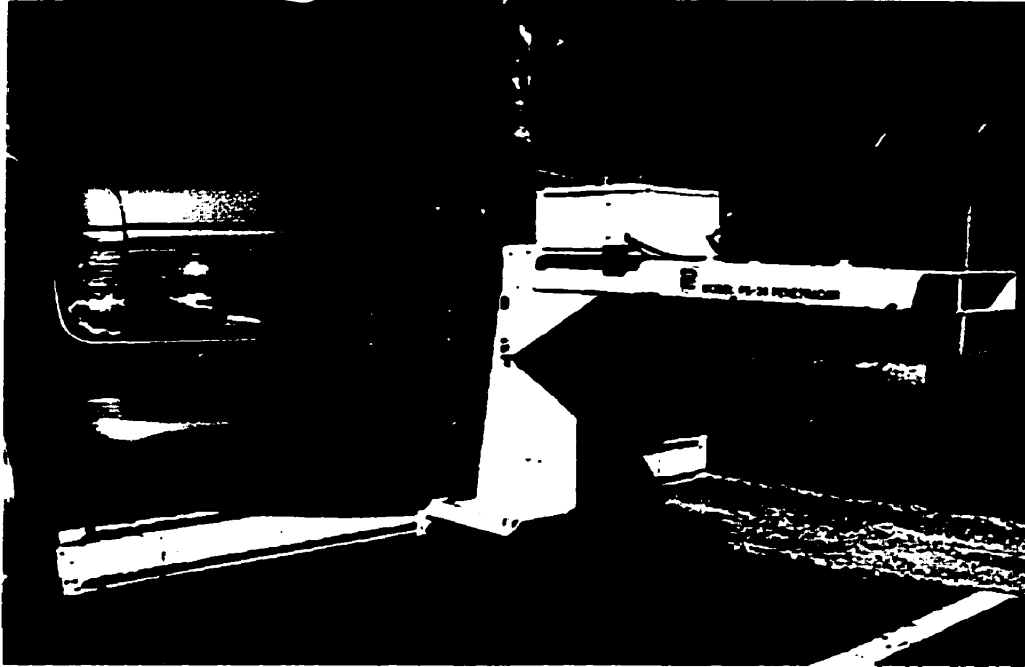


Figure 8 - Exterior antenna assembly on front of van

A steel beam was designed and welded to the frame of the van underneath the front bumper. This beam allows the antenna support structure to be moved to any location across the width of the van for data collection. This ability to shift the position of the radar antenna allows the van to remain in normal traffic lanes to collect data, instead of straddling adjacent lanes. The antenna support structure is bolted into place on the support frame. This support structure is composed of a “post” with two steel Uni-strut channels on either side in which the “arm” can be bolted into place using Uni-strut lock-nuts. This configuration allows the user to choose the vertical air-gap distance between the antenna and the targeted surface. Fixed in place on the arm is the transmitter/receiver unit which sends the transmitted signal to the antenna and receives the reflected signal. This unit is controlled by the master control unit located inside the van. These two devices are connected by the main radar cable which screws into the rear of the transmitter/receiver unit and into a connection port located just above the bumper on the front passenger side of the van. The antenna is connected to the arm using a fixed

bracket on its side and two large plastic bolts that fit into holes located on the end of the arm. The transmitter/receiver unit is connected to the arm by the antenna feed cable that is a semi-rigid coaxial cable. Both of these cables are fragile and care must be taken not to bend them. A single antenna assembly was used in this research to collect the data one pass at a time, along the length of the deck in the direction of traffic flow. The Penetradar IRIS has the capability of acquiring data using 3 to 4 antennae, reducing the number of traverses required along the deck length.

3.2 GPR Background Theory

Beginning with some fundamental concepts of GPR electromagnetic theory, an examination is presented of how the transmitted pulse is affected by the targeted layer systems and how the data may be used to extract information about these layers.

3.2.1 Fundamental Concepts

From an electromagnetic standpoint, a material can be metallic or dielectric in nature, though the transition from metallic to dielectric is gradual, with many materials exhibiting properties of both. Metallic substances have high electrical conductivity and attenuate electromagnetic waves to a high extent, resulting in low penetration depth. Dielectric materials have low electrical conductivity, referred to as insulators, and therefore attenuate electromagnetic waves to a lesser extent. The phase velocity through a material is dependant upon its relative dielectric constant, or relative permittivity, ϵ_r . The dielectric constant of a particular material is referred to as being relative since it is equal to the ratio of the dielectric permittivity of the material, ϵ , to the fundamentally constant dielectric permittivity of free-space, $\epsilon_0 = 8.854 \cdot 10^{-12}$ F/m.

$$\epsilon_r = \epsilon / \epsilon_0 \quad [2]$$

Material permittivity is actually a complex number, $\epsilon = \epsilon' - j\epsilon''$ composed of a real portion, ϵ' , associated with charge storage potential, and an imaginary part, ϵ'' , associated with the conductivity or attenuation of electromagnetic waves in the medium, which is also referred to as the loss factor by Halabe et al. (1993) and by Loulizi and Al-Qadi (1997). In low loss materials, the imaginary part of the material permittivity is often neglected, leading to Equation 2 above.

The propagation velocity of the transmitted RF energy wavefront through a particular material is given by Equation 3 as:

$$v = \frac{c}{\sqrt{\epsilon_r m_r}} \quad [3]$$

where c is the speed of light in free space, $c = 0.3 \cdot 10^9$ m/s and m_r is the relative magnetic permeability of the material. For low loss materials, m_r is usually taken to be unity and the phase velocity of the transmitted energy through a dielectric medium generally reduces to Equation 4:

$$v = \frac{c}{\sqrt{\epsilon_r}} \quad [4]$$

If the signal meets a boundary between two materials that have dissimilar relative dielectric constants, the energy is partially reflected and received again. The amount of energy reflected and transmitted are given by the reflection and transmission coefficients, respectively. These coefficients are dependant on the relative impedance of the two materials at the interface, z_{r1} and z_{r2} , respectively. For low loss dielectrics, the impedance is given in Equation 5:

$$z_r = \sqrt{\frac{m_0}{\epsilon_0 \epsilon_r}} \quad [5]$$

where $m_0 = 4\pi \cdot 10^{-7}$ Henry/meter is the magnetic permeability of free space.

The voltage reflection and voltage transmission coefficients are given by Bungey and Millard (1993) as Equations 6 and 7, respectively:

$$R = \frac{z_{r2} - z_{r1}}{z_{r2} + z_{r1}} = \frac{\sqrt{\epsilon_{r1}} - \sqrt{\epsilon_{r2}}}{\sqrt{\epsilon_{r1}} + \sqrt{\epsilon_{r2}}} \quad [6]$$

$$T = \frac{2z_{r2}}{z_{r1} + z_{r2}} = \frac{2\sqrt{\epsilon_{r1}}}{\sqrt{\epsilon_{r2}} + \sqrt{\epsilon_{r1}}} = 1 - R \quad [7]$$

These coefficients describe the fractions of the incident voltage, and the root of the incident power, to an interface that are reflected and transmitted, respectively. Most of the remaining transmitted energy continues to penetrate past the interface, while a small fraction is lost to spherical losses due to antenna displacement, scattering losses due to roughness of the interface and nonhomogenous layers, and attenuation of the signal by the layer itself. These losses cannot be measured through a particular layer but have been predicted using mathematical models (Bungey and Millard, 1993). Attenuation, α , is a function of the frequency of the transmitted energy, the relative dielectric constant of the medium, and the loss tangent or dissipation factor, δ , which is the ratio of the real to imaginary parts of the medium permittivity, as shown in Eq. 8.

$$\alpha = 12.863 \cdot 10^{-8} f \sqrt{\epsilon_r} \left[\sqrt{(1 + \tan^2 \delta)} - 1 \right]^{1/2} \text{ (dB)} \quad [8]$$

This is simplified to Equation 9 for practical purposes since conductivity is the dominant material property affecting attenuation irregardless of frequency. σ_{dc} is the direct current or ohmic conductivity of the material.

$$\alpha = \frac{1.69 * 10^3 \sigma_{dc}}{\sqrt{\epsilon_r}} \quad [9]$$

It should be noted here that if the electromagnetic wavefront is reflected from an interface of two materials in which the underlying material has a higher relative dielectric constant than the overlying material, then there will be a reversal of polarity in the reflected wave. As the remaining transmitted energy meets successive material interfaces, additional reflections are sent back to the receiver and are recorded over time. In this way, the time required for the energy to travel from the transmitter to each interface and back is recorded with the magnitude of the reflected energy from each interface peak in what is referred to as the radar waveform. Each waveform is composed of the recorded reflections of the initial transmitted signal over time. Each waveform is constructed of eight hundred voltage sample points over a timespan of twenty nanoseconds. Measurements of time and peak amplitudes from the waveform form the basis upon which GPR is used for measuring layer thickness and for more complex predictions of material deterioration such as concrete delaminations and scaling. A typical transmitted signal is shown in Figure 9.

Attenuation plays an important role in determining the penetration depth of the signal into a given medium. Materials that are more conductive will attenuate the energy at a faster rate, reducing the penetration depth. Also affecting penetration depth is the center frequency of the antenna with higher frequencies attenuating faster than lower frequencies. There is a trade-off with penetration depth for depth resolution. Higher frequency antennae produce shorter transmitted pulsewidths. Shorter pulsewidths allow

for measurement of thinner layers, but attenuate more rapidly than longer pulsewidths which have a greater penetration depth, but lower thickness resolution.

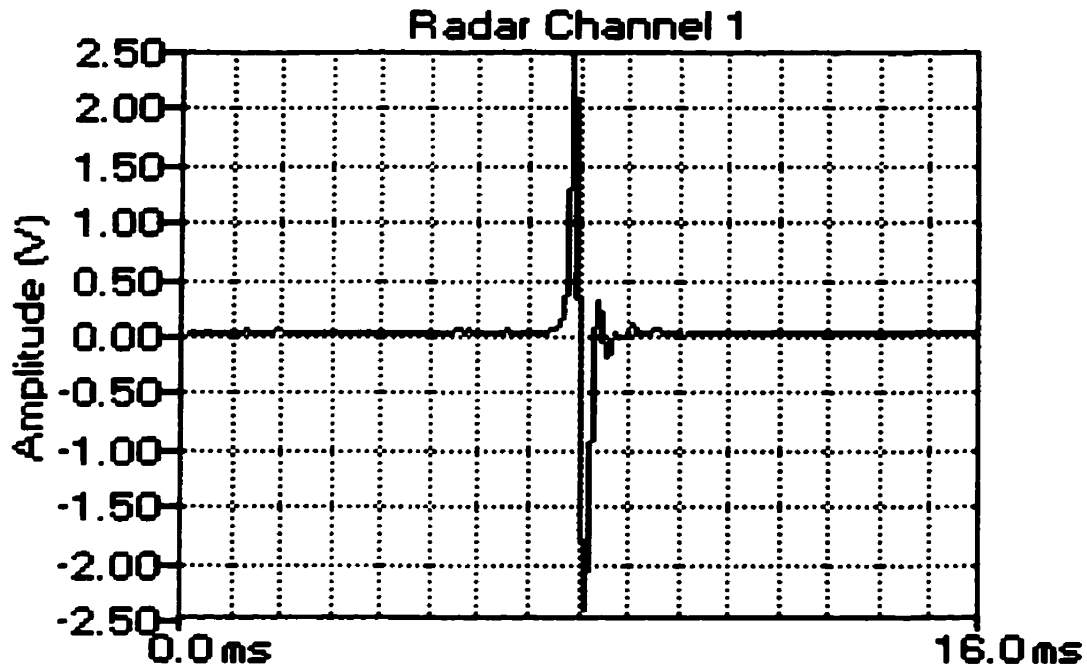


Figure 9 -Typical transmitted radar impulse signal

3.2.2 Interpretation of Layer Characteristics

For the purpose of describing how measurements from the radar waveform are used to extract useful information about the layers, a typical asphalt paved reinforced concrete bridge deck will be used as a target layer system.

An asphalt paved reinforced concrete bridge deck can be considered simply as four dielectric layers. There are the asphalt and concrete layers adjacent to each other and which are bounded above and below by layers of air. Due to dielectric dissimilarities between these layers, energy reflections and transmissions will occur at their interfaces.

Steel reinforcement within the deck does not reflect energy in the same manner as the horizontal and plane interfaces of the air, asphalt, and concrete layers. The reinforcement is metallic and therefore is extremely conductive and reflective of the transmitted energy. The reinforcement is usually arranged into two grids, located near the top and bottom of the concrete slab. The grid is normally composed of longitudinal and transverse bars, used to develop flexural and shear resistance as well as in the control of shrinkage and cracking in the slab. Since the steel occurs as a mat with bar spacing much in excess of the bar diameter, only a portion of the energy transmitted to the level of the mat is reflected. With the radar beam directed orthogonally to the deck, transverse bars have little effect on the reflected signal due to orthogonal polarization, while longitudinal bars have a much greater effect due to parallel polarization. In bridge decks having very closely spaced reinforcement, the reinforcement layer acts more as a plate than a mat, reflecting more energy. When bar spacing is one half of the effective wavelength in the concrete deck the reinforcement layer reflects all of the incident energy. Equation 10 describes the power reflection coefficient, or the square of the voltage transmission coefficient, R , of the layer of reinforcement modeled as an equivalent parallel, or longitudinal mat as reported by Bechtel and Alongi (1976):

$$R = \left[1 + 4(\cos a)^{0.5} \left[d/l \left[\ln \left(\frac{d}{\pi D_1} \right) + F_c \right] \right]^2 \right]^{-1} \quad [10]$$

where: a = angle of incidence, assumed to be zero.

d = longitudinal bar spacing

l = wavelength of the radar wave

D_1 = diameter of the longitudinal reinforcement

F_c = correction factor related to conductor spacing, approximately zero for small spacing.

Figure 10 shows a simple ray diagram depicting the incident and reflected energy portions of the original transmitted beam from the antenna. By accounting for the transmission and reflection of energy from each interface in the system, we can formulate equations to model the expected response in the recorded radar waveform.

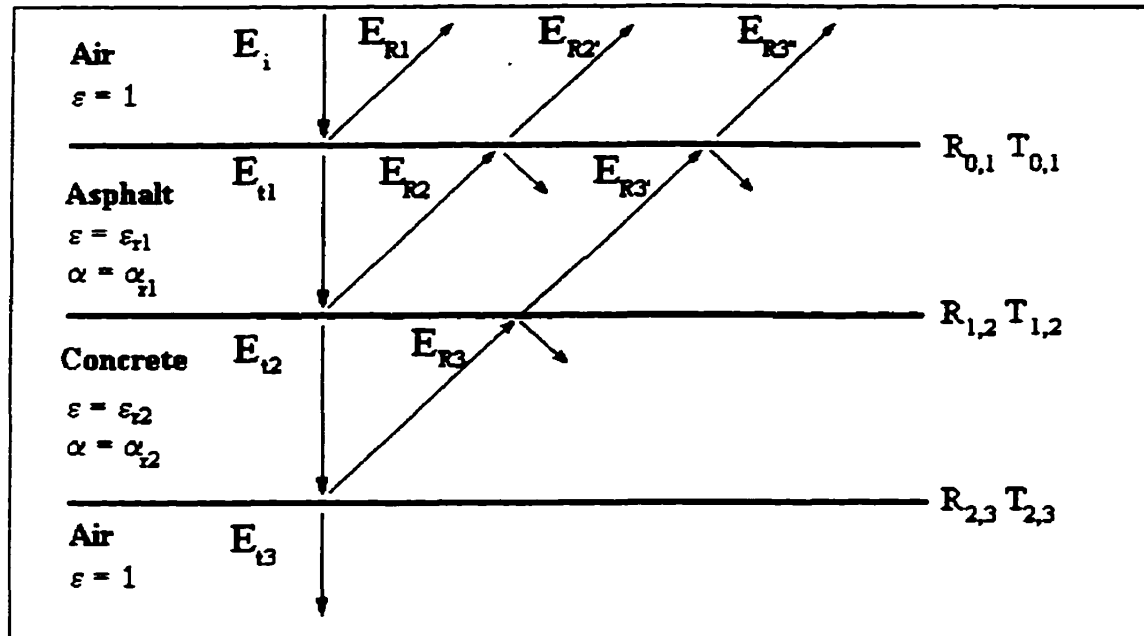


Figure 10 - Ray diagram of energy reflection and transmission from a bridge deck

From Figure 10 it may be observed that there are three reflections which are received by the antenna: the surface reflection from the air/asphalt interface, the reflection from the asphalt/concrete interface and the reflection from the concrete/air interface. The magnitude of the energy reflected from the air/asphalt interface is the product of the voltage reflection coefficient and the incident voltage, E_i , which is the root of the incident power, P_i .

$$E_{R1} = E_i (R_{0,1}) \quad [11]$$

The portion of the energy that is transmitted past the interface is determined by $T_{0,1} = 1 - R_{0,1}$. This energy travels through the asphalt layer and experiences attenuation α_1 before meeting the asphalt/concrete interface. At this interface, the signal is again partially reflected according to the reflection coefficient $R_{1,2}$, and partially transmitted according to the transmission coefficient $T_{1,2}$. The reflected portion is redirected back towards the air/asphalt interface where it is again partially reflected and transmitted according to $R_{0,1}$ and $T_{0,1}$ as before. The resultant magnitude of the peak in the waveform is therefore given by Equation 12 as follows:

$$E_{R2'} = E_i (R_{1,2}) [(T_{0,1}) (\alpha_1)]^2 \quad [12]$$

Using a similar analysis, the resultant peak in the waveform due to the concrete/air interface at the deck bottom is given by Equation 13. Note that there is a change in phase of the peak since the relative dielectric of concrete is higher than that of air.

$$E_{R3'} = E_i (R_{2,3}) [(T_{0,1}) (\alpha_1) (T_{1,2}) (\alpha_2)]^2 \quad [13]$$

Figure 11 shows a waveform recorded from an actual bridge deck. The waveform is the recorded voltage, or signal strength, of the reflected signal versus time. The expected peaks of the air/asphalt, asphalt/concrete, and concrete/air interfaces can be seen within the waveform along with positively oriented peaks corresponding to the upper and lower layers of steel reinforcement. The two initial peaks arriving prior to the four nanosecond location are internal reflections of the antenna and GPR hardware.

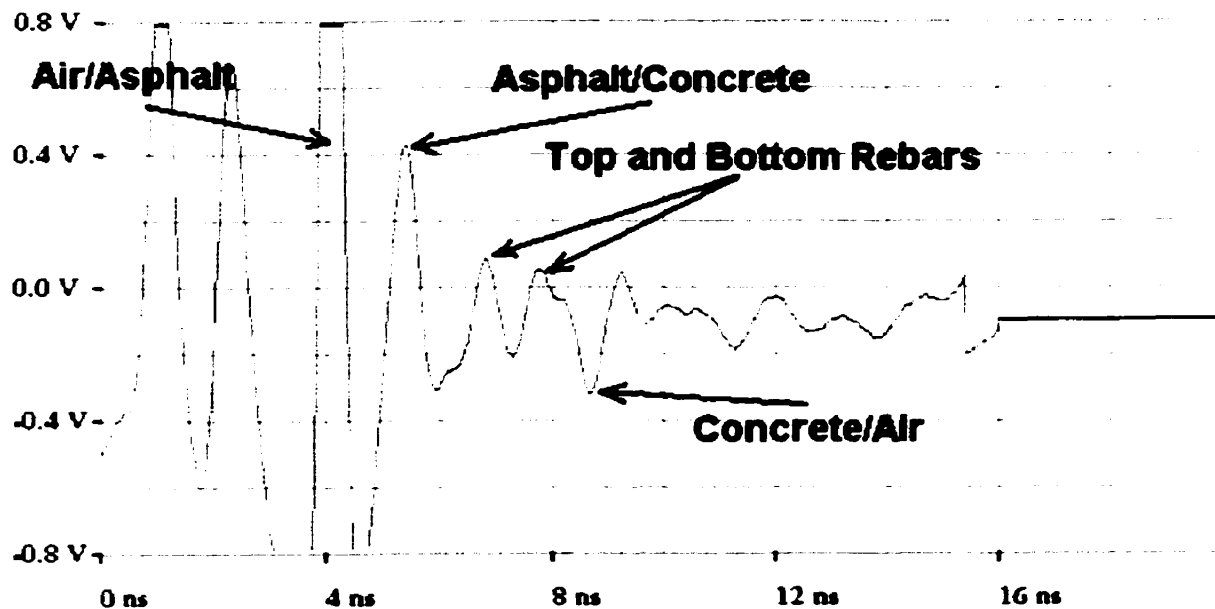


Figure 11 - GPR waveform recorded from typical asphalt paved bridge deck

3.2.3 Measurement of Layer Thicknesses

Since the reflection and transmission coefficients of the radar signal can be expressed in terms of the relative dielectric constants of the layers bounding an interface, the relative dielectric constant of the underlying layer with respect to the relative dielectric constant of the overlying layer is measured using the amplitudes of the reflected peaks in the waveform. Using the amplitude of the reflection from the initial air/asphalt interface, E_r , the relative dielectric constant of the asphalt pavement layer can be computed as shown in Equation 3, if the energy incident to the interface and the relative dielectric constant of the air layer are known. The voltage reflection coefficient is exactly the ratio describing the fraction of the incident energy that is reflected from the interface, or exactly E_r/E_i . This ratio is equated to Equation 6 to yield Equation 14 below.

$$\epsilon_m = \left[\frac{(E_i - E_r)\sqrt{\epsilon_{m-1}}}{E_r + E_i} \right]^2 \quad [14]$$

The propagation time through the asphalt is the time required for the electromagnetic wavefront to pass by the air/asphalt interface, reflect off the asphalt/concrete interface and meet the air/asphalt interface again. This occurs in the data as the time separation between peaks from interfaces bounding a given layer. For the asphalt concrete layer in the simplistic bridge deck model being considered, this is the time difference between the air/asphalt interface peak and the asphalt/concrete interface peak. Knowing that thickness is the product of the phase velocity and the time travelled through a layer, we measure the propagation time, τ , between the $(n-1)^{\text{th}}$ and n^{th} interfaces, the incident and reflected voltages on the $(n-1)^{\text{th}}$ interface, and the relative dielectric constant of the $(n-1)^{\text{th}}$ material, to calculate the thickness of the n^{th} layer by combining Equation 4 and Equation 14 as follows:

$$x_n = \frac{c\tau(E_r + E_i)}{2(E_i - E_r)\sqrt{\epsilon_{m-1}}} \quad [15]$$

This is further simplified to Equation 16 for practical purposes by applying the known value for the speed of light in free space and substituting in the value for the relative dielectric constant of the layer, ϵ_m . This becomes useful if the relative dielectric constant of the material is already known.

$$x_n = \frac{150\tau}{2\sqrt{\epsilon_m}} \quad [16]$$

The propagation time and reflected voltages are both easily measurable quantities from the GPR data. The initial layer encountered by the electromagnetic wavefront is air for an air-coupled antenna system. The relative dielectric constant of air

is generally assumed to be unity, simplifying the problem of calculating the top material layer relative dielectric constant, which is asphalt in the simplistic bridge deck model under consideration. The incident voltage is not obtained from the radar waveform, but from one of two calibration files that are normally recorded during data collection. The first is called the *flat metal plate* file and is recorded to determine the incident voltage at the interface between air and the top material layer. A sample of a flat metal plate calibration file is shown in Figure 12.

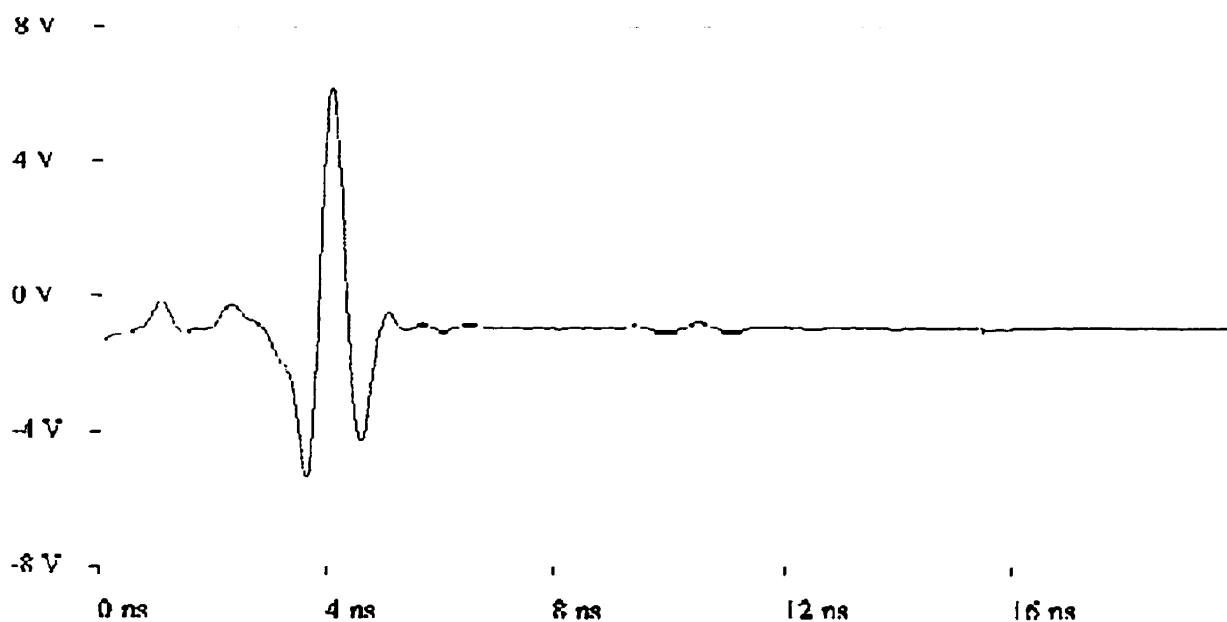


Figure 12 - Sample of a flat metal plate calibration file

Data is recorded with the antenna positioned at operating height over a 36"X48" flat metal plate. The transmitted energy is reflected wholly from the flat metal plate back to the receiver and is recorded. The magnitude of the reflection from the flat metal plate represents the incident voltage transmitted to the interface of the first air layer and the following layer. Figure 13 shows the antenna positioned over the flat metal plate for recording this file.

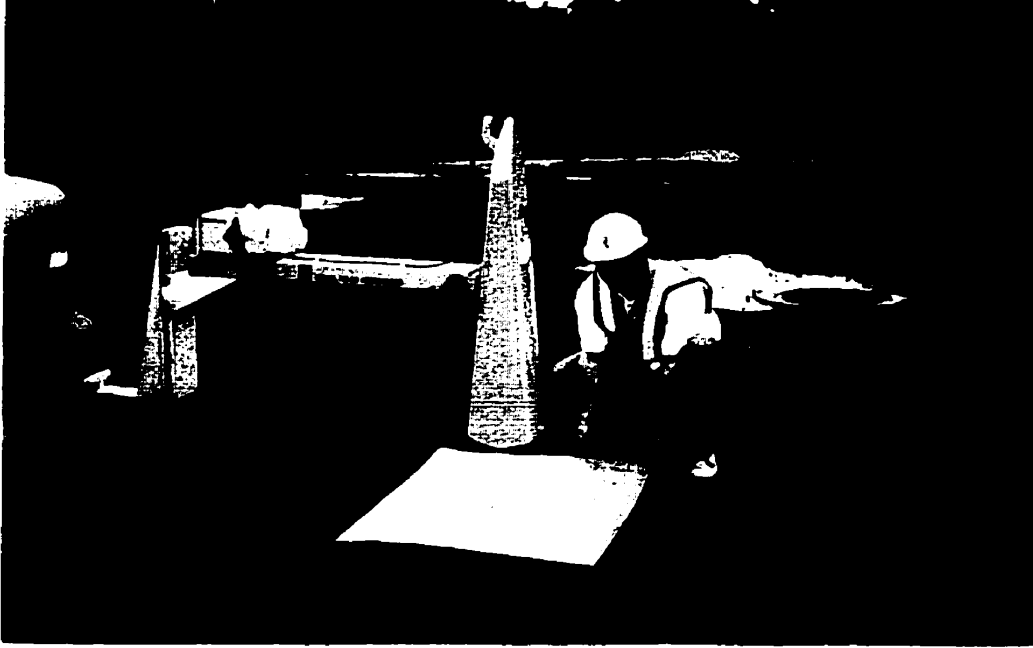


Figure 13 - Antenna positioned over the flat metal plate

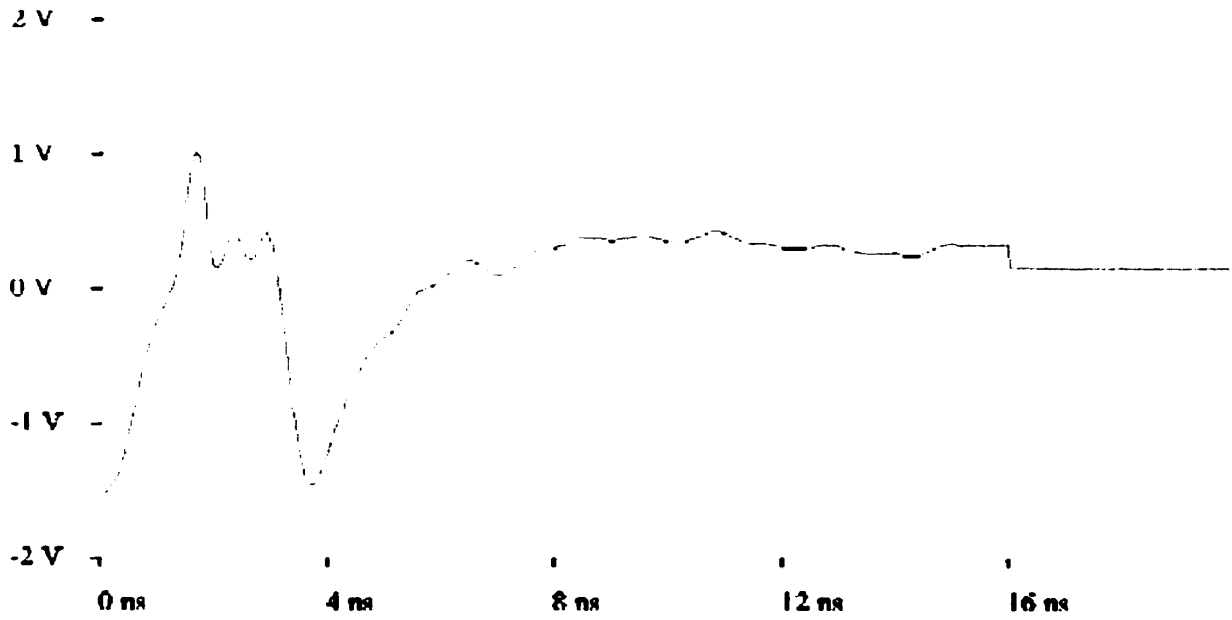


Figure 14 - Sample of a free space calibration file



Figure 15 – Antenna assembly directed into free space

Underlying layer thicknesses are computed using Equation 16, using known values of the relative dielectric constant of the layer. Equation 15 could be used to calculate the relative dielectric constant of the underlying layer, except that the magnitude of the incident energy to that layer is not exactly known since losses in the overlying layer are unknown. Incident energy to an underlying layer is the energy that is transmitted through the overlying layer less the incurred losses. This becomes difficult to determine when using actual data since the losses due to beam dispersion, internal scattering and interface reflections, are not measureable quantities from the data, making the incident energy on underlying layers an estimate with error increasing with depth. Maser (1989) presents the following equation for calculating the relative dielectric constant of the concrete layer beneath an asphalt overlay, assuming no losses in the asphalt layer.

$$\sqrt{\epsilon_{concrete}} = \sqrt{\epsilon_{asphalt}} \left[\frac{F - R2}{F + R2} \right] \quad [17]$$

where F is as follows, in order to simplify Equation 17:

$$F = \frac{4\sqrt{\epsilon_{asphalt}}}{1 - \epsilon_{asphalt}} \quad [18]$$

R2 is the ratio of the peak amplitudes from the asphalt/concrete interface (C) to the air/asphalt interface (A) as shown below in Equation 19.

$$R2 = \frac{C}{A} = \frac{4\sqrt{\epsilon_{asphalt}}}{1 - \epsilon_{concrete}} \left(\frac{\sqrt{\epsilon_{asphalt}} - \sqrt{-\epsilon_{concrete}}}{\sqrt{\epsilon_{asphalt}} + \sqrt{-\epsilon_{concrete}}} \right) \quad [19]$$

The thickness is computed using Equation 16 with the relative dielectric constant of the concrete layer and two-way travel time.

For concrete layers beneath the asphalt surface layer, it can be more practical to use assumed values for the relative dielectric constant and rely on the two-way travel time of the energy through the layer to measure the thickness. This is because the computation of the concrete layer relative dielectric constant is dependant upon the value calculated for the asphalt layer and the errors in measurement accumulate producing increasing error with depth. Errors will also be incurred by using a fixed relative dielectric constant for computing layer thicknesses since variability in material properties, usually due to changes in moisture content, along the data pass will not be considered.

3.3 Evaluation of Pavements Using GPR

Pavement surveys represent the most basic application of GPR in highway infrastructure surveys. The relatively uniform horizontal layers within a pavement system provide an ideal geometry for using GPR to detect the various layers. Changes in electrical properties of the asphalt concrete, base and subbase layers are detected using GPR to estimate layer thicknesses and detect deterioration of the pavement system which traditionally have been unobservable to the inspector. GPR has been used to evaluate highway pavements in both project level deterioration detection and in network level inventories of thicknesses and section types. Information gathered from the surveys is important in many aspects of pavement management including quality assurance of construction, more accurate determination of layer moduli, prediction of remaining life, and design of rehabilitation measures.

Historically, pavement thicknesses have been determined using historical records, core samples and/or test pits at various locations along the pavement section. Often, the extraction of core samples and excavation of test pits is time consuming and expensive, usually requiring closure of traffic in order to conduct the measurements. These discrete thicknesses and section properties are assumed to be representative of the pavement section, resulting in uncertainty regarding variability between locations and requiring assumptions regarding variations between cores. In some applications, such as in the calculation of layer moduli using data from the falling weight deflectometer (FWD), accurate thicknesses are critical since backcalculation methods are most sensitive to small changes in layer thickness. Attoh-Okine (1994) states that a continuous thickness profile, available from GPR surveys, combined with the deflection data from FWD testing, improves the interpretation and characterization of the structural integrity of an entire section of pavement. Failure to account for thickness variability over the section and even within the deflection basin that develops from the impact load of the FWD can

induce errors in the backcalculation of the layer moduli that reduce the effectiveness of the rehabilitation design.

GPR enables engineers to obtain continuous measurements of layer thicknesses such that the variability along the section can be measured instead of assumed to be zero. Reliable determination of layer interfaces is dependant upon significance of the contrast between electrical properties of the individual layers. Since the survey is non-intrusive and can be conducted at speeds up to 80 km/hr, the requirements for traffic control are removed making GPR a very appealing method for collecting pavement thickness data.

There has been a significant amount of research that has focused on the use of GPR for detecting and measuring pavement layer thicknesses. Maser et al. (1994) and Maser (1995) used a 1 GHz air-coupled horn-type antenna and reported accuracies of ± 7.5 percent for asphalt concretes and ± 12 percent for unbound base layers. These results were based on six major studies on over 46 different pavement sections of varying depth, comparing GPR predicted thickness measurements to drilled core and test pit thickness. In some cases, cores were used to calibrate the GPR thickness results to reduce the errors involved. Core calibration becomes important where surface treatments such as chip sealing or slurry sealing will result in relative dielectric constants that are not representative of the entire asphalt concrete layer. Cores may also provide insight into different layers that may have been improperly interpreted in the data. Previously unobserved variations in pavement thickness that could affect predictions of layer moduli over the section were observed in the radar data. The Penetradar Corporation reports that accuracy of ± 5 percent is obtainable for the primary pavement layer if it is homogenous and of sufficient thickness that the next interface is not interfered with by the surface reflection. For asphalt pavements, this is typically limited to a minimum of about 50 mm. Meshner et al. (1995) reported excellent correlation between GPR predicted results and thicknesses as obtained by drilled cores and augers. It was also warned that the use of

cores for calibration may induce errors if a constant propagation velocity is assumed through the calibration.

Clearly, the accuracy in thickness measurement must be a function of the depth and the thickness of the layer being measured if changes in electrical properties occur with depth in the form of moisture content or compaction and due to losses in overlying materials.

There is some debate regarding the reliability of detecting all of the interface reflections in a pavement system. Overlays of asphalt concrete and the previous underlying pavement will be detectable if there is sufficient dielectric contrast between the layers. The effect of weathering and age on the electrical properties of asphalt concrete and the resulting GPR response has not been studied to date. If the interface is detectable, the overlay thickness can be calculated. If the interface is not detectable, the entire asphalt concrete layer thickness may be measurable, but may be subject to errors because the relative dielectric constant of the overlay may be slightly different than the underlying pavement. Slurry and chip seal treatments may induce slight errors in this manner due to scattering losses from the rough surface texture.

Detection of interfaces between the base and subbase and between the subbase and subgrade are more difficult for a variety of reasons. Energy losses increase with depth due to attenuation and scattering effects from nonhomogeneities within the layer and irregular shaped interfaces. The presence of more conductive materials overlying the less conductive base and subbase layers results in less energy being available to penetrate to those depths, producing weaker reflections in the data. Compounding the problem is the compaction of successive lifts of granular materials causing intermingling at the interface between layers such that the deeper interfaces become more convoluted in shape than the assumed plane and parallel layers. Furthermore, the granular materials used for base and subbase layers are often from the same aggregate source, which may be similar

to the subgrade itself. Without sufficient dielectric contrast between the materials, the reflection from the interface becomes difficult to detect from the other lesser reflections within the data. Also, the ability to detect deeper interfaces depends on the type of GPR antenna being used. An air-coupled horn antenna is normally used for data collection at traffic speeds. This type of antenna tends to have more limited depth penetration than a ground-coupled antenna does because a larger proportion of the transmitted energy is reflected from the top of the surface layer and less energy is available to penetrate to deeper layers.

If the reflections between interfaces are detectable, there exists the problem of accurately measuring the dielectric constant from the data. Energy losses occur through layers due to attenuation and scattering effects are an unknown variable when accounting for energy transmissions and reflections in the dielectric system of layers. The incident energy to the surface layer of the pavement system is not measurable from the data, but can be obtained by recording the reflection from a flat metal plate parallel to and at the same distance from the antenna as the top of the surface layer. The proportion of this incident energy reflected from the top of the surface layer is measured from the data. The remaining energy is transmitted past the interface with a portion being lost through attenuation and scattering and a portion arriving incident to the next interface. There are no means by which the energy losses in the surface layer can be measured, other than by placing a reflective metal plate under the layer. In typical field applications, this is possible without digging up the highway. It is possible to construct predictions of energy losses per unit thickness for various materials in a laboratory setting in this manner, but their application in field surveys is again impractical due to the wide range of properties which can occur for any given construction material. The variability of material properties varies widely between highway projects and even within highway sections, making a high degree of error in assumed losses that would undermine their usefulness. Without a measurement or accurate estimation of the losses involved in a given layer, it becomes difficult to accurately account for the amount of energy incident to the next

underlying layer. Errors are introduced into the measurement that accumulate with depth and with successive underlying layers in calculating the relative dielectric constant, and hence the layer thickness. Another approach has been to assume values for the relative dielectric constants of materials and measure only the travel time between reflections in order to compute the thickness. Errors arise in this method since it does not account for variability in the actual relative dielectric constant of the in-situ material due to compaction and moisture content, causing increased or decreased travel time through the layer. Calibration using a sample core thickness or a test pit will reduce the errors involved in the constant dielectric assumption.

Maser et al. (1988) briefly describes the use of GPR to determine the moisture content of base materials, but notes that this is possible if one knows the thickness, relative dielectric constant, and the conductivity of the base material. Unfortunately, all of these quantities can not be independently obtained from GPR data and prior knowledge of these properties of in-situ and in-service materials is virtually impossible to obtain, relegating this exercise strictly to laboratory conditions.

One great advantage of using GPR for surveying pavements sections is the potential for identifying changes in pavement system structure that may be unobservable from the surface. Identifying unknown changes in pavement construction enables better pavement rehabilitation designs and overall management. Wimsatt (1998) reported on the use of GPR by the Texas Department of Transportation as an aid for pavement management decision making. Both air-coupled and ground coupled antennae were used providing nominal penetration depths of 0.6 meters and 9.1 meters, respectively. Along with thickness information, the relative dielectric constants of the layers were found to be of value in predicting an excess of air-voids, or less than optimum density, or conditions in which moisture content was exceedingly high. Excessive air-voids were correlated to lower than normal values of the relative dielectric constant, while excess moisture resulted in higher than normal values. Several case studies were reported in which the

use of GPR provided evidence of failure mechanisms in pavement distress and permitted changes to rehabilitation projects which addressed these problems directly, incurring significant savings. Significantly lower than normal relative dielectric values of a base layer under an asphalt concrete indicated that the base material was less than the optimum density. Investigation showed that the base was coarse graded, lacked fines for cohesion, and allowed excessive water to remain under the pavement leading to distress from truck loadings. Ground coupled GPR was used to investigate the areal extent of a perched water spring under an existing portland cement concrete pavement. Identification of the limits of the spring allowed for an effective drainage design to be placed under the slabs. Another asphalt concrete pavement was surveyed using air-coupled GPR to determine where underdrains would be installed and base repairs made in regions of excessive moisture in the pavement. Higher than normal relative dielectric constants were used to indicate water intrusion through the asphalt concrete as well as saturated base conditions.

GPR can be used to provide managers of highway infrastructure with layer thicknesses and subsurface conditions that are important inputs in the determination of structural capacity and quality assurance of new construction. This information has not been available previously without relying on construction records or resorting to destructive investigations of the roadbed.

3.4 Detecting Deterioration in Bridge Decks

Researchers have identified several characteristics in GPR data as indicators of bridge deck deterioration. Several of these characteristics and the identifying research are discussed in the following subsections.

3.4.1 Air Gap Detection

Early models of delaminations in concrete decks consisted of the typical four dielectric layer model with an extra air layer positioned at the level of the top reinforcement to simulate a crack opening.

Investigations were conducted by Cantor and Kneeter (1982) to study how the radar signal was affected by concrete slabs of various thicknesses, rebar, water and boundary effects, among other variables. The effect of gap width on the radar signal was studied by positioning two concrete slabs on rollers so that the air gap between them could be varied from zero to thirty centimeters. While the air gap distance was found to be measurable over the larger gap distances, the effect is for the negatively pointing bottom echo of the top slab and the positively pointing surface echo of the bottom slab to become superimposed and cancel each other out as the gap distance is decreased. It follows then, that there is a minimum theoretical crack width opening that is completely measurable using GPR that is equal to one half of the pulse width, or 75 mm in air. However, it is possible to resolve distances down to crack widths by taking advantage of algebraically summed overlapped and time-displaced signal according to Alongi et al. (1982). It was reported that this technique may be employed to measure layer thicknesses result in two-way travel times that are less than the one half of the pulse width of the transmitted signal and occur as superimposed reflections in the data.

Manning and Holt (1983) reported 26 percent accuracy in predicting delaminations in bridge decks by identifying strong positively oriented reflections at the top reinforcement level. In this study, a single bridge deck was surveyed with 51 percent of the deck being identified as delaminated, giving a high degree of false indications of sound concrete. It was hypothesized that the strong and positively oriented reflection observed in the data could possibly be due to a large water-filled crack width of the

delamination, instead of the reverse in phase that might be expected if the crack was filled with air.

Detecting and measuring small crack width openings is feasible if material properties are known and remain constant such as in a laboratory environment, but in field conditions, this does not often hold true. Delaminations can produce cracks widths ranging from microns, at their onset, to several millimeters in size. Since the changes in signal characteristics become less measureable as the crack gap decreases, small openings become difficult to resolve in the data. In the field, crack gaps are not often horizontal and planar air-filled gaps, but are irregular in shape and contain sand, organic materials, moisture and chloride. Variations in material properties, coupled with uncertainty as to the contents of the crack void, make measurement, and detection of delaminations based on signal changes due to the presence of crack gaps even more difficult.

Maser (1989) analyzed the likelihood of detecting changes in the radar waveform due to air, water, or other material-filled crack widths in delamination and found that thin delamination cracks have no effect on the radar signal at either the reflection from the top reinforcement layer or at the deck bottom. The theoretical analysis of the magnitude of the net reflected pulse from an air-gap is presented here to demonstrate the futility in using GPR to detect the actual delamination crack. The Net Reflected Pulse (NRP) is the waveform magnitude at a given instance in time and may be computed by accounting for the effects of all reflections from and transmissions through an interface.

Following the approach of Maser (1989) the following consideration of two possible effects of the “gap model” of delaminations on the radar signal is presented. The first effect is a reflection from the concrete/gap and gap/concrete interfaces and the second is a change in the reflection from the bottom of the deck slab. Considering the net reflected pulse from an incident ray to the gap system, it is shown that it is composed of the reflected portion of the incident ray plus the sum of the following reflected

transmissions past the concrete/gap interface. The incident ray, assumed to have a unit magnitude, is reflected according to the reflection coefficient for the concrete/gap interface, $R_{ab} = R$, which is also equal but opposite in phase to the reflection coefficient from the gap/concrete interface, $R_{ba} = -R$. The transmission coefficient are therefore $T_{ab} = 1-R = -T_{ba}$. The incident ray is therefore split into a reflected portion, having magnitude R , and a transmitted portion, having magnitude T_{ab} . The transmitted portion is reflected by the gap/concrete interface according to the reflection coefficient, $R_{ba} = -R$, now with the magnitude RT_{ab} , with the remaining energy being transmitted to the bottom of the slab with magnitude $T_{ab}T_{ba} = T$. The energy reflected from the bottom of the gap is again reflected by the top of the gap, producing a ray with magnitude R^2T_{ab} , while the remaining energy is transmitted into the top concrete layer with magnitude $-RT_{ab}t_{ba} = -RT$, delayed by the two-way travel time in the gap, τ . This reflection again encounters the bottom of the gap and is reflected with magnitude $-R^3T_{ab}$, and transmitted to the deck bottom with magnitude R^2T . This reflection encounters the top of the gap again, resulting in another reflection and a transmission to the top concrete layer with magnitude $-R^3T$, delayed by twice the two-way travel time through the gap, 2τ . The original incident pulse can be represented as $\sin(2\pi t/T)$ where T is the period of the pulse and t is time, allowing the construction of the following relation for the net reflected pulse from the gap:

$$\begin{aligned}
 NRP = R \sin\left(2\pi \frac{t}{T}\right) - R(1 - R^2) \sin\left(2\pi \frac{t - \tau}{T}\right) - R^3(1 - R^2) \sin\left(2\pi \frac{t - 2\tau}{T}\right) \\
 - R^5(1 - R^2) \sin\left(2\pi \frac{t - 3\tau}{T}\right)
 \end{aligned}
 \tag{20}$$

The net reflected pulse is maximized when time is taken to be one half of the radar period, or one-quarter of the assumed sine function. The above equation differs from the work of Maser (1989) in that the transmission effects through the gap are included in the second pulse reflection term and further reflection terms are considered in the equation.

Maser (1989) found that delaminations that are 3 mm or greater in gap width or those that are water filled are detectable in the radar waveform. The above analysis shows that net reflected pulses at the level of the concrete cover are small for both air and damp fine filled gaps, while water filled gaps are highly reflective and should be easily detected, considering that for typical asphalt with a relative dielectric constant of 5, reflection coefficients of 0.382 and 0.124 from the air/asphalt and asphalt/concrete interfaces would result, respectively. For a typical emitted signal strength of 10 volts, neglecting layer attenuation, the incident voltage to the concrete/air interface of the crack gap would be reduced by the layer transmission coefficients to 5.42 volts. On its return to the antenna receiver, the net reflected pulse would be further reduced by these transmission coefficients. Neglecting layer attenuation and peak reduction due to internal reflections between the interfaces, the magnitude of the peak in the waveform for each gap material and gap opening height is shown in Table 2. These values are calculated using a nominal one nanosecond radar period, corresponding to the center frequency of one gigahertz, and relative dielectric constants of 8.22 for normal concrete and 5 for normal asphalt pavement.

Table 2 - Predicted peak magnitude of gap of different thicknesses containing different materials

Gap Material	ϵ_r	R	v (mm/s)	Gap Height (mm)				
				1	3	8.33	15	75
Air	1	0.483	300.0	0.002	0.004	0.017	0.048	0.231
Damp Fines	25	-0.271	60.0	-0.002	-0.018	-0.097	-0.148	-0.148
Water	81	-0.517	33.3	-0.023	-0.131	-0.241	-0.241	-0.241

Table 2 indicates that for small delamination gaps that are filled with air or damp fines, the effect is negligible on the radar waveform. Water filled gaps have a greater effect on the waveform and should be more detectable.

The second proposed effect on the radar waveform due to delamination gap openings was a change in the magnitude of the reflection from the deck bottom. Given the negligible effects shown on the waveform from the gap itself and the increased reductions in the magnitude of the effect as it propagated from the gap to the deck bottom and back to the receiving antenna, it stands to reason that there would be insufficient redistribution of energy from the gap to have an appreciable effect on the magnitude of the deck bottom echo.

Delaminations with such small crack gap openings can be representative of most field conditions, with opening typically 1 mm or less width, but many delaminations tend to be filled with corrosion products consisting primarily of iron oxide. Water entering crack gaps is likely to be absorbed into the concrete slab by capillary action rather quickly, unless the slab is in a saturated condition. The above findings lead to the conclusion that direct detection of delaminations using GPR is not practical.

3.4.2 Signal Distortion

Instead of attempting to detect the actual delamination crack, research has been directed towards detecting other indicators of concrete deterioration. Changes in normal GPR reflected signal shape have been observed and used by researchers to predict concrete deterioration in bridge decks. Waveforms were compared by superposition of each waveform over a baseline waveform shape from the data, representing areas of sound deck.

Clemeña (1983) reported limited success in detecting delamination crack openings by observing depressions and blurred regions about the top reinforcement layer reflection in black and white B-scan or voltage intensity plots.

Research showed that waveforms that were collected from areas of deteriorated deck did vary noticeably from those collected in sound areas of the deck. Superposition of waveforms enabled a qualitative cluster analysis of the data to yield three prediction groups: sound concrete, distressed concrete, and intermediate concrete (in which waveforms were not clearly classified). A wearing test of the deck was conducted by drilling holes at a fixed speed and applied force for 2 minutes, using the penetration depth as a measure of the concrete quality. Of these tests, 90 percent of the distressed concrete predictions proved true, while 91 percent of the sound concrete predictions proved true. Cantor and Kneeter (1982) remark:

“In theory, it is possible to determine the condition of the concrete at any location by examining the radar trace. In practice, this is difficult, because of both the complexity of the trace and the time required to dissect the trace and its component parts.”

These comments support the basic premise that sound concrete will result in well defined and strong reflections from the components within the deck system, while damaged concrete will result in signal losses and distortions in the reflected waveform. Analysis of individual components of the waveform can be difficult due to superposition of the reflections and their close proximity, and also due to damage in the deck slab and the overlying asphalt pavement.

Chung et al. (1984) studied the test data used by Manning and Holt (1983) and developed signal processing techniques which could automate the calculation of the reflection ratios within each waveform. These ratios were used to attempt to predict asphalt/concrete debonding and deck surface scaling and were based on an interpretation of how the radar signal should respond to these conditions. Sound concrete was observed to exhibit a characteristic “W-shape” response in the region of the top reinforcement while delaminations were expected to produce a distortion of the reflection from the top level of reinforcement and were detected by counting the number of slope changes in the waveform in this vicinity.

3.4.3 Signal Attenuation

From the previous discussions, it is noted that detection of actual delaminations has been difficult and inconsistent. Research has instead shifted focus to detecting conditions in which delaminations are likely to occur.

The use of changes in the radar waveform for predicting deck deterioration was refined by analyzing the effects of different variables affecting the reflected energy that were also associated with corrosion of the reinforcement. There must be a supply of oxygen and a potential difference to cause the oxidation. Moisture and chloride play an important role in reinforcement corrosion and their presence in a bridge deck in high quantities can be used as an indicator of probable deterioration. The effects of moisture and chloride on the radar response of a sand bed were studied by Alongi et al. (1993) to establish their use as indicators of bridge deck condition. It was found that signal attenuation increased with increasing chloride concentration and with increasing percent solution content by weight in the sand bed. Al-Qadi et al. (1996) also studied the effects of chloride on the radar waveform and found that increasing chloride content resulted in a time delay shift and a reduction in peak amplitudes. Given the role of excess moisture and chloride in corrosion of the deck reinforcement, this now forms the basis of detecting delaminations for bridge decks in a relatively humid state in areas in which salt is applied for de-icing purposes. Areas of sound concrete in decks are generally less permeable with lower water content and chloride ion concentrations than more permeable or porous areas of concrete that have been damaged by corrosion associated with moisture and salt ingress. Over time with repeated freezing and thawing action, load applications, and cracking, the concrete develops cracking on a microscopic level and will become more porous. Water and chloride ions will migrate into the deck slab and corrosion will initiate as the passive alkaline environment of the concrete surrounding the reinforcement degrades. The effect on the reflected GPR waveform is signal attenuation, an increase in the concrete reflection coefficient, a decrease in the RF propagation velocity through the

deck slab, and further scattering of the signal due to cracking and granulation of the concrete. The increase in the concrete reflection coefficient and decrease in RF propagation velocity are due solely to an increased water content and the resultant increase in the relative dielectric constant. Attenuation is due to the interactive effects of moisture and chloride ion content in the slab. Attenuation is the preferred signal characteristic to correlate to delaminations because of its relationship to the combination of moisture and chloride, the two prime factors leading to corrosion induced deck delamination. An increase in the reflection coefficient can be indicative of an increase in water content at the asphalt/concrete interface and decreasing RF propagation velocity can be indicative of increased water content throughout the slab depth.

Equations 7 and 8, demonstrate how attenuation can be simplified to a function of the relative dielectric constant and the ohmic conductivity of the medium. While the relative dielectric constant is a measureable quantity from the GPR data, the ohmic conductivity is not. In order to know this, it must be measured directly using a sample of the material. This technique is not practical for field applications since the conductivity may vary widely at any point within the bridge deck due to ion concentrations and various degrees of deterioration of the slab. GPR waveforms recorded at a location in the deck where the concrete is known to be sound exhibit clear and strong reflections from the various interfaces. There is a baseline level of signal attenuation due to trace amounts of chloride and moisture and the normal conductivity of the deck slab. In a deteriorated area of the deck, the signal exhibits some higher degree of attenuation due to the excess levels of moisture and chloride in the deck slab. Using a ratio of the amplitudes of the deck bottom reflection, it may be assumed that the change in attenuation due to the excess moisture and chloride in the deteriorated region of the deck can be measured. Another method is to compare the mean square voltage of the waveform data points between the top and bottom of the concrete slab. Alongi et al. (1993) found through experimental verification that when the loss in signal strength was 38.5 percent, the radar would make delamination prediction within .11.2 percent of the ground truth quantities.

Maser (1989) discusses the simplification of signal attenuation that results from increased conductivity through chloride content as a function of concrete cover thickness and the ratio of the reflection from the top reinforcement layer and the reflection from the air/asphalt interface to predict delaminations. However, since the content of reinforcement may vary over the length of a bridge deck, according to its design, this may not represent an accurate prediction since varying reinforcement content will affect the magnitude of the reflection from the reinforcement mats. Even if the reinforcement content is constant along the deck length, the relative transverse position of the antenna over the reinforcement grid does have a small effect on the reflected signal. Given the low probability of exact alignment of the data pass over the longitudinal reinforcement, this reflection would tend to vary along each data pass and potentially yield false predictions using this indicator. Attenuation that is computed based on the signal losses through the entire deck slab can still be affected by reinforcement content variations due to increased energy reflections from increased reinforcement content. However, since the magnitude of the deck bottom reflection is generally much larger than the reinforcement reflection, the effect of the change in reinforcement reflection amplitude is smaller on the bottom echo measured amplitude, while attenuation of the bottom echo peak due to excess moisture and chloride content is increased given the larger distance between the interfaces.

3.4.4 High Asphalt/Concrete Interface Reflectivity

Maser (1990) presented an analysis of GPR and infrared thermography for quantifying the removal areas for bridge deck deterioration. A sample size of twenty eight decks were evaluated using GPR, infrared, and visual observation of the bridge deck underside for direct observation of distress, for a regression analysis based upon the areas found by chain drag and removed from the decks during maintenance. The GPR data was not processed to detect signal attenuation as in the research of Alongi et al. (1993), but a characteristic increase in signal reflectivity from the asphalt/concrete

interface, indicating localized high moisture contents in the near-surface concrete of the deck. This high reflectivity was quantified and normalized as the variable R2 by dividing the magnitude of the asphalt/concrete reflection by the reflection from the air/asphalt interface. Maser computes the dielectric constant of the concrete using Equation 18 assuming no losses in the asphalt layer and a constant value of the relative dielectric constant of the asphalt layer of 5.5 for this calculation. In each data pass the mean value for the relative dielectric constant of the concrete was calculated. Individual values in each pass that exceeded a certain threshold were flagged as indicators of delaminations. Maser found that using a threshold value equal to 1.3 times the mean yielded the best-fit model for predicting delamination quantities. Used independently, underside visual inspection provided the best correlation to actual removal quantities, followed by radar, then infrared techniques. However, the best prediction model yielded a good correlation ($R^2 = 0.83$) between actual removal quantity and predicted area using a combination of GPR and visual detection methods, with a standard error of 4.1 percent of the deck area.

An important difference between the work of Maser (1990) and Alongi et al. (1993) was in the interpretation of this high reflectivity from the asphalt/concrete interface. Alongi et al. (1993) claim that the increase in reflectivity from the deck is due solely to the effect of moisture, while Maser (1990) states that the increase in reflectivity is related to the combined increase in both moisture and chloride ion concentration combined. Corrosion of the reinforcement may be less likely should excess moisture with very low levels of chlorides be present. Although only excess moisture is required to produce the higher reflectivity from the concrete surface, over the lifetime of a bridge deck in an environment where salt is used for deicing purposes, it is unlikely that localized high moisture contents in the deck would not contain high concentration of chloride ions.

Maser (1990) made some important conclusions in that the high reflectivity from the deck may not only indicate deterioration of the concrete cover, but also failure of a

deck membrane without deterioration of the concrete cover. These two different failures are indistinguishable using the high concrete reflectivity alone, but with underside staining maps from visual observations, the cause of the high reflectivity can be inferred.

GPR techniques have been applied only to detecting delaminations at the top layer of reinforcement. Since the signal is directed through the slab from the top downwards, it must be assumed that attenuation as measured by the bottom echo amplitude must be the result of conditions above that interface. This makes sense from a practical standpoint since most water and chloride ingress start from the top of the slab. Detecting delaminations at the level of the bottom layer of reinforcement becomes difficult since it is likely that should they exist, then the deck is delaminated at the top reinforcement layer as well, since the top would be affected first by the water and chloride. Signal attenuation associated with the top bar delamination affects the complete waveform pertaining to the full deck thickness. This effectively masks any further signal degradation that may arise due to delaminations at the bottom reinforcement level. The depth to which moisture and chloride intrusion occurs cannot be determined from the data, but it is inferred that if significant signal attenuation exists, corrosion must affect the top layer of reinforcement first.

A similar argument exists for using the high reflectivity from the asphalt/concrete interface as an indicator of deck deterioration. The indicator is a measure of high moisture conditions at the interface and the adjacent concrete. This condition may be due to moisture intrusion into the slab or simply by cracked and debonded asphalt overlay or even a failed membrane. Assuming that the high reflectivity is due to moisture and chloride intrusion into the slab, the depth of intrusion cannot be measured into the slab, but full depth penetration can be confirmed by visual observation on the deck underside. It must be inferred that the top reinforcement is affected by this condition first and realized that there is a potential for deterioration of the bottom layer reinforcement.

Quantification of the degree of attenuation may lead to a relationship between bottom reinforcement delamination and the most severely attenuated signals.

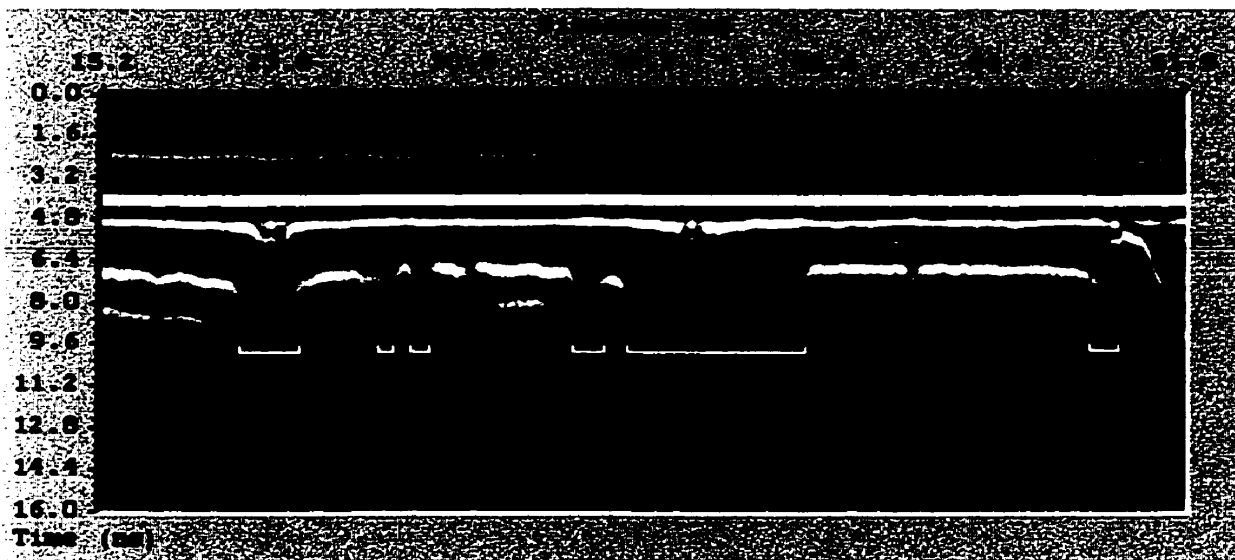


Figure 16 - GPR deck data indicating areas of deterioration

Figure 16 shows a color intensity plot, or B-scan, of a section of a GPR data pass recorded from a typical bridge deck that contains both high reflectivity from the concrete deck and signal attenuation. There is a high probability that delaminations would be found in the deck at these locations. Note that there are three joints shown at the 22.7, 40.8, and 58.8 meter locations along the distance axis as can be seen by increased reflectivity at the level of the asphalt/concrete interface, as well as a distinguishing quadratic-shaped structure that develops in the B-scan at the joint location.

The strong and uniform white line at the 4 ns location is the aligned reflection from the surface of the asphalt pavement. The asphalt/concrete interface and top rebar are located at the 4.9 ns and 5.5 ns locations, on average. This translates to approximately 60 mm of asphalt pavement and 31mm of concrete cover on the deck, assuming relative dielectric constants of 5 and 8.22 for asphalt and concrete, respectively.

The deck bottom is represented by the dark line, an inverted peak due to the change in phase from high to low relative dielectric constants, located approximately at 7.7 ns to 8.2 ns. The variability in the bottom location is due to asphalt thickness and material property variations in the entire deck thickness. The areas above the highlighted lines, located at 9.6 ns, drawn on Figure 16 are interpreted to represent deteriorated areas in the deck. The deteriorations are revealed by the occurrence of excess signal attenuation via the smearing of the reinforcement and deck bottom reflections, and by the occurrence of unusually high peak magnitudes from the asphalt/concrete interface, which can be seen especially well in the areas near the joints.

4. Research Program

The research program for this project was developed by Dalhousie University DalTech and the Nova Scotia Department of Transportation and Public Works. A number of objectives were established to provide a basis for assessing the appropriateness of using GPR for asphalt-covered reinforced concrete bridge deck evaluation for bridge management.

4.1 Objectives

The main objective of the research described within this thesis is to identify and assess ground penetrating radar as a pre-tender estimation tool for bridge management. This main objective will be reached by determining the accuracy and variation between the deterioration estimates predicted using this technology and surveys of the actual deterioration for nine asphalt-covered reinforced concrete bridge decks. The following objectives will be reached to support the main objective of this research:

- 1) Determine the most appropriate method of GPR data processing to optimize the accuracy of the results.
- 2) Determine the network level accuracy and variation of the predicted deterioration quantity with respect to well-established ground-truth measurements of the actual deterioration condition.
- 3) Determine the network level accuracy and variation of the GPR predicted deterioration quantity with respect to the level of accuracy and variation associated with the current deterioration estimation practice.
- 4) Determine the network level spatial correlation between predicted deterioration location and actual deterioration location with respect to well-established ground-truth surveys.

- 5) **Determine limitations of the system with respect to deck design and construction.**

This research program was designed to evaluate the accuracy and reliability of GPR to predict the location and extent of deterioration in asphalt covered reinforced concrete bridge decks. Whereas the exact bridges to be studied were not known prior to their selection for repair, all repair candidate bridges for an upcoming construction season would be surveyed using GPR prior to the tender preparation for the repair work. The data would be processed and an estimate of the deterioration quantity would be made based on the results of the data processing. Also, the GPR predicted deterioration locations would be drawn to scale on a plan map of the deck slab surface area. The GPR quantity estimate and predicted deterioration locations would be compared to deterioration groundtruthing results using the conventional chain drag and half-cell potential survey test methods after the asphalt would be removed from the deck surface. The groundtruthing results would be overlaid on the GPR deterioration prediction maps to assess the level of agreement between predicted and actual deterioration locations. Prediction quantities would thus be compared statistically to establish the percent difference between the methods and associated confidence intervals for individual decks and also for network level performance.

This research program entails an innovative approach to using GPR data for detecting deterioration in asphalt-covered reinforced concrete bridge decks because a comparative study has not been done before where data was collected at traffic speeds for which commercially available processing software has been compared with manual processing methods. Furthermore, previous research has focused on the use of a single deterioration characteristic in the data as the basis of the estimation, whereas the manual processing incorporates the use of high reflectivity from the asphalt/concrete interface and signal attenuation throughout the depth of the deck as the basis of the estimation. The inclusion of these two effects in the data within manual processing was developed to

provide a more robust correlation to the actual deterioration by accounting for multiple phenomena that occur within the processes of deterioration.

4.2 Field Collection of GPR Data

Once the bridges have been identified as potential repair candidates, they were grouped according to geography to minimize travel time and expense during the data collection field trip. Other factors affecting trip scheduling were weather and anticipated traffic flows on each bridge. If heavy traffic was anticipated on a given structure, the survey would be conducted at night when less traffic would be present. Prior to collecting the data, each deck was measured and prepared by placing paint marks over the desired pass location centerlines and the equipment was set up. After collecting the data, each data pass was reviewed for completeness and clarity before the equipment was taken down and stored.

4.2.1 Deck Measurement, Visual Inspection and Marking

On data collection field trips, each bridge was carefully measured to determine the as-built length, width and skew angle of the joints. Other important characteristics were noted such as the direction of magnetic north, the direction of traffic flow, structure type, number of spans, location and type of joints, and location of drains. Before collecting the data, each structure was inspected visually for signs of distress on the deck bottom surface, asphalt pavement surface, and curb, crash wall, support, and abutment conditions. Estimates of the thickness of the deck slab and asphalt pavement were also made by observing the edge of the deck and drainholes, or if they were present, potholes in the pavement. The location and size of efflorescence, moisture and rust staining on the deck underside were recorded on a rough sketch to aid in understanding the characteristics observed in the data.

Fluorescent orange strips of paint were placed at the centerline locations of the data passes across the width of the deck. The paint markings were used by the driver of the van to align the antenna over the desired pass location during the survey. Each group of paint marks was usually spaced at approximately thirty to forty meters apart along the length of the deck, or according to the deck curvature and other factors affecting the visibility of the driver. Fluorescent orange paint was chosen because of its excellent visibility in daylight and good visibility at night. A convention was established that successive passes are aligned from right to left in each traffic direction. The first pass in each direction is placed at a distance of 0.5 meters from the curb edge, with following passes spaced at the desired interval. Early in the project, a one meter wide spacing was employed, but was later reduced to 0.75 meters to increase the spatial resolution of the results.

4.2.2 Equipment Setup

After each bridge was prepared for data collection, the equipment was set up. The first item that was set up was the front and rear roof safety lights. Each set of lights is attached to the roof of the van using large magnetized supports.

A standard procedure was developed to prevent equipment damage when setting up and taking down the exterior hardware. The “arm” portion of the support structure is positioned and bolted into place on the “post”. Once this is completed, the antenna is secured to the arm using the two large plastic bolts. The bolts are tightened enough so that the antenna will not move from the wind gust on it when the van is in motion. The main radar cable is connected to the port on the outside of the van, then to the transmitter/receiver unit. This provides a grounded connection linking the antenna assembly to the van. At this point, the person assembling the antenna system first ground themselves by placing a hand on the aluminum backing of the transmitter/receiver unit,

then inserts a length of solder into the connector at the top of the antenna for the antenna feed cable. Again, the person grounds themselves to discharge any excess charge that may have existed on the antenna to the van. The antenna feed cable is then connected to the top of the antenna. This procedure is very important as it will lessen the likelihood of a transfer of static charge to the transmitter/receiver that may lead to diode failure. Similar care is taken when taking down the antenna assembly. The entire antenna system is positioned in place on the support beam for the initial curbside data passes. After the antenna assembly has been set up, the system is powered up and left on for a short period to stabilize.

To power up the system, the power inverter is first turned on, then the computer system. After the radar data acquisition software is running, the radar MCU and distance measuring instrument control are turned on, completing the hardware preparations for data collection.

4.2.3 Recording Data and Calibration Files

With the antenna hardware setup and the signal checks confirming proper transmission, the system is ready to collect data. Each data pass is usually set up one at a time on the computer, using an even-odd sign convention for traffic flow direction. When each file has been prepared, data collection is initiated after the distance counter button is held in to zero the count. With the counter held in the zero position, no waveforms are collected even though data acquisition has commenced. The van is driven up to the deck at traffic speed with the antenna aligned over the appropriate pass location paint mark on the deck surface. About ten meters before the initial abutment joint, the distance counter is released to begin collecting waveforms. Data collection is terminated by pressing the F1 key when the antenna is located approximately ten meters past the final abutment joint. All data passes are collected in this manner by driving the van over the deck in each direction. Periodically, the antenna support post is moved along the

steel support beam such that it is centered over the next pass location with the van remaining in the center of the proper traffic lane. "Authorized vehicle only" turnabouts connecting opposite lanes of divided highways, and side roads or driveways are used to turn the van around when each pass is completed. The driver uses extreme caution when choosing appropriate times to merge with traffic flow, giving preference to occasions with no oncoming traffic.

After all the data passes are recorded, the van is parked off of the roadway and each data file reviewed for clarity, completeness and an initial assessment of layer boundaries, deterioration and other features that could be seen in the data. If all files are found to be satisfactory, the flat metal plate and free space calibration files are then recorded prior to taking down the antenna hardware. The takedown procedure for the antenna hardware is simply the reverse of the set up procedure, with similar care to disconnect the antenna before the grounded link to the van is interrupted. The antenna and arm are stored in the rear compartment of the van. The support post is centered on the steel support beam to avoid covering the van headlights and the cap is screwed back on the main radar cable port to prevent soiling the connections.

Data is transferred from the computer in the van to an office desktop computer using an Iomega Jaz drive that can be connected externally to each system and uses individual disks having a one gigabyte capacity. A typical bridge with a surface area of 400 m² produces approximately 15 Mb of data.

After the accuracy of GPR as a repair quantity prective tool has been demonstrated, it is at this point in the data collection that sufficient information has been recorded to produce a quantity estimation report of the deck deterioration. The total time required onsite to observe the deck and collect this data is minimal, typically one hour for an average 400 m² bridge deck surface. In this study, the additional chain drag and half-

cell potential survey data serves only to provide the ground-truth data by which the accuracy and effectiveness of the GPR estimates may be judged.

4.3 Chain Drag Survey Data Collection

The chain drag survey was conducted after the asphalt pavement and waterproofing have been stripped from the concrete deck slab. Due to traffic restrictions, one lane was closed to traffic for repairs at one time. This means that the data collected on each lane is taken at a different time, but basically under similar conditions. The deck is usually swept clean of excess dirt and debris that may interfere with the test procedure. Another effect that interferes with the test procedure is nearby traffic. Oncoming traffic in remaining lanes that are not closed for repair produce sufficient background noise that a small deteriorated area can be missed while conducting the test. Hence, each area was usually chained several times before moving on to other locations. The chain drag survey is used to locate and determine the extent of the cracked and debonded areas of concrete cover over the top layer of reinforcement by dragging the chain over the exposed concrete surface and listening to the tone produced, as may be seen in Figure 17.

The test is simple, but relies on the operator's interpretation of the sound resulting from the chain being dragged over the exposed concrete surface. On undamaged concrete, the chain results in a sharp, ringing sound whereas on deteriorated concrete, the sound is dull and hollow. Various degrees of cracking severity and gap opening will affect the sound produced. The entire surface of the deck is sounded using the chain in this manner. The boundary of each detected deteriorated area found with the chain are delineated using spray paint. These areas are simplified into rectangular shapes for ease of saw-cutting, removal and repair. Also, groups of small designated repairs are often grouped together to form a larger rectangular area or interconnected group of rectangular shapes to simplify the repair work, including sound areas of concrete with deteriorated areas in the repair.



Figure 17 - Conducting the chain drag survey

Accompanying the chain drag testing is visual observation of surface deterioration due to scaling and freezing and thawing. While these areas may not produce a noticeable effect in the sound of the chain on the deck, they are also encompassed by painted rectangles for removal if they are found to be severe enough.

Prior to each chain drag survey, a plan map of the deck was drawn to scale with a 0.25 meter by 0.25 meter grid superimposed on the deck surface for sketching the chain drag results. Each vertex of the rectangular shapes describing the deteriorated areas is drawn on the deck map to the nearest 0.05 meter and rectangular areas are shaded in to denote the deteriorated regions of the deck surface.

4.4 Half-Cell Potential Survey Data Collection

The half-cell potential survey was also conducted after the pavement and waterproofing membrane had been stripped from the deck surface. Due to traffic

restrictions, one lane is closed to traffic for repairs at one time. This means that the data was collected from each lane at different times and may be influenced slightly due to different moisture contents in the deck. A grid system was established on each deck span to identify the point measurement locations for the survey. Data points were spaced at half meter intervals across the width of the deck, with the first set of points being placed at 0.1 meters from the curb edge. A surveying tape was stretched from one joint to the next to measure point location spacing. The initial and final point in each longitudinal series of points in each span was located at approximately 10 centimeters from the abutment joint, just alongside of the steel section, and the others were placed at each meter mark on the tape. Each longitudinal strip of data points would be placed after the data had been collected on the previous strip. Using this arrangement, the density of data collection points was greater than the minimum requirement of 4 feet spacing as specified in ASTM C 876-91.

Since the half-cell potential survey was conducted during rehabilitation work on each structure, the contractor was able to jackhammer away an area of concrete cover on each deck span, exposing sufficient reinforcement to provide a suitable connection. A large copper clamp was attached to the exposed reinforcement after it has been cleaned with a wire brush and coarse emery cloth to remove any remaining concrete and dirt. The clamp was connected to a voltmeter, set to read measurements to one thousandth of a volt, by approximately one hundred and eighty feet of 18 gauge wire. The voltmeter was connected to a copper-copper sulfate half-cell electrode by approximately six feet of the same wire. A damp sponge was placed over the ceramic plug on the electrode, after removing the plastic cap, to provide a good moist contact between the electrode and the deck surface.

As each longitudinal strip of data points was placed on the deck surface, each point was pre-wetted using a solution of water and dishwashing detergent. The soapy solution ensures that there is a good electrical contact between the deck surface and the

electrode via the dampened sponge. The potential was measured at each point on the grid network and recorded along with the its location. Data were also recorded in each longitudinal strip of points at 0.05 meters on either side of a steel joint.

After both the chain drag and half-cell potential survey, several locations on the deck were chosen, after referring to the GPR survey map, to extract core sample to corroborate with the GPR predicted deterioration locations. Core samples were inspected, then tested for water soluble chloride content to provide evidence in agreement or disagreement with the GPR survey.



Figure 18 - Conducting the half-cell potential survey

5. Presentation and Discussion of Data Analysis and Results

All of the data gathered required processing to produce an estimate of the deterioration quantity and to present the data in a graphical format. This allowed for comparison of GPR predicted deterioration locations to actual deterioration locations found using the chain drag and half-cell potential survey data to establish spatial correlation. Half-cell and radar data were compared to a threshold value to differentiate between deteriorated and sound areas of deck. The chain drag data was already processed or differentiated as per the audible test procedure of the survey, but required transfer to AutoCAD to measure the deteriorated areas.

The following sections will examine how these data are processed and converted into a graphical format for comparison and will also examine the issues related to their interpretation.

5.1 Automatic Processing of GPR Data

Penetradar Corporation produces in-house designed software to analyze the GPR data recorded using their hardware. The scope of this research is based solely on bridge deck data analysis. Bridge data analysis is divided into two steps using two different analysis programs that were included with the IRIS package: bridge processing and bridge post-processing.

Bridge processing involves the observation and identification of layer interfaces using other Penetradar-designed graphical display software, the creation of a processing setup file, and the production of processing output files containing basic measurements from the raw data. The setup file identifies which data files were recorded on the deck and requires the user to specify the time location of the surface reflection,

asphalt/concrete interface, top rebar peak, and deck bottom peak. The user should first examine the data before creating the setup file to study and determine the interfacial reflections to ensure that the proper peaks are identified in the setup file. The user then inputs the location of these peaks by observing the data either in A-scan or in waterfall plot format and by placing lines over the appropriate peaks during this observation. The exception to this is the surface echo, for which the time location (less one nanosecond) is inputted numerically in the initial stages of creating the setup file. This allows the software to align the data according to the surface echo to simplify viewing the data. The selection of the other peak locations establishes a fixed-position gate or window around each peak that the software uses to track the peak location as it fluctuates in its time position. Once these gate locations are established for all the data passes, the software processes the setup file, recording such measurements as peak amplitude and time location. Processed file information is stored in a new file used as the input for post-processing of the data.

Bridge post-processing uses the new processed data information files to predict the location and extent of deterioration based on one of four optional characteristics to look for in the data. These four characteristics are signal attenuation, changes in the signal shape and consistency, changes in the asphalt/concrete interface echo amplitude, and changes in the bottom echo amplitude. Of these characteristics, signal attenuation is the most recommended and applicable characteristic that is associated with deck deterioration, due to the effect of excess of moisture and chloride in the deck slab on the signal. The user is required to input the bridge name, skew angle, pass width, and the length of the unit deck area in each data pass. Each pass in this research was subdivided into sections of 0.25 meter length. Finally, the user selects the desired deterioration characteristic to identify in the data and the results are presented graphically on the computer monitor and can be printed on paper. The degree of signal attenuation is determined by computing the sum of the mean square voltages in each waveform between the user-defined top and bottom of the deck slab. The mean square voltage is

the power reflected from within the deck slab. Regions of deck that are high in moisture and chloride content will exhibit reduced peak amplitudes and therefore smaller mean square voltages, or power. The analysis software was designed using a sign convention of a measurement exceeding a threshold value corresponding to a deterioration prediction. A change in polarity of the power was required by multiplying it by negative one to suit this sign convention. The reversed polarity power of each waveform is compared to a threshold value that is equal to the median plus some portion of the median. This coefficient for the additional portion of the mean is set by default in the automatic processing software according to the findings of SHRP S-325 to 0.385. This portion of the median value was found to balance the number of false deterioration predictions to the number of false sound deck predictions such that an accurate overall deterioration quantity resulted. The bridge post-processing software does allow the user to change the threshold value, adjusting the results to seem more appropriate. After the calculations have been made using the bridge processing data results, the calculated deterioration characteristic quantities are shown for each waveforms in each data pass. Post-processing results consist of a bridge deterioration map showing the location of the unit deck areas that were found to exceed the threshold power and therefore exhibit deterioration characteristics in the data. These deterioration maps can be printed for reporting purposes.

The processing software was designed to allow technicians or laypersons to process the GPR data requiring only minimal experience in locating the interfacial peaks in the data. The software applications were specifically designed for use on typical slab on girder deck designs where the data exhibits reflections from the surface, asphalt/concrete interface, top and bottom layers of reinforcement, and the deck bottom. More complex decks such as prestressed and voided slab designs may not be interpreted properly by the software.

The time required to automatically process and post-process the data is dependant on the amplitude and clarity of the interfacial peaks. After inspecting all the data passes, the user may be able to produce the processing setup file within ten or fifteen minutes. Processing may take another ten or fifteen minutes depending on the number of waveforms collected per pass and the processing speed of the computer being used. Post-processing results can be achieved after just a few minutes of preparation and observation of the results. Repair estimates can be produced using the quantities produced from the post-processing output, but for this research the results were tabulated and re-drawn on a plan scaled map of the deck surface using AutoCAD and a brief report was written. This report production generally required two days of results tabulation and drawing.

Unfortunately, the software presents a “black-box” approach that does not permit the user to observe and control the tracking and measurement of every waveform. The power measured in each waveform in each pass can be observed after post-processing of the data, but can not be directly compared visually to each waveform. The power is graphed along the length of the data pass, and shows the position of the deterioration threshold. Values that appear significantly different from the normal range and that are close to the threshold can be included in the predicted deterioration results by adjusting the threshold. However, the user must trust the resulting output without ensuring the proper peaks were identified and tracked in the analysis.

5.2 Manual Processing of GPR Data

As this research project progressed, a need for an alternative technique of processing the GPR data was realized. Initial results obtained using the automatic processing software indicated that there was a poor correlation between the actual and the predicted deterioration quantity and locations and are discussed in Section 5.6.1. The alternative to automatic processing using the Penetradar software was to observe and evaluate the deterioration characteristics in the GPR data manually. An in-house manual

processing software program, called *pushbutn.exe*, was obtained from Penetradar that allows the user to identify in the data the start and end of the bridge, input the pass width, spacing and deck skew, measure thicknesses, and flag regions of the data that are found to exhibit deterioration characteristics. A similar peak tracking algorithm is used in the manual processing software for calculating thicknesses that is used in the automatic processing software, except that the manual processing software allows the user to see the peak being tracked within the gate as the data is being processed. The user also has the benefit of adjusting the tracking gate position to follow the desired peak should it migrate out of range of the gate. The user can browse through a series of data files and make a qualitative judgement on the condition of the deck based on the observed waveform qualities such as peak amplitude or signal attenuation. While totally subjective, this technique gives the user control over the analysis. The software allows the user to flag more than one characteristic, although only one characteristic may be examined individually per pass. Output consists of a bridge map drawn using simple ASCII characters in a MS-DOS file.

For this research, an innovative combination of signal attenuation and high reflectivity from the surface of the concrete slab (high relative dielectric constant) were used as deterioration characteristics in the data. Attenuation is apparent in the data through a significant reduction in all of the peaks contained within the waveform corresponding to the thickness of the slab. Most affected is the deck bottom echo, which makes an excellent indication of signal attenuation. Also accompanying a reduction in the slab peak amplitudes can be a slight increase in time position of the peak as the propagation velocity of the energy through the slab is increased due to the higher relative dielectric constant of the slab in deteriorated areas. Further attenuative characteristics in the data include a reduction in the clarity, or smoothness, of the individual peaks within the waveform resulting from scattering losses. Changes in the relative dielectric constant of the concrete near the surface of the slab are detectable by a significant increase in the asphalt/concrete peak amplitude. Both signal attenuation and changes in concrete relative

dielectric are detected through manual processing by relative comparison of a waveform to those near it in the data pass and to all waveforms observed in a given file. Changes in a particular waveform associated with deterioration can range from subtle to very pronounced contrast to waveforms representing sound concrete.

In both automatic and manual processing methods for the GPR data, the software will calculate the percent of the deck area that is predicted to be deteriorated and both provide simple deterioration maps of the deck. These deterioration locations found on these maps were tabulated for reporting purposes and also as an aid in drawing the deterioration locations on plan maps of the decks using AutoCAD. The deteriorated area was calculated based on the sum of these predicted deterioration areas in each pass and was divided by the surveyed deck surface area to obtain an estimate of the percent of the total deck area deterioration. Where passes overlapped, the resulting deterioration prediction quantities were corrected by subtracting the superimposed deterioration prediction areas to avoid double-counting these areas.

Each data pass was subdivided into unit areas of 0.25 meter length by the pass width. These passes and unit areas were drawn onto scaled plan maps of the deck surface areas on AutoCAD to denote the predicted deteriorated and sound regions of the slab.

The time required to inspect and analyze the radar data was dependant on the amplitude and clarity of the interfacial peaks with each data pass, but took approximately one full day for a typical data set of good clarity from a 400 m² deck surface area. Vague data required considerably more inspection time in order to decide where the various interfacial reflections existed and to make judgements regarding the data characteristics associated with the predicted sound and deteriorated regions of the deck surface. Subsequent tabulation and production of plan scaled maps of the deck surface area showing the predicted deteriorations generally required an additional two days. Compared to automatic processing, the manual processing is much more labour intensive

and time consuming, but gives the user more confidence in the results and allows the user to influence the results according to intuition and consideration of other factors.

5.3 Chain Drag Data Processing

The chain drag field data was sketched to the nearest 0.05 meter on scaled plan drawings of the deck surface. The vertices of each area found to be deteriorated on the deck using the chain drag method was drawn onto the plan map of the deck surface to form polygons using AutoCAD. The deterioration locations found using the chain drag method were then compared to those predicted by both GPR processing methods. The total deteriorated area found using the chain drag method was easily measured from the plan map of each deck using AutoCAD.

5.4 Half-Cell Potential Survey Data Processing

The half-cell potential survey data were tabulated using their longitudinal and transverse location on the deck and the measured voltage. Isopotential contour maps were produced to demonstrate the distribution of voltage across the deck surface. According to ASTM C 876-91, a voltage that is more negative than -0.35 volts indicates that there is at least a ninety percent probability that active corrosion exists on the top layer of reinforcement at that location. Since contours were produced in 0.02 volt increments, the -0.36 volt contour lines provided a boundary by which the area predicted to have active corrosion could be measured. These lines were imported into the AutoCAD drawings of the deck surfaces for measurement and comparison to the GPR predicted deterioration locations.

5.5 Issues Regarding Data Interpretation

It is important to understand that each of the test methods used in this research is an estimate of a deterioration symptom of the entire deterioration process. These symptoms can correspond to timeframes of the entire deterioration process ranging from initial moisture and chloride ingress into the slab to complete corrosion and delamination of the slab. Figure 19 describes how these methods approximate the actual deterioration regime by considering different symptoms. The predicted areas of these methods based on these symptoms will tend to have areas of confluence and divergence depending on the age of the deterioration process for each localized area of the bridge deck under study. GPR is used to locate areas of excess moisture and chloride, the half-cell potential survey is used to locate areas of active corrosion, and the chain drag survey is used to locate areas of concrete that have cracked or debonded from the top mat of reinforcement due to corrosion. Using these methods to assess the accuracy of GPR implies that all methods are expected to produce similar results. However, given the range of time frames that different symptoms represent, it follows that a significant level of divergence among the results must be expected.

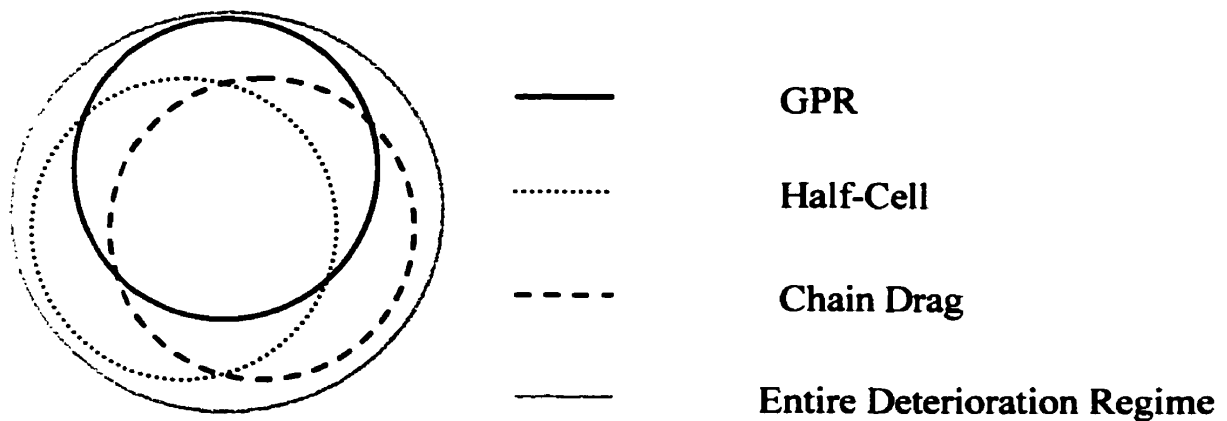


Figure 19 - Diagram showing convergence and divergence of test methods

There exist assumptions, experimental errors, and simplifications in each test method that need to be comprehended when a comparison between these methods is made. These effects must be included in the justification of differences between the results of each test method.

5.5.1 GPR Data

Deterioration in bridge decks is correlated to the presence of excess moisture and chloride in the deck. Excesses of moisture and chloride are found to generally exist under usual conditions in the Atlantic Canadian climate at most of the deck deterioration phases. The exception to this is at the onset of moisture and chloride ingress into the concrete cover and also periods of extremely dry weather that tend to remove the interior excesses of moisture from the deck slab. It is the combined interactive effect of moisture and chloride that leads to noticeable attenuation of the radar waveform. Without sufficient amounts of chloride, the effect of excess moisture is small on signal attenuation and vice versa according to Alongi et al. (1993). Except in very dry periods of weather, sufficient excesses of moisture and chloride can be found within deteriorated areas in reinforced concrete decks when chloride is applied in wintertime as a deicing agent.

Attenuative effects on the radar waveform may not be due exclusively to the combined interaction of moisture and chloride in the concrete deck slab. The effects of other phenomena on the GPR waveform such as alkali-aggregate reactivity and its associated chemical products and cracking have not been studied to date. Certainly, energy losses in the data will occur from other forms of deck deterioration that result in local changes in relative dielectric constant and in increased signal scattering from layer non-homogeneity or cracks. Not all energy losses that are due to moisture and chloride can be correlated to observed phenomena from the half-cell and chain drag surveys. A

portion of these attenuative effects will represent phases of the deterioration process that are not detectable using these survey methods.

Detection of deck deterioration is based on a relative comparison of waveforms within a data pass or series of passes on a single deck. If there is good contrast between the areas of sound concrete and deteriorated concrete, then the difference is easily noticeable and less error can be expected in the results. Decks that have very low and very high quantities of deterioration may present difficulties in making a correct deterioration prediction. On decks that exhibit high levels of deterioration, the areas of sound concrete may exhibit signs of moisture and chloride ingress, alkali-aggregate reactivity, poor asphalt concrete quality, and micro-cracking that may cause signal attenuation, leaving little contrast between delaminated and non-delaminated regions of the deck. These problems lead to a higher level of background attenuation levels in the data, making detection of localized, corrosion related, signal attenuation more difficult. The probability of detecting deteriorated and sound areas of concrete is reduced, while the probability of false predictions is increased. Identification of the bottom echo can be difficult in data from such decks because the bottom echo amplitude can be reduced to the level of the background clutter or pseudo-peaks created by superposition of near interfaces. Decks in very good condition can also be misleading as slight changes in the signal characteristics can be misinterpreted as signal attenuation, leading to increased potential for false predictions of deterioration. Establishing a known location of deterioration on the deck allows the processor to establish a threshold level of attenuation by which the remainder of the data can be assessed.

Signal processing of several decks that were analyzed in this research revealed that some physical constraints can result in difficulties in data interpretation. Since the data processing is based on a relative comparison of the waveforms, changes in the waveform due to different numbers of prestressing tendons, that may also vary in depth on the deck cross-section, can create substantial internal scattering that may render a

relative comparison useless. Tendons that vary in position at different locations along the length of the deck will result in peaks that are located at different time positions, and hence slightly different amplitudes due to background signal attenuation as a function of depth, making the relative comparison of waveforms very difficult. Another type of deck, such as a monolithic deck, devoid of supporting girders, of varying thickness provides similar difficulties with the added effect of non-orthogonal reflection from the deck bottom. Depth penetration is another issue on extremely thick decks and also those which contain high chloride contents. Steel fiber reinforced concretes may present a signal penetration and signal scattering problems because of the more homogenous distribution of steel throughout the deck thickness and the random orientation of each fiber causing reflections from unknown depths and non-orthogonal reflections to the direction of transmission. Synthetic fiber reinforced concrete decks may behave similarly to a normal concrete deck, depending on the dielectric properties of the material and its addition rate to the concrete.

Other decks that were examined in this research contained epoxy coated steel reinforcement. This epoxy coating is used as a barrier to prevent moisture and chloride from contacting the steel and therefore protecting the steel from corrosion. Unfortunately, this epoxy barrier also undermines the assumption that deterioration will be found where excessive moisture and chloride are detected in the deck using GPR. It is also unfortunate that the presence of epoxy coating on the reinforcement cannot be detected in the GPR signal. Hence, unless there is prior knowledge of the use of epoxy coated reinforcement in a given deck, the GPR survey may severely overestimate the level of deterioration.

The nature and condition and even existence of asphalt pavement overlay on a deck will affect the ability to interpret deterioration characteristics in the radar data. The lack of an asphalt overlay on a deck will allow moisture not just to penetrate more easily into cracks and highly permeable regions of the concrete, but will also allow them to dry

out more quickly. This means that the interactive effect between moisture and chloride on signal attenuation can be reduced on exposed concrete decks, making the contrast between probable deterioration and sound concrete less obvious. A porous asphalt pavement layer, designed using primarily coarse aggregates and containing substantial voids for drainage, can entrap water in the short term, but also facilitate drying. Furthermore, these pavements will tend to accumulate chloride and tend to cause signal scattering due to the voids, reducing the signal penetration into the deck.

The automatic processing software allows the user to vary a threshold level to affect the processing results. Raising or lowering the threshold affects the severity of the deterioration condition that is desired in the result. The location of clusters of problematic areas are unaffected by changing the threshold but their extent and density on the deck and the predicted quantity are affected. In manual processing of the data, there is no such numerical threshold by which the user compares calculated coefficients to determine the condition of each unit area on the deck. With experience, the user becomes accustomed to observe sufficient relative change in the signal that deterioration is likely in a particular area. Each deck, and the associated level of signal change, is different depending on background attenuation levels and the contrast between obviously sound and deteriorated areas of the deck slab. It may be hypothesized that a higher degree of attenuation may be associated with a higher degree of deterioration severity, but it becomes difficult to use an absolute threshold level of as a decision tool considering the other potential factors affecting the signal, that are unknown to the inspector. Instead, a variable threshold is used depending on the clarity and contrast observed in the data in particular regions of a given deck slab. Again, this is a highly subjective process that is operator-dependant.

There are interpretative errors that can be made in both automatic and manual modes of processing GPR data. Multiple asphalt pavement layers often exhibit reflections of varying intensity that can make identifying and tracking the

asphalt/concrete interface difficult, especially if those layers are thin and/or deteriorated. Thin layers provide an additional challenge when measuring thickness because of interference between the surface and interfacial reflections. The true amplitude of the interfacial reflection can be observed and measured by subtracting a replica of the flat metal plate file that is scaled to the same amplitude of the surface reflection from the waveform. Top reinforcement layers can be difficult to distinguish and track in the waveform if the concrete cover is thin for this same reason. The depth to reinforcement can vary substantially from deck to deck as well as within the same deck.

Other interpretative errors arise due to the bridge design. Structures that have multiple interior supports and continuous girders supporting the deck are subject to negative moments at these supports. The decks are therefore designed to contain more steel at the top layer of reinforcement at these locations. The effect on the signal is to increase the amplitude of the top reinforcement layer reflection. In some cases, the steel content is so high that the reinforcement grid reflects most of the transmitted energy and information cannot be obtained from deeper within the slab. Where decks experience positive moments, the steel content is increased at the bottom layer of reinforcement, causing a similar increase in the bottom reinforcement layer reflection. In these conditions, the entire data pass may contain regions of varying reinforcement reflection intensities. Other deck designs such as full-depth slabs and pre-stressed voided slabs present different waveforms than the typical slab-on-girder design. These types of bridges have a slab depth that tends to exceed the penetration depth capability of the radar system. Data from these structures tend to exhibit no deck bottom echo and varying reinforcement reflection intensities. Furthermore, on thick slabs, the deeper reflections tend to be weaker due to increased background attenuation which is a function of the depth of the slab. This may pose a problem with automated processing of the data if the algorithm is based on assumed constancy of all the reflected peaks. Manual processing of these structures is also difficult because of the discontinuous nature of the data along

the entire pass length. Relative comparison must be made within similar regions of the data.

Deck conditions are assumed to be constant over the entire surface area, but this is not so. Regions of pavement nearest the curbs are more likely to be deteriorated with age and are more likely to contain moisture as surface runoff is directed to drains located in these areas. Metallic trash and soil and debris that tend to hold moisture tend to accumulate in the curbs of the bridges. These conditions have an effect on the surface dielectric measurement and the amount of energy that can be directed into the deck.

Diaphragms that are placed transversely across the deck width between the girders and diaphragms at joint locations can cause “apparent attenuation” in the signal. In steel members, the positively oriented reflection from the stringer or diaphragm counteracts the negatively oriented reflection from the concrete/air interface at the deck slab bottom. The net effect is a reduction in the deck bottom echo that may appear as though it was caused by moisture/chloride effects in the slab. However, signal attenuation caused by excesses of moisture and chloride normally affect the entire waveform, inducing distortion in the shape and a reduction in reflected peak amplitudes.

Increased asphalt/concrete reflection amplitudes can be an indicator of excess moisture in the concrete slab adjacent to the interface, asphalt pavement that has become debonded from the concrete slab and contains moisture at the separation, or may indicate moisture intrusion through a waterproofing membrane and/or surface scaling. Debonded asphalt and failed membranes are not accounted for by the chain drag or the half-cell potential surveys and will increase the quantitative difference between these two methods and the GPR predictions.

The position of the antenna relative to the location of the deterioration will affect the attenuative effect in the radar waveform, as will the size of the defect. At the

operating height of the antenna, the beam produces a “footprint” or coverage area on the deck surface that is oval in shape and is approximately one meter wide by sixty centimeters wide, and increases in size with depth. Deterioration effects in the data are maximized when they are located directly under the antenna since the transmitted beam is more concentrated nearest the center. Deterioration effects that are located farther from the center of the beam are weaker in the data. Deteriorated areas that are small relative to the size of the beam coverage area will have a lesser effect than large areas of deterioration.

The condition of the deck slab surrounding joints is more difficult to ascertain than deck slab condition from interior areas of the structure. The geometry is much more complex, depending on the joint design, and can not be modeled without prior knowledge of the components. This is very impractical for field testing as the joint can be covered by asphalt pavement and the design may be unknown. Certainly, joints produce a different waveform than the deck slab does. Steel content and positions at joints are usually higher and different, respectively, than in slabs and tend to create multiple higher intensity reflections in the waveform when the joint is in good condition. This may pose a problem for automated processing of the data that compares waveform peak amplitudes and construction along an entire section of a data pass. Joints in poor condition can be detected manually by observing the adjacent data on either side of the joint and by observing the reflections at the joint. The transition from typical deck waveforms to joint waveforms tends to gradually decrease with the bottom echo decreasing in amplitude and becoming more distorted in shape as the data changes from sound deck to deteriorated joint material. Joints that are in good condition tend to exhibit more abrupt changes in deck bottom reflection as the data changes from slab to joint.

GPR data is organized for processing by dividing each pass into unit areas of length and pass-width. These unit areas are drawn onto the deck surface to represent zones of predicted deterioration. It is important to understand that a unit area may not be

entirely deteriorated, but contains sufficient deteriorated area that it is detectable in the data. Quantitative dissimilarity due to size differences between the unit area prediction and the actual extent of deterioration area must be expected.

Longitudinal position of the radar on the deck is determined from the data by observing the number of pulses recorded from the distance measuring instrument of the ABS braking system on the van. The number of pulses is multiplied by a constant to obtain distance. Small errors in calibration of this constant can cause slight misposition of the predicted area with the actual test location. This error increases with increasing deck length. Careful calibration of the distance measuring instrument constant is therefore very important.

5.5.2 Chain Drag Data

Conducting the chain drag survey is simple, using a subjective test criteria where the sound of the chain impacting the deck surface is interpreted as hollow sounding or not by the operator. Interpretative errors can arise due to a number of conditions such as the chain size used, traffic, operator fatigue, presence of debris or waterproofing membrane on some areas of the deck surface, non-corrosion induced cracking, and the proximity and size of delaminations.

Typically, a six foot length of one-half to three-eighths inch diameter chain is used for the survey. Other configurations include a series of shorter, smaller diameter chains attached to an arm on the end of a long handle, in similar fashion to a rake. Chain weight and size affect the amount of energy directed into the deck and the frequency of that energy. This affects the depth from which the energy will be reflected with sufficient amplitude that a significant difference between sound and unsound concrete can be detected by the operator. Heavier chains direct more energy deeper into the slab than lighter chains. The pitch and tone of the reflected sound from the delamination also differs according to the weight of chain used.

A major contributing factor to misinterpretation of chain drag sounding is traffic noise. Surveys are normally conducted on a single closed lane of a structure, while the other lane or lanes remain open to traffic. Often, the traffic is passing within four to ten feet of the operator while the deck is being surveyed. Noise from large trucks can make it very difficult to detect a change in the sound produced that identifies a delamination.

Operator fatigue can play a role in misinterpretation of chain drag sounding. On bridge decks that are in good condition, the operator can begin to “detect” suspicious areas of deck that sound somewhat different than other areas, but do not produce obvious sounds indicative of delaminations.

lighter chains. The pitch and tone of the reflected sound from the delamination also differs according to the weight of chain used.

A major contributing factor to misinterpretation of chain drag sounding is traffic noise. Surveys are normally conducted on a single closed lane of a structure, while the other lane or lanes remain open to traffic. Often, the traffic is passing within four to ten feet of the operator while the deck is being surveyed. Noise from large trucks can make it very difficult to detect a change in the sound produced that identifies a delamination.

Operator fatigue can play a role in misinterpretation of chain drag sounding. On bridge decks that are in good condition, the operator can begin to “detect” suspicious areas of deck that sound somewhat different than other areas, but do not produce obvious sounds indicative of delaminations.

Rehabilitation construction of decks is a dirty and dusty procedure that requires the deck surfaces to be swept clean of dirt and debris after the asphalt pavement and waterproofing membranes have been stripped from the deck. Sometimes not all of the debris is swept from the deck or all of the membrane stripped from the deck surface. Both debris and partially bonded membranes can produce hollow sounds that are similar to delaminated concrete.

In some cases, the asphalt pavement has been so well bonded to the deck surface that work crews needed to use light jackhammers to remove the pavement from the deck surface. The impact of the hammer on the deck surface tends to spall small pieces of the cover concrete from the remainder of the deck, inducing small surficial “delaminations” that will be detected by the chain drag survey.

Lastly, it is important to remember that results from the chain drag survey are a combination of visual assessment of the deck surface, areas that produced a hollow

delaminated sound from the chain drag test, and also areas of deck that is not deteriorated. These non-deteriorated areas of the deck become included into the chain drag survey results by grouping clusters of delaminations into simple parallelograms for removal and repair. In some cases, small areas of sound deck are found within large areas of deteriorated deck and are removed intentionally to simplify the repair operation as a whole.

While GPR is used to detect moisture and chloride ingress into the deck, and the half-cell potential survey is used to detect active corrosion, both of which may be precursory to the formation of a delamination, the chain drag survey will not detect areas of excess moisture and chloride or active corrosion that has induced insufficient stress in the deck to form a delamination.

5.5.3 Half-Cell Potential Data

The half-cell potential survey is a more objective test than the manual processing technique of radar data interpretation or chain drag survey methods because it uses a fixed standard threshold instead of relying on subjective test criteria. The test procedure and density of data collection points are standardized in ASTM C 876-91 as are means of data interpretation. In this research, the data collection points were assigned coordinates representing the longitudinal and transverse distance from a fixed point on the deck surface. After tabulating the data, contour plots were produced using a software package called Surfer. Contours were generated for every step of 0.02 volts using a Kriging interpolative curve-fitting model with smoothing effects. It must be re-emphasized that the -0.35 volt threshold only gives an indication that there is a ninety percent probability of active corrosion. Certain effects may occur that tend to shift the actual threshold that may best represent the active corrosion on a given deck.

Since the half-cell electrode is used to measure the electrical potential field surrounding the corrosion induced current in the reinforcement, the moisture content and electrical connectivity of the concrete cover over the reinforcement play an important role in the value of the measured potential. Concrete cover that is very dry will be more insulated and cause values that are less negative to be observed in areas overlying active corrosion. In regions of deck deterioration where the concrete cover has completely debonded from the reinforcement and underlying concrete, potentials can result that may not indicate deterioration at all due to the insulating effect of the air gap between the cover and the remainder of the slab. Furthermore, the interpolation tends to falsely include areas of sound concrete into the reported active corrosion areas, and vice versa, due to the curve fitting approximation.

Aside from moisture and electrical connectivity effects causing misinterpretation in the results, the smoothing effect of the Kriging interpolation model used to create the contour lines from the raw data may also tend to obscure some areas of deterioration within areas of sound concrete, and vice versa, if the respective potentials are close to the -0.35 volt threshold. As a result, some small areas of deterioration that may be observed in the other detection methods results may not be observed in the half-cell method results.

5.6 Comparison of Bridge Deck Survey Results

Results from the GPR, chain drag and half-cell potential survey methods were compared both graphically and statistically to describe the correlation and differences among them. The resulting quantities and spatial distribution of deterioration was analyzed statistically to establish the accuracy and level of difference to be expected of the GPR survey relative to the chain drag and half-cell potential survey methods. Numerical accuracy of both GPR processing techniques relative to the ground-truthing survey methods was computed based on the basic estimate and total measured deteriorated surface area, respectively. Spatial correlation was described statistically by

observing the prediction and outcome of each unit radar prediction area of 0.25-meter length by pass width. Agreement, or convergence, between the predicted and observed deterioration was considered to be confirmed if at least one-third of the unit prediction area contained observed deterioration. There are four scenarios that can result from each unit area prediction:

- 1) A true detection of deterioration, (A);
- 2) A false detection of deterioration, (B);
- 3) A true detection of sound concrete, (C); and
- 4) A false detection of sound concrete, (D).

Of these scenarios, the actual deterioration area will be described by the sum of the true deterioration and false sound predictions (A+D), while the actual area of sound concrete will be described by the sum of the false deterioration and true sound concrete predictions, (B+C). Obviously, to maximize spatial correlation the best method would maximize the true predictions and minimize the false predictions. Statistics were constructed to describe the accuracy, false alarm rates, and probability of correct detections for manual and automatic processing techniques relative to the chain drag and half-cell potential surveys by counting the various outcomes of all of the unit prediction areas, as follows:

$$\text{Percent Correct Deterioration Prediction} = A/(A+B)$$

$$\text{Percent Correct Sound Concrete Prediction} = C/(C+D)$$

$$\text{Percent Total Correct Predictions} = (A+C)/(A+B+C+D)$$

$$\text{Percent Total Incorrect Predictions} = (B+D)/(A+B+C+D)$$

$$\text{Probability of Correctly Detecting Deterioration} = A/(A+D)$$

$$\text{Probability of Correctly Detecting Sound Concrete} = C/(B+C)$$

$$\text{False Alarm Rate of Detecting Deterioration in Sound Concrete} = B/(B+C)$$

$$\text{False Alarm Rate of Detecting Sound Concrete in Deterioration} = D/(A+D)$$

These statistics were used not just to describe how the predicted quantity compares to the quantity found by the ground-truthing methods, but also how the locations of predicted deterioration compare to the deterioration locations as found by the ground-truthing methods. However, it must be remembered that the actual deterioration quantities must be compared to the predicted quantity, not just the percent of correct deterioration predictions, since the false deterioration predictions are counteracted by the false sound concrete predictions.

5.6.1 Preliminary GPR Automatic Processing Results

The earliest GPR surveys in this research project were processed using version 1.10 of the Penetradar automatic processing software. Comparison between these results and the observed deterioration made the accuracy of these surveys questionable. Results from seven of these early structures are listed in

The Robie Street Overpass, McClures Overpass, and Lower truro Road Overpass were constructed using epoxy coated reinforcement. It can be observed that the GPR predictions did not correlate well with the actual quantity of deterioration observed for these three decks. It is hypothesized that although the automatic processing did not perform well for the other decks listed in Table 3, the differences for these three decks is more attributable to the epoxy coating preventing the chloride depassivation, and hence the ensuing corrosion, of the reinforcement. Even if the automatic processing had perfectly identified the areas of excessive moisture and chloride ingress into the deck, the usual correlation between excess moisture and chloride cannot be assumed because of this barrier effect of the epoxy.

Table 3 showing the GPR predicted deterioration estimates and the actual deterioration quantity found using the chain drag method. Unfortunately, no records

were retained of the location and spatial extent of the observed deterioration to compare to the GPR predicted deterioration. These early results were found to have poor correlation between the GPR predicted and actual deterioration quantities. Poor spatial correlation between the GPR predicted and actual deterioration locations was observed on the decks.

The Robie Street Overpass, McClures Overpass, and Lower Truro Road Overpass were constructed using epoxy coated reinforcement. It can be observed that the GPR predictions did not correlate well with the actual quantity of deterioration observed for these three decks. It is hypothesized that although the automatic processing did not perform well for the other decks listed in Table 3, the differences for these three decks is more attributable to the epoxy coating preventing the chloride depassivation, and hence the ensuing corrosion, of the reinforcement. Even if the automatic processing had perfectly identified the areas of excessive moisture and chloride ingress into the deck, the usual correlation between excess moisture and chloride cannot be assumed because of this barrier effect of the epoxy.

Table 3 - GPR predictions and actual deterioration quantities on initial structures

Structure ID	Chain Drag Deterioration Quantity (m ²)	GPR Predicted Deterioration Quantity (m ²)	Difference (m ²)	Difference (%)
McClures OP	37.9	77.2	-39.3	-103.7%
Robie Street OP	65.0	129.3	-64.3	-98.9%
Lower Truro Rd	148.3	164.9	-16.6	-11.2%
Joseph Howe OP	171.5	487.5	-316.0	-184.3%
Dutch Village OP	13.1	73.2	-60.1	-458.8%
CNR OP	15.9	31.4	-15.5	-97.5%
Middle R. Bridge	286.7	39.8	246.9	86.1%

From these early results, it became apparent that the automatic processing did not appear to perform as well as described in SHRP S-325 where accuracy of ± 11.2 percent of the ground truth quantities was reported. It was unknown if the poor correlation between actual deterioration quantities and those predicted using the automatic processing software was due to a lack of experience in interpreting the radar waveforms, improper use of the software, or perhaps a problem with the software itself. After supervision was provided by the Penetradar Corporation, it was determined that improper usage of the software was not likely to be the cause of the poor results. At this point, manual processing of the radar data was introduced into the research program to address these correlation problems. Future structures that were surveyed using GPR were processed both using the newer version 3.10 of the automatic processing software and using the manual processing technique for this research. The inclusion of processing the GPR data manually resulted in a significant increase in the amount of time and effort required to process the data. At the same time, manual processing introduced a significantly higher degree of subjectivity into the data analysis. Minimal operator influence was one of the selection criteria for the most appropriate method in identifying deterioration in asphalt paved reinforced concrete bridge decks, but as the results from the following nine structures will show, the manual processing technique offers the user better opportunity to apply quality control on the analysis that results in a more accurate estimate that better represents the actual deterioration that exists in each deck.

5.6.2 Glendale Bridge

The Glendale Bridge is located on Highway 105 approximately 22 km north of Port Hastings, Inverness County. It is a slab on steel girder design with a length of 37.5 meters and a width of 8.4 meters. The deck was surveyed using GPR on March 19, 1997 and rehabilitated during the summer of 1997. The GPR data appeared to be of good to very good clarity in which the reflections from interfaces and reinforcement were well formed and easily distinguishable.

Appendix A1.1 shows a plan view map of the deck surface using red hatching to designate where signal attenuation was detected in the GPR data using manual processing. Green hatching is used to designate where debonded concrete; delaminations and surface scaling were detected using the chain drag method. Good correlation between the manual GPR results and the chain drag results are apparent in the region of the abutment joints and interior joints. However, poor correlation can be seen in radar data pass “B” and “G” where a significant amount of deterioration was found using the chain drag method, but not found using GPR in the central and northern spans. Appendix A1.2 shows a similar plan map of the deck surface using red hatching to designate where signal attenuation was detected in the GPR data using manual processing and a solid black line representing the -0.36 volt contour line established using the half-cell potential survey. The area bounded by this contour represents zones of active corrosion in the deck as stipulated by ASTM C 876-91. The data shows good correlation between active corrosion detected about the joints of the deck and the GPR detections similarly located. GPR resulted in no detections in the central span along radar pass “B” where several major areas of active corrosion were detected. One group of manually processed GPR detections on the northern span does occupy a similar region as a large area of active corrosion. Overall, the half-cell potential survey did not detect similar quantities or all of the locations as the chain drag survey method, but there exists good correlation between these two ground-truthing methods at several of the deteriorated areas on the northern interior joint, and on the eastern edge of the central and northern spans.

Appendix A1.3 shows a similar plan map of the deck surface using black hatching to designate where signal attenuation was detected in the GPR data using automatic processing and green hatching to designate where debonded concrete, delaminations and surface scaling were detected using the chain drag method. The automatic processing results correlate more favorably with the actual deterioration found on the deck using the chain drag method, particularly with the deteriorated areas found along pass “B” of the

radar survey, but resulted in numerous false detections in the central span. Two major zones of deterioration were not detected in the northern span using the automatic processing method for the GPR data. Appendix A1.4 shows a similar plan map of the deck surface using black hatching to designate where signal attenuation was detected in the GPR data using automatic processing and a solid black line bounding the zones of active corrosion detected in the deck. Again, little active corrosion was detected throughout the central span where the majority of GPR detections were located. Good correlation between the automatic processing results and the areas of active corrosion can be observed in radar pass “B” on the eastern edge of the central and northern spans and along the joints of the deck.

Appendix A1.5 shows a similar plan map of the deck surface using black hatching to designate where signal attenuation was detected in the GPR data using automatic processing and red hatching to designate where signal attenuation was detected in the GPR data using manual processing. It is evident that both methods detect attenuation near the joints of the deck, while the automatic processing detected more attenuation throughout the central span than could be observed using manual processing. Both manual and automatic processing detected attenuation in the southern span that neither the half-cell or chain drag methods detected deterioration. While the automatic processing detected more of the deterioration found using the ground-truthing methods, it also resulted in more false detections of deterioration, leading one to the conclusion that, based on graphical observation alone, the manual and automatic processing techniques performed at similar levels of accuracy on this particular deck.

Considering the graphical spatial correlation of results, the automatic processing seems to identify the areas of deterioration detected by the half-cell potential and chain drag surveys better than the manual processing of the GPR data for the Glendale bridge. The quantitative and spatial estimate statistics are listed in Table 4 for the Glendale Bridge.

Table 4 – Quantitative and spatial estimate statistics – Glendale Bridge

Glendale Bridge				
Predicted versus Actual and Ground-truth Quantities (Expressed as a Percentage of Deck Surface Area)				
GPR Predicted Quantity (Automatic)	29.1%			
GPR Predicted Quantity (Manual)	16.2%			
Actual Quantity Removed	22.6%			
Chain Drag Quantity	20.1%			
Half-Cell Quantity	9.3%			
GPR Spatial Correlation Statistics	Total GPR Unit Areas on Deck = 1350			
	Relative to Chain Drag		Relative to Half-Cell	
	Manual	Automatic	Manual	Automatic
True Deterioration Predictions	106	174	61	114
False Deterioration Predictions	68	188	114	254
True Sound Predictions	996	866	1088	950
False Sound Predictions	180	122	87	32
% Correct Deterioration Predictions	60.9%	48.1%	34.9%	31.0%
% Correct Sound Predictions	84.7%	87.7%	92.6%	96.7%
% Total Correct Predictions	81.6%	77.0%	85.1%	78.8%
% Total Incorrect Predictions	18.4%	23.0%	14.9%	21.2%
Probability of correctly detecting deterioration	37.1%	58.8%	41.2%	78.1%
Probability of correctly detecting sound concrete	93.6%	82.2%	90.5%	78.9%
False alarm rate of detecting deterioration	6.4%	17.8%	9.5%	21.1%
False alarm rate of detecting sound concrete	62.9%	41.2%	58.8%	21.9%

The half-cell potential survey quantity resulted in significantly less deterioration detection than the chain drag method due to a lack of electrical activity detected along the abutment joints and in the area of surface scaling found on the northern edge of the easternmost span. These areas did not produce a hollow sound using the chain drag test, that would indicate delamination, but were outlined for removal because of the economy in replacing all joints at one time and because of the high probability of future reinforcement corrosion below the scaled concrete.

The quantities obtained using the manual processing were closer to the chain drag and the half-cell quantities than the those obtained using the automatic processing of the GPR data. The percent of correct deterioration predictions using manual processing exceeded that obtained using the automatic processing relative to both ground-truthing methods. However, the correct prediction rate of sound concrete was approximately the same for each method, giving a higher percent correct prediction rate for the manual technique than the automatic processing software due to the increased correct deterioration prediction rate of the manual processing technique on this particular deck. The fair correlation observed in the figures contained in Appendix A1 between the manual processing results and the chain drag and half-cell potential surveys is described well by the low 37.1% probability of correctly detecting deterioration and the moderately high 62.9% false alarm rate of detecting sound concrete using manual processing on this particular bridge deck. The majority of deterioration that was unidentified by the manual GPR processing results occurred in Pass "B". Extensive deterioration that is found along one strip of data that is bounded by two other strips of sound concrete data can sometimes be difficult to detect because the user may believe that the deck geometry is influencing that particular pass, rather than deck deterioration. Deck deterioration does not usually remain confined longitudinally along one strip of data, but can be identified at the same general distance in adjacent passes. The automatic processing also exhibited a moderately high false alarm rate of 58.8% in detecting sound concrete due to the lack of deterioration detections in the western edge of the northern span.

5.6.3 Rough Brook Bridge

The Rough Brook Bridge is located on Highway 105, approximately 15 km north of Port Hastings, Inverness County. It is a slab on steel girder design with a length of 34.2 meters and a width of 8.6 meters. The deck was surveyed using GPR on March 19, 1997 and rehabilitated during the summer of 1997. The data in general was of poor to fair clarity, exhibiting much distortion and a lack of well defined reflections from the

interfaces and reinforcement. These poor quality data may be due to general excesses of moisture and chloride and/or deteriorated asphalt pavement on the deck that may cause signal scattering and losses at all points on the deck rather than just excess losses at the deteriorated areas.

Appendix A2.1 shows a plan view map of the deck surface using red hatching to designate where signal attenuation was detected and blue hatching to designate where high concrete reflectivity, or high concrete relative dielectric constant was found in the GPR data using manual processing. Green hatching is used to designate where debonded concrete; delaminations and surface scaling were detected using the chain drag method. Good correlation between the manual GPR results and the chain drag results are apparent in the region of the abutment and interior joints as well as in numerous small delaminations in all spans. However, there are also numerous small areas of deterioration that were found using the chain drag method, but not found using GPR. The half-cell potential survey was not conducted on this deck.

Appendix A2.2 shows a similar plan map of the deck surface using black hatching to designate where signal attenuation was detected in the GPR data using automatic processing and green hatching to designate where debonded concrete, delaminations and surface scaling were detected using the chain drag method. The automatic processing results seem to correlate as well with the actual deterioration found on the deck along the joints, but appears not to detect deterioration in many of the delaminated areas found in on the deck spans. Rather, the automatic processing results appear to identify small groups of detections in areas that were found to be in good condition by the chain drag survey.

Appendix A2.3 shows a similar plan map of the deck surface using black hatching to designate where signal attenuation was detected in the GPR data using automatic processing and red and blue hatching to designate where signal attenuation and high

concrete reflectivity, respectively, were detected in the GPR data using manual processing. It is evident that both methods detect attenuation in some similar regions of the deck, but a large number of non-similar areas were detected as deteriorated by each processing method. Considering the graphical spatial correlation of results, both GPR processing methods appeared to perform equally well for this bridge. Table 5 lists the quantitative and spatial estimate statistics for the Rough Brook Bridge.

Table 5 – Quantitative and spatial estimate statistics – Rough Brook Bridge

Rough Brook Bridge				
Predicted versus Actual and Ground-truth Quantities (Expressed as a Percentage of Deck Surface Area)				
GPR Predicted Quantity (Automatic)	21.7%			
GPR Predicted Quantity (Manual)	21.2%			
Actual Quantity Removed	29.4%			
Chain Drag Quantity	27.2%			
Half-Cell Quantity	N/A			
GPR Spatial Correlation Statistics		Total GPR Unit Areas on Deck = 1233		
	Relative to Chain Drag		Relative to Half-Cell	
	Manual	Automatic	Manual	Automatic
True Deterioration Predictions	203	150	N/A	N/A
False Deterioration Predictions	54	112	N/A	N/A
True Sound Predictions	661	694	N/A	N/A
False Sound Predictions	315	277	N/A	N/A
% Correct Deterioration Predictions	79.0%	57.3%	N/A	N/A
% Correct Sound Predictions	67.7%	71.5%	N/A	N/A
% Total Correct Predictions	70.1%	68.5%	N/A	N/A
% Total Incorrect Predictions	29.9%	31.5%	N/A	N/A
Probability of correctly detecting deterioration	39.2%	35.1%	N/A	N/A
Probability of correctly detecting sound concrete	92.4%	86.1%	N/A	N/A
False alarm rate of detecting deterioration	7.6%	13.9%	N/A	N/A
False alarm rate of detecting sound concrete	60.8%	64.9%	N/A	N/A

Both GPR processing methods resulted in similar quantity estimates, but the manual processing technique exhibited a higher percentage of correct deterioration predictions than the automatic processing software results. Both processing techniques exhibited similar correct prediction rates for the existence of sound concrete. In spite of

the higher percent correct sound concrete prediction rates for each method, the manual processing technique correctly predicted less sound concrete areas than the automatic processing. Both GPR processing methods exhibited similar probabilities of correctly detecting deteriorated and sound concrete. As observed in the figures of Appendix A.2, both methods performed similarly in predicting the quantity and extent of deterioration on this particular deck, however, the low probabilities of the manual and automatic GPR processing methods of correctly predicting deterioration locations may be attributed the poor clarity of the data and the resulting lack of significant contrast of the signal shape and amplitude between the deteriorated and sound regions of the deck.

5.6.4 Victoria Bridge

The Victoria Bridge is located on Highway 105, approximately 19 km north of Port Hastings over the River Inhabitants, Inverness County. It is a slab on steel girder design with a length of 28.0 meters and a width of 8.5 meters. The deck was surveyed using GPR on March 19, 1997 and rehabilitated during the summer of 1997. The data in general was of good clarity, exhibiting some distortion and generally well defined reflections from the interfaces and reinforcement. This level of clarity indicates that the deck materials are generally in sound condition and free of scattering losses due to cracks and non-homogeneities.

Appendix A3.1 shows a plan view map of the deck surface using red hatching to designate where signal attenuation and high concrete reflectivity were detected in the GPR data using manual processing. Green hatching is used to designate where debonded concrete; delaminations and surface scaling were detected using the chain drag method. Good correlation between the manual GPR results and the chain drag results are apparent in the region of the abutment and interior joints. Many apparently random detections can be seen that were detected using the manual processing technique, of which two of the larger areas occur in proximity to the two areas of deterioration detected within the

northern span. The manual GPR processing appears to have a fair correlation to the deterioration quantity and locations found using the chain drag method.

Appendix A3.2 shows a similar plan map of the deck surface using red hatching to designate where signal attenuation was detected in the GPR data using manual processing and a solid black line representing the -0.36 volt contour line established using the half-cell potential survey. The area bounded by this contour represents zones of active corrosion in the deck. Virtually no active corrosion was detected on the entire slab, except for a small area located on the northern span that lies in close proximity to a group of detections found using the manual GPR processing technique. The half-cell potential survey results do not seem to represent the deterioration levels detected using the chain drag survey method very well. The manual GPR processing results seem to correlate poorly with the results of the half-cell potential survey on this particular deck.

Appendix A3.3 shows a similar plan map of the deck surface using black hatching to designate where signal attenuation was detected in the GPR data using automatic processing and green hatching to designate where debonded concrete, delaminations and surface scaling were detected using the chain drag method. The automatic processing results correlate more favorably with the actual deterioration found on the deck, but show many more detections than what was found using the chain drag method.

Appendix A3.4 shows a similar plan map of the deck surface using black hatching to designate where signal attenuation was detected in the GPR data using automatic processing and a solid black line bounding the zones of active corrosion detected in the deck. Again, little active corrosion was detected throughout the deck where the majority of GPR detections were located. The major area of active corrosion detected on the northern span correlates very well to a group of automatic processing detections in the same area.

Appendix A3.5 shows a similar plan map of the deck surface using black hatching to designate where signal attenuation was detected in the GPR data using automatic processing and red hatching to designate where signal attenuation and high concrete reflectivity were detected in the GPR data using manual processing. It is evident that both methods detect attenuation near the joints of the deck, while the automatic processing detected more attenuation throughout the deck spans than could be observed using manual processing.

Table 6 – Quantitative and spatial estimate statistics – Victoria Bridge

Victoria Bridge				
Predicted versus Actual and Ground-truth Quantities (Expressed as a Percentage of Deck Surface Area)				
GPR Predicted Quantity (Automatic)	40.7%			
GPR Predicted Quantity (Manual)	13.6%			
Actual Quantity Removed	11.1%			
Chain Drag Quantity	5.2%			
Half-Cell Quantity	0.1%			
GPR Spatial Correlation Statistics	Total GPR Unit Areas on Deck = 864			
	Relative to Chain Drag		Relative to Half-Cell	
	Manual	Automatic	Manual	Automatic
True Deterioration Predictions	27	37	0	1
False Deterioration Predictions	82	408	109	278
True Sound Predictions	715	399	754	585
False Sound Predictions	40	20	1	0
% Correct Deterioration Predictions	24.8%	8.3%	0.0%	0.4%
% Correct Sound Predictions	94.7%	95.2%	99.9%	100.0%
% Total Correct Predictions	85.9%	50.5%	87.3%	67.8%
% Total Incorrect Predictions	14.1%	49.5%	12.7%	32.2%
Probability of correctly detecting deterioration	40.3%	64.9%	0.0%	100.0%
Probability of correctly detecting sound concrete	89.7%	49.4%	87.4%	67.8%
False alarm rate of detecting deterioration	10.3%	50.6%	12.6%	32.2%
False alarm rate of detecting sound concrete	59.7%	35.1%	100.0%	0.0%

The manual processing seems to describe the areas of deterioration detected by the half-cell potential and chain drag surveys better than the automatic processing of the GPR data for the Victoria Bridge because of the much higher number of false

deterioration predictions observed with the automatic processing results. Table 6 lists the quantitative and spatial estimate statistics for the Victoria Bridge.

The half-cell potential survey resulted in significantly less deterioration detected than the chain drag survey. It is likely that the deck was in a very dry condition at the time of the test causing the concrete cover to act as an insulator, decreasing the negativity of the corrosion field potential. The quantity estimate obtained using the manual GPR processing method was much closer to the deterioration quantity measured using the chain drag survey than the estimate obtained using the automatic GPR processing software. The manually processed GPR estimate was actually very close to the final deterioration removal quantity that was measured after the repairs have been completed. This value is based on the chain drag areas that were detected, but is increased as repair work follows the existence of corrosion visible on the exposed reinforcement. Although the manual processing method resulted in a higher percent correct deterioration prediction, the probability of correct deterioration detection is less than the automatic processing results because of the relatively higher percentage of false predictions of sound concrete. The automatic processing results, however, exhibited a substantially lower probability of detecting sound concrete than the manual processing because of the high number of false deterioration predictions which also contributed to a high false alarm rate of detecting deterioration.

The manual GPR processing performed much better than the automatic GPR processing on the Victoria Bridge. This was evident by the higher total correct prediction rate for the manual processing compared to the percent correct and incorrect prediction rates for the automatic processing, which were similar. The automatic processing results detected a higher percentage of the actual deterioration than the manual processing results but also resulted in a much higher false deterioration prediction.

5.6.5 Deep Hollow Overpass

The Deep Hollow Overpass is located on Highway 101 over the Deep Hollow road near New Minas, Kings County. It is a slab on steel girder design with a length of 54.5 meters and a width of 12.3 meters. The deck was surveyed using GPR on July 17, 1998 and rehabilitated during the autumn of 1998. The data was of fair to good clarity, exhibiting some distortion and well defined reflections from the interfaces and reinforcement where deck in good condition could be found. The majority of data from the internal areas of the deck exhibited poor clarity and a high degree of distortion. These effects can be attributed to the relatively sound areas of concrete that were found near the curbs, and the heavily delaminated interior regions of the spans.

Appendix A4.1 shows a plan view map of the deck surface using red hatching to designate where signal attenuation and blue hatching to designate where high concrete reflectivity, or high concrete relative dielectric, were detected in the GPR data using manual processing. Green hatching was used to designate where debonded concrete; delaminations and surface scaling were detected using the chain drag method. Excellent correlation between the manual GPR results and the chain drag results are apparent on the entire deck surface, with the exception of radar passes "A", "B" and "C" on the northern curb edge. Manual processing detected many instances of signal attenuation in these areas, but no indication of deterioration was found using the chain drag method. The shape of the deteriorated areas found using the chain drag match up very well with the manual processing results on all three spans, but is more notably similar in the central span at the 34m southbound distance location. The manual processing appears to have an excellent correlation to the deterioration quantity and locations found using the chain drag method.

Appendix A4.2 shows a similar plan map of the deck surface using red hatching to designate where signal attenuation was detected in the GPR data using manual

processing and a solid black line representing the -0.36 volt contour line established using the half-cell potential survey. The area bounded by this contour represents zones of active corrosion in the deck. Only the northbound lane of the deck was tested using the half-cell potential survey. As with the chain drag results, the manual processing technique compares very favorably with the half-cell survey results. The half-cell survey did not locate any active corrosion in much of the GPR predicted deterioration areas in the southern span, in spite of obvious signs of distress observed during the half-cell survey. The deck was so severely delaminated that there was sufficient air gap between the delaminated concrete cover and the remainder of the slab to act as an insulator, reducing the negativity of the corrosion potential measurements in this area. The half-cell potential survey results do not seem to represent the deterioration levels detected using the chain drag survey method very well. The manual processing technique seems to correlate reasonably well to the results of the half-cell potential survey on this particular deck, except for the excess deterioration detections found using the manual processing of the GPR data where it is known that the half-cell potential survey incorrectly detected no deterioration. Some further excess GPR detections were evident in the central and northern spans, but these seem within reasonable proximity to the half-cell potential detected deterioration that they may be justified as highly-probable future active corrosion areas.

Appendix A4.3 shows a similar plan map of the deck surface using black hatching to designate where signal attenuation was detected in the GPR data using automatic processing and green hatching to designate where debonded concrete, delaminations and surface scaling were detected using the chain drag method. The automatic processing results correlate well with the actual deterioration found on the deck with respect to location of those detections found, but the number of detections is far less than the actual quantity of deterioration found using the chain drag method. The automatic processing results appear sparse and mostly lie within deterioration found using the chain drag,

except for some scattered detections along the curbs and a grouping of detections in the northern span.

Appendix A4.4 shows a similar plan map of the deck surface using black hatching to designate where signal attenuation was detected in the GPR data using automatic processing and a solid black line bounding the zones of active corrosion detected in the deck. Again, the automatic processing detected attenuation in the GPR data in the areas incorrectly defined as being concrete in good condition by the half-cell potential survey. The other automatic processing detections lie within the active corrosion areas denoted by the half-cell potential survey except for some scattered, and typically singular, predictions.

Appendix A4.5 shows a similar plan map of the deck surface using black hatching to designate where signal attenuation was detected in the GPR data using automatic processing and red hatching to designate where signal attenuation and high concrete reflectivity were detected in the GPR data using manual processing. It is evident that both methods detected attenuation in similar areas of the deck surface, but the automatic processing detected far less attenuation throughout the deck than what the manual processing achieved.

The manual processing seems to describe the areas of deterioration detected by the half-cell potential and chain drag surveys much better than the automatic processing of the GPR data for the Deep Hollow Overpass because of the much higher number of correct deterioration predictions observed with the manual processing method. Table 7 lists the quantitative and spatial estimate statistics for the Deep Hollow Overpass.

Table 7 – Quantitative and spatial estimate statistics – Deep Hollow Overpass

Deep Hollow Overpass				
Predicted versus Actual and Ground-truth Quantities (Expressed as a Percentage of Deck Surface Area)				
GPR Predicted Quantity (Automatic)	20.2%			
GPR Predicted Quantity (Manual)	70.1%			
Actual Quantity Removed	54.6%			
Chain Drag Quantity	54.0%			
Half-Cell Quantity	31.4%			
GPR Spatial Correlation Statistics	Total GPR Unit Areas on Deck = 3488			
	Relative to Chain Drag		Relative to Half-Cell	
	Manual	Automatic	Manual	Automatic
True Deterioration Predictions	1705	543	589	236
False Deterioration Predictions	756	185	620	153
True Sound Predictions	699	1304	488	964
False Sound Predictions	328	1456	47	391
% Correct Deterioration Predictions	69.3%	74.6%	48.7%	60.7%
% Correct Sound Predictions	68.1%	47.2%	91.2%	71.1%
% Total Correct Predictions	68.9%	53.0%	61.8%	68.8%
% Total Incorrect Predictions	31.1%	47.0%	38.2%	31.2%
Probability of correctly detecting deterioration	83.9%	27.2%	92.6%	37.6%
Probability of correctly detecting sound concrete	48.0%	87.6%	44.0%	86.3%
False alarm rate of detecting deterioration	52.0%	12.4%	56.0%	13.7%
False alarm rate of detecting sound concrete	16.1%	72.8%	7.4%	62.4%

The manual method of GPR data processing resulted in a much more accurate quantity estimate of the deterioration found by the chain drag survey. It is known that the half-cell potential survey resulted in misleading data over a portion of the deck due to severe delaminations causing electrical discontinuity. The percent of correct deterioration predictions for the automatic GPR data processing were slightly improved over the manual GPR processing due to the smaller total number of deterioration predictions made by the automatic processing. This severe shortfall of deterioration predictions using the automatic processing method caused the probability of correct detection of deterioration to be much smaller than that observed for the manual processing with respect to both the chain drag and half-cell potential results. The observed probability of correct detection of sound concrete is lower for the manual

processing technique than the automatic processing technique because of the relatively low number of occurrences of sound concrete on the deck and a higher false deterioration detection rate observed with the manual processing on this deck.

Overall, with a more accurate estimate of the chain drag and actual deterioration quantity estimates and with a much higher probability of correctly detecting deterioration than the automatic processing results, the manual processing method appears to be give more accurate results on this particular deck.

5.6.6 Grand Pre Overpass

The Grand Pre Overpass is located on Highway 101 over the Grand Pre Road, near Grand Pre, Kings County. It is a concrete slab on steel girder design with a length of 53.9 meters and a width of 14.2 meters. The deck was surveyed using GPR on July 17, 1998 and rehabilitated during the autumn of 1998. The data in general was of fair to good clarity, exhibiting good reflections from the top and bottom mats of reinforcement, but a very weak to non-existent deck bottom echo. The good clarity in the data is indicative of sound asphalt and concrete that does not exhibit significant scattering losses. The weak bottom echo amplitude in the data may be due to a slightly thicker deck than usual and slightly higher background losses in the asphalt pavement and/or concrete of the deck.

Appendix A5.1 shows a plan view map of the deck surface using red hatching to designate where signal attenuation and blue hatching to designate where high concrete reflectivity, or high concrete relative dielectric, were detected in the GPR data using manual processing. Green hatching was used to designate where debonded concrete; delaminations and surface scaling were detected using the chain drag method. Excellent correlation between the manual GPR results and the chain drag results are apparent on the entire deck surface, with the exception of radar pass "A" in the the western span where

attenuation was detected along the curb edge, but the chain drag survey found no evidence of deterioration. Also, several small delaminations were located along a crack that was found along the centerline of the deck, but no evidence of these were found using the manual GPR processing. Small and scattered false deterioration detections from the manual processing of the GPR data can be observed in all spans. The shape of the deteriorated areas found using the chain drag match up very well with the manual processing results around the abutment and interior joints and along the southern curb in the central span where an area of surface scaling was outlined during the chain drag survey. The manual processing appears to have an excellent correlation to the deterioration quantity and locations found using the chain drag method.

Appendix A5.2 shows a similar plan map of the deck surface using red hatching to designate where signal attenuation was detected in the GPR data using manual processing and a solid black line representing the -0.36 volt contour line established using the half-cell potential survey. The area bounded by this contour represents zones of active corrosion in the deck. As with the chain drag results, the manual processing technique compares very favorably with the half-cell survey results with the major detections being located about the joints. The manual processing results and half-cell potential survey results do find signal attenuation and active corrosion, respectively, in radar pass "A" in the western span where there was disagreement between the manual processing and chain drag results. The half-cell potential survey did identify two areas of active corrosion that were found along the centerline crack in the deck, but only identified one similar area as the chain drag method in this region. The manual processing technique seems to correlate reasonably well to the results of the half-cell potential survey on this particular deck, except for the small and scattered deterioration detections found using the manual processing of the GPR data through the deck spans.

Appendix A5.3 shows a similar plan map of the deck surface using black hatching to designate where signal attenuation was detected in the GPR data using the automatic

processing and green hatching to designate where debonded concrete, delaminations and surface scaling were detected using the chain drag method. The automatic processing results correlate well with the actual deterioration found on the deck with respect to location of those detections found, but the number of detections is much higher than the actual quantity of deterioration found using the chain drag method. The automatic processing results appear to contain more scattered and random detections with some small groupings in the decks and along the southern curb in the eastern span that appear as though they may represent actual phenomena. These apparent phenomena were undetected using the chain drag survey.

Appendix A5.4 shows a similar plan map of the deck surface using black hatching to designate where signal attenuation was detected in the GPR data using automatic processing and a solid black line bounding the zones of active corrosion detected in the deck. The automatic processing detected attenuation in the GPR data in the areas defined as being active corrosion by the half-cell potential survey, but with only sparse detections along the southern curb in the western span, and without any detections in the active corrosion identified along the centerline crack of the deck. The other automatic processing detections lie outside the active corrosion areas detected using the half-cell potential survey.

Appendix A5.5 shows a similar plan map of the deck surface using black hatching to designate where signal attenuation was detected in the GPR data using automatic processing and red hatching to designate where signal attenuation and high concrete reflectivity were detected in the GPR data using manual processing. It is evident that both methods found deterioration detections in similar areas of the deck surface, with some degree of scattering in each method, but the automatic processing detected more attenuation about the area adjacent to the joints and throughout the deck than what was observed using the manual processing.

Table 8 – Quantitative and spatial estimate statistics – Grand Pre Overpass

Grand Pre Overpass				
Predicted versus Actual and Ground-truth Quantities (Expressed as a Percentage of Deck Surface Area)				
GPR Predicted Quantity (Automatic)	32.6%			
GPR Predicted Quantity (Manual)	15.0%			
Actual Quantity Removed	11.2%			
Chain Drag Quantity	9.1%			
Half-Cell Quantity	8.3%			
GPR Spatial Correlation Statistics		Total GPR Unit Areas on Deck = 4104		
		Relative to Chain Drag		Relative to Half-Cell
		Manual	Automatic	Manual
True Deterioration Predictions	302	224	290	227
False Deterioration Predictions	358	695	393	654
True Sound Predictions	3355	2996	3292	3067
False Sound Predictions	89	189	129	156
% Correct Deterioration Predictions	45.8%	24.4%	42.5%	25.8%
% Correct Sound Predictions	97.4%	94.1%	96.2%	95.2%
% Total Correct Predictions	89.1%	78.5%	87.3%	80.3%
% Total Incorrect Predictions	10.9%	21.5%	12.7%	19.7%
Probability of correctly detecting deterioration	77.2%	54.2%	69.2%	59.3%
Probability of correctly detecting sound concrete	90.4%	81.2%	89.3%	82.4%
False alarm rate of detecting deterioration	9.6%	18.8%	10.7%	17.6%
False alarm rate of detecting sound concrete	22.8%	45.8%	30.8%	40.7%

The manual processing seems to describe the areas of deterioration detected by the half-cell potential and chain drag surveys much better than the automatic processing of the GPR data for the Grand Pre Overpass. The deteriorated areas defined by the half-cell potential and chain drag surveys were filled in more densely by the manual processing results than by the automatic processing results. Also, less false deterioration detections were observed in the regions of sound concrete in the manual processing results than in the automatic processing results. Table 8 lists the quantitative and spatial estimate statistics for the Grand Pre Overpass.

The deterioration quantity estimate obtained using the manual processing was closer than the quantity obtained using the automatic processing to the quantity detected

using both the chain drag and half-cell potential surveys and to the actual deterioration removal quantity. The automatic processing overestimated the deterioration quantity by approximately three hundred percent.

While the rate of correct sound concrete predictions was very similar for the automatic and manual GPR data processing methods, the manual rate of correct deterioration predictions was slightly less than twice as accurate as that provided by the automatic processing. The false alarm rates of detecting deterioration in sound concrete and in detecting sound concrete in deterioration observed using the manual GPR data processing method were approximately half of the rates observed in the automatic processing results for this particular structure.

Based on observed graphical and on statistical comparison, the manual GPR data processing results best predicted the deterioration quantities and locations found on the Grand Pre Overpass due to accurate quantity estimation, improved correct deterioration prediction rates, and reduced false alarm prediction rates.

5.6.7 Shubenacadie CNR Overpass

The Shubenacadie CNR Overpass is on Highway 104 near the Halifax-Hants county line. It is a concrete slab on steel girder design with a length of 98.5 meters and a width of 9.3 meters. The deck was surveyed using GPR on November 5, 1997 and rehabilitated during the summer of 1998. The data in general was of good clarity, exhibiting good reflections from the layer interfaces and good contrast between the very good and very deteriorated areas of the deck. This is probably because the background levels of moisture and chloride contained in the sound concrete were much lower than excessive levels of moisture and chloride found in the deteriorated regions of the deck.

Appendix A6.1 shows a plan view map of the deck surface using red hatching to designate where signal attenuation was detected in the GPR data using manual processing. Although the data was processed to seek areas of high concrete reflectivity, none were found in the data. Green hatching was used to designate where debonded concrete; delaminations and surface scaling were detected using the chain drag method. Fair correlation between the manual GPR processing results and the chain drag results can be observed on the entire deck surface. The manual GPR processing detected much less deterioration than what was found using the chain drag survey. In general, the detections that were made using the manual GPR processing coincided well with the chain drag survey results. Two areas of GPR predicted deterioration, located on the eastern edge of the northern span, did not correlate to any deterioration found using the chain drag survey. The manual processing appears to only have a poor correlation to the deterioration quantity using the chain drag method. This is probably due to the use of a threshold level of signal attenuation during manual processing that was too conservative, resulting in reduced overall quantity estimate and a lack of detection density in the deteriorated areas that were found using the manual GPR processing method. Manual GPR processing is subjective and can be liable to overestimations or underestimations of the appropriate threshold level to differentiate the sound from deteriorated concrete signal characteristics. By choosing a more conservative or liberal threshold, the user affects the overall estimation quantity, while the general shape and location of deterioration changes little. The lack of high concrete reflectivity detections in the manual processing results indicate that the deck slab was probably in a dry condition at the time of the GPR data collection resulting in a decreased level of attenuation due to the interactive effects of moisture and chloride.

Appendix A6.2 shows a similar plan map of the deck surface using red hatching to designate where signal attenuation was detected in the GPR data using manual processing and a solid black line representing the -0.36 volt contour line established using the half-cell potential survey. The area bounded by this contour represents zones of

active corrosion in the deck. Results were obtained using the half-cell survey for only the western lane of the overpass. As with the chain drag survey results, the manual processing results seem to underestimate the quantity of active corrosion that was found using the half-cell potential survey. However, the manual processing detections do seem to fill out the active corrosion areas more densely and describe their shape much better than in the case of the chain drag results. The majority of manual processing detections fall within the bounds of the -0.36 volt contour line, indicating that very few false deterioration detections should be observed. The manual processing technique seems to correlate reasonably well to the results of the half-cell potential survey on this particular deck.

Appendix A6.3 shows a similar plan map of the deck surface using black hatching to designate where signal attenuation was detected in the GPR data using the automatic processing and green hatching to designate where debonded concrete, delaminations and surface scaling were detected using the chain drag method. The automatic processing results correlate well with the actual deterioration found on the deck with respect to location of those detections found, but the number of detections is much lower than the actual quantity of deterioration found using the chain drag method. The use of a less conservative threshold in processing the data may result in a more accurate quantity estimate by the automatic processing.

Appendix A6.4 shows a similar plan map of the deck surface using black hatching to designate where signal attenuation was detected in the GPR data using automatic processing and a solid black line bounding the zones of active corrosion detected in the deck. The automatic processing detected attenuation in the GPR data in the areas defined using the half-cell survey as containing active corrosion, but also predicted less detections than the area defined by the half-cell potential survey. The automatic processing detections correlate well with the shape of the areas found to be actively corroding by the half-cell potential survey, but not the overall quantity. Again, the use of

a less conservative threshold in processing the data may result in a more accurate quantity estimate by the automatic processing.

Table 9 – Quantitative and spatial estimate statistics – Shubenacadie CNR Overpass

Shubenacadie CNR Overpass					
Predicted versus Actual and Ground-truth Quantities (Expressed as a Percentage of Deck Surface Area)					
GPR Predicted Quantity (Automatic)	15.5%				
GPR Predicted Quantity (Manual)	28.5%				
Actual Quantity Removed	35.3%				
Chain Drag Quantity	35.1%				
Half-Cell Quantity	39.5%				
GPR Spatial Correlation Statistics		Total GPR Unit Areas on Deck = 5122			
		Relative to Chain Drag		Relative to Half-Cell	
		Manual	Automatic	Manual	Automatic
True Deterioration Predictions		698	470	462	314
False Deterioration Predictions		638	285	97	88
True Sound Predictions		2540	2864	1524	2265
False Sound Predictions		1246	1503	675	91
% Correct Deterioration Predictions		52.2%	62.3%	82.6%	78.1%
% Correct Sound Predictions		67.1%	65.6%	69.3%	96.1%
% Total Correct Predictions		63.2%	65.1%	72.0%	93.5%
% Total Incorrect Predictions		36.8%	34.9%	27.0%	6.5%
Probability of correctly detecting deterioration		35.9%	23.8%	40.6%	77.5%
Probability of correctly detecting sound concrete		79.9%	90.9%	94.0%	96.3%
False alarm rate of detecting deterioration		20.1%	9.1%	6.0%	3.7%
False alarm rate of detecting sound concrete		64.1%	76.2%	59.4%	22.5%

Appendix A6.5 shows a similar plan map of the deck surface using black hatching to designate where signal attenuation was detected in the GPR data using automatic processing and red hatching to designate where signal attenuation and high concrete reflectivity were detected in the GPR data using manual processing. Both manual and automatic GPR processing methods describe similar attenuated areas of the deck surface, but the automatic processing seemed to yield less detections than the manual processing of the GPR data. The automatic processing results did not include detections on the

eastern edge of the northern span where two areas of detections were located using the manual processing.

The manual processing seems to describe the areas of deterioration detected by the half-cell potential and chain drag surveys as well as the automatic processing of the GPR data for the Shubenacadie CNR Overpass. While both GPR processing techniques underestimated the overall deterioration quantities, the deteriorated areas defined by the half-cell potential and chain drag surveys were filled in more densely by the manual processing results than by the automatic processing results. Table 9 lists the quantitative and spatial estimate statistics for the Shubenacadie CNR Overpass.

Both GPR processing methods underestimated the chain drag and half-cell potential survey quantities, but the manual processing technique yielded a much closer estimate than the automatic processing technique. With the underestimation of deterioration, both processing methods exhibited low correct prediction rates of sound concrete and low total correct prediction rates. Both GPR processing methods resulted in similarly poor estimates of the deterioration quantities, yet modelled the shape of the active corrosion found on the deck very well with approximately eighty percent correct deterioration prediction rates with respect to the half-cell potential survey results. The manual processing exhibited almost half the probability of correctly detecting active corrosion as shown by the automatic processing in this particular bridge.

5.6.8 Baddeck River Bridge

The Baddeck River Bridge is on Highway 105 over the Baddeck River in Victoria County. It is a concrete slab on steel girder design with a length of 83.5 meters and a width of 8.0 meters. The deck was surveyed using GPR on October 17, 1996 and rehabilitated during the summer of 1998. The data in general was of excellent clarity, exhibiting very strong and well-developed reflections from the layer interfaces and very

good contrast between the sound and deteriorated areas of the deck. The clarity and good contrast in the data tend to indicate that there is little scattering losses due to cracking or non-homogeneities in the deck and that there significant difference in moisture and chloride content between the sound and deteriorated regions of the deck.

Appendix A7.1 shows a plan view map of the deck surface using red and blue hatching to designate where signal attenuation and high concrete reflectivity were detected, respectively, in the GPR data using manual processing. Green hatching was used to designate where debonded concrete, delaminations and surface scaling were detected using the chain drag method. Excellent correlation between the manual GPR results and the chain drag results can be observed on the entire deck surface. The manual processing resulted in an area of deterioration detections along the western abutment joint where considerably less deterioration was detected using the chain drag survey. Two small areas that were observed in the manual GPR results near the deck centerline at the 8-meter and 11-meter westbound locations on the deck do not coincide with any of the chain drag results. However, the correlation between the manual processing results and the chain drag results appear excellent on the remainder of the deck surface with the manual GPR describing the shape of the chain drag results very well. Notable examples of this can be observed at internal joints, at the triangular area of deterioration located at the 40-meter to 44-meter distance in the eastbound lane, and at the two areas of deterioration located at the 74-meter location in the westbound lane. Also of note is the apparently sound concrete located at the internal joint located near the 57-meter westbound location. This area was a previously repaired area of the deck that produced strong attenuation characteristics in the GPR data. The chain drag survey produced no evidence of deterioration at this location, but a core sample was drilled because the GPR indication was so strong. The concrete observed in the core was extremely porous and lacking in cement paste. Subsequent analysis revealed a water-soluble chloride content of 0.238%, very close to the 0.25% threshold used by the Ontario Ministry of Transportation as an indication for probable corrosion. With the high levels of

attenuation observed in the GPR data and the observation of the core sample, the site inspector decided to replace this previously repaired area. In general, the manual processing estimation appeared to produce an accurate estimation of the quantity and location of the deterioration detected using the chain drag survey, resulting in an excellent correlation.

Appendix A7.2 shows a similar plan map of the deck surface using red and blue hatching to designate where signal attenuation and high concrete reflectivity, respectively, were detected in the GPR data using manual processing and a solid black line representing the -0.36 volt contour line established using the half-cell potential survey. The area bounded by this contour represents zones of active corrosion in the deck. Results were obtained using the half-cell survey for only the westbound lane of the bridge. As with the chain drag survey results, the manual processing results seem to overestimate the quantity of active corrosion that was found using the half-cell potential survey near the western abutment joint. The manual processing also appeared to underestimate the deterioration quantity in several locations on the deck as well. The manual processing detections do appear to fall within the boundary established by the -0.36 volt contour line, indicating that very few false deterioration detections should be observed. It is interesting to note that the two small areas of GPR detections on the eastern span coincide with areas of active corrosion detected using the half-cell potential survey where no coincidence was observed with the chain drag survey results. The manual processing technique seems to correlate very well with the results of the half-cell potential survey on this particular deck.

Appendix A7.3 shows a similar plan map of the deck surface using black hatching to designate where signal attenuation was detected in the GPR data using the automatic processing and green hatching to designate where debonded concrete, delaminations and surface scaling were detected using the chain drag method. The automatic processing results correlate fairly well with the actual deterioration found on the deck with respect to

some of their locations, with the number of detections appearing similar to the actual quantity of deterioration found using the chain drag method. However, the automatic processing tended to produce excess detections surrounding some of the deterioration found using the chain drag survey and few detections in and near other similar areas. The automatic processing also detected signal attenuation in the region of the previously repaired joint and excess detections near the western abutment joint.

Appendix A7.4 shows a similar plan map of the deck surface using black hatching to designate where signal attenuation was detected in the GPR data using automatic processing and a solid black line bounding the zones of active corrosion detected in the deck. The automatic processing detected most of the signal attenuation in the GPR data in the areas defined as being active corrosion, with an apparent similar quantity as that defined by the half-cell potential survey. The automatic processing detections correlate well with the shape of the areas found to be actively corroding by the half-cell potential survey except for one major group of detections located at the westbound 41-meter location that fall outside that boundary.

Appendix A7.5 shows a similar plan map of the deck surface using black hatching to designate where signal attenuation was detected in the GPR data using automatic processing and red hatching to designate where signal attenuation and high concrete reflectivity were detected in the GPR data using manual processing. Both manual and automatic GPR processing methods describe similar attenuated areas of the deck surface, with approximately the same quantity of non-coincident detections.

The manual processing seems to describe the areas of deterioration detected by the half-cell potential and chain drag surveys marginally better than the automatic processing of the GPR data for the Baddeck River Bridge. Both methods appeared to accurately predict the location and extent of the deterioration detected by both the chain

drag and the half-cell potential surveys. The quantitative and spatial estimate statistics for the Baddeck River Bridge are listed in Table 10.

Table 10 – Quantitative and spatial estimate statistics – Baddeck River Bridge

Baddeck River Bridge				
Predicted versus Actual and Ground-truth Quantities (Expressed as a Percentage of Deck Surface Area)				
GPR Predicted Quantity (Automatic)	30.9%			
GPR Predicted Quantity (Manual)	37.4%			
Actual Quantity Removed	40.1%			
Chain Drag Quantity	34.9%			
Half-Cell Quantity	46.0%			
GPR Spatial Correlation Statistics	Total GPR Unit Areas on Deck = 2672			
	Relative to Chain Drag		Relative to Half-Cell	
	Manual	Automatic	Manual	Automatic
True Deterioration Predictions	661	523	416	345
False Deterioration Predictions	314	323	104	108
True Sound Predictions	1226	1182	575	581
False Sound Predictions	471	644	241	302
% Correct Deterioration Predictions	67.8%	61.8%	80.0%	76.2%
% Correct Sound Predictions	72.2%	64.7%	70.5%	65.8%
% Total Correct Predictions	70.6%	63.8%	74.2%	69.3%
% Total Incorrect Predictions	29.4%	36.2%	25.8%	30.7%
Probability of correctly detecting deterioration	58.4%	44.8%	63.3%	53.3%
Probability of correctly detecting sound concrete	79.6%	78.5%	84.7%	84.3%
False alarm rate of detecting deterioration	20.4%	21.5%	15.3%	15.7%
False alarm rate of detecting sound concrete	41.6%	55.2%	36.7%	46.7%

The manual processing of the GPR data yielded a more accurate prediction of the chain drag and half-cell potential surveys and of the final removal quantity from the deck than the automatic processing. Both methods exhibited good percent correct prediction rates with the manual processing results giving generally better accuracy than the automatic processing results. This is evident as well by the slightly better probability shown by manual processing than automatic processing to correctly detect deterioration and its associated false alarm rate of detecting sound concrete in deteriorated areas. The probability of correctly detecting sound concrete and false alarm rate of detecting

deterioration in sound concrete were almost identical for both GPR data processing methods.

5.6.9 Skye River Bridge

The Skye River Bridge is on Highway 105 over the Skye River at Whycocomagh in Inverness County. It is a concrete slab on steel girder design with a length of 46.8 meters and a width of 8.1 meters. The deck was surveyed using GPR on October 17, 1996 and rehabilitated during the summer of 1998. The data in general was of fair to good clarity, exhibiting sometimes weak reinforcement layers. This may indicate some degree of scattering losses, possibly due to deteriorated asphalt pavement, and can also arise due to elevated background levels of signal attenuation in the concrete.

Appendix A8.1 shows a plan view map of the deck surface using red and blue hatching to designate where signal attenuation and high concrete reflectivity, respectively, were detected in the GPR data using manual processing. Green hatching was used to designate where debonded concrete; delaminations and surface scaling were detected using the chain drag method. Ground-truthing data was only collected on the the eastbound lane of the bridge. Good correlation between the manual GPR results and the chain drag results can be observed on the entire deck surface. Notable examples of this can be observed at the internal joints, and at the two major areas of deterioration located the eastbound 25 to 28-meter and 35-meter locations. Also, the manual GPR results predicted the northern curbside deterioration very well, found using the chain drag survey. Two major areas of apparent false deterioration detections can be observed at the eastbound 10 to 13-meter and 37 to 43-meter locations. In general, the manual processing estimation appeared to produce a slight over-estimation of the quantity and location of the deterioration detected using the chain drag survey.

Appendix A8.2 shows a similar plan map of the deck surface using red and blue hatching to designate where signal attenuation and high concrete reflectivity were detected in the GPR data, respectively, using manual processing and a solid black line representing the -0.36 volt contour line established using the half-cell potential survey. The area bounded by this contour represents zones of active corrosion in the deck. Results were obtained using the half-cell survey for only the eastbound lane of the bridge. The manual processing results seem to accurately estimate the quantity of active corrosion that was found using the half-cell potential survey, but with a portion of this predicted deterioration lying outside of the zones of active corrosion and some false sound concrete predictions lying within the zones of active corrosion. The deterioration predictions that did not correlate to areas of deterioration found using the chain drag survey at the eastbound 37 to 43-meter locations does correlate well with active corrosion as determined using the half-cell potential survey. A portion of the deterioration detections located at the eastbound 10 to 13-meter locations correlates to active corrosion. The deterioration detections appear to mostly fall within the -0.36 volt contour line, but do not satisfactorily fill in the area, leaving many false predictions of sound concrete within this area. The manual processing technique seems to correlate reasonably well with the results of the half-cell potential survey on this particular deck. It should be noted that there was poor correlation between the half-cell and chain drag survey results, with the majority of chain drag defined deterioration not coinciding with active corrosion defined by the half-cell potential survey.

Appendix A8.3 shows a similar plan map of the deck surface using black hatching to designate where signal attenuation was detected in the GPR data using the automatic processing and green hatching to designate where debonded concrete, delaminations and surface scaling were detected using the chain drag method. The automatic processing results do not correlate well with the actual deterioration on the deck found using the chain drag survey with some sparse detections located within. In spite of this poor spatial

correlation, the predicted quantity from the automatic processing appears to approximate deterioration quantity found using the chain drag survey.

Appendix A8.4 shows a similar plan map of the deck surface using black hatching to designate where signal attenuation was detected in the GPR data using automatic processing and a solid black line bounding the zones of active corrosion detected in the deck. The automatic processing detected most of the signal attenuation in the GPR data in the areas defined as being active corrosion and appears to correlate much better with the half-cell potential survey than the chain drag survey. The automatic processing detections correlate well with the shape of the areas found to be actively corroding by the half-cell potential survey except for a number of false deterioration predictions that fall outside the -0.36 volt boundary.

Appendix A8.5 shows a similar plan map of the deck surface using black hatching to designate where signal attenuation was detected in the GPR data using automatic processing and red hatching to designate where signal attenuation and high concrete reflectivity were detected in the GPR data using manual processing. Both manual and automatic GPR processing methods described generally similar attenuated areas of the deck surface, but with different densities of detection in different locations. Automatic processing results tended to congregate within the boundary defined by the half-cell potential survey, whereas the manual processing results tended to occupy areas within the regions defined by both the chain drag and half-cell potential survey as areas of deterioration.

The manual processing seems to describe the areas of deterioration detected by the half-cell potential and chain drag surveys better than the automatic processing of the GPR data for the Skye River Bridge. Table 11 lists the quantitative and spatial estimate statistics for the Skye River Bridge.

Table 11 – Quantitative and spatial estimate statistics – Skye River Bridge

Skye River Bridge					
Predicted versus Actual and Ground-truth Quantities (Expressed as a Percentage of Deck Surface Area)					
GPR Predicted Quantity (Automatic)	30.4%				
GPR Predicted Quantity (Manual)	42.3%				
Actual Quantity Removed	38.7%				
Chain Drag Quantity	34.4%				
Half-Cell Quantity	41.9%				
GPR Spatial Correlation Statistics		Total GPR Unit Areas on Deck = 744			
		Relative to Chain Drag		Relative to Half-Cell	
		Manual	Automatic	Manual	Automatic
True Deterioration Predictions		197	104	191	153
False Deterioration Predictions		114	122	121	76
True Sound Predictions		339	337	290	333
False Sound Predictions		94	181	142	182
% Correct Deterioration Predictions		63.3%	46.0%	61.2%	66.8%
% Correct Sound Predictions		78.3%	65.1%	67.1%	64.7%
% Total Correct Predictions		72.0%	59.3%	64.7%	65.3%
% Total Incorrect Predictions		28.0%	40.7%	35.3%	34.7%
Probability of correctly detecting deterioration		67.7%	36.5%	57.4%	45.7%
Probability of correctly detecting sound concrete		74.8%	73.4%	70.6%	81.4%
False alarm rate of detecting deterioration		25.2%	26.6%	29.4%	18.6%
False alarm rate of detecting sound concrete		32.3%	63.5%	42.6%	54.3%

The manual processing of the GPR data yielded a more accurate prediction of the chain drag and half-cell potential surveys and of the final removal quantity from the deck than the automatic processing. The manual processing results exhibited a better percent correct deterioration prediction rate with respect to the chain drag survey, but the automatic processing results exhibited a better percent correct deterioration prediction rate with respect to the half-cell potential survey. However, manual processing resulted in higher probabilities of correct deterioration prediction than the automatic processing for both the chain drag and half-cell potential surveys. This was due to the better false alarm rate of detecting sound concrete in deteriorated areas for the manual method of GPR data processing.

5.6.10 Stewiacke River Bridge

The Stewiacke River Bridge is on the Trunk 2 highway over the Stewiacke River, approximately 1 kilometer north of Stewiacke, Colchester County. It is a concrete slab on steel girder design with a length of 84.0 meters and a width of 8.3 meters. The deck was surveyed using GPR on October 16, 1997 and rehabilitated during the summer of 1998. The data in general was of very good clarity, exhibiting strong reflections from the interfacial and reinforcement layers indicating low levels of scattering losses due to cracks and layer nonhomogeneity. Good contrast between sound and deterioration concrete could be observed in the data indicating low background levels moisture and chloride, and hence signal attenuation, in the concrete.

Appendix A9.1 shows a plan view map of the deck surface using red and blue hatching to designate where signal attenuation and high concrete reflectivity, respectively, were detected in the GPR data using manual processing. Green hatching was used to designate where debonded concrete; delaminations and surface scaling were detected using the chain drag method. Excellent correlation between the manual GPR results and the chain drag results can be observed on the entire deck surface, except for two distinct areas of GPR detections at the southbound 4-meter and the interior joint located at the southbound 56-meter location. The former area appears to describe deterioration along a transverse bar, while the latter describes deterioration surrounding a joint. This joint and the asphalt pavement overlying it were left in place as it was repaired a few years just prior to the total deck repair. In spite of this, strong evidence of signal attenuation was observed in the GPR data in this area. In general, the manual processing provides excellent correlation between the predicted and actual deterioration quantities and the overall shape of the deteriorated areas found using the chain drag survey. Slight underestimation of the small and scattered delaminations found in the northern span and about the edges of the major deteriorated areas in the southern span were observed in the manual processing results.

Appendix A9.2 shows a similar plan map of the deck surface using red and blue hatching to designate where signal attenuation and high concrete reflectivity, respectively, were detected in the GPR data using manual processing and a solid black line representing the -0.36 volt contour line established using the half-cell potential survey. The area bounded by this contour represents zones of active corrosion in the deck. The manual processing results appeared to accurately estimate the quantity of active corrosion that was found using the half-cell potential survey, but with some underestimation of the deterioration quantity and therefore some false sound concrete predictions lying near the edges of the active corrosion areas. It is interesting to note that the GPR detections located at the southbound 4-meter location that did not correlate with any chain drag results correlate very well with the results of the half-cell potential survey. The overall shape of the half-cell potential survey results is described very well by the manual processing results, except for the eastern region of the southern abutment joint where the manual processing results detected signal attenuation but no evidence of active corrosion was found. The manual processing technique appeared to exhibit excellent correlation with the results of the half-cell potential survey on this particular deck.

Appendix A9.3 shows a similar plan map of the deck surface using black hatching to designate where signal attenuation was detected in the GPR data using the automatic processing and green hatching to designate where debonded concrete, delaminations and surface scaling were detected using the chain drag method. The automatic processing results correlate fairly well with the location of deterioration on the deck found using the chain drag survey but severely underestimate the quantity of deterioration actually found. In spite of this poor quantitative correlation, the predicted deterioration locations from the automatic processing tend to approximate the interior of the deterioration areas found using the chain drag survey. It is possible that a less conservative threshold may have resulted in a higher and more accurate deterioration estimate.

Table 12 – Quantitative and spatial estimate statistics – Stewiacke River Bridge

Stewiacke River Bridge				
Predicted versus Actual and Ground-truth Quantities (Expressed as a Percentage of Deck Surface Area)				
GPR Predicted Quantity (Automatic)	22.8%			
GPR Predicted Quantity (Manual)	44.5%			
Actual Quantity Removed	59.7%			
Chain Drag Quantity	53.9%			
Half-Cell Quantity	50.5%			
GPR Spatial Correlation Statistics			Total GPR Unit Areas on Deck = 3586	
	Relative to Chain Drag		Relative to Half-Cell	
	Manual	Automatic	Manual	Automatic
True Deterioration Predictions	1166	708	1311	781
False Deterioration Predictions	204	87	219	54
True Sound Predictions	1407	1203	1533	1573
False Sound Predictions	809	1588	523	1178
% Correct Deterioration Predictions	85.1%	89.1%	85.7%	93.5%
% Correct Sound Predictions	63.5%	43.1%	74.6%	57.2%
% Total Correct Predictions	71.8%	53.3%	79.3%	65.6%
% Total Incorrect Predictions	28.2%	46.7%	20.7%	34.4%
Probability of correctly detecting deterioration	59.0%	30.8%	71.5%	39.9%
Probability of correctly detecting sound concrete	87.3%	93.3%	87.5%	96.7%
False alarm rate of detecting deterioration	12.7%	6.7%	12.5%	3.3%
False alarm rate of detecting sound concrete	41.0%	69.2%	28.5%	60.1%

Appendix A9.4 shows a similar plan map of the deck surface using black hatching to designate where signal attenuation was detected in the GPR data using automatic processing and a solid black line bounding the zones of active corrosion detected in the deck. While there is good spatial correlation with the half-cell potential survey results, the automatic processing detections are sparse and severely underestimate the overall deterioration quantity.

Appendix A8.5 shows a similar plan map of the deck surface using black hatching to designate where signal attenuation was detected in the GPR data using automatic processing and red hatching to designate where signal attenuation and high concrete reflectivity were detected in the GPR data using manual processing. Both manual and

automatic GPR processing method results coincided well, but the number of automatic processing detections is much less than the number of detections found using the manual GPR processing method.

The manual processing provides a more accurate prediction than the automatic GPR processing for the Stewiacke River Bridge because of better quantitative correlation to the actual deterioration found using the ground-truthing methods. Both methods exhibited similar spatial correlation to the chain drag and half-cell potential survey method results. Table 12 lists the quantitative and spatial correlation statistics for the Stewiacke River bridge.

The manual processing of the GPR data yielded a more accurate prediction of the chain drag and the final removal quantity from the deck than the automatic processing, while the automatic processing results predicted the half-cell potential deterioration quantity better than the manual processing results. The manual processing results exhibited a better percent correct deterioration prediction rate with respect to the chain drag survey, but the automatic processing results exhibited a marginally better percent correct deterioration prediction rate with respect to the half-cell potential survey. However, manual processing resulted in higher probabilities of correct deterioration prediction than the automatic processing for both the chain drag and half-cell potential surveys. This was due to the better false alarm rate of detecting sound concrete in deteriorated areas for the manual method of GPR data processing. The automatic GPR processing exhibited a better probability of detecting sound concrete than the manual GPR processing method because of the sparsity of detections and the lack of false deterioration detections in the areas on sound concrete.

The manual processing of the GPR data yielded a more accurate prediction of the chain drag and the final removal quantity from the deck than the automatic processing, while the automatic processing results predicted the half-cell potential deterioration

quantity better than the manual processing results. The manual processing results exhibited a better percent correct deterioration prediction rate with respect to the chain drag survey, but the automatic processing results exhibited a marginally better percent correct deterioration prediction rate with respect to the half-cell potential survey. However, manual processing resulted in higher probabilities of correct deterioration prediction than the automatic processing for both the chain drag and half-cell potential surveys. This was due to the better false alarm rate of detecting sound concrete in deteriorated areas for the manual method of GPR data processing. The automatic GPR processing exhibited a better probability of detecting sound concrete than the manual GPR processing method because of the sparsity of detections and the lack of false deterioration detections in the areas on sound concrete.

The manual processing method provided a more accurate estimate and better spatial correlation to the ground-truthing results than the automatic processing results for the Stewiacke River Bridge.

In general, the preceding project level comparisons of manual and automatic GPR processing results to the actual and ground-truthing deterioration detections on each deck tended to indicate that the manual GPR processing outperformed the automatic GPR processing by providing more accurate predictions of the location and extent of the actual deterioration. This is because of the higher degree of control the user has in manual processing in that they can apply their own intuition and judgement in the interpretation of the signal characteristics. The automatic processing allows the user judgement only on the general time location of the interfacial peaks and some influence on the threshold level that may be applied. With manual GPR processing, the user can recognize and account for such phenomena as potholes, joints, diaphragms, and the influence on the data of girders or stringers that support the deck, as well as recognize signal changes like distortion or reflectivity where excessive attenuation may not be apparent as in the case of very dry concrete.

5.7 Network Level Comparison of Results

Comparisons of the manual and automatic processing of the GPR data to the chain drag and half-cell potential survey results on individual bridge decks showed that the manual processing generally outperformed the automatic processing with higher qualitative accuracy and improved spatial correlation to actual deterioration found on each deck. While differences in accuracy have been recognized on a project level, it is important to study the accuracy of the predictions on a network level to determine if GPR provides satisfactory level of performance as a deterioration prediction tool for bridge management. A network level analysis in which all of the data from all of the structures surveyed provides an overall comparison of the GPR processing results as well as establishes confidence limits that may be used as an aid in applying future GPR surveys to bridge management decisions. These accuracies are presented in terms of the percent of the ground-truthing detected or actual quantity detected or repaired, respectively, and also in terms of these quantities as percentages of the total deck surface area. Table 13 lists the predicted, ground-truth and repair quantities for the nine structures observed in this research project.

The actual repaired area listed in is based on the chain drag quantity, for it is the outlined areas from the chain drag that are repaired. These quantities are increased when repairs exceed the boundaries of these outlines when corrosion is followed along the reinforcement until clean steel is encountered. The half-cell potential survey quantities listed for the Deep Hollow Overpass and Shubenacadie CNR Overpass represent only a portion of the entire deck surface and are neglected from the quantitative comparisons regarding half-cell potential survey values since the other test method values represent measurements from the entire deck surface area. The extremely small quantity found using the half-cell potential survey on the Victoria bridge resulted in some extremely high difference percentages and was also neglected from the quantitative comparison.

Table 13 – Predicted, ground-truth and actual bridge deck deterioration quantities

Structure ID	Predicted Quantities		Ground-truth		Actual
	Manual (m ²)	Automatic (m ²)	Chain Drag (m ²)	Half-Cell (m ²)	Repaired (m ²)
Stewiacke River Bridge	310.2	158.9	375.7	352.0	416.2
Skye River Bridge	79.1	56.9	64.4	78.3	72.4
Baddeck River Bridge	249.5	206.3	233.0	292.6	267.5
Shubenacadie CNR Overpass	261.0	141.9	321.4	187.0	323.4
Grand Pre Overpass	115.1	249.4	69.9	63.8	85.9
Deep Hollow Overpass	468.6	138.7	361.2	99.5	365.0
Victoria Bridge	28.5	85.4	12.5	0.1	23.3
Rough Brook Bridge	62.3	63.9	80.0	n/a	86.4
Glendale Bridge	50.9	44.4	63.3	29.4	71.0

The difference between the ground-truthing or the actual repair quantity and the predicted GPR quantity, by manual or automatic processing, was calculated for each bridge deck to determine the average difference and standard deviation between these measurements. These statistics were then used to construct 95% confidence intervals to describe the expected range of difference between future predictions and what should be found using the chain drag or half-cell potential survey.

Table 14 lists the average, standard deviation, and 95% confidence limits for comparisons of the ground-truthing and actual repair quantities and the GPR predicted quantities.

With respect to the overall quantity the manual GPR processing provides a more accurate prediction of the chain drag survey quantity results than the automatic GPR processing by an average reduction in the overestimated quantity by 46.4%. The variability in the difference between the chain drag survey quantity and the manual GPR

processing was found to be approximately four times less than the difference between the chain drag survey quantity and the automatic GPR processing quantity, resulting in a much smaller confidence interval.

Table 14 - Statistical comparisons of actual ground-truth and repair quantities to GPR predicted quantities as a percent of the ground-truth or actual quantity

Comparison	Average (%)	Standard Deviation (%)	Upper 95% Confidence Limit (%)	Lower 95% Confidence Limit (%)
Chain Drag - Manual GPR	-19.4%	50.2%	18.1%	-56.9%
Chain Drag - Automatic GPR	-65.8%	217.6%	96.9%	-228.4%
Half-cell - Manual GPR	-25.6%	47.2%	21.7%	-72.9%
Half-cell - Automatic GPR	-46.1%	142.5%	96.8%	-188.9%
Actual Repair - Manual GPR	1.5%	25.4%	20.5%	-17.5%
Actual Repair - Automatic GPR	-18.8%	121.6%	72.0%	-109.7%
Manual GPR - Automatic GPR	-10.7%	88.8%	55.7%	-77.0%

Alongi et al. (1993) reported that the GPR predicted deterioration area that is formulated using the default threshold of the automatic processing is expected to be within ± 11.2 percent of the ground truth quantities. The results of this research indicated that with average overestimates of $65.8\% \pm 162.6\%$ and $46.1\% \pm 142.9\%$ for the chain drag and half-cell potential survey quantities, respectively, the automatic processing results disagree with the accuracy reported by Alongi. Manual GPR processing was found to yield more accurate quantity overestimates of $19.4\% \pm 37.5\%$ and $25.6\% \pm 47.3\%$ of the chain drag and half-cell potential survey quantities, respectively. While the chain drag and half-cell potential surveys provide estimates of the repairs that will be made on the deck surface, the most important comparison, in terms of bridge management, is between the GPR predictions and the actual repair quantity. This quantity is based on the chain drag survey results, but is normally a larger quantity because repairs usually follow corrosion on the reinforcement until clean steel is observed. The automatic GPR processing resulted in an overestimate of $18.8\% \pm 90.8\%$, while the manual GPR processing resulted in an underestimate of $1.5\% \pm 19.0\%$ of the

actual repair quantity. Clearly, the manual GPR processing results provide, on average, a more accurate and precise estimate of the ground-truthing and actual repair quantities than do the automatic GPR processing results. The automatic GPR processing underestimated the manual GPR processing quantity by 10.7% \pm 66.4%.

Table 15 – Predicted, ground-truth and actual bridge deck deterioration quantities as percentages of the bridge deck surface area

Structure ID	Predicted Quantities		Ground-truth		Actual
	Manual (%)	Automatic (%)	Chain Drag (%)	Half-Cell (%)	Repaired (%)
Stewiacke River Bridge	44.5	22.8	53.9	50.5	59.7
Skye River Bridge	42.3	30.4	34.4	41.9	38.7
Baddeck River Bridge	37.4	30.9	34.9	46.0	40.1
Shubenacadie CNR Overpass	28.5	15.5	35.1	39.5	35.3
Grand Pre Overpass	15.0	32.6	9.1	8.3	11.2
Deep Hollow Overpass	70.1	20.2	54.0	31.4	54.6
Victoria Bridge	13.6	40.7	5.2	0.1	11.1
Rough Brook Bridge	21.2	21.7	27.2	n/a	29.4
Glendale Bridge	16.2	14.1	20.1	9.3	22.6

Alternatively, the deterioration estimates and actual findings can be expressed as a percentage of the deck surface area to normalize the statistical results. For example, the quantitative error of a fifty percent difference between predicted and actual deterioration quantities is more significant on a 300 m² deck surface than on a 2000 m² deck surface. Table 15 lists the average, standard deviation, and 95% confidence limits for comparisons of the ground-truthing and actual repair quantities and the GPR predicted quantities as percentages of the deck surface areas.

As with the quantitative comparison, the Deep Hollow and Shubenacadie CNR Overpasses were neglected from the computations regarding half-cell potential survey

results since only a portion of the entire deck surface was surveyed using that method. Furthermore, the statistics representing the difference between the GPR predictions and the actual repair quantities do not include the last seven structures listed in Table 15 because they were processed with an earlier version of the software than the other structures.

Table 16 lists the average, standard deviation, and 95% confidence limits for comparisons of the ground-truthing and actual repair quantities and the GPR predicted quantities as percentages of the bridge deck surface area.

Table 16 - Statistical comparisons of ground-truth and repair quantities to GPR predicted quantities as a percent of the bridge deck surface area

Comparison	Average (%)	Standard Deviation (%)	Upper 95% Confidence Limit (%)	Lower 95% Confidence Limit (%)
Chain Drag - Manual GPR	-1.7%	8.6%	4.8%	-8.1%
Chain Drag - Automatic GPR	5.0%	22.9%	22.1%	-12.1%
Half-cell - Manual GPR	-2.2%	8.5%	5.6%	-9.9%
Half-cell - Automatic GPR	-2.6%	22.3%	17.8%	-22.9%
Actual Repair - Manual GPR	1.5%	9.0%	8.3%	-5.2%
Actual Repair - Automatic GPR	3.6%	19.5%	14.5%	-7.3%
Manual GPR - Automatic GPR	6.7%	22.3%	23.3%	-10.0%

The results of this research indicated that with an average underestimate of 5.0% \pm 17.1% of the deck surface area for the chain drag and an overestimate of 2.6% \pm 16.6% for the half-cell potential survey quantities, respectively, the automatic GPR processing exhibits excessive variability in predicting the ground-truthing survey quantities. Manual GPR processing was found to yield more accurate quantity overestimates of 1.7% \pm 6.4% and 2.2% \pm 6.3% of the chain drag and half-cell potential survey quantities, respectively. The automatic GPR processing resulted in an underestimate of 3.6% \pm 14.5%, while the manual GPR processing resulted in an underestimate of 1.5% \pm 6.7% of the actual repair quantity. As with the quantitative comparisons, the manual GPR processing results

provide, on average, a more accurate and precise estimate of the ground-truthing and actual repair quantities than the automatic GPR processing results. The automatic GPR processing underestimated the manual GPR processing quantity by $6.7\% \pm 16.6\%$.

Table 17 lists the spatial correlation statistics for the nine bridge decks that were studied in this research.

Table 17 – Network level statistics of GPR spatial correlation with actual and ground-truth deterioration

Network Level Comparison of GPR Processing Methods	Relative to Chain Drag Results		Relative to Half-cell Results	
	Manual	Automatic	Manual	Automatic
Total Predicted Locations	20799	20799	12056	12056
Total Deterioration/True	5065	2933	2254	1476
Total Deterioration/False	2588	2405	939	1150
Total Sound/True	9574	9481	7393	6969
Total Sound/False	3572	5980	1470	2461
Overall % Correct Deterioration Predictions	66.2%	54.9%	70.6%	56.2%
Overall % Correct Sound Predictions	72.8%	61.3%	83.4%	73.9%
Overall % Total Correct Predictions	70.4%	59.7%	80.0%	70.0%
Overall % Total Incorrect Predictions	29.6%	40.3%	20.0%	30.0%
Overall Probability of correctly detecting deterioration	58.6%	32.9%	60.5%	37.5%
Overall Probability of correctly detecting sound concrete	78.7%	79.8%	88.7%	85.8%
Overall False alarm rate of detecting deterioration	21.3%	20.2%	11.3%	14.2%
Overall False alarm rate of detecting sound concrete	41.4%	67.1%	39.5%	62.5%

From these statistics, it is observed that the manual GPR data processing resulted in more accurate correct deterioration, correct sound concrete and therefore overall correct predictions, than the automatic GPR processing. The overall correct deterioration prediction rate with respect to the chain drag survey was 66.2%, which agrees well with the similar rate of 73.8% agreement as shown by core sampling of the decks during their repair. The core sampling data was analyzed in a similar fashion to the unit GPR prediction areas by confirming or disproving a deterioration or sound concrete prediction.

Confirmation of the prediction was based on water soluble chloride content that exceeded 0.25%, as per Ontario Ministry of Transportation practice, and also by identifying cracks or corrosion in the core sample.

The manual radar processing results exhibited a higher probability of detecting deterioration than the automatic processing by 25.7% and 23.0 % for the deterioration locations as determined by the chain drag and half-cell potential surveys, respectively. Similar probabilities of correct detection of sound concrete were observed for both GPR processing methods.

5.8 Effectiveness of Manual GPR Processing Deterioration Prediction

It has been shown that the manual GPR processing has provided the most reliable and accurate estimations of the quantity and location of the chain drag and half-cell potential survey results. This method must be compared against the criteria established in Section 2.1. While the GPR data is collected non-destructively from the deck without interfering with normal traffic flow, and can be processed manually to provide accurate and reliable results, the remaining three criteria may not be well satisfied. The manual processing method is completely subjective, relying on the operator's understanding of the radar waveform structure and the test subject itself. The operator must make qualitative decisions regarding the level of attenuation or reflectivity observed in the data. This affects the reproducibility of the results in that a given operator may feel differently about the threshold to use in deciding whether the deck is sound or deteriorated and certainly will result in different interpretations of the data by different operators. The hardware and manual processing software are simple to use, but the data interpretation and processing can be complex. Regardless, the method has been shown to be effective and still represents the most appropriate technology for deck assessment at traffic speeds.

How good is good enough with respect to the accuracy of the manual GPR processing results? Table 18 lists quantities of deterioration that were found by previous investigators using the chain drag survey and quantities that were predicted using traditional visual estimation methods. The statistics were selected from a list of estimates reported by Maser (1990) that fell within the range of the deterioration levels observed in this research.

Table 18 - Actual and estimated deterioration - visual estimation

Bridge ID	Actual Deterioration % Deck Surface Area	Engineer's Estimate % Deck Surface Area	Difference % Deck Surface Area
V2.1 - 2.5	8.4%	21.9%	-13.5%
V3.1 - 3.4	10.9%	16.3%	-5.4%
Mi6	14.7%	5.0%	9.7%
R5	34.4%	13.0%	21.4%
R6	40.0%	23.3%	16.7%
N2	20.0%	31.0%	-11.0%
Average			3.0%
Standard Deviation			14.9%
Confidence			13.6%
Lower 95% confidence limit			-10.7%
Upper 95% confidence limit			16.6%

Traditional visual estimation resulted in an average underestimation of the deterioration of 3.0% . 13.6% of the deck surface area. Manual GPR processing was observed in this research to result in an overestimate of 1.7% . 6.4% of the deck surface area, resulting in a slightly improved accuracy, but approximately half of the variability observed in the visual estimation results. The difference between 1.7% and 3.0% is minimal with respect to the cost of repairs, but with manual GPR processing yielding half of the variability that is observed when using traditional visual estimation, significant savings can be expected by decreasing unanticipated repair costs.

In Sections 5.6, 5.7 and 5.8 it was shown that the manual GPR processing technique can produce an relatively accurate estimate of the ground-truthing and actual repair quantities on a given bridge deck. However, the ability of the GPR results to clearly demonstrate the location and extent of all deterioration on a given deck seems to be insufficient to allow bridge managers to order specific sections of a deck span to be repaired. This predictive capability is not important with respect to saving time and materials since decks are usually stripped of all the asphalt in one lane at a time to allow for repairs. Identifying particular areas from a GPR survey report on a scale drawing of the deck, then transferring those areas onto the actual deck surface would be just as time consuming as using the chain drag survey to outline the unknown deterioration on the deck surface. Spatial correlation is therefore important only academically, to ensure that the processing procedure is utilizing the proper characteristics in the data to correlate with the actual deterioration. Spatial correlation provides a means of checking that the inverse problem of finding the flaw through a characteristic in the data, instead of the characteristic in the data by finding the flaw, is being solved effectively.

The most important benefit of GPR as a bridge management tool is the ability to predict within a known range of difference, the quantity of deterioration that is expected to be found on a given deck, within a subgroup of decks. This will allow managers to effectively prioritize the subgroup of bridges for repair, ensuring that the available budget is spent most efficiently. The degree of uncertainty that accompanied the traditional visual estimation of deterioration can be substantially reduced as a greater number of bridges throughout all districts can be assessed by a single operator with less variability in the results. A reduction in the variability of the difference between estimated and actual deterioration quantities will reduce the occurrences of gross underestimation, resulting in high unit prices and budget overruns and will also tend to reduce long-term unit prices as the variability of predictions is decreased. As discussed in Section 5.8, traditional visual estimation was observed, on average, to underestimate the actual deterioration levels and tends to drive up the unit cost. Manual GPR processing results

tend to slightly overestimate the deterioration quantities and hence, drive the immediate cost up, but tend to reduce the unit price over time.

Given the nondestructive capability of GPR to collect data at traffic speeds and given the improvements in accuracy and variability of the estimated deterioration quantities with respect to traditional visual estimation, GPR appears to provide a very effective method of condition assessment for asphalt-covered reinforced concrete bridge decks.

6. Conclusions and Recommendations

A collaborative research program was designed by Dalhousie University DalTech and the Nova Scotia Department of Transportation and Public Works to examine the accuracy and confidence with which GPR can be used to predict the quantity and location of delaminations and concrete scaling on asphalt covered bridge decks. Seventy-two bridge decks were surveyed at traffic speeds using GPR for deterioration estimation. The GPR data was processed manually using a novel combination of excess signal attenuation and areas of high concrete relative dielectric constant as deterioration indicators in the data. Deterioration predictions made using GPR were also compared quantitatively and spatially to ground-truthing data obtained from nine bridge decks using the well-established chain drag and half-cell potential surveys after the asphalt was removed from each bridge deck just prior to repair. These comparisons were used to construct statistics describing the accuracy and variation between the GPR predictions and the actual deterioration quantities for each deck and on a network level.

The results of this research indicated that the correlation using the default threshold of the automatic processing using signal attenuation with the chain drag results did not agree with the accuracy reported by Alongi et al. (1993). Adjustment of the statistical accuracy of this threshold, or better understanding of the relationship between the threshold and the waveform characteristics of the data representing the sound concrete, and therefore improved application of a threshold value, may improve the accuracy of the automatic processing results.

The automatic processing software requires only minimal user inputs including the location of stationary peak-tracking gates on the waveforms for a given data file. Since there are no visual means to monitor the tracking of the peaks, it must be assumed that the peaks are properly and consistently tracked during the automatic data processing. The incorporation of a graphic display during processing to ensure that the peaks are

being properly identified and tracked would be an asset, allowing the user to feel confident in the proper interpretation of the data. Furthermore, instead of using a fixed position for the peak-tracking gate, the software would be improved by allowing the user to use a variable-positioned gate to track the peaks in the data. Layer thicknesses and electrical properties can be subject to a high degree of variability on and between each deck such that the time position of the peaks will fluctuate significantly and may fall outside of the bounds of its normal position. The most appropriate way to achieve the definition of the variable-position tracking gate would be to view the data pass on the color intensity plot software and input a connected series of line segments over the peak locations, such that the tracking window is always positioned over the peak location. The width of the gate can then be reduced to avoid tracking nearby peaks that may interfere with the desired peak.

The manual processing results were based on a combination of signal attenuation and high concrete reflectivity, or high concrete relative dielectric constant. The automatic software allows the user to only produce output consisting of one deterioration characteristic at a time. Multi-characteristic processing results may improve the accuracy of the automatic GPR processing.

The manual processing relies on the user's capability to distinguish changes in the signal characteristics to denote areas of deterioration. This method requires the operator to be highly skilled at GPR data interpretation and therefore may be unsuitable for general use by a layperson. This research has shown that this has yielded a more accurate and precise result than the automatic processing provided with the GPR system. It follows that incorporation of manual processing into the automatic processing will improve the accuracy and precision of the results. This can be achieved by presenting a graphical depiction of a measured waveform characteristic for all waveforms on a scaled plan map of the deck surface, using a grey-scale intensity to represent the range of the value measured. For example, on a given data file, the bottom echo peak amplitude can

be automatically measured by the software and aligned in position of the deck surface. The most negative amplitudes can be represented by the darkest shades and the most positive amplitudes represented by the brightest shades. This will present a spatial depiction of the deck bottom echo on the deck surface by which the user can detect sufficient decrease in the peak magnitude to assign a deterioration detection within that data file. All data files can be represented in this fashion on the deck surface, using the full range of peak amplitudes to scale the shade intensity. Graphic displays of the waveform properties can allow the user to also detect changes in the waveform due to such objects as drains or diaphragms under the deck that may be falsely interpreted as deterioration. Furthermore, other measured phenomena in the data can be represented in this way, such as peak amplitude at the asphalt/concrete interface or signal attenuation. Combining the automatic measurement and comparison to a statistical threshold with the intuitive graphical deterioration detection of the manual processing will improve the accuracy and variability of the deterioration prediction.

The following conclusions were made on the basis of this research:

- 1) Manual processing of the GPR data based on both signal attenuation and high reflectivity from the asphalt/concrete interface provided the most accurate and least variable estimate of the actual deterioration repair quantity and location.
- 2) Manual processing of the GPR data underestimated the actual deterioration repair quantity by 1.5% \pm 6.7% of the total deck surface area. Manual processing of the GPR data also overestimated the chain drag designated deteriorated by 1.7 \pm 6.4% and overestimated the half-cell potential designated deterioration by 2.2% \pm 6.3%.

- 3) **Manual processing of the GPR data provided an increase in accuracy of 1.3% of the deck surface area and a reduction in variability of 7.2% of the deck surface area with respect to the performance of traditional visual estimations of deck deterioration.**
- 4) **Manual processing of the data exhibited the highest rates of correct spatial deterioration prediction of 66.2% and 70.6% with respect to the chain drag and half-cell potential surveys, respectively. Manual processing of the data also exhibited the highest probability of correctly detecting deterioration of 58.6% and 60.5% with respect to the chain drag and half-cell potential surveys, respectively.**
- 5) **Certain types of deck construction surveyed during this research program presented difficulties in data interpretation. These decks include prestressed and continuous spans where signal scattering and variable reflections from increased reinforcement content and tendons can occur. Monolithic decks that are in excess of 200 to 250 mm in thickness make full-depth signal penetration difficult. Variable thickness decks provide inconsistent locations of the deck bottom and incur losses through non-orthogonal reflections. Epoxy coated reinforcement in bridge decks prevents the depassivation of the reinforcement steel, thus disabling the correlation between excesses of moisture and chloride and reinforcement corrosion and delamination of the concrete cover.**

It is recommended that a number of factors that may have resulted in the inferior performance of the automatic GPR processing results, relative to the manual GPR processing results, be addressed.

An improvement to the manual processing results can be made by removing obvious misinterpretations from the reported deterioration quantity and locations, such as underlying diaphragms or drains on the deck. These can often be observed on the scaled plan maps of the deterioration locations on the deck surface after processing has been completed. These misinterpretations are obvious as regularly spaced thin lines across the deck width, in the case of diaphragms.

This research has led to the hypothesis that the accuracy and variability of the manual GPR processing estimate may increase with increasing levels of deterioration on a given deck. This phenomenon cannot be proven or disproven given the number of results presented in this research, but should be further investigated. If this phenomenon is found to exist, then new statistics must be computed to describe the quantitative relationship between the manual GPR processing predictions and the ground-truth or actual repair quantities. The predicted quantities should then be transformed by a mathematical function to establish a constant variance for all predicted levels of deterioration.

Improvements in efficiency in reporting the survey results can be achieved by changing the software or producing other software to tabulate the deterioration locations that form the output of both the manual and automatic processing software. These locations can then be used as inputs in a program to automatically draw the deck surface and deterioration locations in AutoCAD, reducing the time and effort required to produce the plan maps of the deck deterioration.

GPR provides a fast and nondestructive method of data collection through asphalt pavements, removing the need for traffic control during the actual inspection. This research has demonstrated that estimates of deck deterioration due to corrosion induced delamination and surface scaling or damage due to freezing and thawing can be estimated with slight improvements in accuracy, but less than half of the variability of traditional

visual estimation methods. The average difference between the manual GPR processing results and the actual repair quantities was an underestimate of 1.5% to 6.7% of the deck surface area. These improvements and this research will allow the Nova Scotia Department of Transportation to incorporate the deterioration surveys into a bridge management system. Management decisions can be made for a network of bridge decks before tendering repairs that will result in more efficient spending of the annual repair budget. Less variability between the predicted and actual repair quantities will lead to long term reductions in unit price of the work as contractors become comfortable with the accuracy and variability of the GPR predictions. GPR has been shown to be an effective method for condition assessment of asphalt-covered reinforced concrete bridge decks in Nova Scotia that should result in savings through reduced variability on a network level between estimates and actual quantities of deterioration.

The 5-year collaborative research project between the Nova Scotia Department of Transportation and Public Works will be completed on January 1, 2001. In the remaining two years of the project, further refinements will be made in the manual data processing and more ground-truth data will be collected to improve the statistical confidence of the relationships between the GPR estimates and the actual repair quantities. Furthermore, the application of GPR for pavement thickness measurement and evaluation will be investigated.

7. References

- Akroyd, T. N. W., and Jones, R. Non-Destructive Testing of Structural Concrete by the Ultrasonic Pulse Technique. Proceedings of the Fourth International Conference on Non-Destructive Testing, London, England, September 9-13, 1964, pp. 230-234
- Aktan, A., Farhey, D., Hunt, V., Helmicki, A., Brown, D., and Shelley, S. Objective Bridge Condition Assessment. International Symposium Non-Destructive Testing in Civil Engineering (NDT-CE), Vol. 1, September 26-28, 1995, pp. 51-59
- Allred, J. C. Rebar Location and Cover Measurements to Aid Corrosion Potential Surveys. <http://www.intercorr.com/intercorr/techsess/papers/session1/abstracts/allred.html>, December 14, 1998
- Alongi, A. J., Clemeña, G. G., and Cady, P. D. Condition Evaluation of Concrete Bridges Relative to Reinforcement Corrosion, Volume 3: Method of Evaluating the Condition of Asphalt-Covered Decks. Strategic Highways Research Program, Report SHRP-S-325, National Research Council, Washington DC, 1993
- Alongi, A. V., Cantor, T. R., Kneeter, C. P., and Alongi, A., Jr. Concrete Evaluation by Radar Theoretical Analysis, Transportation Research Record 853, Concrete Analysis and Deterioration, Transportation Research Board, National Research Council, National Academy of Sciences, Washington DC, 1982, pp. 31-37
- Al-Qadi, I. L., Riad, S. M., Su, W., and Haddad, R. H. Detecting flaws in Portland cement concrete using TEM horn antennae, Proceedings of Nondestructive Evaluation in Bridges and Highways, SPIE, S. Chase, Ed., SPIE, Scottsdale, AZ, Dec. 4-5, 1996, pp.2946-2951.

- American Society for Testing and Materials. Standard Test Method for Half-Cell Potentials of Uncoated Reinforcing Steel in Concrete. ASTM C 876 – 91, 1991, pp. 440-445**
- Attoh-Okine, N. O., and Roddis, W. M. Kim. Pavement Thickness Variability and its Effect on Determination of Moduli and Remaining Life. Transportation Research Record 1449, Design and Rehabilitation of Pavements, Transportation Research Board, National Research Council, Washington DC, 1994, pp. 39-45**
- Bechtel, M. E., and Alongi, A. V. Reflection from Wire-Mesh Shielding Structures. Technical Report SC-1, Penetradar Corporation, Niagara Falls, NY., 1976**
- Bungey, J. H., and Millard, S. G. Radar Inspection of Structures. Proc. Instn Civ. Engrs Structs & Bldgs, vol. 99, May, 1993, pp. 173-186**
- Cantor, T. R., and Kneeter, C. P. Radar as Applied to Evaluation of Bridge Decks. Transportation Research Record 853, Concrete Analysis and Deterioration, Transportation Research Board, National Research Council, National Academy of Sciences, Washington DC, 1982, pp. 37-42**
- Chung, T., Carter, C. R., Manning, D. G., and Holt, F. B. Signature Analysis of Radar Waveforms Taken on Asphalt-Covered Bridge Decks. Technical Report ME-84-01, Ontario Ministry of Transport and Communications, 1984**
- Clemeña, G. G. Nondestructive Inspection of Overlaid Bridge Decks with Ground Penetrating Radar, Transportation Research Record 899, Bridge inspection and rehabilitation, Transportation Research Board, National Research Council, National Academy of Sciences, Washington DC, 1983, pp. 21-32**

- Gannon, E. J., and Cady, P. D. **Condition Evaluation of Concrete Bridges Relative to Reinforcement Corrosion, Volume 1: State-of-the-art of existing methods, Report SHRP-S-323, Strategic Highways Research Program, National Research Council, Washington DC, 1993**
- Halabe, U., Sotoodehnia, A., Maser, K. R., and Kausel, E. A. **Modeling the Electromagnetic Properties of Concrete. ACI Materials Journal, Vol. 90, No. 6, November-December, 1993, pp. 552-563**
- Kemp, S. **Reinforcement Electropotentials Halfcell Potential Measurements. <http://www.techtest.demon.co.uk/half1.htm>, December 14, 1998**
- Lin, J. M., and Sansalone, M. **A Procedure for Determining P-wave Speed in Concrete for Use in Impact-Echo Testing Using a Rayleigh Wave Speed Measurement Technique. Innovation in Non-Destructive Testing of Concrete. ACI International SP-168. Farmington Hills, Michigan, 1997, pp.137-151**
- Loulizi, A. and Al-Qadi, I. L. **Use of Electromagnetic Waves to Evaluate Civil Infrastructure. Recent Advances in Bridge Engineering, Advanced Rehabilitation, Durable Materials, Nondestructive Evaluation, and Management, U. Meiers and R. Betti, Eds., Zurich, Switzerland, Jul 15-16, 1997, pp. 335-345**
- Manning, D. G., and Masliwec, T. **The Application of Radar and Thermography to Bridge Deck Condition Surveys, Technical Report MAT-90-11, Ontario Ministry of Transportation and Communications, November, 1990**
- Manning, D. G., and Holt, F. B. **Detecting Deterioration in Asphalt-Covered Bridge Decks, Transportation Research Record 899, Bridge Inspection and Rehabilitation,**

Transportation Research Board, National Research Council, National Academy of Sciences, Washington DC, 1983, pp. 10-20

Maser, K. R. Radar Pavement Thickness Evaluations for Varying Base Conditions. Transportation Research Record 1355, National Research Council, National Academy Press, Washington, DC, 1995, pp. 90-98

Maser, K. R., and Scullion, T. R. Automated Pavement Subsurface Profiling using Radar: Case Studies of Four Experimental Field Sites. Transportation Research Record 1344, Transportation Research Board, National Research Council, National Academy Press, Washington, DC, 1994, pp.148-154

Maser, K. R. New Technology for Bridge Deck Assessment, Phase II Report. Report No. FHWA-NETC-90-01, Massachusetts Institute of Technology, Center for Transportation Studies, Federal Highways Administration, McLean, VA., 1990

Maser, K. R. New Technology for Bridge Deck Assessment, Phase I Report. Report No. FHWA-NETC-89-01, Massachusetts Institute of Technology, Center for Transportation Studies, Federal Highways Administration, McLean, VA., 1989

Maser, K., Brademeyer, B., and Littlefield, R. Pavement Condition Diagnosis Based on Multisensor Data. Transportation Research Record 1196, Pavement Evaluation and Rehabilitation, Transportation Research Board, National Research Council, National Academy Press, Washington, DC, 1988, pp.62-71

Mesher, D. E., Dawley, C. B., Davis, J. L., and Rossiter, J. R. Evaluation of New Ground Penetrating Radar Technology to Quantify Pavement Structures. Transportation Research Record 1505, Transportation Research Board, National Academy Press, Washington, DC, 1995, pp. 17-26

- Neville, A. M., and Brooks, J. J. **Concrete Technology**. John Wiley & Sons, Inc., New York, 1987, pp. 275-278
- Poston, R., and Sansalone, M. **Detecting Cracks in the Beams and Columns of a Post-Tensioned Parking Garage Using the Impact-Echo Method**. **Innovation in Non-Destructive Testing of Concrete**, ACI International SP-168. Farmington Hills, Michigan, 1997, pp.199-219
- Rösch, A., Hillemeier, B., Porzig, E., Krause, M., and Maierhofer, C. **Air Voids, Poor Compaction and Areas of Low Concrete Strength Detection in Concrete by Pulse Velocity Measurements**, **International Symposium Non-Destructive Testing in Civil Engineering (NDT-CE)**, Berlin, Germany, September 26-28, 1995, pp. 895-902
- Sansalone, M., and Streett, W. **Use of the Impact-Echo Method and Field Instrument for Non-Destructive Testing of Concrete Structures**. **International Symposium Non-Destructive Testing in Civil Engineering (NDT-CE)**, Berlin, Germany, September 22-28, 1995. pp. 495-502
- Sansalone, M., Carino, N. J. **Detecting Delaminations in Concrete Slabs With and Without Overlays Using the Impact-Echo Method**, **ACI Materials Journal Technical Paper**, **ACI Materials Journal**, Vol. 86, No.2, March-April, 1989
- Shaw, P., and Xu, A. **Assessment of the Deterioration of Concrete in NPP – Causes, Effects and Investigative Methods**, <http://www.ndt.net/article/0298/shaw/shaw.htm>, February, 1998
- Unknown, **Concrete Repair Digest**, August/September 1996, Vol. 7, No. 4, pp. 179-181.

- Volkwein, A. Potential Measurements on Prestressed Concrete Bridges Required Additional Informations for a Durable Repair, International Symposium Non-Destructive Testing in Civil Engineering (NDT-CE), Berlin, Germany, September 26-28, 1995, pp. 887-893**
- Wimsatt, A. J. The Use of Ground Penetrating Radar in Pavement Rehabilitation Strategy Selection and Pavement Condition Assessment.
<http://www.flash.net/~awimsatt/GPR3g.html>, December 14, 1998**
- Wollbold, F., and Neisecke, J. Ultrasonic-Impulse-Echo-Technique – Advantages of an Online Imaging Technique for the Inspection of Concrete, International Symposium Non-Destructive Testing in Civil Engineering (NDT-CE), Berlin, Germany, September 26-28, 1995, pp. 1135-1143**

8. Appendices

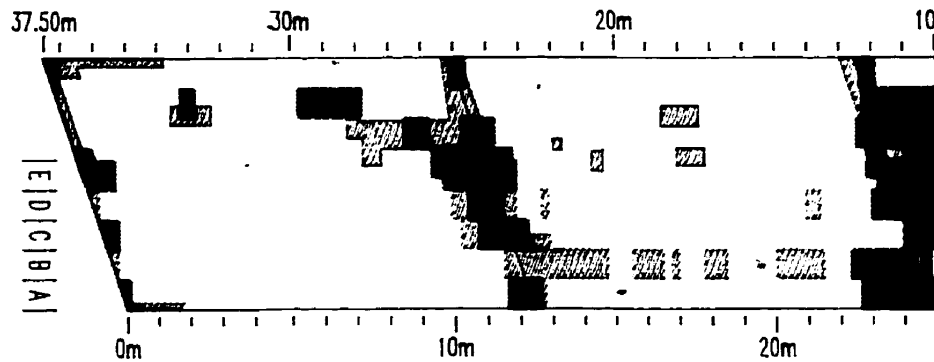
Glendale Bridge

GPR Deck Survey
March 19, 1997

Chain Drag Area = 63.3 m²
Percent Chain Drag Area = 20.1%

Combined Radar Indicator Area = 50.9 m²
Percent Combined Radar Indicator Area = 16.2%

Surface Area = 315.0 m²
Surveyed Surface Area = 315.0 m²



Glendale_Thesis.dwg 99/03/12



DALHOUSIE
University

DalTech
Architecture
Computer Science
Engineering

REFERENCE

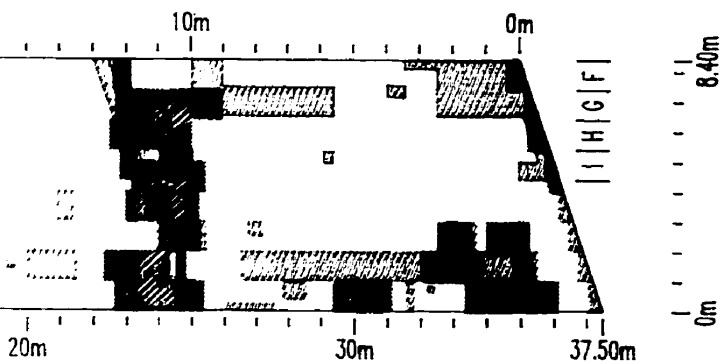
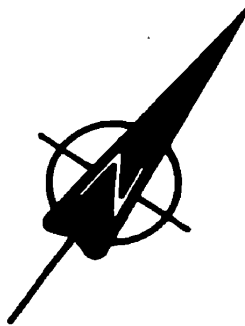
SCALE : 1cm = 250 cm

DATE : 99/03/12





DRAWN BY : C. BARNES

APPROVED BY :

NONA SC
TRANSPORTA
GROUNDTRU
GLD



Legend

-  - SIGNAL ATTENUATION (MANUAL)
-  - HIGH CONCRETE REFLECTIVITY (MANUAL)
-  - SIGNAL ATTENUATION AND HIGH CONCRETE REFLECTIVITY (MANUAL)
-  - CURB DRAG AREAS

NOVA SCOTIA DEPARTMENT OF
TRANSPORTATION AND PUBLIC WORKS
ROUNDTRUTHING COMPARISON
GLENDALE, NOVA SCOTIA

GLENDALE BRIDGE

DRAWING NO.

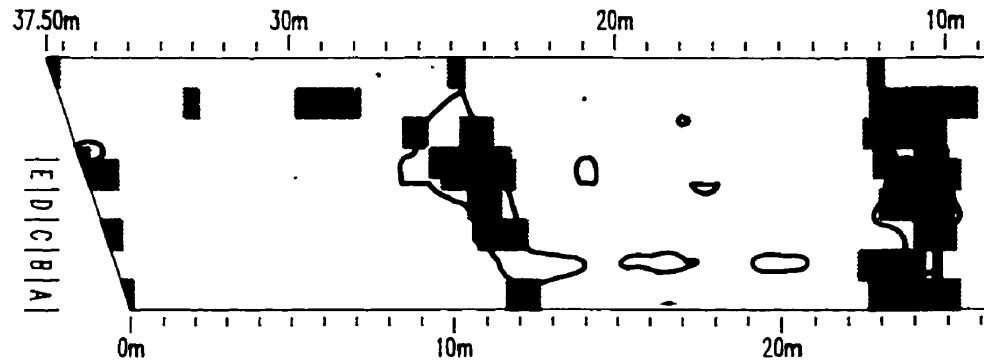
Appendix A1.1

Glendale Bridge

GPR Deck Survey
March 19, 1997

Surface Area = 315.0 m²
Surveyed Surface Area = 315.0 m²

Half Cell Potential Area = 29.1 m²
Percent Half Cell Potential Area = 9.3%
Combined Radar Indicator Area = 50.9 m²
Percent Combined Radar Indicator Area = 16.2%



Glendale_Thesis.dwg 99/03/12



DALHOUSIE
University

DalTech
Architecture
Computer Science
Engineering

REFERENCE

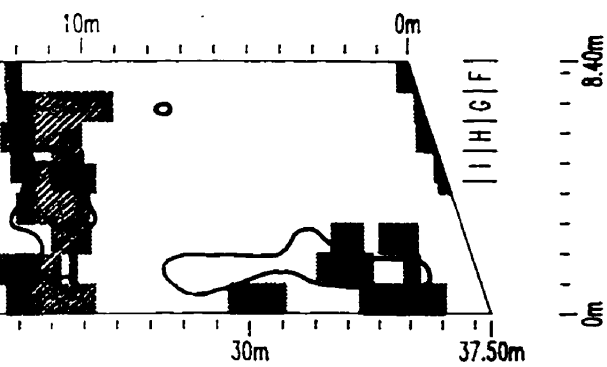
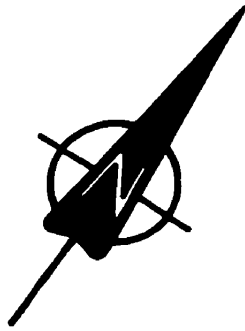
SCALE : 1cm = 250 cm

DATE : 99/03/12





DRAWN BY : C. BARNES

APPROVED BY :

NOVA SCOTIA
TRANSPORTATION
GROUNDTRUTHI
GLENDALE



Legend

-  - SIGNAL ATTENUATION (NORMAL)
-  - HIGH CONCRETE REFLECTIVITY (NORMAL)
-  - SIGNAL ATTENUATION AND HIGH CONCRETE REFLECTIVITY (NORMAL)
-  - HALFCELL POTENTIAL < -0.35 VOLTS

NOVA SCOTIA DEPARTMENT OF
 TRANSPORTATION AND PUBLIC WORKS
 TRUTHING COMPARISON
 GLENDALE, NOVA SCOTIA

GLENDALE BRIDGE

DRAWING NO.

Appendix A1.2

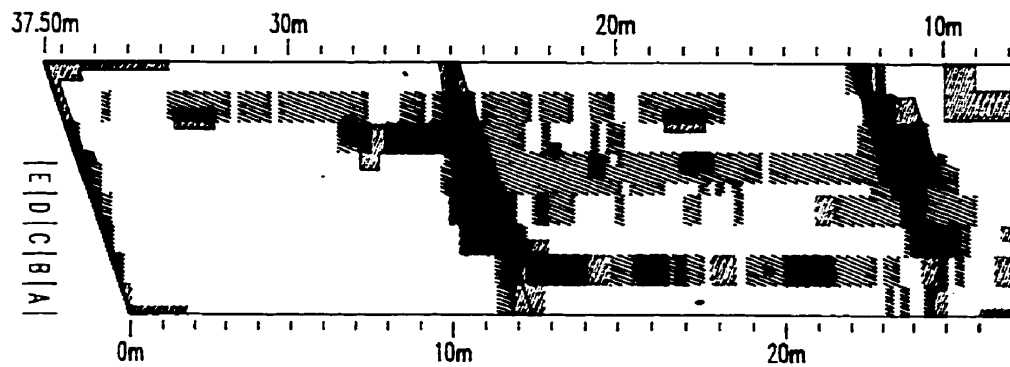
Glendale Bridge

GPR Deck Survey
 March 19, 1997

Chain Drag Area = 63.3 m²
 Percent Chain Drag Area = 20.1%

Surface Area = 315.0 m²
 Surveyed Surface Area = 315.0 m²

Automatic Processing Indicator Area = 44.4 m²
 Percent Automatic Processing Indicator Area = 14.1%



Glendale_Thesis.dwg 99/03/12



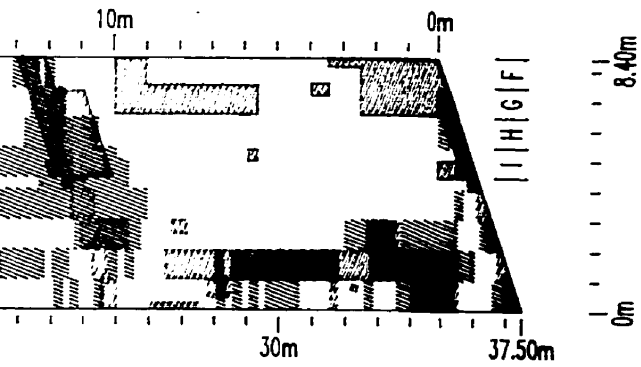
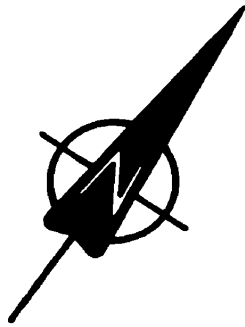
DALHOUSIE
 University

DalTech
 Architecture
 Computer Science
 Engineering

REFERENCE

SCALE : 1cm = 250 cm
 DATE : 99/03/12
 DRAWN BY : C. BARNES
 APPROVED BY :

NOVA SCOTIA DEPARTMENT OF
 TRANSPORTATION AND
GROUNDTRUTHING
 GLENDALE, NS



Legend

 - SIGNAL ATTENUATION (AUTOMATIC)

 - CURB DRAG AREAS

NOVA SCOTIA DEPARTMENT OF
TRANSPORTATION AND PUBLIC WORKS
IDTRUTHING . COMPARISON
GLENDALE, NOVA SCOTIA

GLENDALE BRIDGE

DRAWING NO.

Appendix A1.3

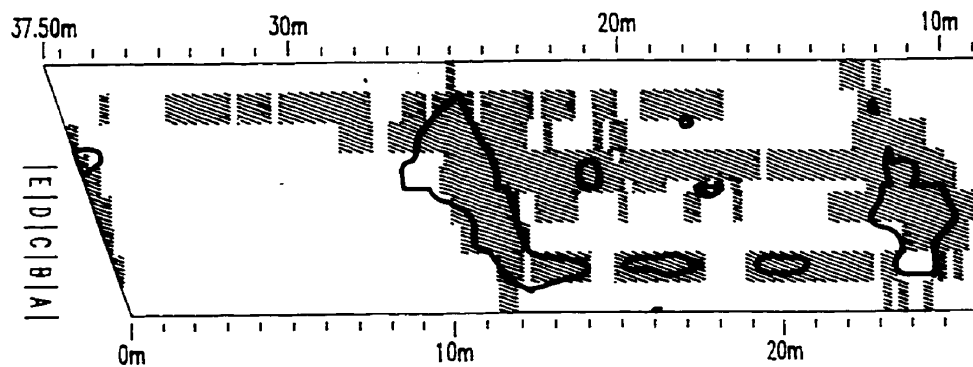
Glendale Bridge

GPR Deck Survey
March 19, 1997

Half Cell Potential Area = 29.1 m²
Percent Half Cell Potential Area = 9.3%

Surface Area = 315.0 m²
Surveyed Surface Area = 315.0 m²

Automatic Processing Indicator Area = 44.4 m²
Percent Automatic Processing Indicator Area = 14.1%



Glendale_Thesis.dwg 99/03/12



DALHOUSIE
University

DalTech
Architecture
Computer Science
Engineering

REFERENCE

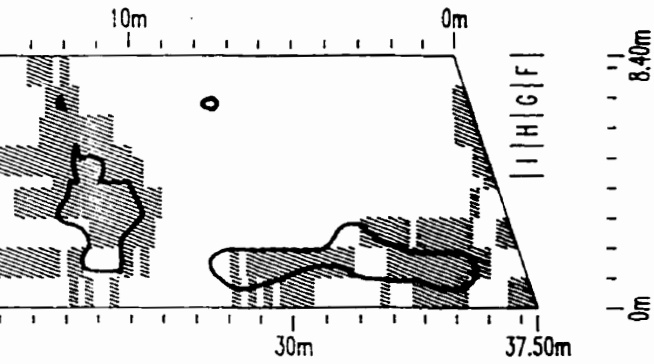
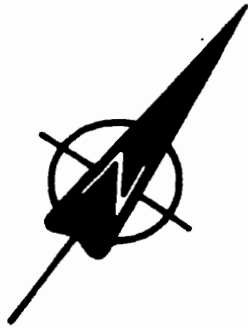
SCALE : 1cm = 250 cm

DATE : 99/03/12

DRAWN BY : C. BARNES


APPROVED BY :

NOVA SCOTIA
TRANSPORTATION
GROUNDTRUTH
GLENDALE



Legend

 - SIGNAL ATTENUATION (AUTOMATIC)

 - HALFCELL POTENTIAL
< -0.35 VOLTS

NOVA SCOTIA DEPARTMENT OF
TRANSPORTATION AND PUBLIC WORKS
CORROSION MONITORING AND
VALIDATION COMPARISON
GLENDALE, NOVA SCOTIA

GLENDALE BRIDGE

DRAWING NO.

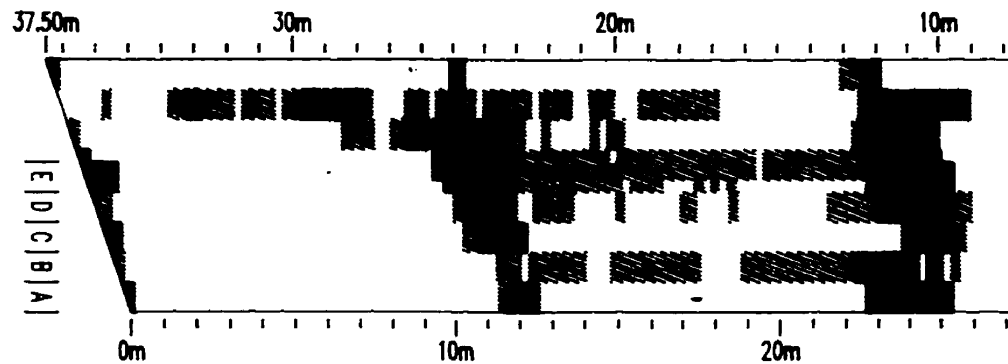
Appendix A1.4

Glendale Bridge

GPR Deck Survey
March 19, 1997

Surface Area = 315.0 m²
Surveyed Surface Area = 315.0 m²

Combined Radar Indicator Area = 50.9 m²
Percent Combined Radar Indicator Area = 16.2%
Automatic Processing Indicator Area = 44.4 m²
Percent Automatic Processing Indicator Area = 14.1%



Glendale_Thesis.dwg 99/03/12



DALHOUSIE
University

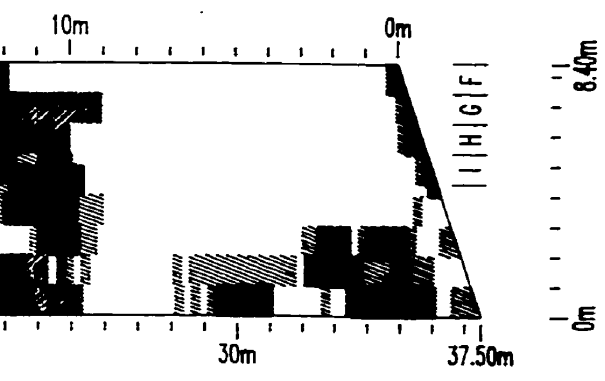
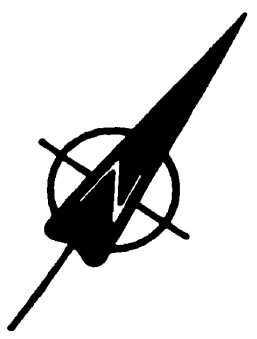
DalTech
Architecture
Computer Science
Engineering

REFERENCE





SCALE : 1cm = 250 cm
DATE : 99/03/12
DRAWN BY : C. BARNES
APPROVED BY :

NOVA SCOTIA DEPARTMENT OF
TRANSPORTATION AND
INFRASTRUCTURE

GPR PROCESSING
GLENDALE, NOVA SCOTIA



Legend

-  - SIGNAL ATTENTION (AUTOMATIC)
-  - SIGNAL ATTENTION (NORMAL)
-  - HIGH CONCRETE REFLECTIVITY (NORMAL)
-  - SIGNAL ATTENTION AND HIGH CONCRETE REFLECTIVITY (NORMAL)

NOVA SCOTIA DEPARTMENT OF
TRANSPORTATION AND PUBLIC WORKS
PROCESSING COMPARISON
GLENDALE, NOVA SCOTIA

GLENDALE BRIDGE

DRAWING NO.

Appendix A1.5

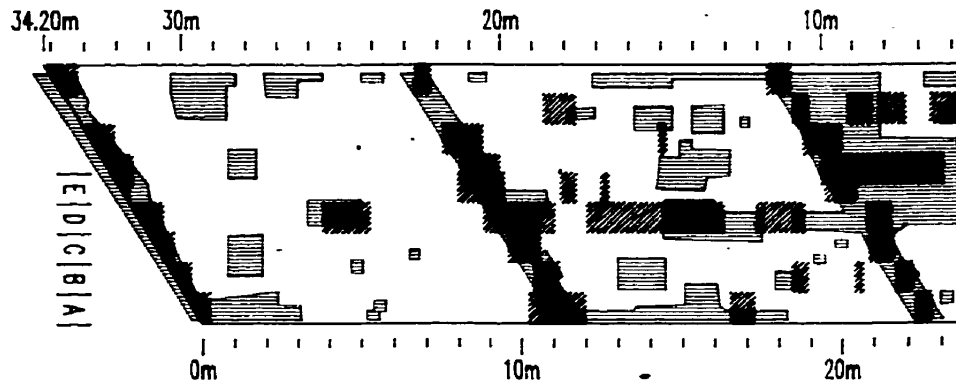
Rough Brook Bridge

GPR Deck Survey
 March 19, 1997

Chain Drag Area = 80.0 m²
 Percent Chain Drag Area = 27.2%

Combined Radar Indicator Area = 62.3 m²
 Percent Combined Radar Indicator Area = 21.2%

Surface Area = 315.0 m²
 Surveyed Surface Area = 315.0 m²



Rough_Brook_Thesis.dwg 99/03/12



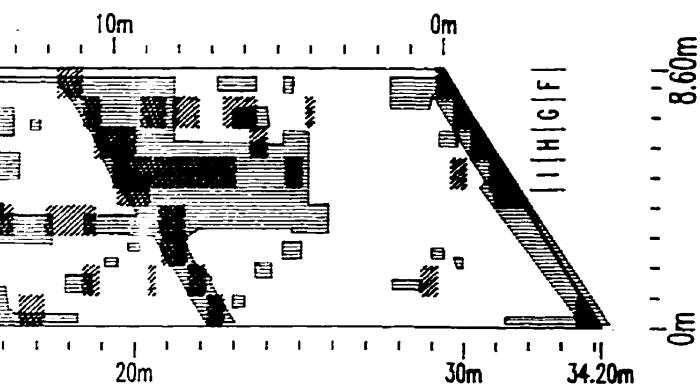
DALHOUSIE
 University

DalTech
 Architecture
 Computer Science
 Engineering





REFERENCE

SCALE : 1cm = 250 cm
 DATE : 99/03/12
 DRAWN BY : C. BARNES
 APPROVED BY :

NOVA SCOTIA DEPARTMENT OF
 TRANSPORTATION AND
GROUNDTRUTHING
 MCINTYRE'S MOUND



Legend

-  - SIGNAL ATTENUATION (NORMAL)
-  - HIGH CONCRETE REFLECTIVITY (NORMAL)
-  - SIGNAL ATTENUATION AND HIGH CONCRETE REFLECTIVITY (NORMAL)
-  - CHURN DRAG AREAS

NOVA SCOTIA DEPARTMENT OF
TRANSPORTATION AND PUBLIC WORKS
FOUNDTRUTHING COMPARISON
MCINTYRES MOUNTAIN, NOVA SCOTIA

ROUGH BROOK BRIDGE

DRAWING NO.

Appendix A2.1

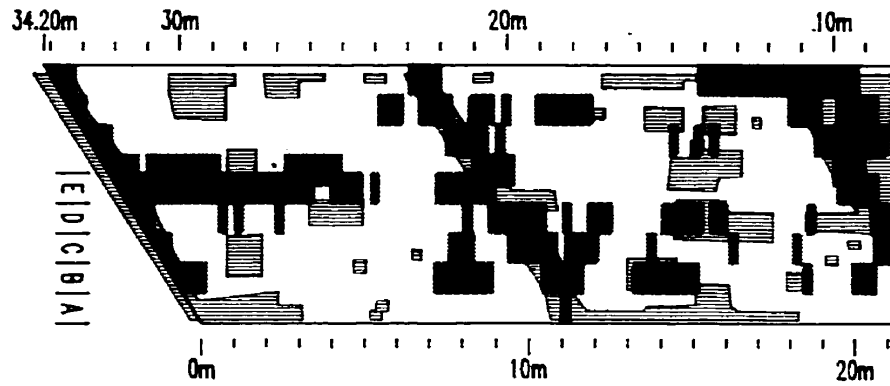
Rough Brook Bridge

GPR Deck Survey
March 19, 1997

Chain Drag Area = 80.0 m²
Percent Chain Drag Area = 27.2%

Surface Area = 315.0 m²
Surveyed Surface Area = 315.0 m²

Automatic Processing Indicator Area = 63.9 m²
Percent Automatic Processing Indicator Area = 21.7%



Rough_Brook_Thesis.dwg 99/03/12



DALHOUSIE
University

DalTech
Architecture
Computer Science
Engineering

REFERENCE

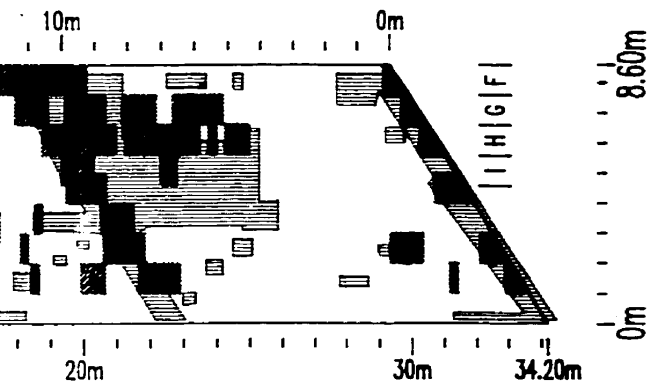
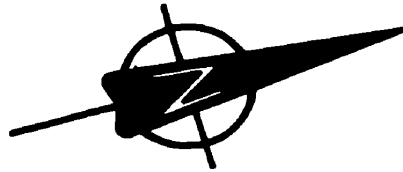
SCALE : 1cm = 250 cm

DATE : 99/03/12

DRAWN BY : C. BARNES

APPROVED BY :

NOVA SCOTIA
TRANSPORTATION
GROUNDTRUTH
MCINTYRE



Legend

 - SEWAL ATTENUATION (AUTOMATIC)

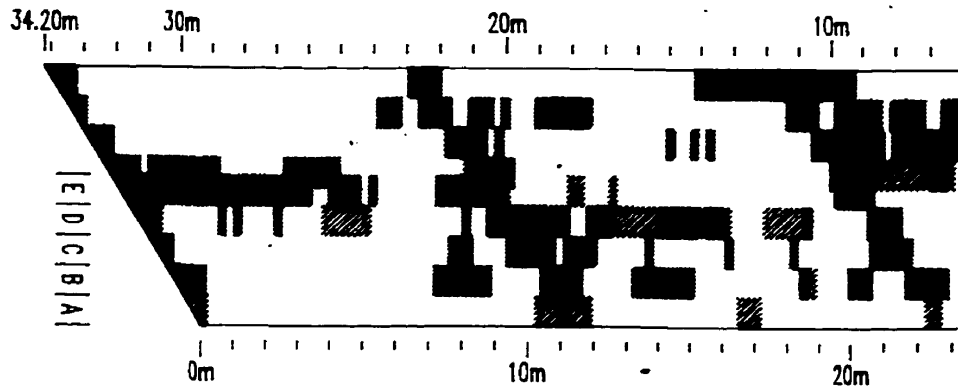
 - CIVIL BRG MEAS

Rough Brook Bridge

GPR Deck Survey
March 19, 1997

Surface Area = 315.0 m²
Surveyed Surface Area = 315.0 m²

Combined Radar Indicator Area = 62.3 m²
Percent Combined Radar Indicator Area = 21.2%
Automatic Processing Indicator Area = 63.9 m²
Percent Automatic Processing Indicator Area = 21.7%



Rough_Brook_Thesis.dwg 99/03/12



DALHOUSIE
University

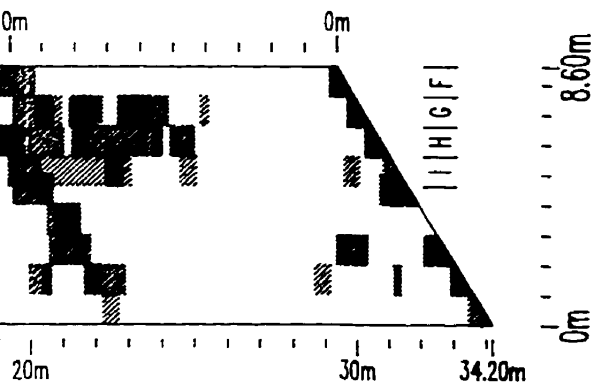
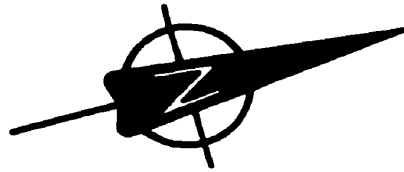
DalTech
Architecture
Computer Science
Engineering

REFERENCE

SCALE : 1cm = 250 cm
DATE : 99/03/12
DRAWN BY : C. BARNES
APPROVED BY :

NOVA SCOTIA DE
TRANSPORTATION AN

GPR PROCESSING
MCINTYRES MOUNTAIN



Legend

- SIGNAL ATTENUATION (AUTOMATIC)
- SIGNAL ATTENUATION (MANUAL)
- HIGH CONCRETE REFLECTIVITY (MANUAL)
- SIGNAL ATTENUATION AND HIGH CONCRETE REFLECTIVITY (MANUAL)

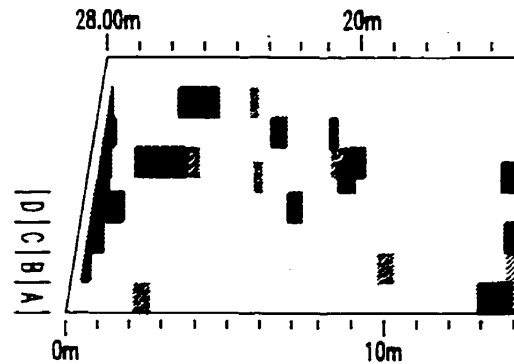
Victoria Bridge

GPR Deck Survey
March 19, 1997

Chain Drag Area = 12.5 m²
Percent Chain Drag Area = 5.2%

Combined Radar Indicator Area = 28.5 m²
Percent Combined Radar Indicator Area = 13.6%

Surface Area = 315.0 m²
Surveyed Surface Area = 315.0 m²



Victoria_Thesis.dwg 99/03/12



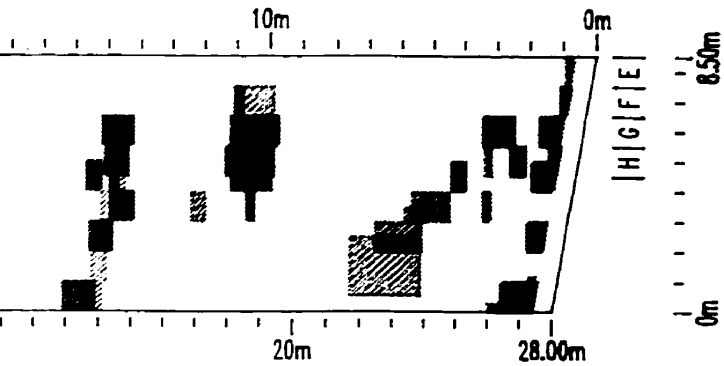
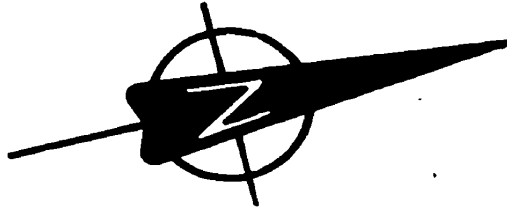
DALHOUSIE
University

DalTech
Architecture
Computer Science
Engineering


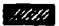


REFERENCE

SCALE : 1cm = 250 cm
DATE : 99/03/12
DRAWN BY : C. BARNES
APPROVED BY :

NOVA SCOTIA
TRANSPORTATION
GROUNDTRUTH
KENNEDY



Legend

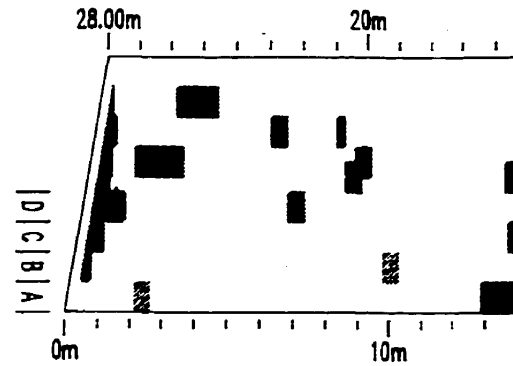
-  - SIGNAL ATTENUATION (ANNUAL)
-  - HIGH CONCRETE REFLECTIVITY (ANNUAL)
-  - SIGNAL ATTENUATION AND HIGH CONCRETE REFLECTIVITY (ANNUAL)
-  - CHWV DRAG AXES

Victoria Bridge

GPR Deck Survey
March 19, 1997

Half Cell Potential Area = 0.1 m^2
Percent Half Cell Potential Area = 0.0%
Combined Radar Indicator Area = 28.5 m^2
Percent Combined Radar Indicator Area = 13.6%

Surface Area = 315.0 m^2
Surveyed Surface Area = 315.0 m^2



Victoria_Thesis.dwg 99/03/12



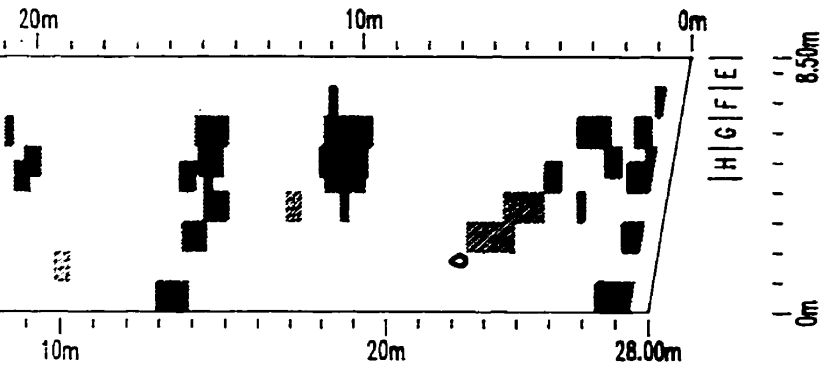
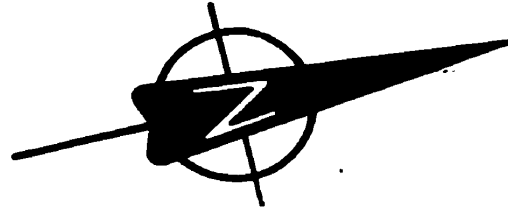
DALHOUSIE
University

DalTech
Architecture
Computer Science
Engineering





REFERENCE

SCALE : 1cm = 250 cm
DATE : 99/03/12
DRAWN BY : C. BARNES
APPROVED BY :

NOVA SCOTIA
TRANSPORTATION
GROUNDTRUTH
GENERAL



Legend

-  - SIGNAL ATTENUATION (UNUSUAL)
-  - HIGH CONCRETE REFLECTIVITY (UNUSUAL)
-  - SIGNAL ATTENUATION AND HIGH CONCRETE REFLECTIVITY (UNUSUAL)
-  - HALFCELL POTENTIAL < -0.35 VOLTS

NOVA SCOTIA DEPARTMENT OF
TRANSPORTATION AND PUBLIC WORKS
FOUNDTRUTHING COMPARISON
KINGSVILLE, NOVA SCOTIA

VICTORIA BRIDGE

DRAWING NO.

Appendix A3.2

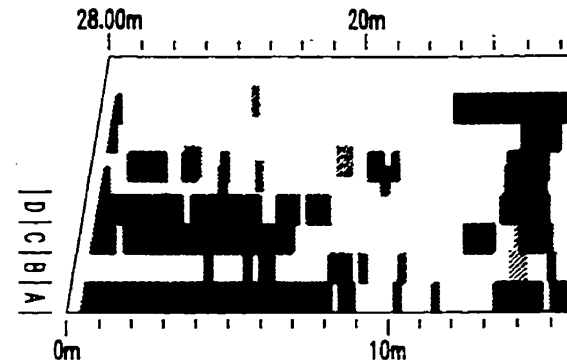
Victoria Bridge

GPR Deck Survey
March 19, 1997

Chain Drag Area = 12.5 m²
Percent Chain Drag Area = 5.2%

Surface Area = 315.0 m²
Surveyed Surface Area = 315.0 m²

Automatic Processing Indicator Area = 85.4 m²
Percent Automatic Processing Indicator Area = 40.7%



Victoria_Thesis.dwg 99/03/12



DALHOUSIE
University

DalTech
Architecture
Computer Science
Engineering

REFERENCE

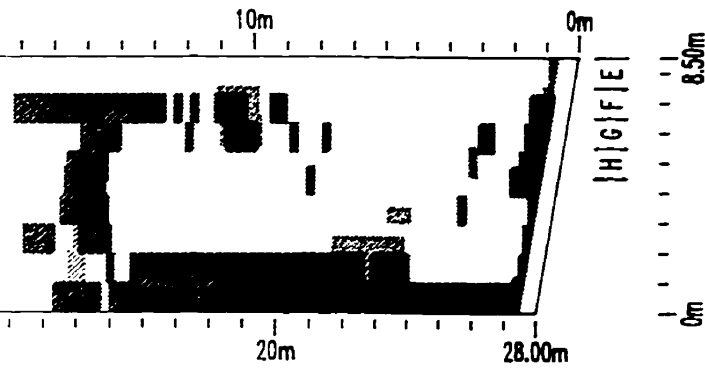
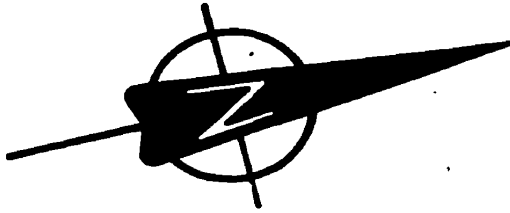
SCALE : 1cm = 250 cm

DATE : 99/03/12

DRAWN BY : C. BARNES

APPROVED BY :

NOVA SCOTIA DEPARTMENT OF
TRANSPORTATION AND
GROUNDTRUTHING
KINGVILLE, N.S.



Legend

 - SIGNAL ATTENUATION (AUTOMATIC)

 - CONSTRUCTION AREAS

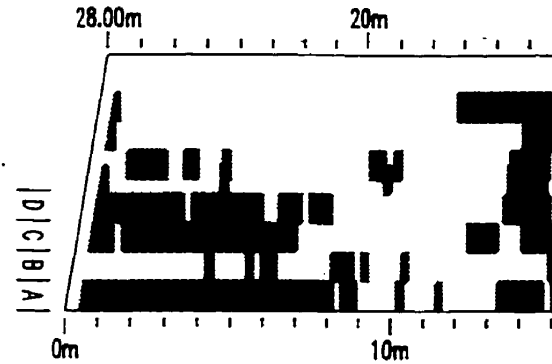
Victoria Bridge

GPR Deck Survey
March 19, 1997

Half Cell Potential Area = 0.1 m²
Percent Half Cell Potential Area = 0.0%

Surface Area = 315.0 m²
Surveyed Surface Area = 315.0 m²

Automatic Processing Indicator Area = 85.4 m²
Percent Automatic Processing Indicator Area = 40.7%



Victoria_Thesis.dwg 99/03/12



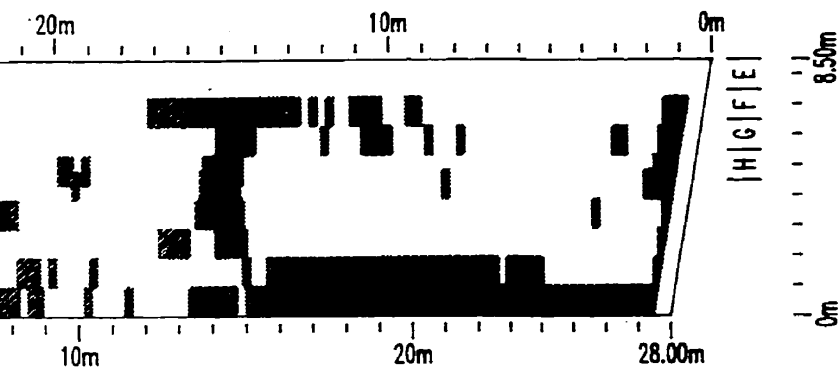
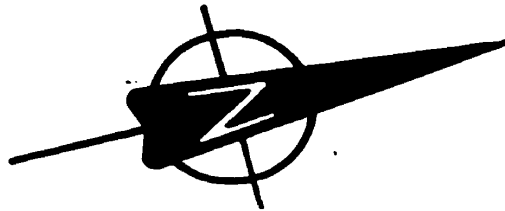
DALHOUSIE
University

DalTech
Architecture
Computer Science
Engineering

REFERENCE

SCALE : 1 cm = 250 cm
DATE : 99/03/12
DRAWN BY : C. BARNES
APPROVED BY :

NOVA SCOTIA
TRANSPORTATION
GROUNDTRUTHING
KINGVILLE



Legend

■ - SIGNAL ATTENUATION (AUTOMATIC)

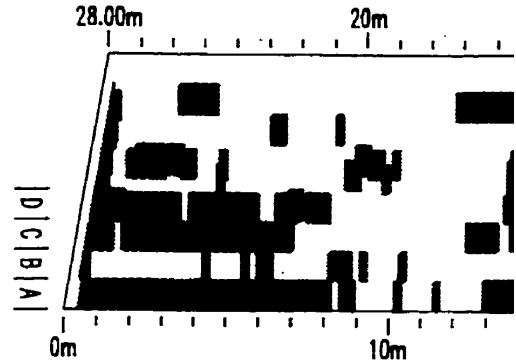
~ - HALFCELL POTENTIAL
< -0.35 VOLTS

Victoria Bridge

GPR Deck Survey
March 19, 1997

Surface Area = 315.0 m²
Surveyed Surface Area = 315.0 m²

Combined Radar Indicator Area = 28.5 m²
Percent Combined Radar Indicator Area = 13.6%
Automatic Processing Indicator Area = 85.4 m²
Percent Automatic Processing Indicator Area = 40.7%



Victoria_Thesis.dwg 99/03/12



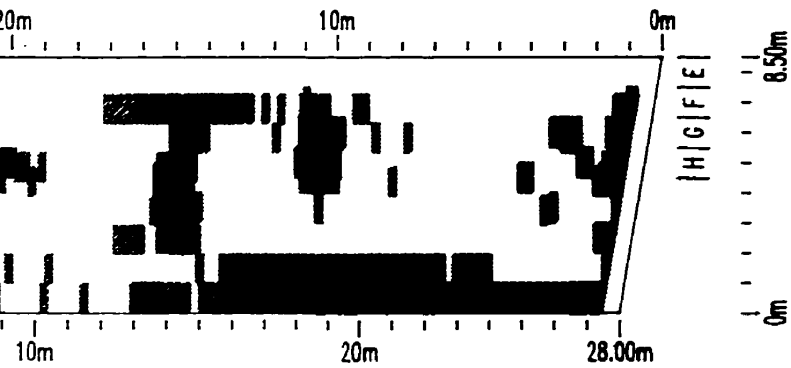
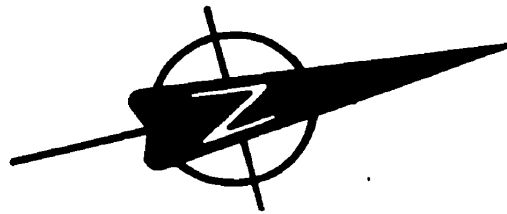
DALHOUSIE
University

DalTech
Architecture
Computer Science
Engineering





REFERENCE

SCALE : 1cm = 250 cm
DATE : 99/03/12
DRAWN BY : C. BARNES
APPROVED BY :

NOVA SCOTIA
TRANSPORTATION
GPR PROCESSING
KINGSTON



Legend

-  - SIGNAL ATTENUATION (AUTOMATIC)
-  - SIGNAL ATTENUATION (MANUAL)
-  - HIGH CONCRETE REFLECTIVITY (MANUAL)
-  - SIGNAL ATTENUATION AND HIGH CONCRETE REFLECTIVITY (MANUAL)

<p>NOVA SCOTIA DEPARTMENT OF TRANSPORTATION AND PUBLIC WORKS PROCESSING COMPARISON KINGSVILLE, NOVA SCOTIA</p>	<p>VICTORIA BRIDGE</p>	<p>FIGURE NO. Appendix A3.5</p>
---	-------------------------------	--

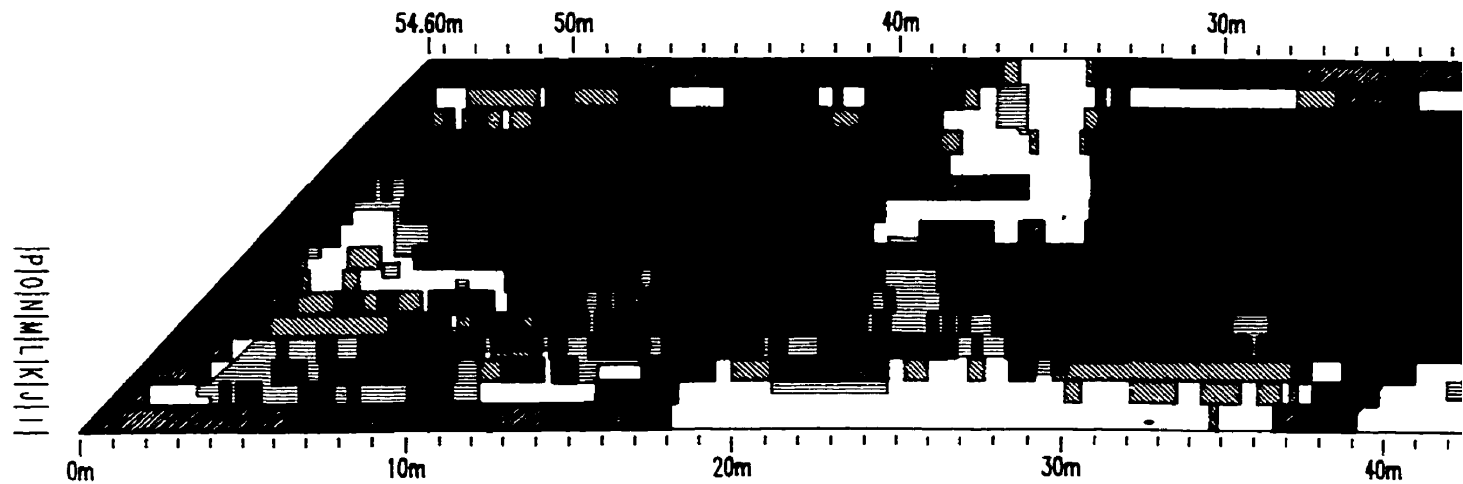
Deep Hollow Overpass

GPR Deck Survey
October 17, 1996

Chain Drag Area = 361.2 m²
Percent Chain Drag Area = 54.0%

Combined Radar Indicator Area = 468.6 m²
Percent Combined Radar Indicator Area = 70.1%

Surface Area = 671.3 m²
Surveyed Surface Area = 668.5 m²



Deep_Hollow_Thesis.dwg 99/03/12



DALHOUSIE
University

DalTech
Architecture
Computer Science
Engineering

REFERENCE

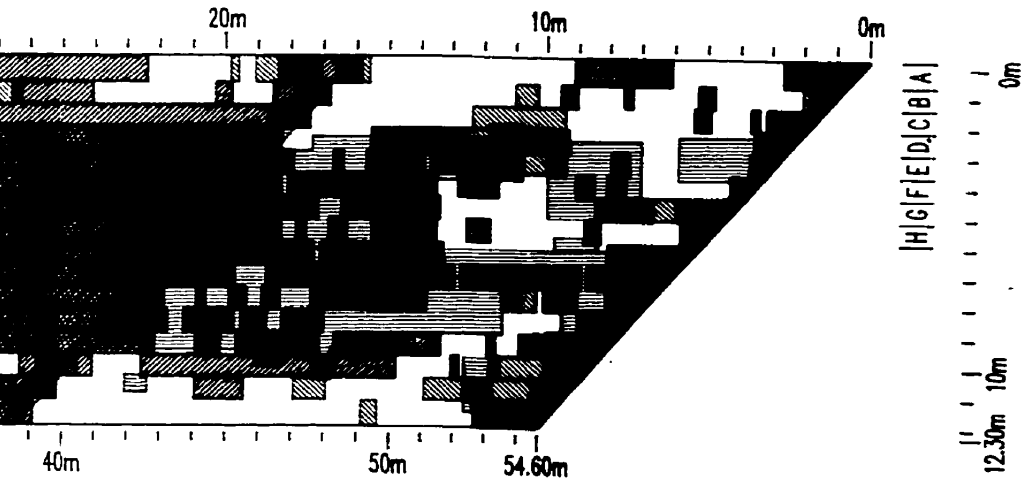
SCALE : 1cm = 250 cm

DATE : 99/03/12





DRAWN BY : C. BARNES

APPROVED BY :

Nova Scotia
TRANSPORTATION
GROUNDTRUTH
WOLFEMILL



Legend

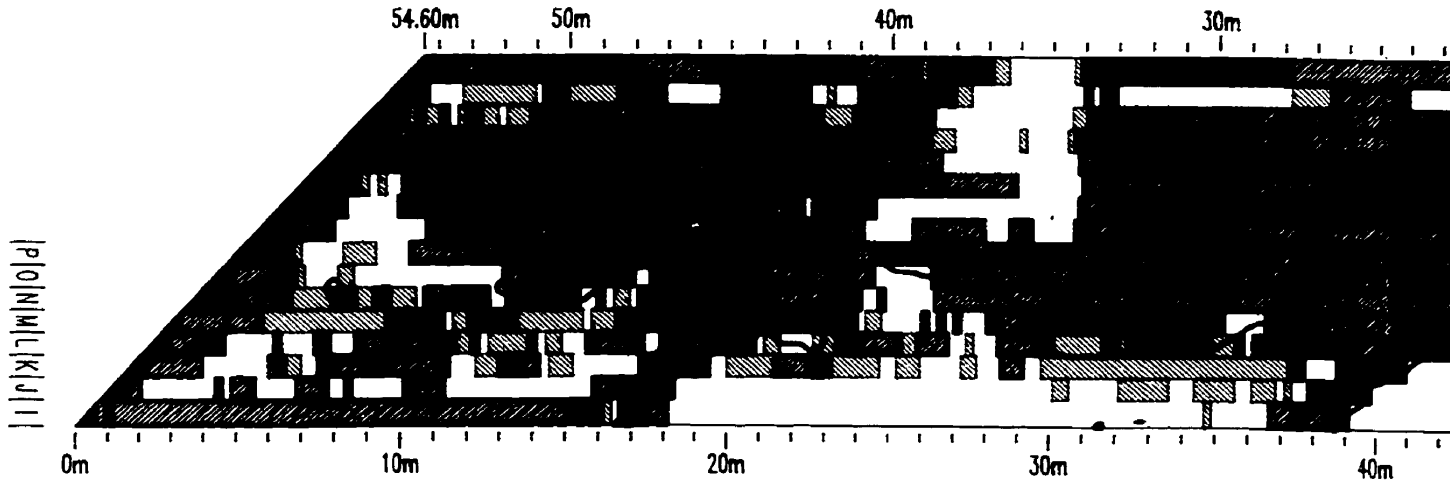
-  - SIGNAL ATTENUATION (MINIMAL)
-  - HIGH CONCRETE REFLECTIVITY (MINIMAL)
-  - SIGNAL ATTENUATION AND HIGH CONCRETE REFLECTIVITY (MINIMAL)
-  - CURB DRAG AREAS

Deep Hollow Overpass

GPR Deck Survey
 October 17, 1996

Half Cell Potential Area = 99.5 m²
 Percent Half Cell Potential Area = 99.5/316.9 = 31.4%
 Combined Radar Indicator Area = 468.6 m²
 Percent Combined Radar Indicator Area = 70.1%

Surface Area = 671.3 m²
 Surveyed Surface Area = 668.5 m²



Deep_Hollow_Thesis.dwg 99/03/12



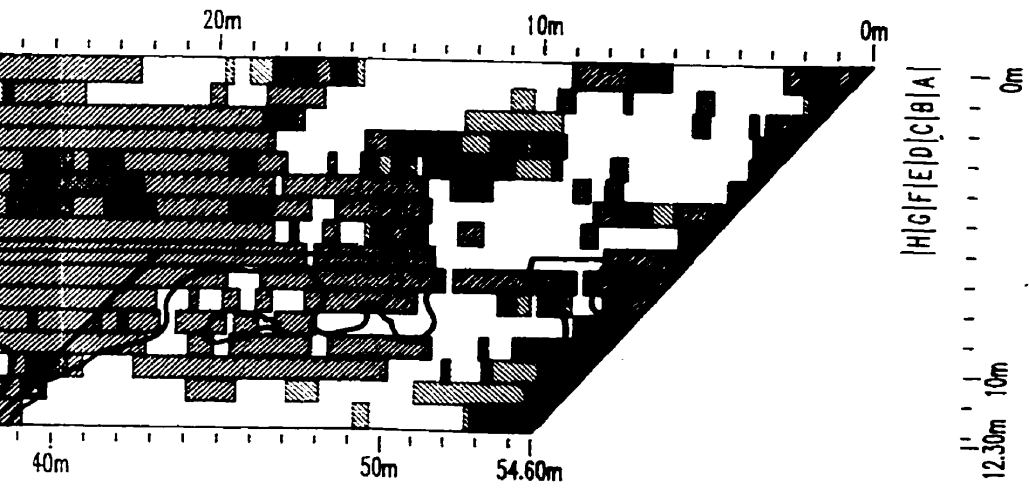
DALHOUSIE
 University

DalTech
 Architecture
 Computer Science
 Engineering





REFERENCE

SCALE :	1cm = 250 cm
DATE :	99/03/12
DRAWN BY :	C. BARNES
APPROVED BY :	

NOVA SCOTIA
 TRANSPORTATION
GROUNDTRUTH-
 WOLFVALL



Legend

-  - SIGNAL ATTENUATION (MINIMAL)
-  - HIGH CONCRETE REFLECTIVITY (MINIMAL)
-  - SIGNAL ATTENUATION AND HIGH CONCRETE REFLECTIVITY (MINIMAL)
-  - HALFCELL POTENTIAL < -0.35 VOLTS

NOVA SCOTIA DEPARTMENT OF
TRANSPORTATION AND PUBLIC WORKS
CORROSION TRUTHING COMPARISON
WOLFVILLE, NOVA SCOTIA

DEEP HOLLOW OVERPASS

DRAWING NO.
Appendix A4.2

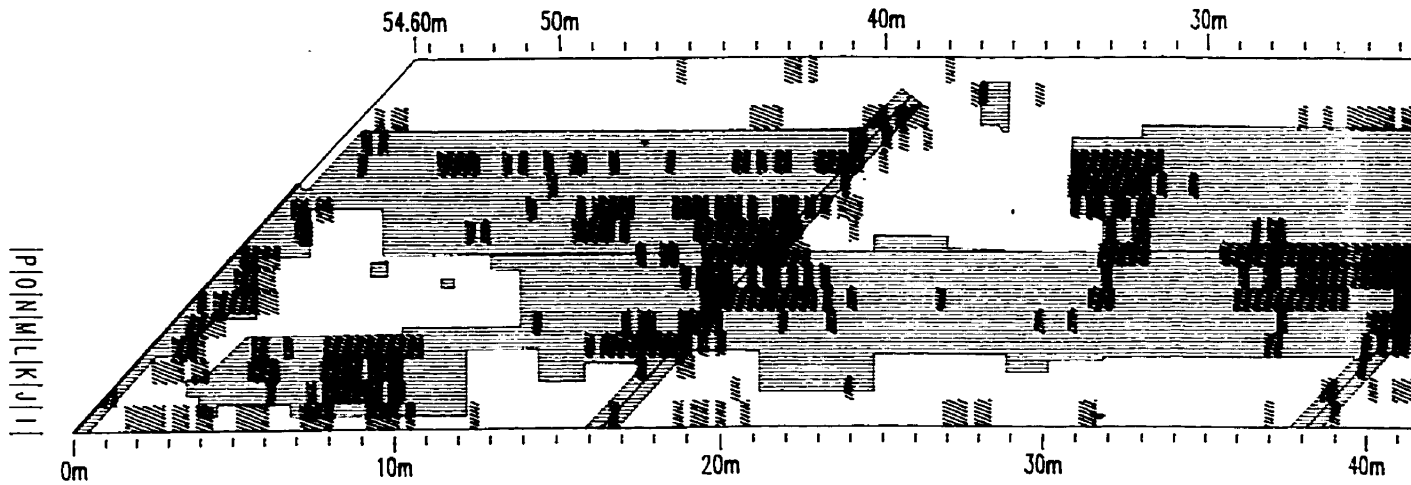
Deep Hollow Overpass

GPR Deck Survey
October 17, 1996

Chain Drag Area = 361.2 m²
Percent Chain Drag Area = 54.0%

Surface Area = 671.3 m²
Surveyed Surface Area = 668.5 m²

Automatic Processing Indicator Area = 138.7 m²
Percent Automatic Processing Indicator Area = 20.2%



Deep_Hollow_Thesis.dwg 99/03/12



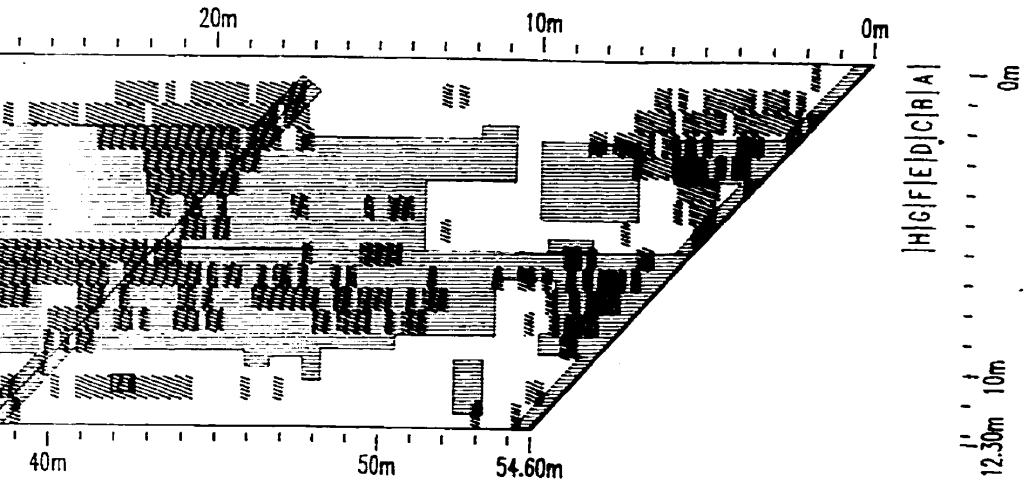
DALHOUSIE
University

DalTech
Architecture
Computer Science
Engineering

REFERENCE

SCALE: 1cm = 250 cm
DATE: 99/03/12
DRAWN BY: C. BARNES
APPROVED BY:

NOVA SCOTIA
TRANSPORTATION
GROUNDTRUTH
WOLFE



Legend

 - SIGNAL ATTENUATION (AUTOMATIC)

 - CHAIN DRAG MEAS

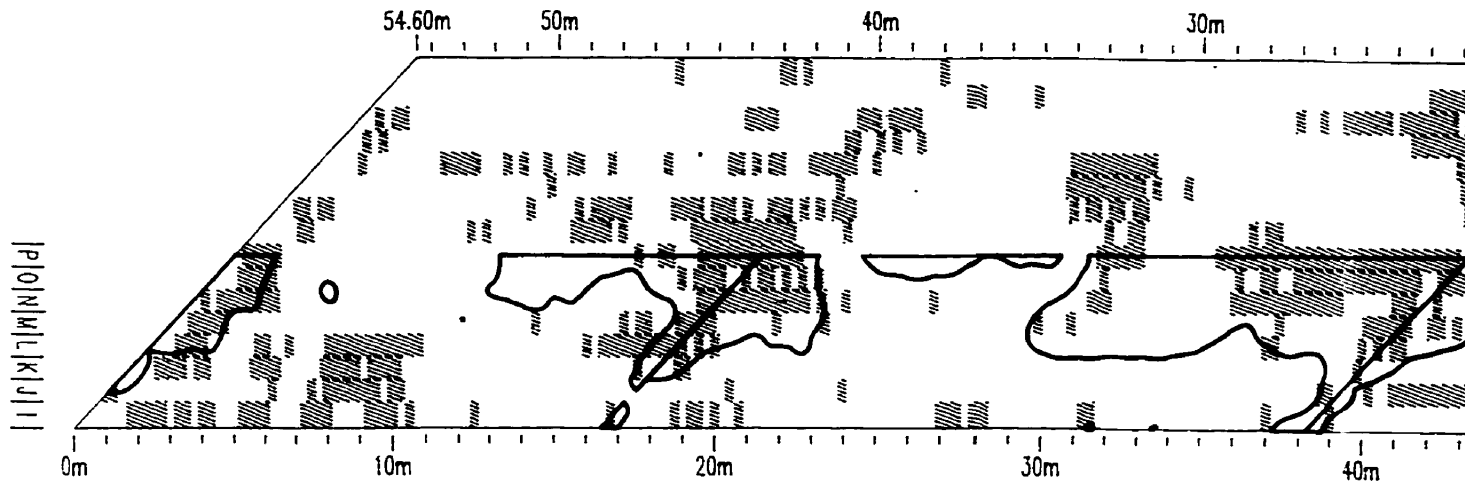
Deep Hollow Overpass

GPR Deck Survey
October 17, 1996

Half Cell Potential Area = 99.5 m²
Percent Half Cell Potential Area = 99.5/316.9 = 31.4%

Surface Area = 671.3 m²
Surveyed Surface Area = 668.5 m²

Automatic Processing Indicator Area = 138.7 m²
Percent Automatic Processing Indicator Area = 20.2%



Deep_Hollow_Thesis.dwg 99/03/12



DALHOUSIE
University

DalTech
Architecture
Computer Science
Engineering

REFERENCE

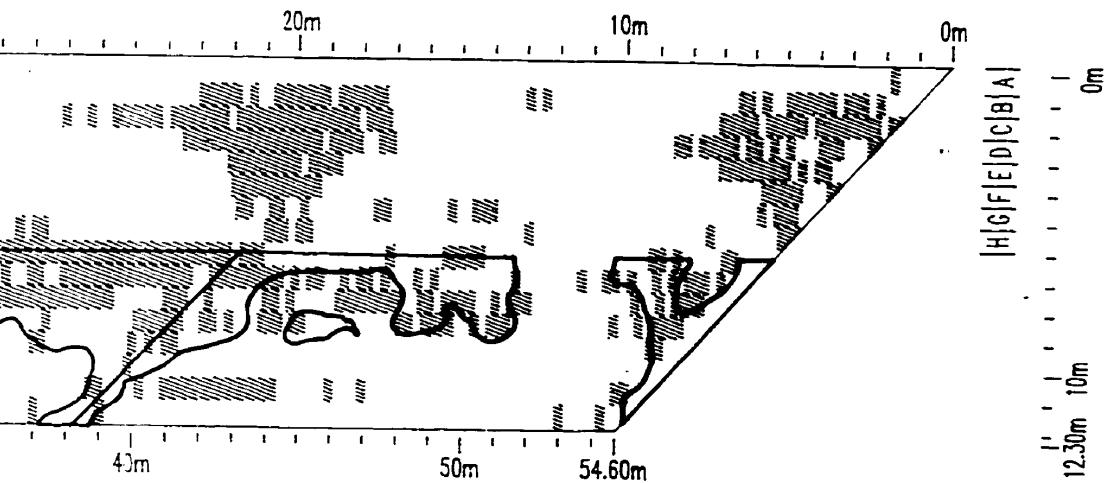
SCALE : 1cm = 250 cm

DATE : 99/03/12

DRAWN BY : C. BARNES

APPROVED BY :

NOVA SCOTIA
TRANSPORTATION
GROUNDTRUTHING
WOLFVILLE



Legend

 - SIGNAL ATTENUATION (AUTOMATIC)

 - HALFCELL POTENTIAL
< -0.35 VOLTS

NOVA SCOTIA DEPARTMENT OF
TRANSPORTATION AND PUBLIC WORKS
ROUNDTRUTHING COMPARISON
WOLFEVILLE, NOVA SCOTIA

DEEP HOLLOW OVERPASS

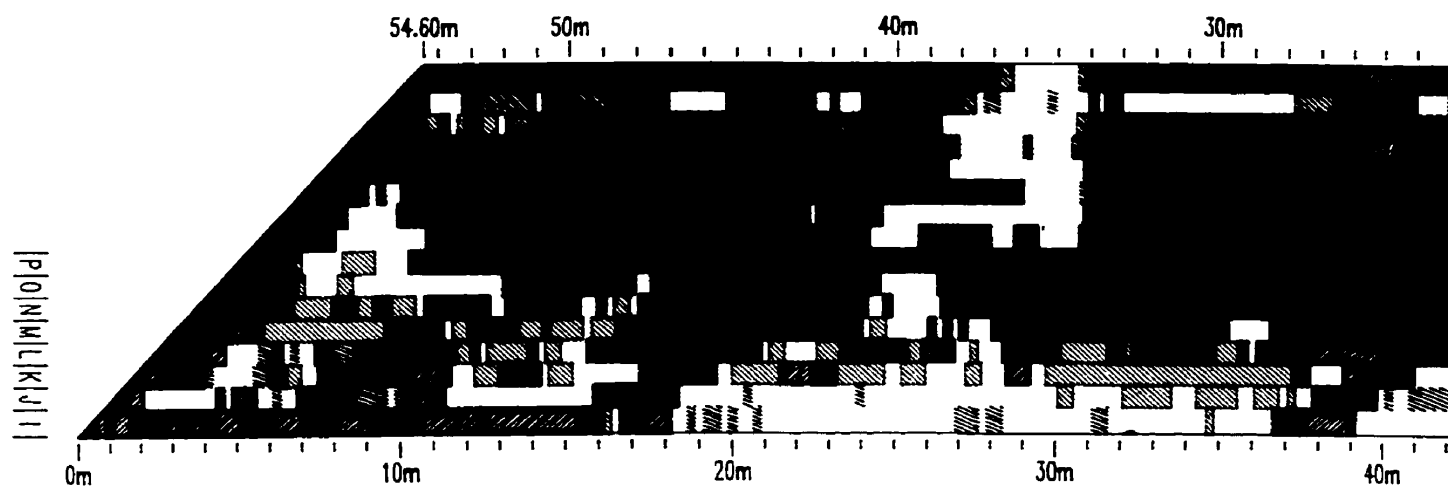
DRAWING NO.

Appendix A4.4

Deep Hollow Overpass (KIN095)

GPR Deck Survey
 October 17, 1996

Surface Area = 671.3 m²
 Surveyed Surface Area = 668.5 m²
 Combined Radar Indicator Area = 468.6 m²
 Percent Combined Radar Indicator Area = 70.1%
 Automatic Processing Indicator Area = 138.7 m²
 Percent Automatic Processing Indicator Area = 20.2%



Deep_Hollow_Thesis.dwg 99/03/12



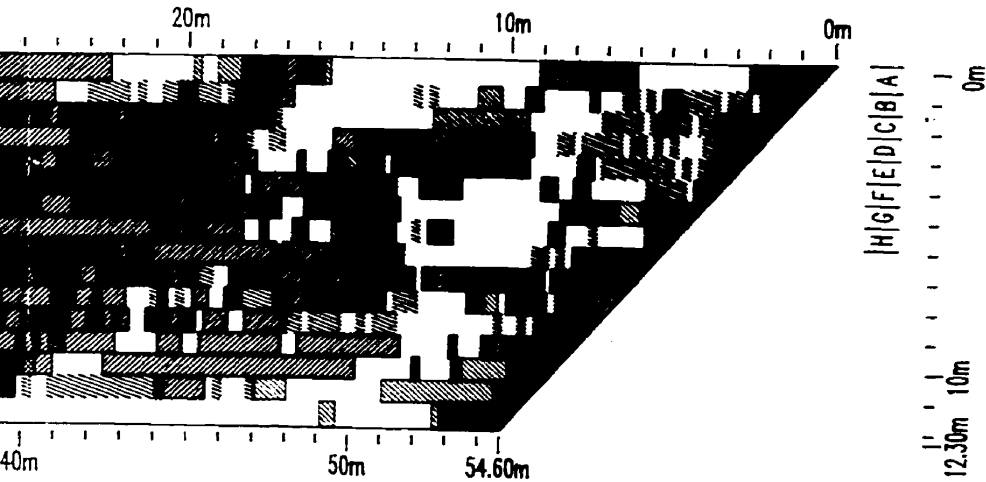
DALHOUSIE
 University

DalTech
 Architecture
 Computer Science
 Engineering





REFERENCE

SCALE :	1cm = 250 cm
DATE :	99/03/12
DRAWN BY :	C. BARNES
APPROVED BY :	

NOVA SCOTIA
 TRANSPORTATION
GPR PROCES
 WOLFEN



Legend

-  - SIGNAL ATTENUATION (AUTOMATIC)
-  - SIGNAL ATTENUATION (MANUAL)
-  - HIGH CONCRETE REFLECTIVITY (MANUAL)
-  - SIGNAL ATTENUATION AND HIGH CONCRETE REFLECTIVITY (MANUAL)

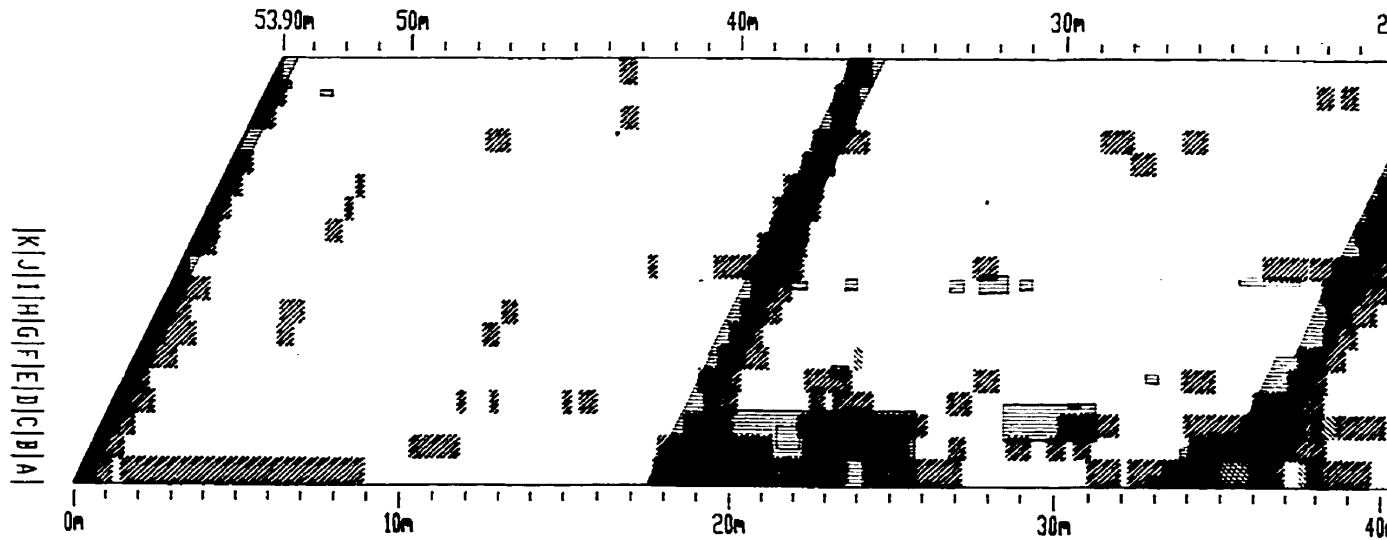
Grand Pre Overpass

GPR Deck Survey
July 17, 1998

Chain Drag Area = 69.9 m²
Percent Chain Drag Area = 9.1%

Combined Radar Indicator Area = 115.1 m²
Percent Combined Radar Indicator Area = 15.0%

Surface Area = 765.4 m²
Surveyed Surface Area = 765.4 m²



Grand Pre_Thesis.dwg 99/03/12



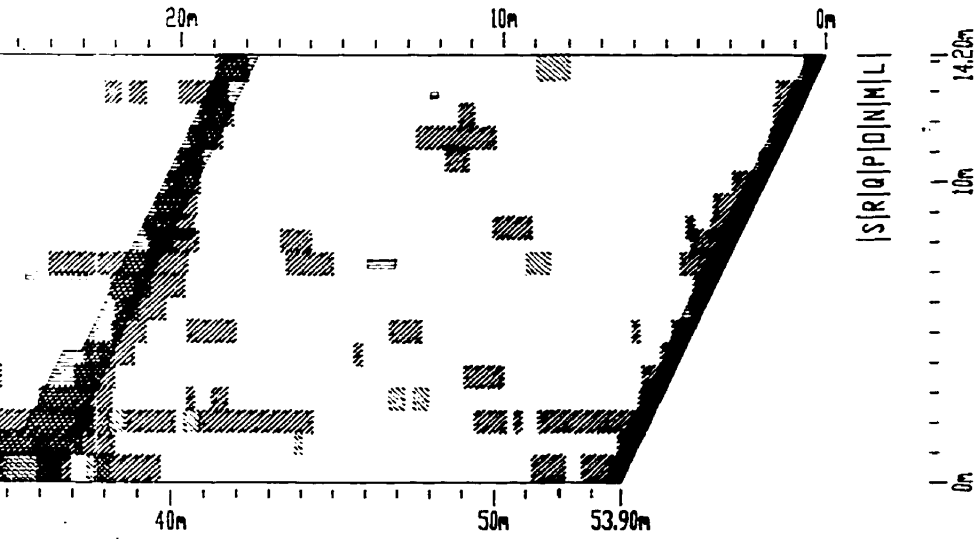
DALHOUSIE
University

DalTech
Architecture
Computer Science
Engineering





REFERENCE

SCALE : 1cm = 250 cm
DATE : 99/03/12
DRAWN BY : C. BARNES
APPROVED BY :

NOVA SCOTIA
TRANSPORTATION
GROUNDTRUTH
GRAND PRE



Legend

-  - SIGNAL ATTENUATION (MANUAL)
-  - HIGH CONCRETE REFLECTIVITY (MANUAL)
-  - SIGNAL ATTENUATION AND HIGH CONCRETE REFLECTIVITY (MANUAL)
-  - CHAIN DRAG AREAS

NOVA SCOTIA DEPARTMENT OF
TRANSPORTATION AND PUBLIC WORKS
UNDBTRUTHING COMPARISON
GRAND PRE, NOVA SCOTIA

GRAND PRE OVERPASS

DRAWING NO.

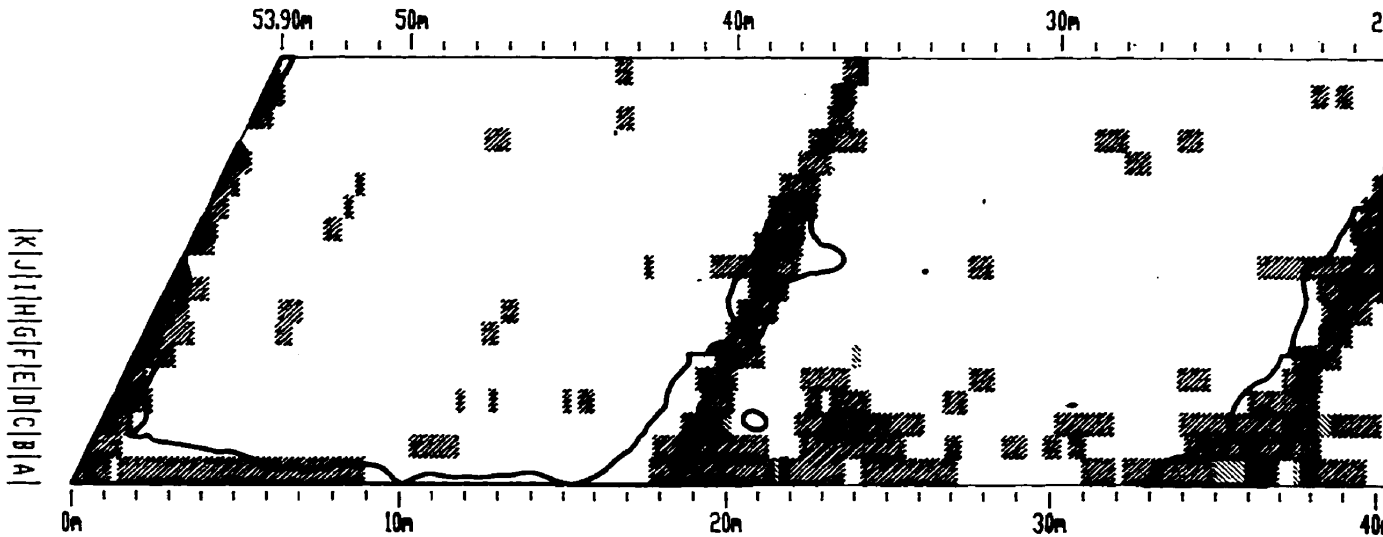
Appendix A5.1

Grand Pre Overpass

GPR Deck Survey
July 17, 1998

Half Cell Potential Area = 63.8 m²
Percent Half Cell Potential Area = 8.3%
Combined Radar Indicator Area = 115.1 m²
Percent Combined Radar Indicator Area = 15.0%

Surface Area = 765.4 m²
Surveyed Surface Area = 765.4 m²



Grand Pre_Thesis.dwg 99/03/12



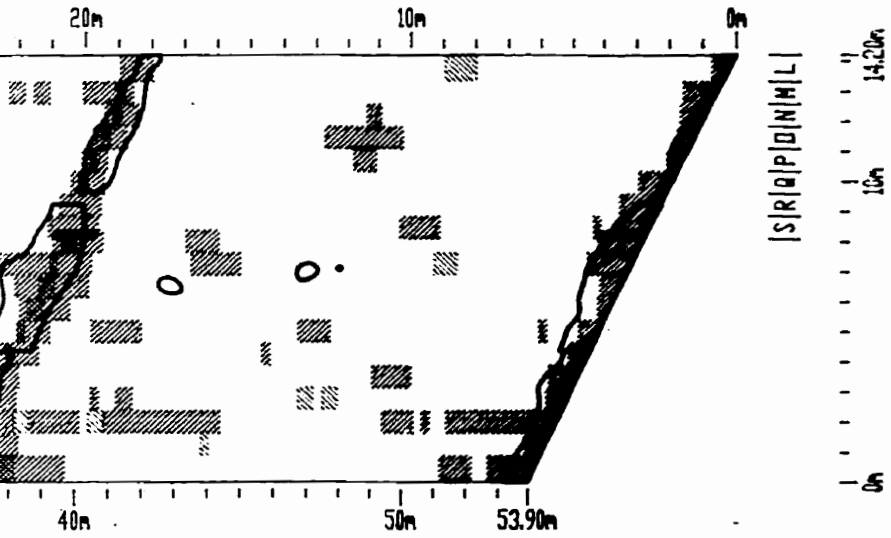
DALHOUSIE
University

DalTech
Architecture
Computer Science
Engineering

REFERENCE

SCALE : 1cm = 250 cm
DATE : 99/03/12
DRAWN BY : C. BARNES
APPROVED BY :

NOVA SCOTIA
TRANSPORTATION
GROUNDTRUTH
GRAND PRE



|S|R|Q|P|D|M|L|

Legend

- SIGNAL ATTENUATION (ANNUAL)
- HIGH CONCRETE REFLECTIVITY (ANNUAL)
- SIGNAL ATTENUATION AND HIGH CONCRETE REFLECTIVITY (ANNUAL)
- HALFCELL POTENTIAL <math>< -0.35 \text{ VOLTS}</math>

NOVA SCOTIA DEPARTMENT OF
TRANSPORTATION AND PUBLIC WORKS
ROUTING COMPARISON
AND PRE, NOVA SCOTIA

GRAND PRE OVERPASS

DRAWING NO.
Appendix A5.2

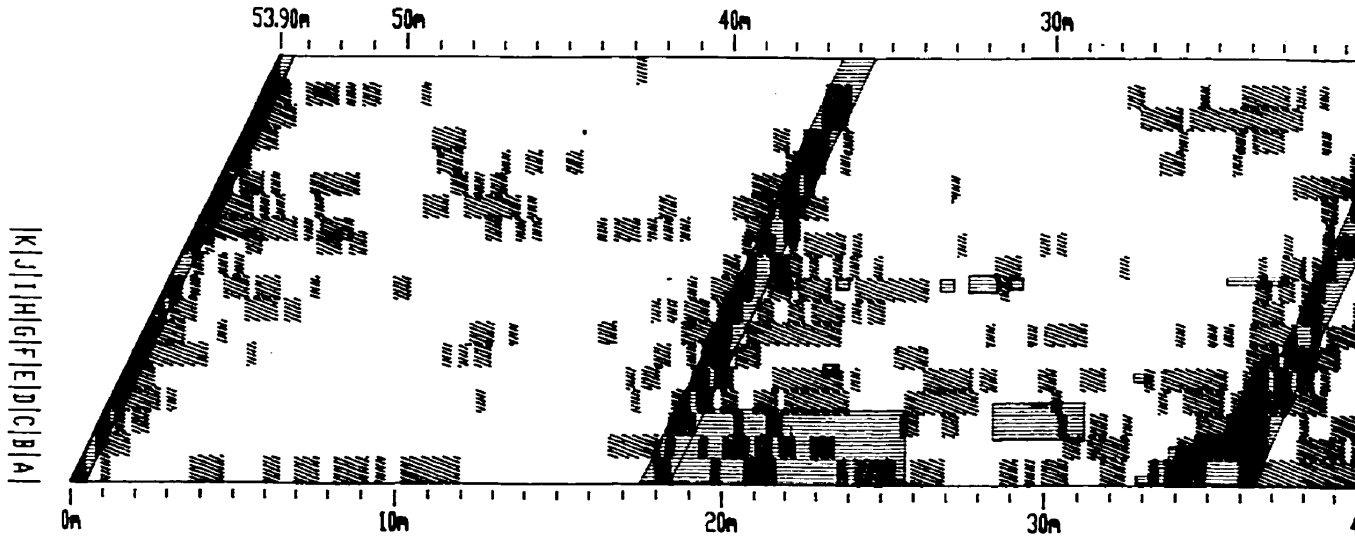
Grand Pre Overpass

GPR Deck Survey
July 17, 1998

Chain Drag Area = 69.9 m²
Percent Chain Drag Area = 9.1%

Surface Area = 765.4 m²
Surveyed Surface Area = 765.4 m²

Automatic Processing Indicator Area = 249.4 m²
Percent Automatic Processing Indicator Area = 32.6%



Grand Pre_Thesis.dwg 99/03/12



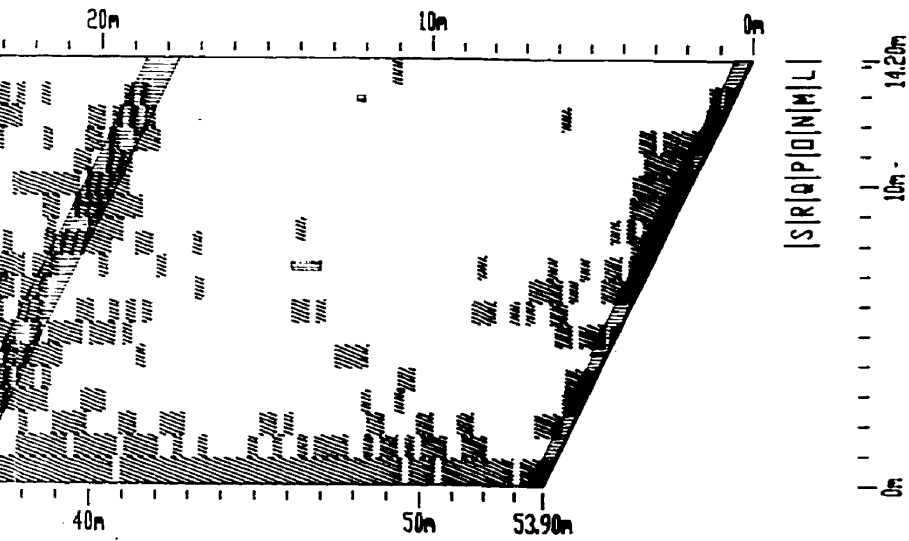
DALHOUSIE
University

DalTech
Architecture
Computer Science
Engineering

REFERENCE

SCALE : 1cm = 250 cm
DATE : 99/03/12
DRAWN BY : C. BARNES
APPROVED BY :

NOVA SCOTIA
TRANSPORTATION
GROUNDTRUTH
GRAND P



Legend

 - SIGNAL ATTENUATION (AUTOMATIC)

 - CURB DRAG MEAS

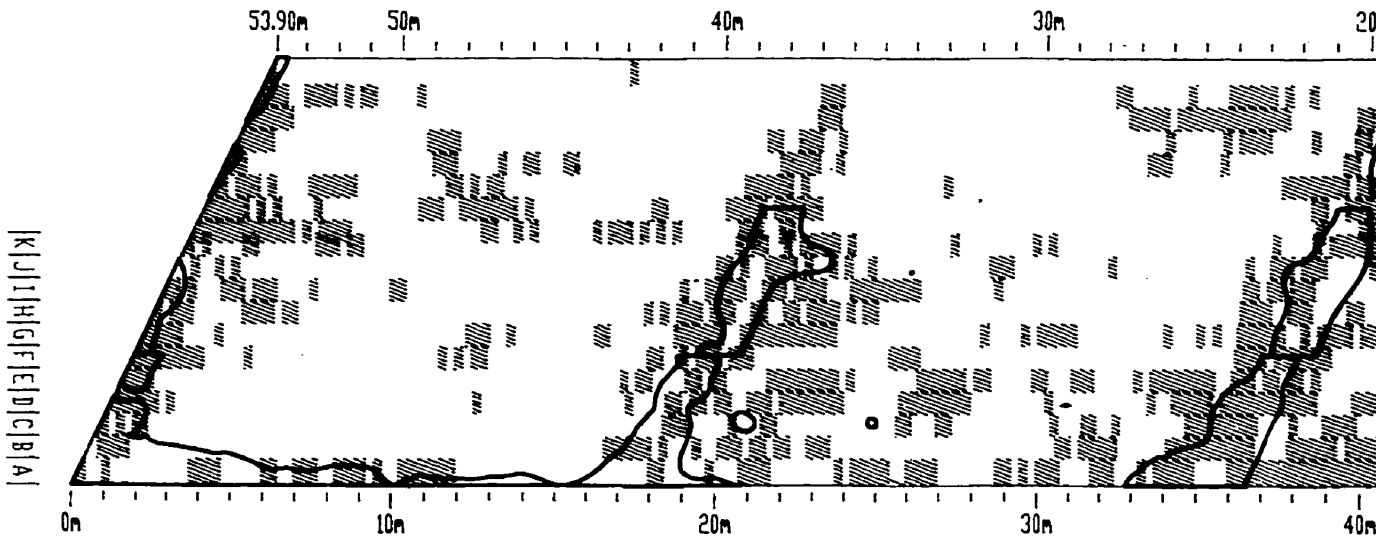
Grand Pre Overpass

GPR Deck Survey
July 17, 1998

Half Cell Potential Area = 63.8 m²
Percent Half Cell Potential Area = 8.3%

Surface Area = 765.4 m²
Surveyed Surface Area = 765.4 m²

Automatic Processing Indicator Area = 249.4 m²
Percent Automatic Processing Indicator Area = 32.6%



Grand Pre_Thesis.dwg 99/03/12



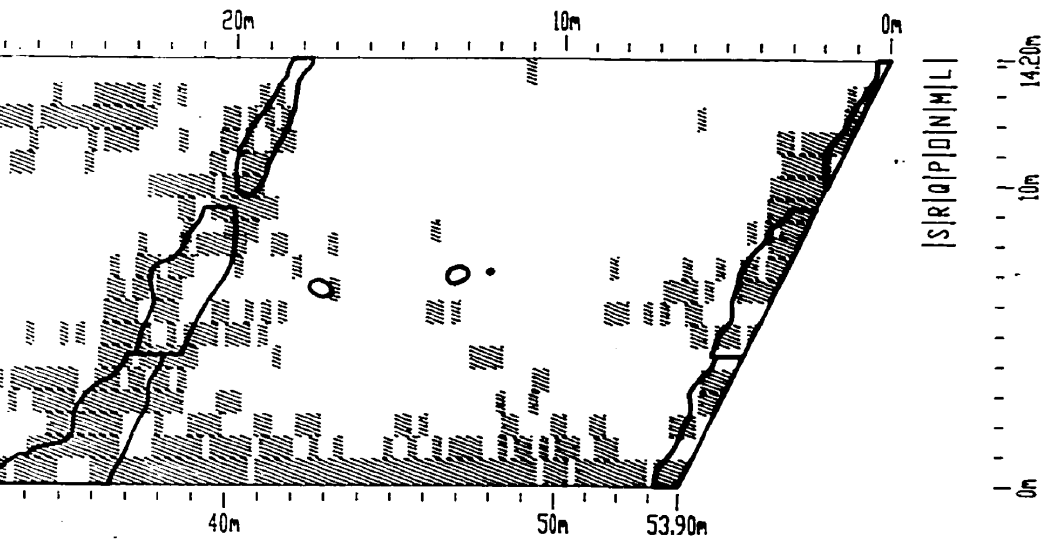
DALHOUSIE
University

DalTech
Architecture
Computer Science
Engineering

REFERENCE


SCALE : 1cm = 250 cm
DATE : 99/03/12
DRAWN BY : C. BARNES
APPROVED BY :

NOVA SCOTIA
TRANSPORTATION
GROUNDTRUTH
GRAND PRE



Legend

 - SIGNAL ATTENUATION (AUTOMATIC)

 - HALFCCELL POTENTIAL
< -0.35 VOLTS

NOVA SCOTIA DEPARTMENT OF
TRANSPORTATION AND PUBLIC WORKS
ROUNDRUTHING COMPARISON
GRAND PRE, NOVA SCOTIA

GRAND PRE OVERPASS

DRAWING NO.

Appendix A5.4

Grand Pre Overpass

GPR Deck Survey

July 17, 1998

Surface Area = 765.4 m²

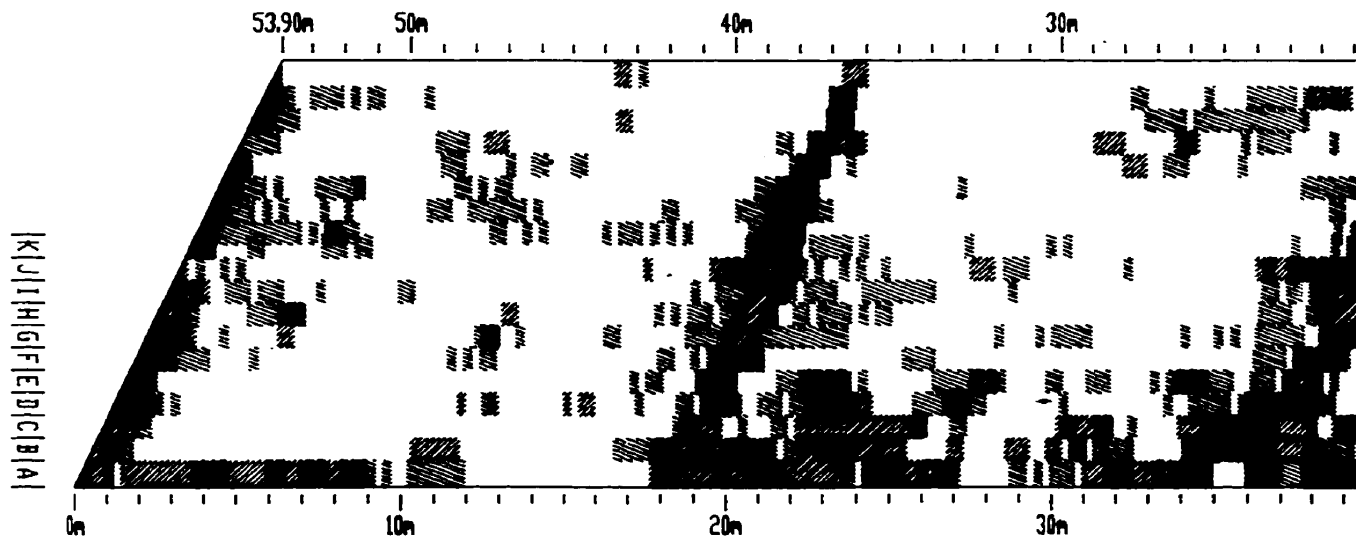
Surveyed Surface Area = 765.4 m²

Combined Radar Indicator Area = 115.1 m²

Percent Combined Radar Indicator Area = 15.0%

Automatic Processing Indicator Area = 249.4 m²

Percent Automatic Processing Indicator Area = 32.6%



Grand Pre_Thesis.dwg 99/03/12



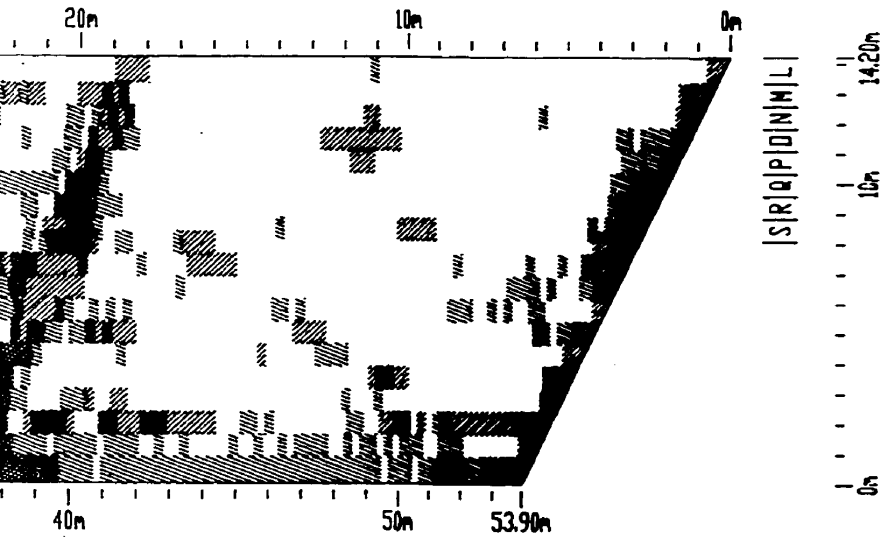
DALHOUSIE
University





DalTech
Architecture
Computer Science
Engineering

REFERENCE

SCALE :	1cm = 250 cm
DATE :	99/03/12
DRAWN BY :	C. BARNES
APPROVED BY :	

NOVA SCOTIA
TRANSPORTATION
GPR PROCESSING
GRAND PRE



- Legend**
-  - SIGNAL ATTENUATION (AUTOMATIC)
 -  - SIGNAL ATTENUATION (MANUAL)
 -  - HIGH CONCRETE REFLECTIVITY (MANUAL)
 -  - SIGNAL ATTENUATION AND HIGH CONCRETE REFLECTIVITY (MANUAL)

SCOTIA DEPARTMENT OF
 TRANSPORTATION AND PUBLIC WORKS
 PROCESSING COMPARISON
 GRAND PRE, NOVA SCOTIA

GRAND PRE OVERPASS

DRAWING NO.
 Appendix A5.5

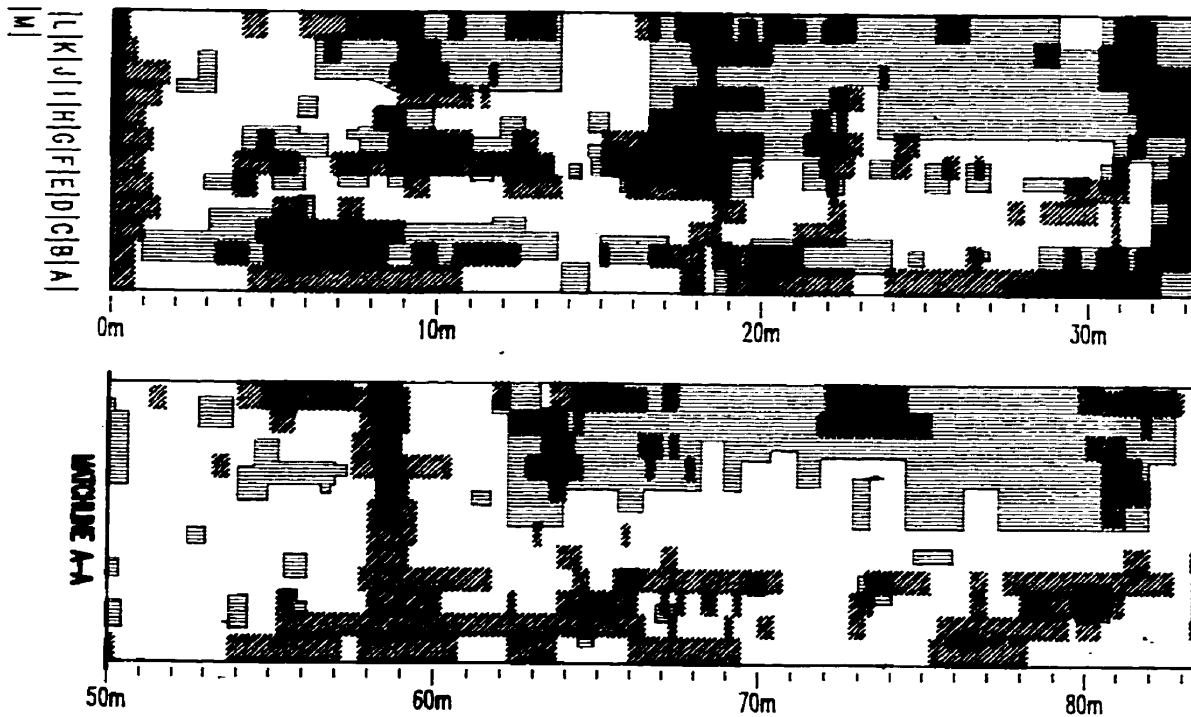
Shubenacadie Canal CNR Overpass

GPR Deck Survey
November 5, 1997

Chain Drag Area = 321.4 m²
Percent Chain Drag Area = 35.1%

Combined Radar Indicator Area = 261.0 m²
Percent Combined Radar Indicator Area = 28.5%

Surface Area = 472.8 m²
Surveyed Surface Area = 460.5 m²



Shubenacadie_Thesis.dwg 99/03/12



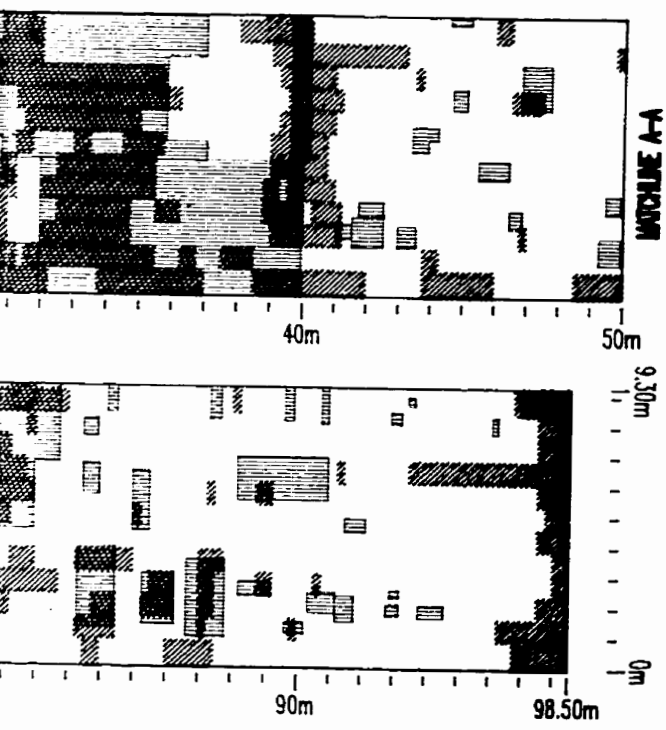
DALHOUSIE
University

DalTech
Architecture
Computer Science
Engineering





REFERENCE

SCALE : 1cm = 250 cm
DATE : 99/03/12
DRAWN BY : C. BARNES
APPROVED BY :

NOVA SCOTIA
TRANSPORTATION
GROUNDTRUTH
SHUBENACADIE



Legend

-  - SIGNAL ATTENUATION (ANNUAL)
-  - HIGH CONCRETE REFLECTIVITY (ANNUAL)
-  - SIGNAL ATTENUATION AND HIGH CONCRETE REFLECTIVITY (ANNUAL)
-  - CURB DRAG AREAS

SCOTIA DEPARTMENT OF
TRANSPORTATION AND PUBLIC WORKS
MATERIALS TESTING DIVISION
SHUBENACADIE, NOVA SCOTIA

SHUBENACADIE CANAL CNR OVERPASS

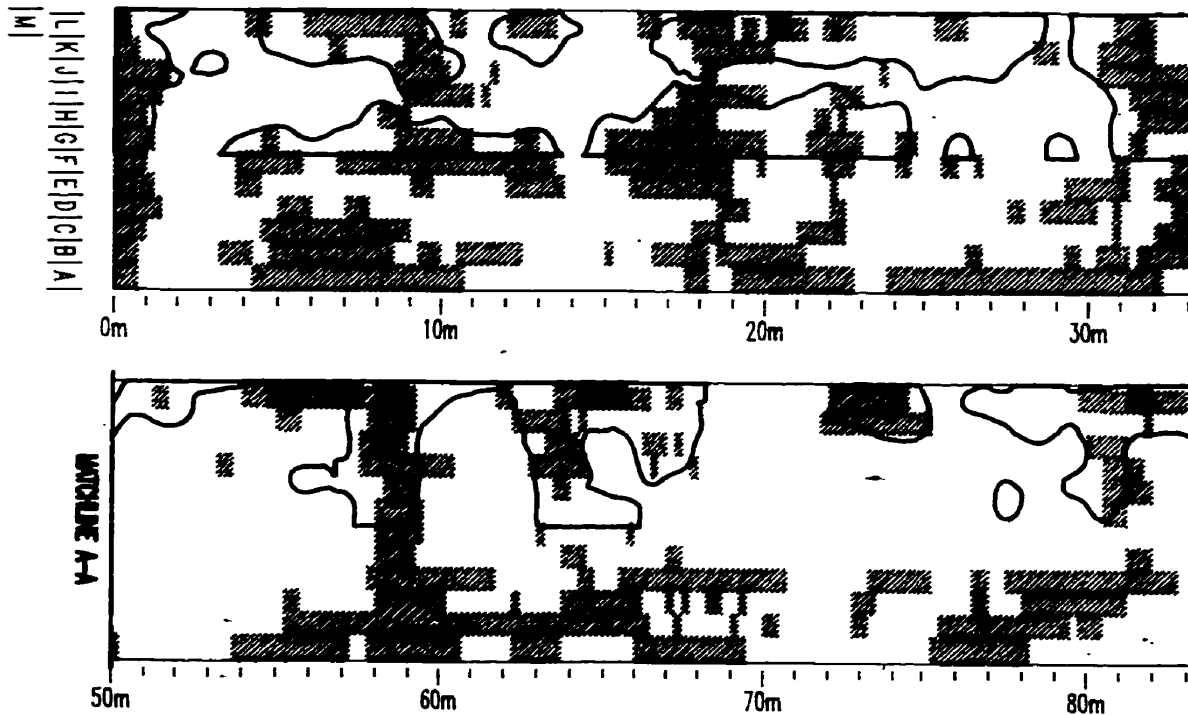
DRAWING NO.
Appendix A6.1

Shubenacadie Canal CNR Overpass

GPR Deck Survey
November 5, 1997

Half Cell Potential Area = 187.0 m²
 Percent Half Cell Potential Area = 39.5%
 Combined Radar Indicator Area = 261.0 m²
 Percent Combined Radar Indicator Area = 28.5%

Surface Area = 472.8 m²
 Surveyed Surface Area = 460.5 m²



Shubenacadie_Thesis.dwg 99/03/12



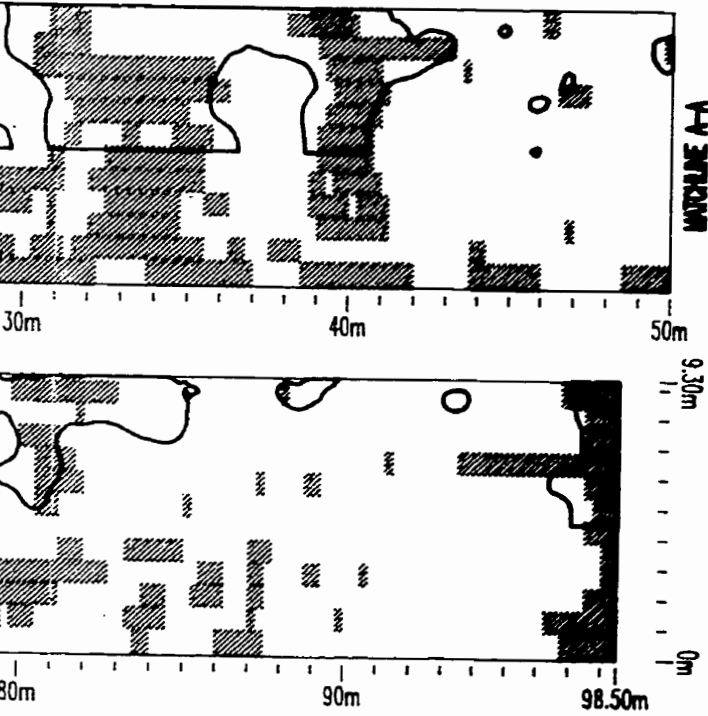
DALHOUSIE
University

DalTech
Architecture
Computer Science
Engineering

REFERENCE

SCALE : 1cm = 250 cm
 DATE : 99/03/12
 DRAWN BY : C. BARNES
 APPROVED BY :

NOVA SCOTIA
TRANSPORTATION
GROUNDTRUTH-
SHUBENACADIE



Legend

-  - SIGNAL ATTENUATION (NORMAL)
-  - HIGH CONCRETE REFLECTIVITY (NORMAL)
-  - SIGNAL ATTENUATION AND HIGH CONCRETE REFLECTIVITY (NORMAL)
-  - HALFCELL POTENTIAL < -0.35 VOLTS

NOVA SCOTIA DEPARTMENT OF
TRANSPORTATION AND PUBLIC WORKS
CORROSION TRUTHING COMPARISON
SHUBENACADIE, NOVA SCOTIA

SHUBENACADIE CANAL CNR OVERPASS

DRAWING NO.
Appendix A6.2

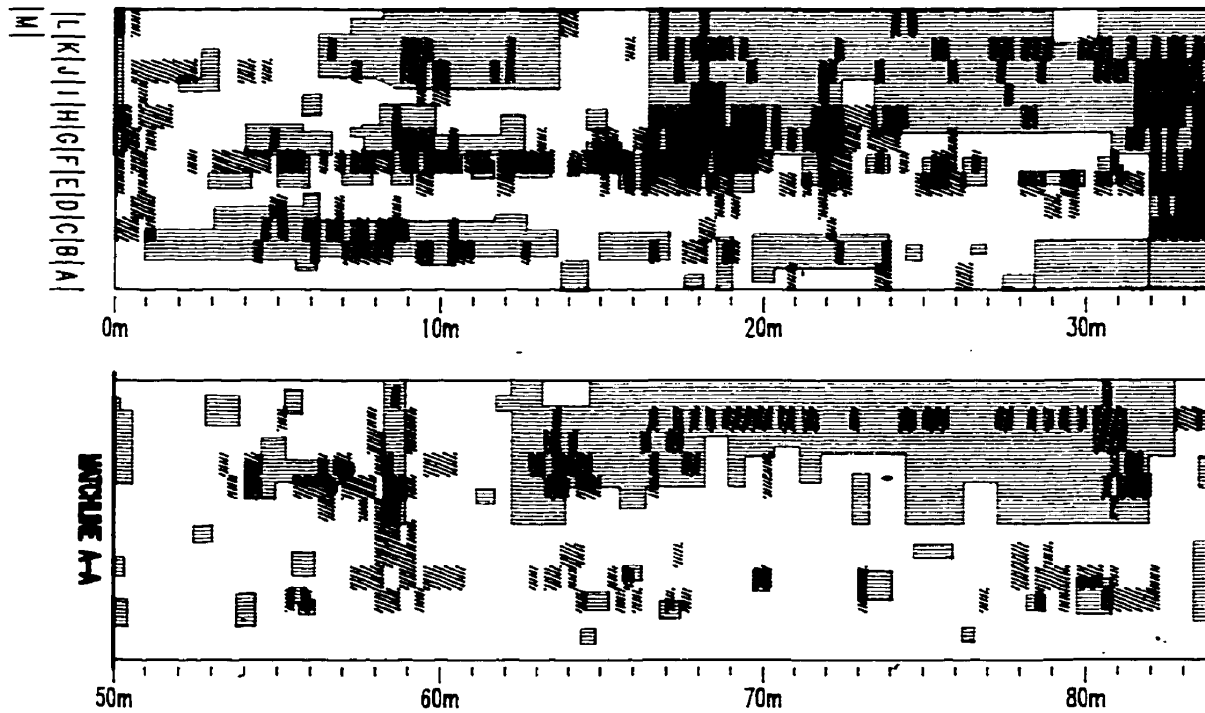
Shubenacadie Canal CNR Overpass

GPR Deck Survey
November 5, 1997

Chain Drag Area = 321.4 m²
Percent Chain Drag Area = 35.1%

Surface Area = 472.8 m²
Surveyed Surface Area = 460.5 m²

Automatic Processing Indicator Area = 138.7 m²
Percent Automatic Processing Indicator Area = 15.5%



Shubenacadie_Thesis.dwg 99/03/12



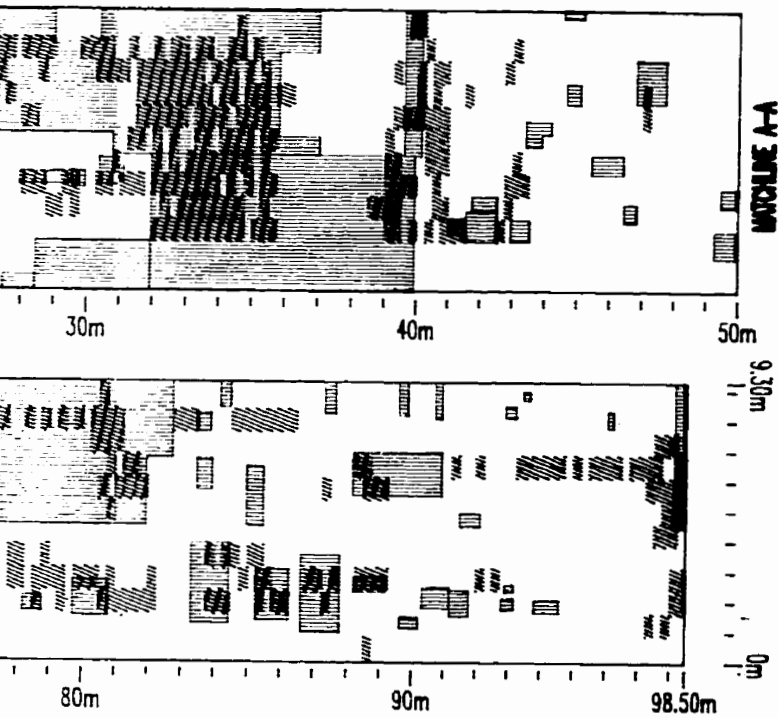
DALHOUSIE
University

DalTech
Architecture
Computer Science
Engineering


REFERENCE

SCALE : 1cm = 250 cm
DATE : 99/03/12
DRAWN BY : C. BARNES
APPROVED BY :

NOVA SCOTIA
TRANSPORTATION
GROUNDTRUTH
SHUBENACADIE



Legend

 - SIGNAL ATTENUATION (AUTOMATIC)

 - CON DRG AREAS

NOVA SCOTIA DEPARTMENT OF
TRANSPORTATION AND PUBLIC WORKS

UNDERTRUTHING COMPARISON
SHUBENACADIE, NOVA SCOTIA

SHUBENACADIE CANAL CNR OVERPASS

DRAWING NO.

Appendix A6.3

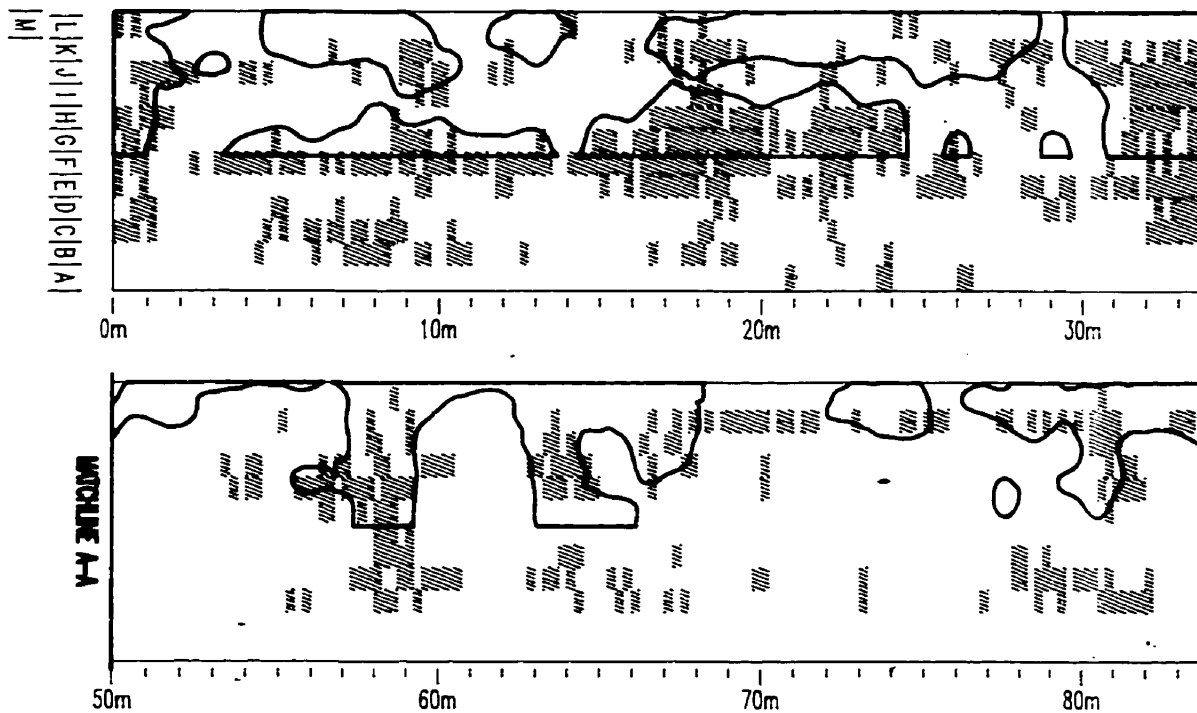
Shubenacadie Canal CNR Overpass

GPR Deck Survey
November 5, 1997

Half Cell Potential Area = 187.0 m²
Percent Half Cell Potential Area = 39.5%

Surface Area = 472.8 m²
Surveyed Surface Area = 460.5 m²

Automatic Processing Indicator Area = 138.7 m²
Percent Automatic Processing Indicator Area = 15.5%



Shubenacadie...Thesis.dwg 99/03/12



DALHOUSIE
University

DalTech
Architecture
Computer Science
Engineering

REFERENCE

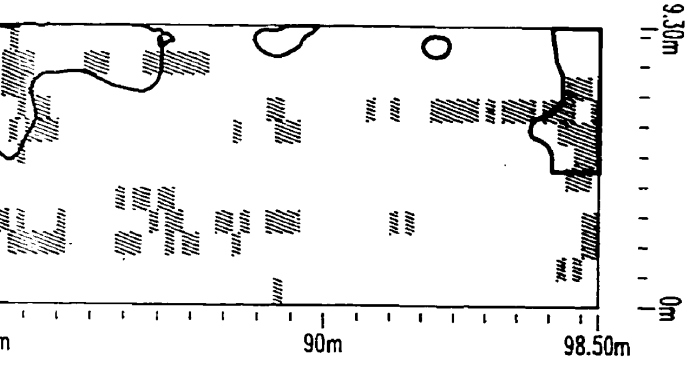
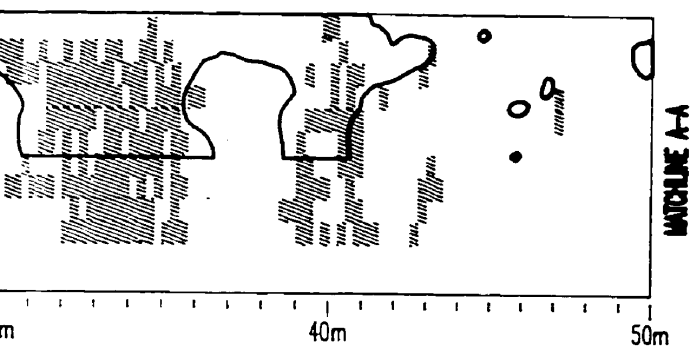
SCALE : 1cm = 250 cm



DATE : 99/03/12

DRAWN BY : C. BARNES

APPROVED BY :

NOVA SCOTIA
TRANSPORTATION
GROUNDTRUTH
SHUBENACADIE



- Legend
-  - SIGNAL ATTENUATION (AUTOMATIC)
 -  - HALFCELL POTENTIAL < -0.35 VOLTS

NOVA SCOTIA DEPARTMENT OF
TRANSPORTATION AND PUBLIC WORKS
CORROSION MONITORING
CORROSION COMPARISON
SHUBENACADIE, NOVA SCOTIA

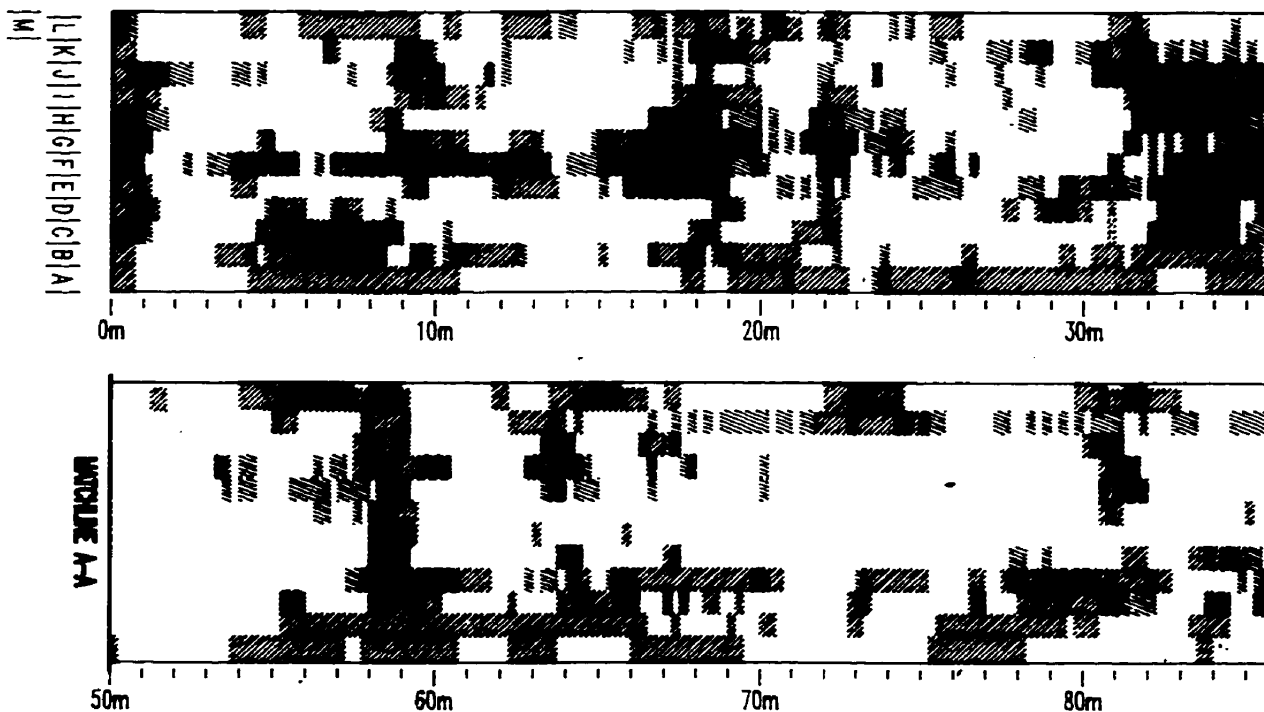
SHUBENACADIE CANAL CNR OVERPASS

DRAWING NO.
Appendix A6.4

Shubenacadie Canal CNR Overpass

GPR Deck Survey
November 5, 1997

Surface Area = 472.8 m²
 Surveyed Surface Area = 460.5 m²
 Combined Radar Indicator Area = 261.0 m²
 Percent Combined Radar Indicator Area = 28.5%
 Automatic Processing Indicator Area = 138.7 m²
 Percent Automatic Processing Indicator Area = 15.5%



Shubenacadie_Thesis.dwg 99/03/12



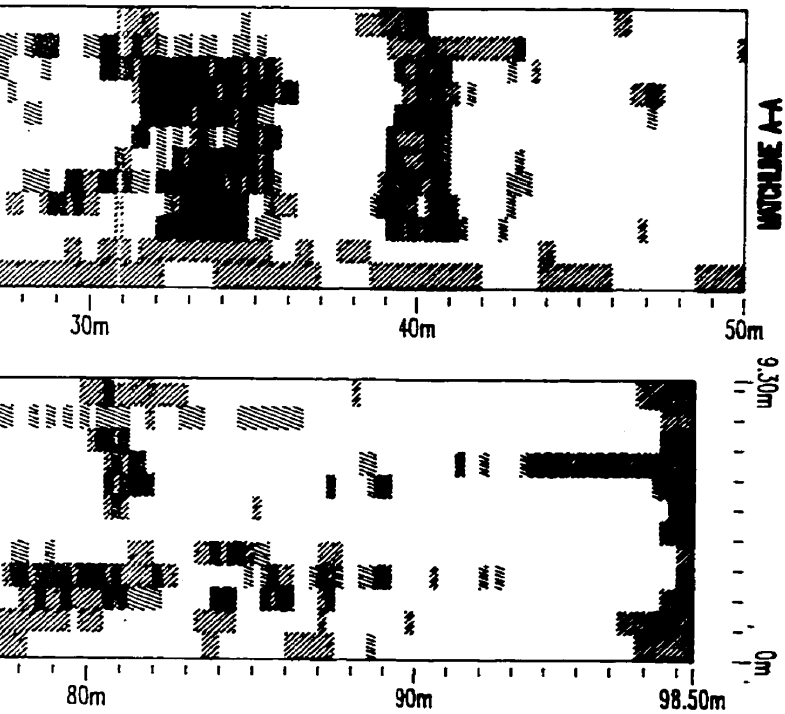
DALHOUSIE
University





DalTech
Architecture
Computer Science
Engineering

REFERENCE

SCALE : 1cm = 250 cm
 DATE : 99/03/12
 DRAWN BY : C. BARNES
 APPROVED BY :

NOVA SCOTIA DEPT
TRANSPORTATION AND
GPR PROCESSING
SHUBENACADIE, NS



- Legend
-  - SIGNAL ATTENUATION (AUTOMATIC)
 -  - SIGNAL ATTENUATION (MANUAL)
 -  - HIGH CONCRETE REFLECTIVITY (MANUAL)
 -  - SIGNAL ATTENUATION AND HIGH CONCRETE REFLECTIVITY (MANUAL)

NOVA SCOTIA DEPARTMENT OF
TRANSPORTATION AND PUBLIC WORKS
PROCESSING COMPARISON
SHUBENACADIE, NOVA SCOTIA

SHUBENACADIE CANAL CNR OVERPASS

DRAWING NO.

Appendix A6.5

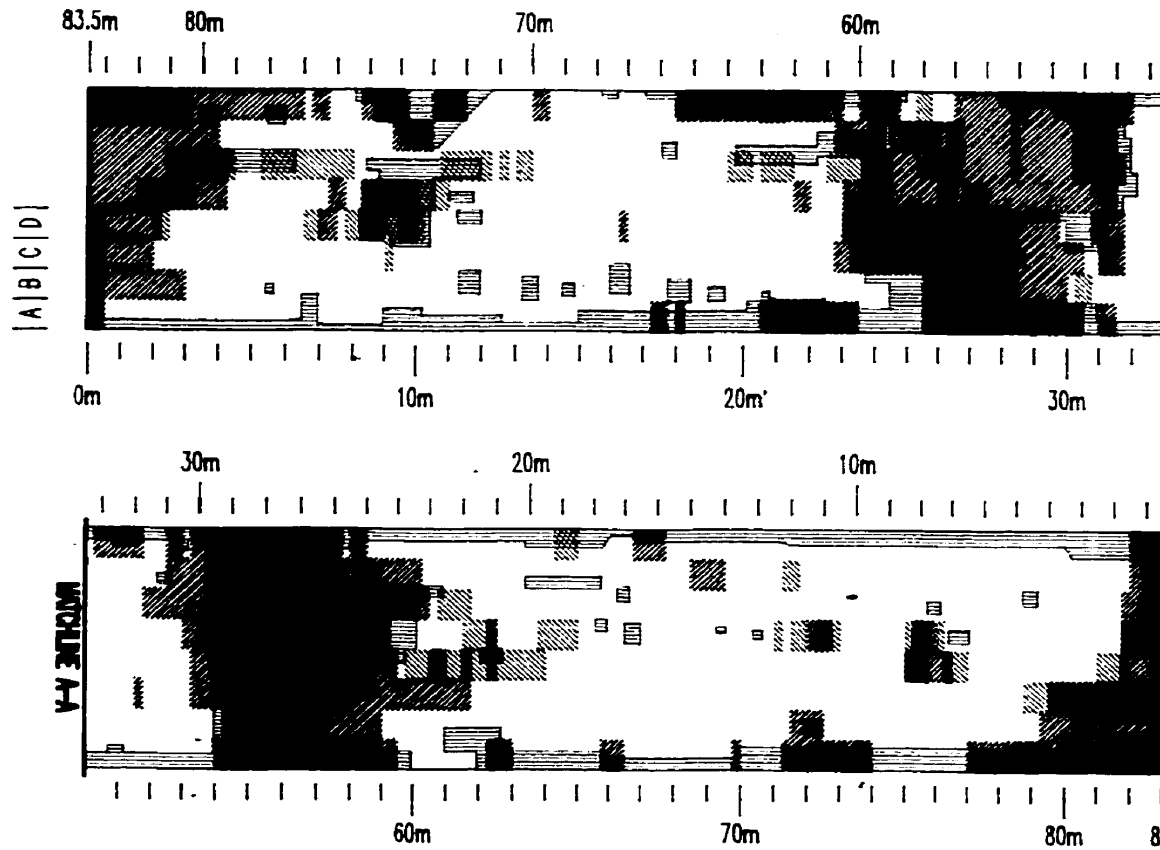
Baddeck River Bridge

GPR Deck Survey
October 17, 1996

Chain Drag Area = 233.0 m²
Percent Chain Drag Area = 34.9%

Combined Radar Indicator Area = 249.5 m²
Percent Combined Radar Indicator Area = 37.4%

Surface Area = 668.0 m²
Surveyed Surface Area = 668.0 m²



Baddeck_Thesis.dwg 99/03/12



DALHOUSIE
University

DalTech
Architecture
Computer Science
Engineering

REFERENCE

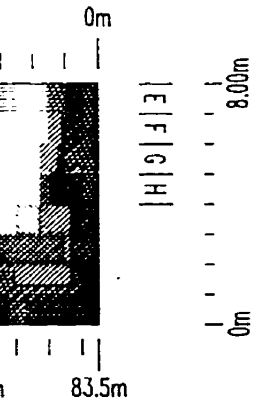
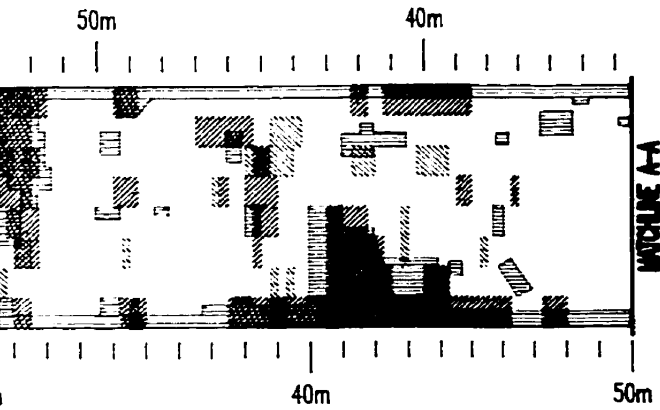
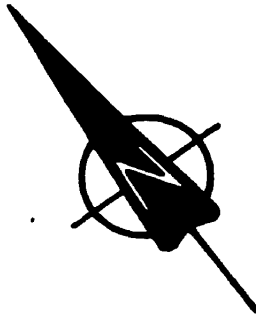
SCALE : 1cm = 250 cm

DATE : 99/03/12





DRAWN BY : C. BARNES

APPROVED BY :

NOVA SCOTIA
TRANSPORTATION
GROUNDTRUTH
BADDECK



Legend

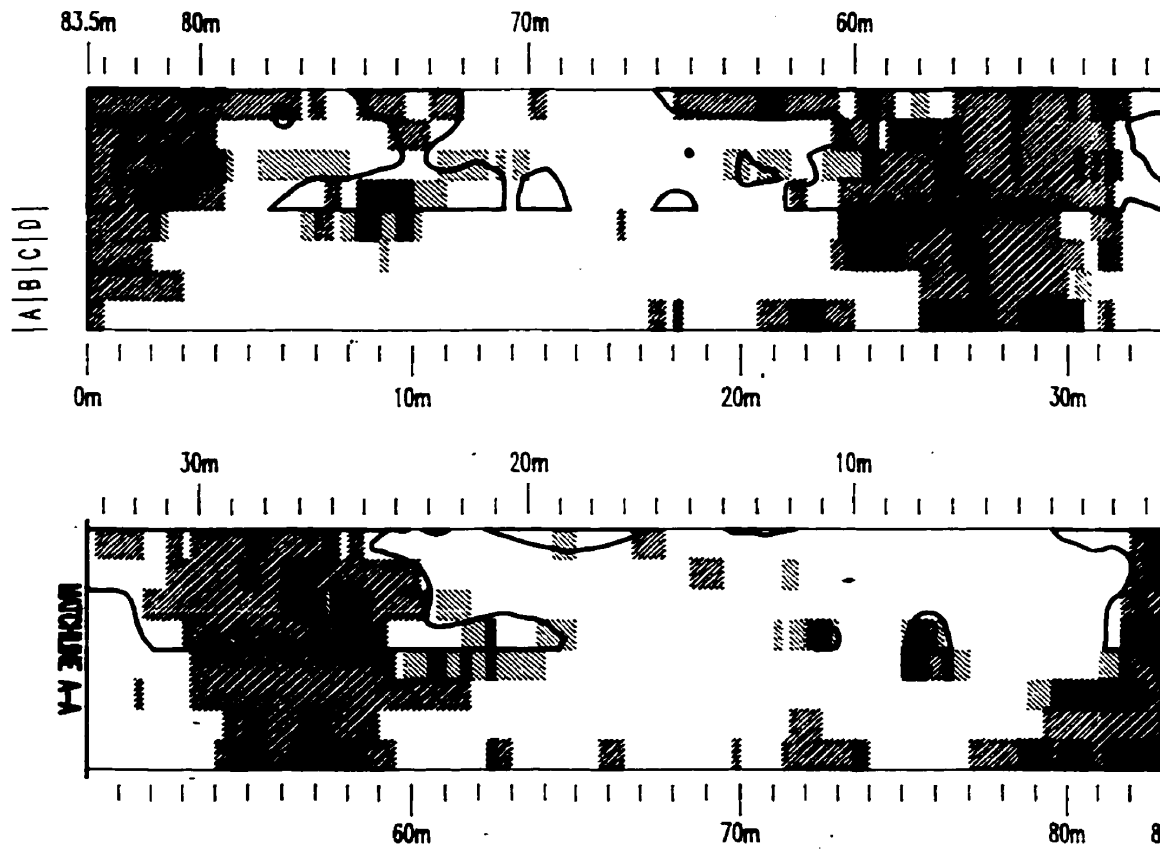
-  - SIGNAL ATTENUATION (NORMAL)
-  - HIGH CONCRETE REFLECTIVITY (NORMAL)
-  - SIGNAL ATTENUATION AND HIGH CONCRETE REFLECTIVITY (NORMAL)
-  - CHIM DRAG AREAS

Baddeck River Bridge

GPR Deck Survey
October 17, 1996

Half Cell Potential Area = 153.7 m²
Percent Half Cell Potential Area = 46.0%
Combined Radar Indicator Area = 249.5 m²
Percent Combined Radar Indicator Area = 37.4%

Surface Area = 668.0 m²
Surveyed Surface Area = 668.0 m²



Baddeck_Thesis.dwg 99/03/12



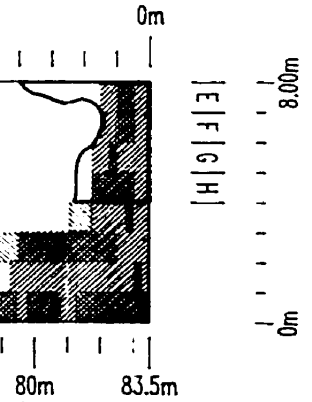
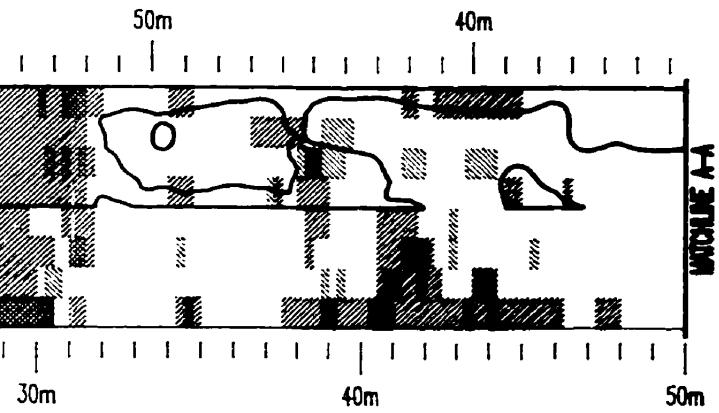
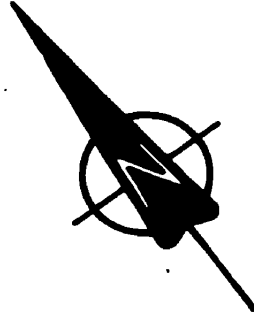
DALHOUSIE
University

DalTech
Architecture
Computer Science
Engineering





REFERENCE

SCALE : 1cm = 250 cm
DATE : 99/03/12
DRAWN BY : C. BARNES
APPROVED BY :

NOVA SCOTIA
TRANSPORTATION
GROUNDTRUTH
BADDECK



Legend

-  - SIGNAL ATTENUATION (ANNUAL)
-  - HIGH CONCRETE REFLECTIVITY (ANNUAL)
-  - SIGNAL ATTENUATION AND HIGH CONCRETE REFLECTIVITY (ANNUAL)
-  - HALF CELL POTENTIAL < -0.35 VOLTS

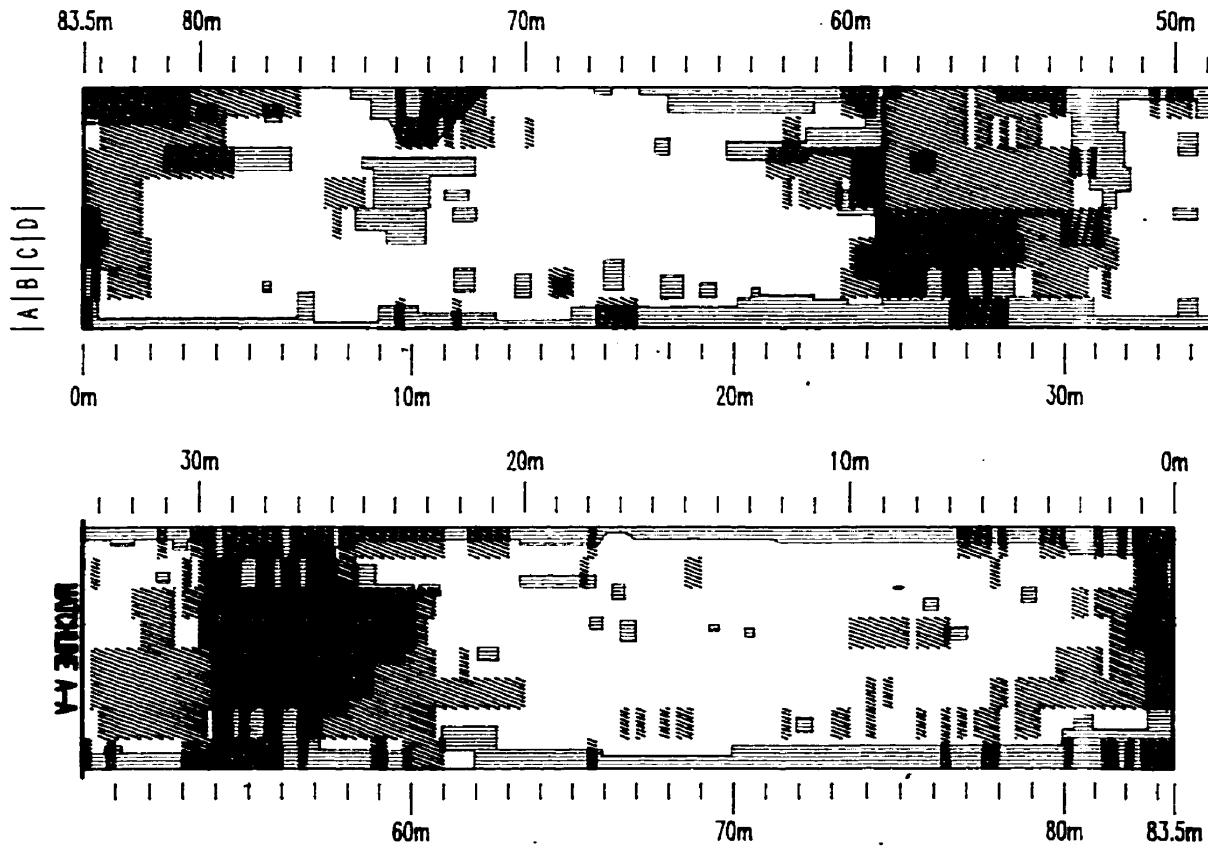
Baddeck River Bridge

GPR Deck Survey
October 17, 1996

Chain Drag Area = 233.0 m²
Percent Chain Drag Area = 34.9%

Surface Area = 668.0 m²
Surveyed Surface Area = 668.0 m²

Automatic Processing Indicator Area = 206.3 m²
Percent Automatic Processing Indicator Area = 30.9%



Baddeck_Thesis.dwg 99/03/12



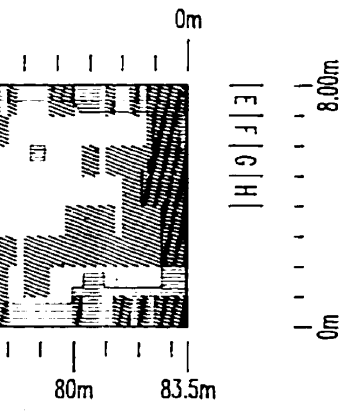
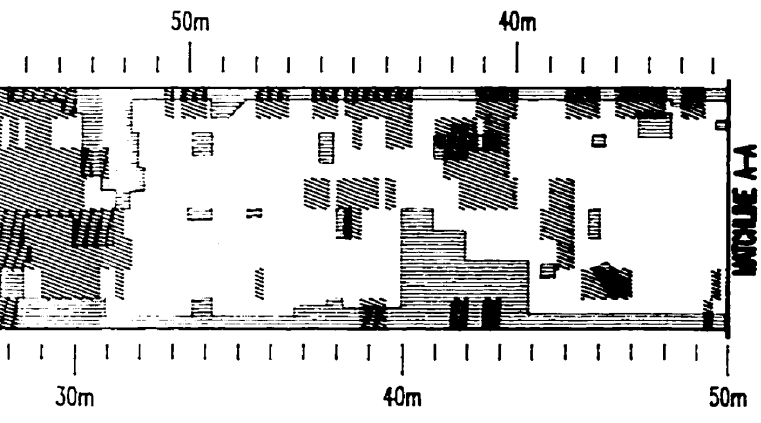
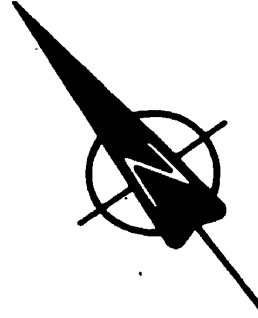
DALHOUSIE
University

DalTech
Architecture
Computer Science
Engineering

REFERENCE

SCALE : 1cm = 250 cm
DATE : 99/03/12
DRAWN BY : C. BARNES
APPROVED BY :

NOVA SCOTIA DEPARTMENT OF
TRANSPORTATION AND
GROUNDTRUTHING
BADDECK, NS



Legend

 - SIGNAL ATTENUATION (AUTOMATIC)

 - CHURN DRAG AREAS

NOVA SCOTIA DEPARTMENT OF
 TRANSPORTATION AND PUBLIC WORKS
UNDRUTHING COMPARISON
 BADDECK, NOVA SCOTIA

BADDECK RIVER BRIDGE

DRAWING NO.
Appendix A7.3

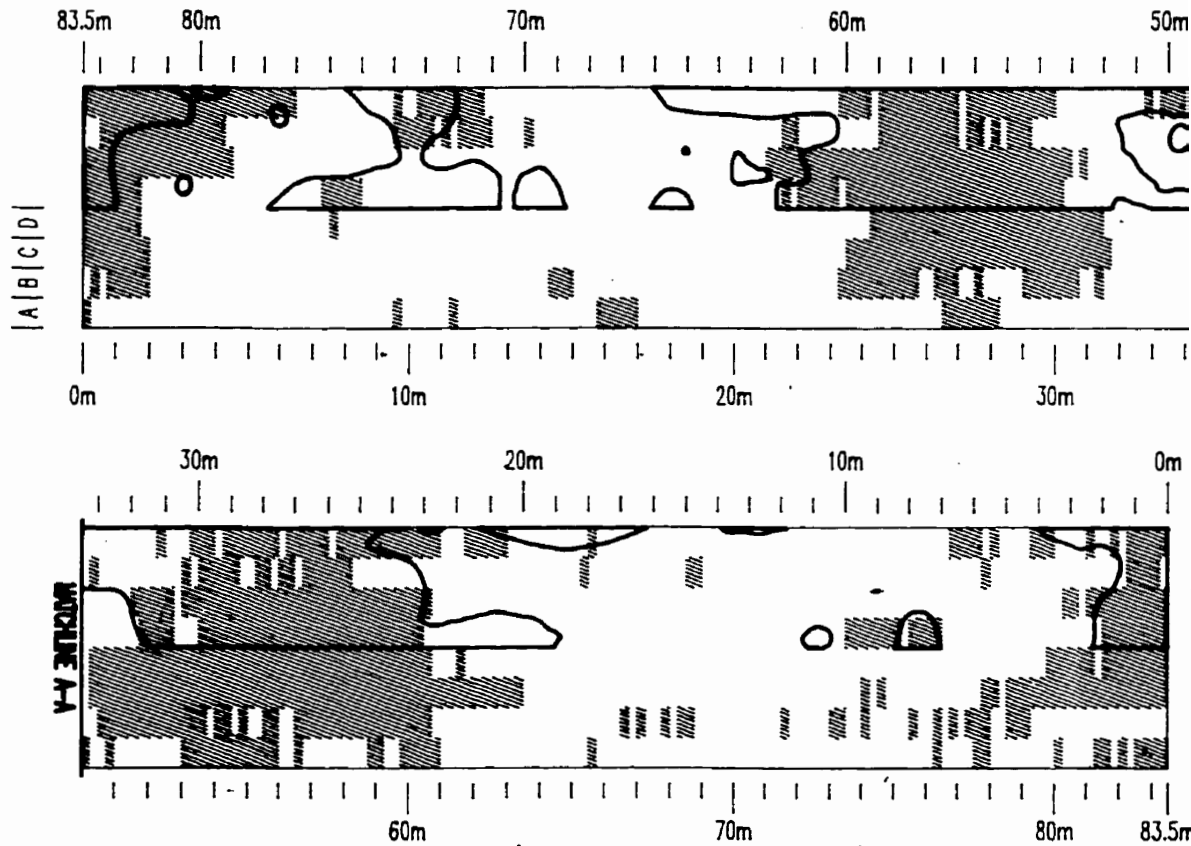
Baddeck River Bridge

GPR Deck Survey
 October 17, 1996

Half Cell Potential Area = 153.7 m²
 Percent Half Cell Potential Area = 46.0%

Surface Area = 668.0 m²
 Surveyed Surface Area = 668.0 m²

Automatic Processing Indicator Area = 206.3 m²
 Percent Automatic Processing Indicator Area = 30.9%



Baddeck_Thesis.dwg 99/03/12



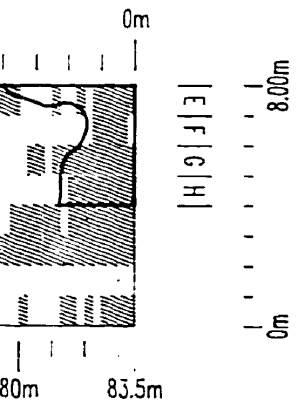
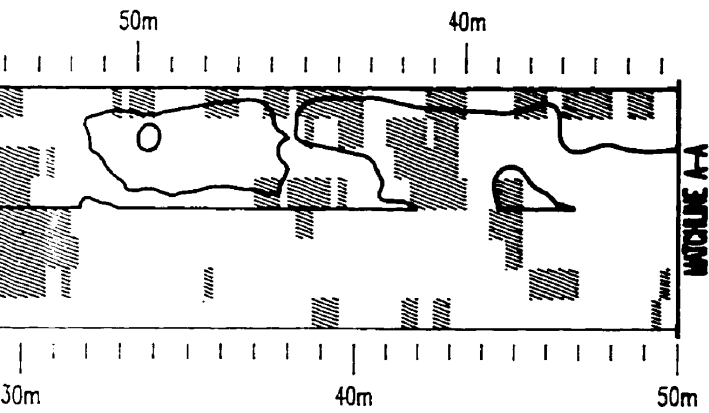
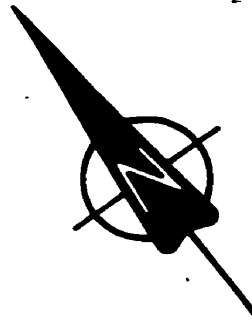
DALHOUSIE
 University

DalTech
 Architecture
 Computer Science
 Engineering

REFERENCE


SCALE : 1cm = 250 cm
 DATE : 99/03/12
 DRAWN BY : C. BARNES
 APPROVED BY :

NOVA SCOTIA
 TRANSPORTATION
GROUNDTRUTHING
 BADDECK, N



Legend

 - SIGNAL ATTENUATION (AUTOMATIC)

 - HALFCELL POTENTIAL < -0.35 VOLTS

NOVA SCOTIA DEPARTMENT OF
TRANSPORTATION AND PUBLIC WORKS

TRUTHING COMPARISON

BADDECK, NOVA SCOTIA

BADDECK RIVER BRIDGE

DRAWING NO.

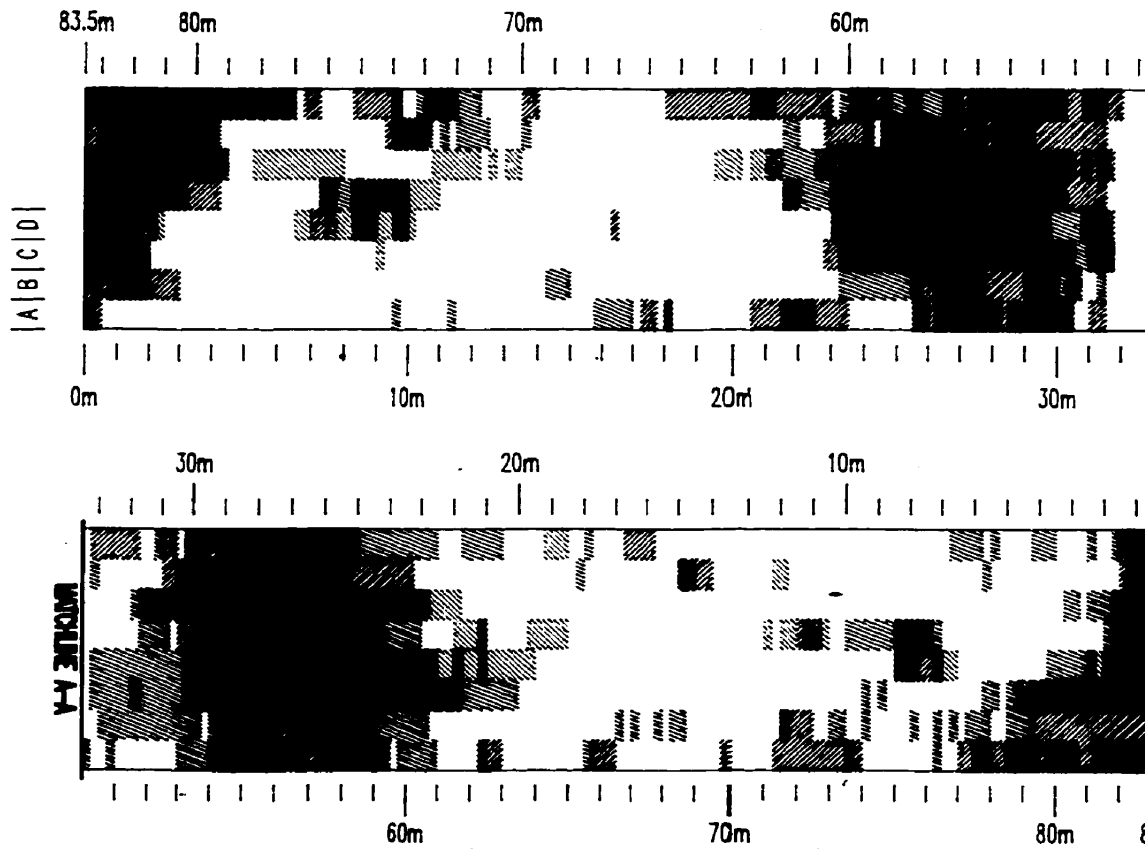
Appendix A7.4

Baddeck River Bridge

GPR Deck Survey
October 17, 1996

Surface Area = 668.0 m²
Surveyed Surface Area = 668.0 m²

Combined Radar Indicator Area = 249.5 m²
Percent Combined Radar Indicator Area = 37.4%
Automatic Processing Indicator Area = 206.3 m²
Percent Automatic Processing Indicator Area = 30.9%



Baddeck_Thesis.dwg 99/03/12



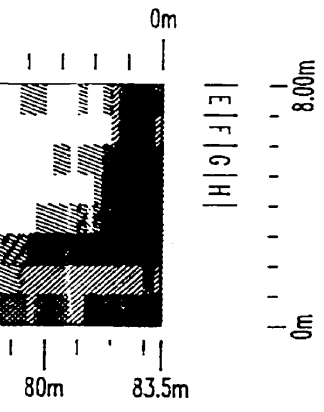
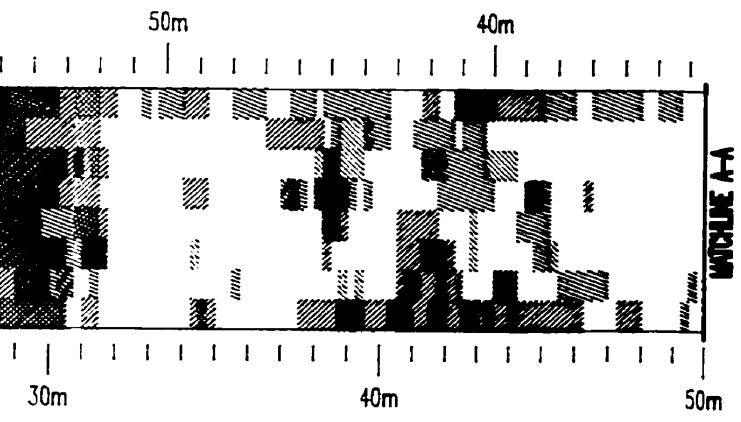
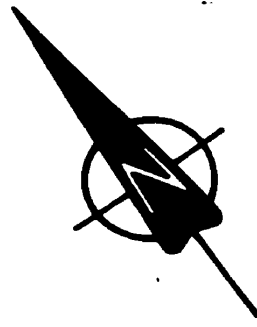
DALHOUSIE
University





DalTech
Architecture
Computer Science
Engineering

REFERENCE

SCALE : 1cm = 250 cm
DATE : 99/03/12
DRAWN BY : C. BARNES
APPROVED BY :

NOVA SCOTIA
TRANSPORTATION
GPR PROCES
BADDECK



- Legend**
-  - SIGNAL ATTENUATION (AUTOMATIC)
 -  - SIGNAL ATTENUATION (MANUAL)
 -  - HIGH CONCRETE REFLECTIVITY (MANUAL)
 -  - SIGNAL ATTENUATION AND HIGH CONCRETE REFLECTIVITY (MANUAL)

NOVA SCOTIA DEPARTMENT OF
TRANSPORTATION AND PUBLIC WORKS
PROCESSING COMPARISON
BADDECK, NOVA SCOTIA

BADDECK RIVER BRIDGE

DRAWING NO.
Appendix A7.5

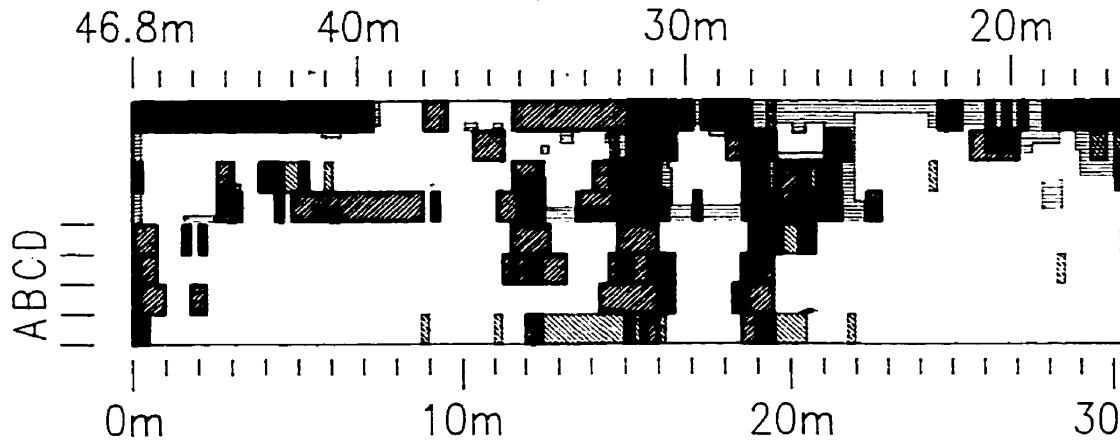
Skye River Bridge

GPR Deck Survey
October 17, 1996

Chain Drag Area = 64.4 m²
Percent Chain Drag Area = 34.4%

Combined Radar Indicator Area = 79.1 m²
Percent Combined Radar Indicator Area = 42.3%

Surface Area = 379.1 m²
Surveyed Surface Area = 374.4 m²



Skye_River_Thesis.dwg 99/03/12



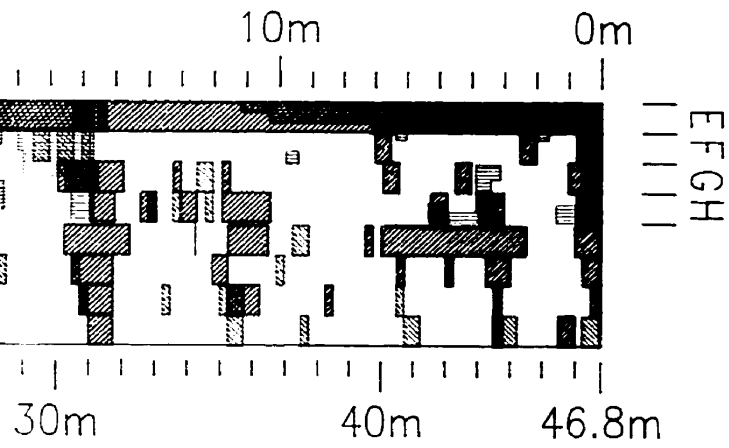
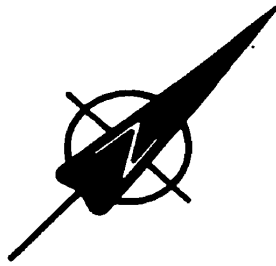
DALHOUSIE
University

DalTech
Architecture
Computer Science
Engineering





REFERENCE

SCALE : 1cm = 250 cm
DATE : 99/03/12
DRAWN BY : C. BARNES
APPROVED BY :

NOVA SCOTIA
TRANSPORTATION
GROUNDTRUTH
WHYCOCK



Legend

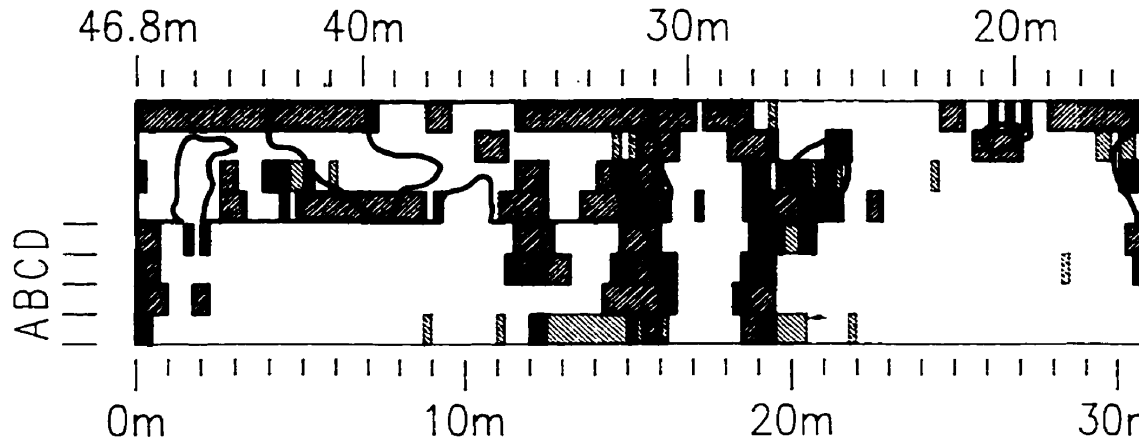
-  - SIGNAL ATTENUATION (MANUAL)
-  - HIGH CONCRETE REFLECTIVITY (MANUAL)
-  - SIGNAL ATTENUATION AND HIGH CONCRETE REFLECTIVITY (MANUAL)
-  - CHURN DRAG AREAS

Skye River Bridge

GPR Deck Survey
October 17, 1996

Half Cell Potential Area = 78.3 m²
Percent Half Cell Potential Area = 41.9%
Combined Radar Indicator Area = 79.1 m²
Percent Combined Radar Indicator Area = 42.3%

Surface Area = 379.1 m²
Surveyed Surface Area = 374.4 m²



Skye_River_Thesis.dwg 99/03/12



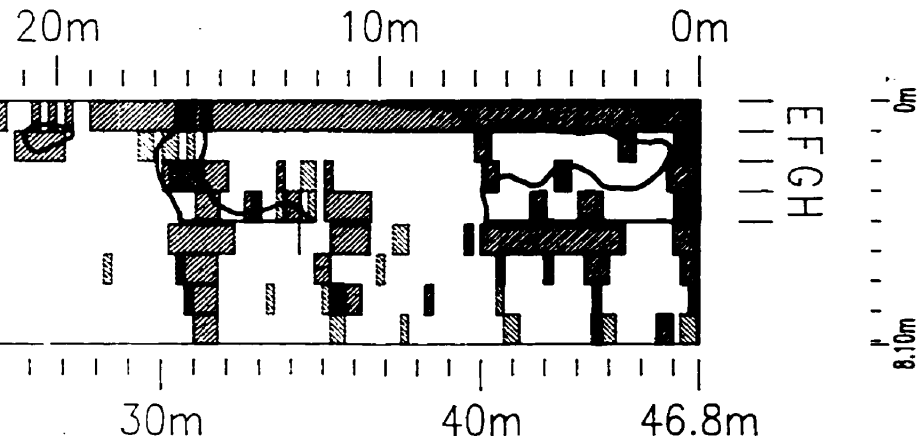
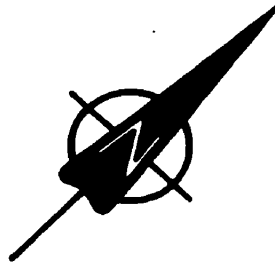
DALHOUSIE
University

DalTech
Architecture
Computer Science
Engineering





REFERENCE

SCALE : 1cm = 250 cm
DATE : 99/03/12
DRAWN BY : C. BARNES
APPROVED BY :

NOVA SCOTIA
TRANSPORTATION
GROUNDTRUTH
WHYCOCK



Legend

-  - SIGNAL ATTENUATION (ANNUAL)
-  - HIGH CONCRETE REFLECTIVITY (ANNUAL)
-  - SIGNAL ATTENUATION AND HIGH CONCRETE REFLECTIVITY (ANNUAL)
-  - HALFCELL POTENTIAL < -0.35 VOLTS

NOVA SCOTIA DEPARTMENT OF
TRANSPORTATION AND PUBLIC WORKS
FOUNDTRUTHING COMPARISON
WHYCOMAGH, NOVA SCOTIA

SKYE RIVER BRIDGE

DRAWING NO.

Appendix A8.2

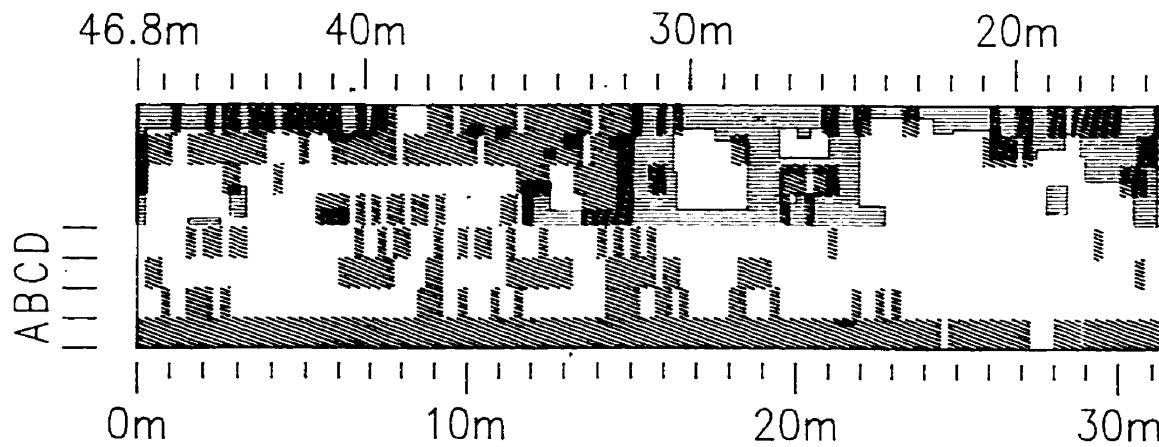
Skye River Bridge

GPR Deck Survey
October 17, 1996

Chain Drag Area = 64.4 m²
Percent Chain Drag Area = 34.4%

Surface Area = 379.1 m²
Surveyed Surface Area = 374.4 m²

Automatic Processing Indicator Area = 56.9 m²
Percent Automatic Processing Indicator Area = 30.4%



Skye_River_Thesis.dwg 99/03/12



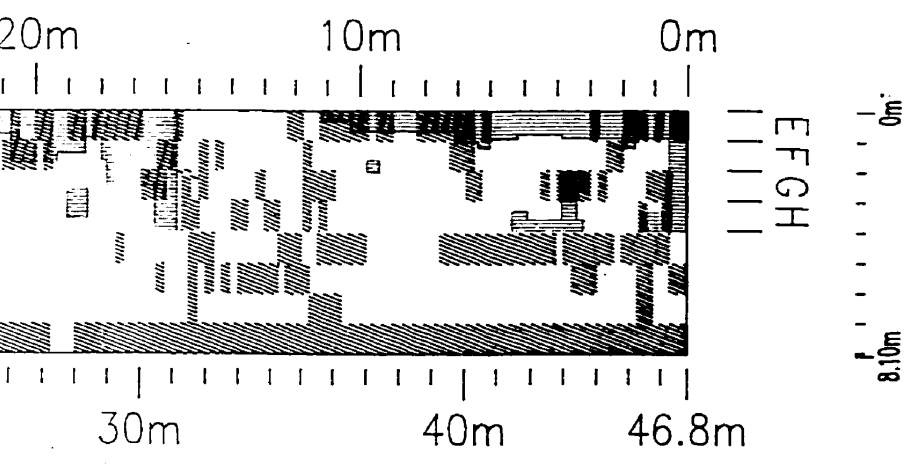
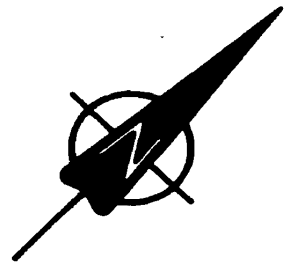
DALHOUSIE
University

DalTech
Architecture
Computer Science
Engineering



REFERENCE

SCALE : 1cm = 250 cm
DATE : 99/03/12
DRAWN BY : C. BARNES
APPROVED BY :

NOVA SCOTIA
TRANSPORTATION
GROUNDTRUTH
WHYCOMB



Legend

-  - SIGNAL ATTENUATION (AUTOMATIC)
-  - CHOW DRAG AREAS

NOVA SCOTIA DEPARTMENT OF
TRANSPORTATION AND PUBLIC WORKS
UNDTRUTHING COMPARISON
WHYCOCOMAGH, NOVA SCOTIA

SKYE RIVER BRIDGE

ENCLOSURE NO.
Appendix A8.3

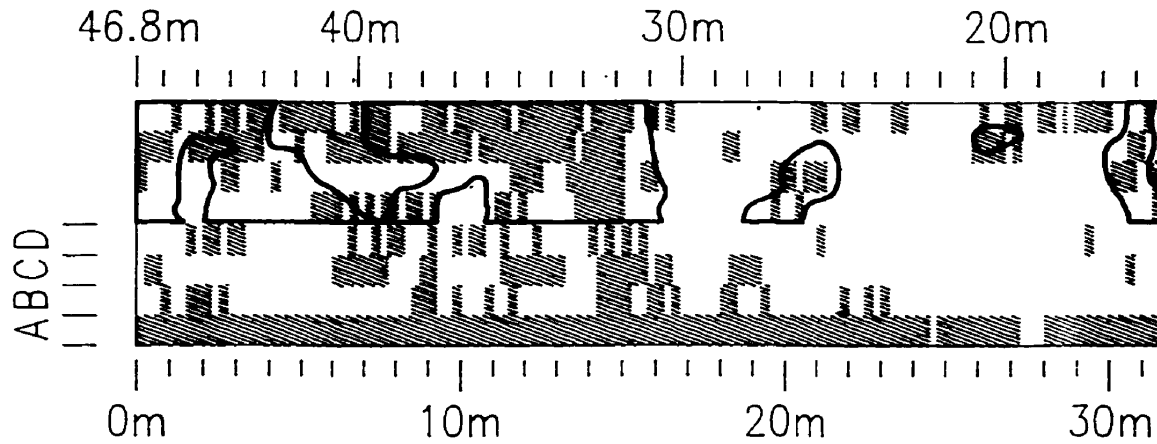
Skye River Bridge

GPR Deck Survey
October 17, 1996

Half Cell Potential Area = 78.3 m²
Percent Half Cell Potential Area = 41.9%

Surface Area = 379.1 m²
Surveyed Surface Area = 374.4 m²

Automatic Processing Indicator Area = 56.9 m²
Percent Automatic Processing Indicator Area = 30.4%



Skye_River_Thesis.dwg 99/03/12



DALHOUSIE
University

DalTech
Architecture
Civil Engineering
Computer Science
Engineering

REFERENCE

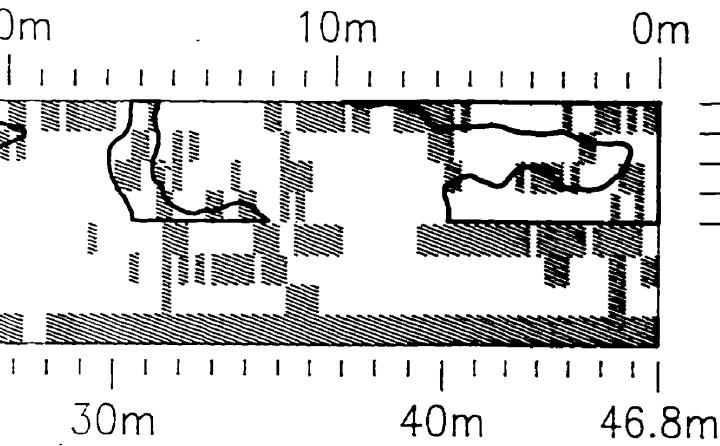
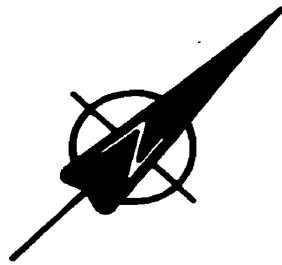
SCALE : 1cm = 250 cm

DATE : 99/03/12

DRAWN BY : C. BARNES

APPROVED BY :

NOVA SCOTIA
TRANSPORTATION
GROUNDTRUTH
WHYCOMBE



EFGH

8.10m

Legend:

 - SIGNAL ATTENUATION (AUTOMATIC)

 - HALFCELL POTENTIAL
< -0.35 VOLTS

NOVA SCOTIA DEPARTMENT OF
TRANSPORTATION AND PUBLIC WORKS
INDENTRUTHING COMPARISON
WHYCOMAGH, NOVA SCOTIA

SKYE RIVER BRIDGE

DRAWING NO.

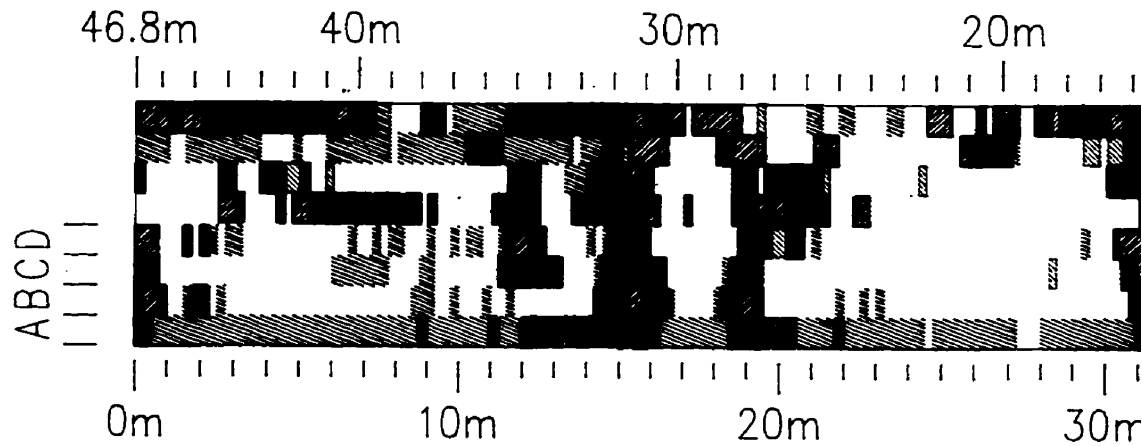
Appendix A8.4

Skye River Bridge

GPR Deck Survey
October 17, 1996

Surface Area = 379.1 m²
Surveyed Surface Area = 374.4 m²

Combined Radar Indicator Area = 79.1 m²
Percent Combined Radar Indicator Area = 42.3%
Automatic Processing Indicator Area = 56.9 m²
Percent Automatic Processing Indicator Area = 30.4%



Skye_River_Thesis.dwg 99/03/12



DALHOUSIE
University

DalTech
Architecture
Computer Science
Engineering

REFERENCE

SCALE : 1cm = 250 cm

DATE : 99/03/12

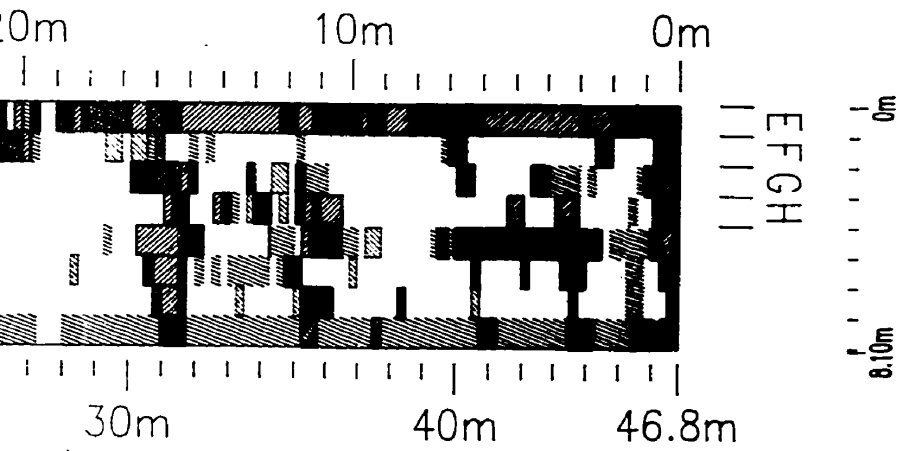
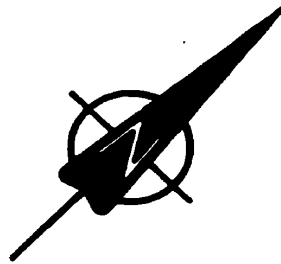
DRAWN BY : C. BARNES

APPROVED BY :

NOVA SCOTIA
TRANSPORTATION

GPR PROCESS

WNYCOCOMA



Legend

- SIGNAL ATTENUATION (ALUMINUM)
- SIGNAL ATTENUATION (MORNING)
- HIGH CONCRETE REFLECTIVITY (MORNING)
- SIGNAL ATTENUATION AND HIGH CONCRETE REFLECTIVITY (MORNING)

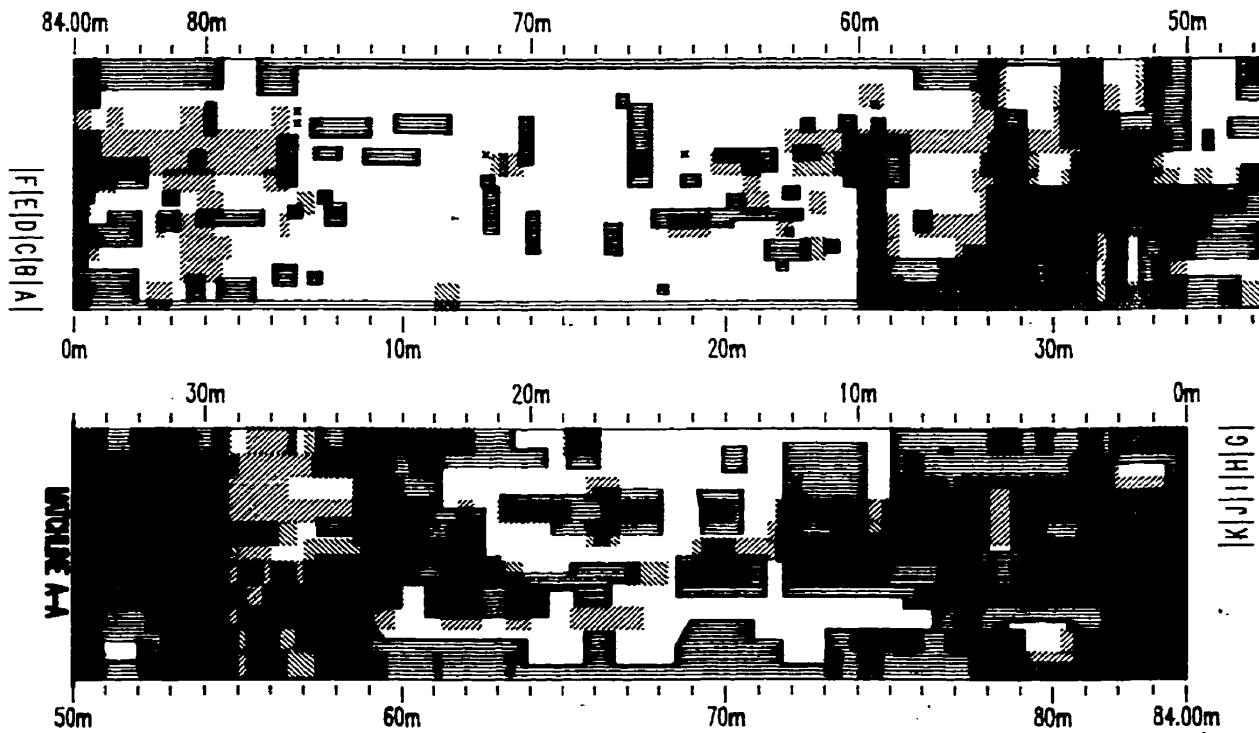
Stewiacke River Bridge

GPR Deck Survey
October 16, 1997

Chain Drag Area = 376.0 m²
Percent Chain Drag Area = 53.9%

Combined Radar Indicator Area = 310.2 m²
Percent Combined Radar Indicator Area = 44.5%

Surface Area = 697.2 m²
Surveyed Surface Area = 697.2 m²



Stewiacke_River_Thesis.dwg 98/03/12



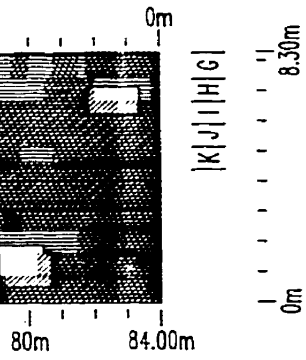
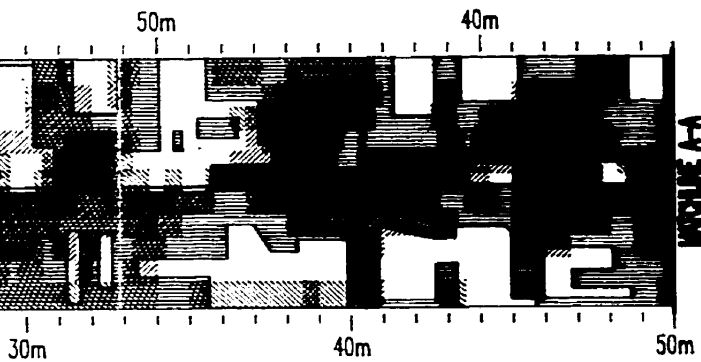
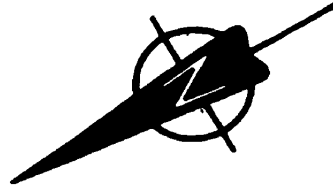
DALHOUSIE
University

DalTech
Architecture
Civil/Environmental
Engineering





REFERENCE

SCALE : 1cm = 250 cm
DATE : 98/03/12
DRAWN BY : C. BARNES
APPROVED BY :

NOVA SCOTIA DEPARTMENT OF
TRANSPORTATION AND
GROUNDTRUTHING
STEWIACKE, N.S.



Legend

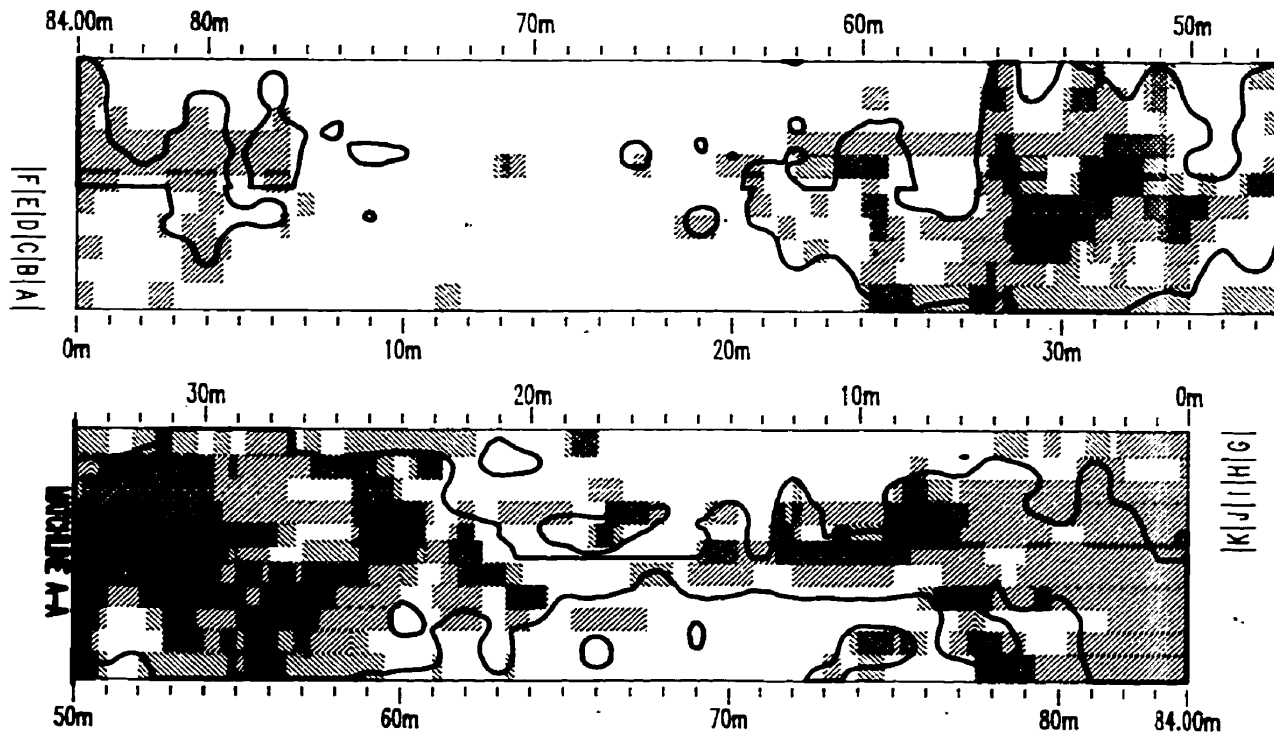
-  - SIGNAL ATTENUATION (MANUAL)
-  - HIGH CONCRETE REFLECTIVITY (MANUAL)
-  - SIGNAL ATTENUATION AND HIGH CONCRETE REFLECTIVITY (MANUAL)
-  - CHAIN DRAG AREAS

Stewiacke River Bridge

GPR Deck Survey
 October 16, 1997

Half Cell Potential Area = 352.0 m²
 Percent Half Cell Potential Area = 50.5%
 Combined Radar Indicator Area = 310.2 m²
 Percent Combined Radar Indicator Area = 44.5%

Surface Area = 697.2 m²
 Surveyed Surface Area = 697.2 m²



Stewiacke_River_Thesis.dwg 98/03/12



DALHOUSIE
 University

DalTech
 Architecture
 Computer Science
 Engineering

REFERENCE

SCALE : 1cm = 250 cm

DATE : 98/03/12

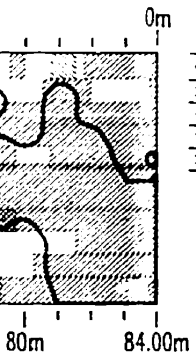
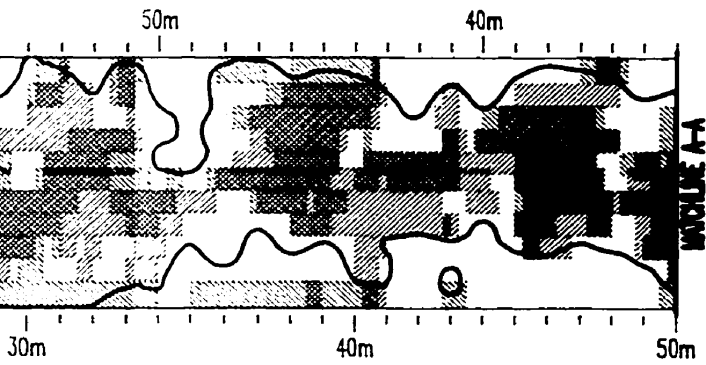
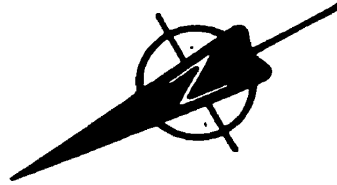
DRAWN BY : C. BARNES

APPROVED BY :





NOVA SCOTIA DEPARTMENT OF
 TRANSPORTATION AND
 INFRASTRUCTURE

GROUNDTRUTHING

STEWIACKE, NS



Legend

-  - SIGNAL ATTENUATION (MINIMAL)
-  - HIGH CONCRETE REFLECTIVITY (MINIMAL)
-  - SIGNAL ATTENUATION AND HIGH CONCRETE REFLECTIVITY (MINIMAL)
-  - HALFCELL POTENTIAL < -0.35 VOLTS

NOVA SCOTIA DEPARTMENT OF
TRANSPORTATION AND PUBLIC WORKS
FOUNDTRUTHING COMPARISON
STEWIACKE, NOVA SCOTIA

STEWIACKE RIVER BRIDGE

DRAWING NO.
Appendix A9.2

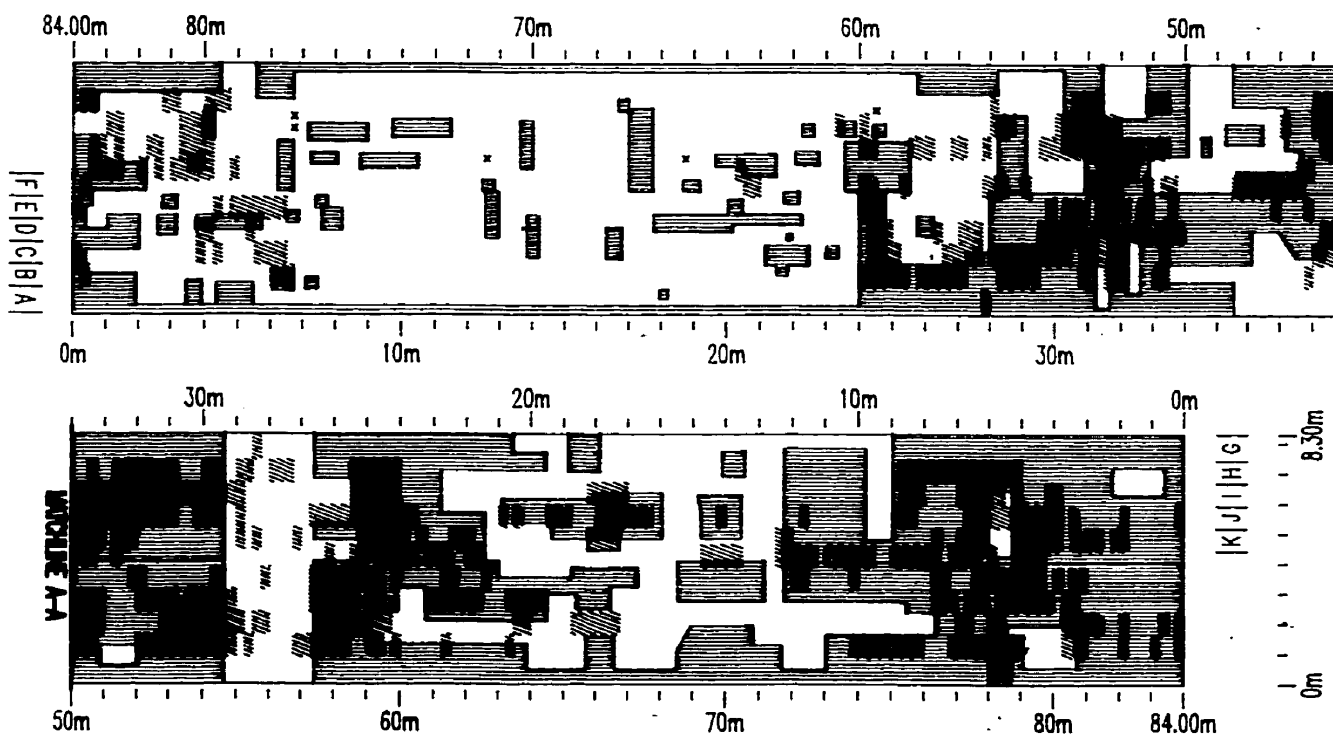
Stewiacke River Bridge

GPR Deck Survey
October 16, 1997

Chain Drag Area = 376.0 m²
Percent Chain Drag Area = 53.9%

Surface Area = 697.2 m²
Surveyed Surface Area = 697.2 m²

Combined Radar Indicator Area = 158.9 m²
Percent Combined Radar Indicator Area = 22.8%



Stewiacke_River_Thesis.dwg 98/03/12



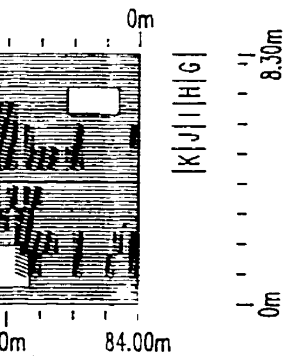
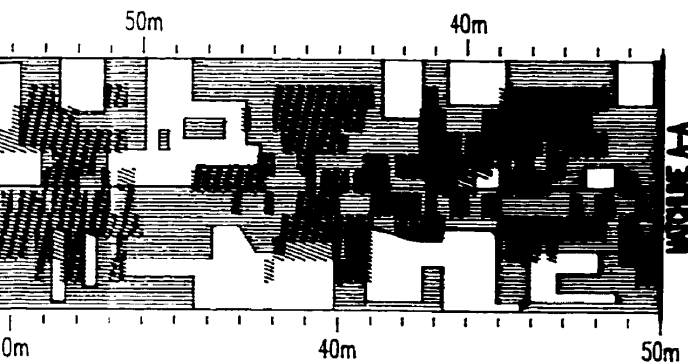
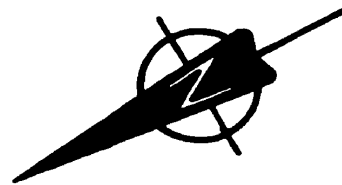
DALHOUSIE
University

DalTech
Architecture
Computer Science
Engineering


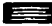
REFERENCE

SCALE : 1cm = 250 cm
DATE : 98/03/12
DRAWN BY : C. BARNES
APPROVED BY :

NOVA SCOTIA DEPARTMENT
TRANSPORTATION AND PUBLIC
GROUNDTRUTHING C
STEWIACKE, NOVA SC



Legend

-  - SIGNAL ATTENUATION (AUTOMATIC)
-  - CHAIN DRAG AREAS

NOVA SCOTIA DEPARTMENT OF
TRANSPORTATION AND PUBLIC WORKS
UNDERTRUTHING COMPARISON
STEWIACKE, NOVA SCOTIA

STEWIACKE RIVER BRIDGE

DRAWING NO.

Appendix A9.3

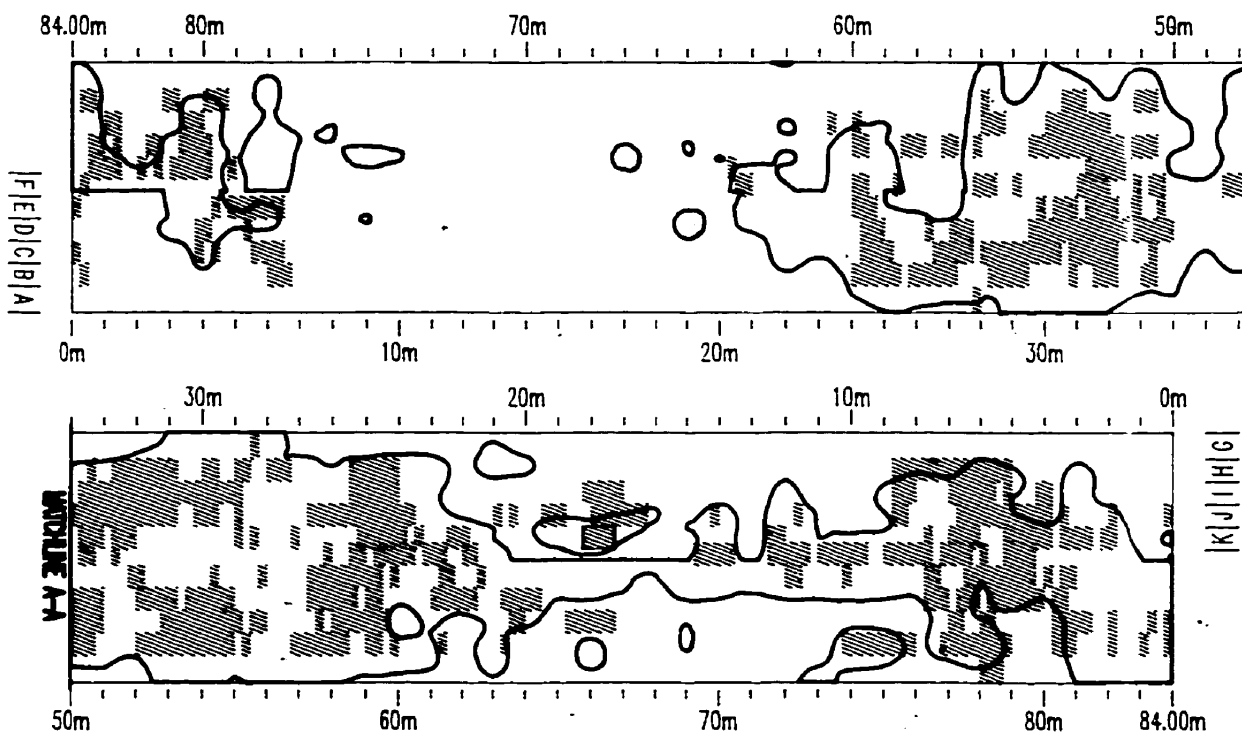
Stewiacke River Bridge

GPR Deck Survey
October 16, 1997

Half Cell Potential Area = 352.0 m²
Percent Half Cell Potential Area = 50.5%

Surface Area = 697.2 m²
Surveyed Surface Area = 697.2 m²

Combined Radar Indicator Area = 158.9 m²
Percent Combined Radar Indicator Area = 22.8%



Stewiacke_River_Thesis.dwg 98/03/12



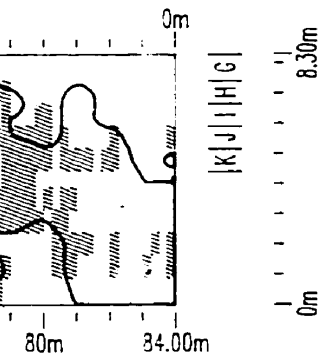
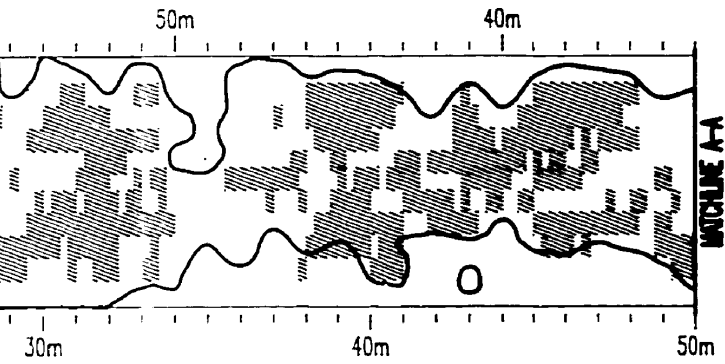
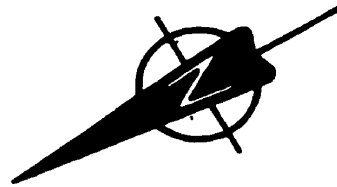
DALHOUSIE
University



DalTech
Architecture
Computer Science
Engineering

REFERENCE

SCALE : 1cm = 250 cm
DATE : 98/03/12
DRAWN BY : C. BARNES
APPROVED BY :

NOVA SCOTIA DEPARTMENT OF
TRANSPORTATION AND
INFRASTRUCTURE
GROUNDTRUTHING
STEWIACKE RIVER BRIDGE



- Legend**
-  - SIGNAL ATTENUATION (AUTOMATIC)
 -  - HALFCELL POTENTIAL < -0.35 VOLTS

NOVA SCOTIA DEPARTMENT OF
TRANSPORTATION AND PUBLIC WORKS
ROUNDRUTHING COMPARISON
STEWIACKE, NOVA SCOTIA

STEWIACKE RIVER BRIDGE

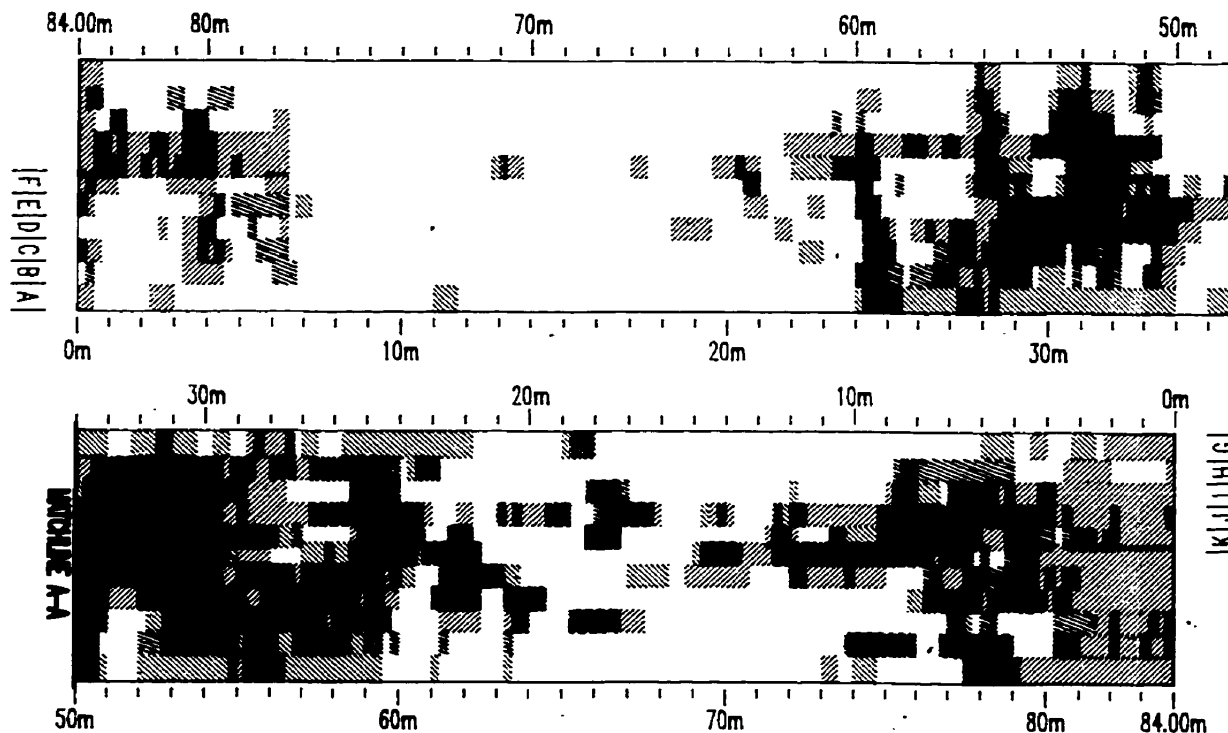
DRAWING NO.
Appendix A9.4

Stewiacke River Bridge

GPR Deck Survey
October 16, 1997

Surface Area = 697.2 m²
Surveyed Surface Area = 697.2 m²

Combined Radar Indicator Area = 310.2 m²
Percent Combined Radar Indicator Area = 44.5%
Combined Radar Indicator Area = 158.9 m²
Percent Combined Radar Indicator Area = 22.8%



Stewiacke_River_Thesis.dwg 98/03/12



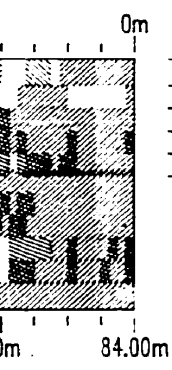
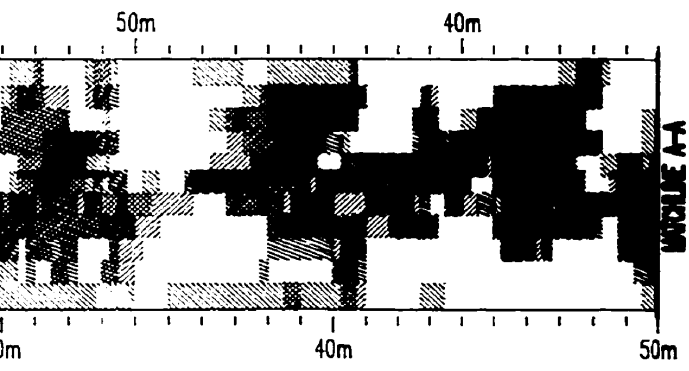
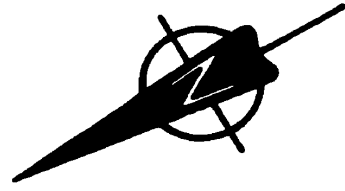
DALHOUSIE
University

DalTech
Architecture
Computer Science
Engineering





REFERENCE

SCALE : 1cm = 250 cm
DATE : 98/03/12
DRAWN BY : C. BARNES
APPROVED BY :

NOVA SCOTIA
TRANSPORTATION
GPR PROCESSING
STEWIACKE



Legend

-  - SIGNAL ATTENUATION (AUTOMATIC)
-  - SIGNAL ATTENUATION (MANUAL)
-  - HIGH CONCRETE REFLECTIVITY (MANUAL)
-  - SIGNAL ATTENUATION AND HIGH CONCRETE REFLECTIVITY (MANUAL)

NOVA SCOTIA DEPARTMENT OF
 TRANSPORTATION AND PUBLIC WORKS
PROCESSING COMPARISON
 STEWACKE, NOVA SCOTIA

STEWACKE RIVER BRIDGE

DRAWING NO.
Appendix A9.5

